LIFE E-VIA: Prototype implementation and tyre/road noise performances

Julien Cesbron, Marie-Agnès Pallas, Simon Bianchetti, Philippe Klein, Veronique Cerezo, Antonino Moro, Francesco Bianco

LIFE E-VIA

"Electric Vehicle noIse control by Assessment and optimisation of tyre/road interaction"

LIFE18 ENV/IT/000201

Deliverable	Report on action B2
Content	Prototype implementation and tyre/road noise performances
Action/Sub-action	B2: Tyre-pavement coupling study and prototype implementation
Status - date	Final version - 13-05-2022

Authors	Julien CESBRON, Marie-Agnès PALLAS, Simon BIANCHETTI, Philippe KLEIN and Véronique CEREZO (UNI EIFFEL) Antonino MORO and Francesco BIANCO (IPOOL)
Beneficiaries	UNI EIFFEL CRD IPOOL UNIRC
Contact person	Julien CESBRON
E-mail	julien.cesbron@univ-eiffel.fr
Project Website	https://life-evia.eu/

Document history

Version	Date	Contributor	Input
0.0	19-02-2021	J. Cesbron	Document created
1.0	28-02-2022	S. Bianchetti, J. Cesbron, P. Klein, M-A. Pallas	Draft of the document completed
1.1	11-03-2022	J. Cesbron and M-A. Pallas	Checking of the final draft version
1.2	13-05-2022	J. Cesbron and M-A. Pallas	Final version after Scientific Committee review

Keywords: electric vehicles, vehicle noise emission, tyre-road noise, pass-by noise, microphone array, close-proximity noise, low-noise asphalt concretes, very thin asphalt concrete, rubberised asphalt concrete, crumb rubber, surface texture, sound absorption, dynamic stiffness, friction.

Table of contents

Executive Summary

Action B2 of the LIFE E-VIA project, entitled "Tyre-pavement coupling study", focuses on tyre/road interaction in the specific context of growing electric vehicle (EV) fleet. The main goal is to select the optimal combination of road surface and tyre in order to reduce noise in urban area, prior to the implementation of the pilot test section in Florence (Italy) within Action B3. Action B2 mainly consists of gathering experimental data in France on the reference test track of Université Gustave Eiffel (UNI EIFFEL) Nantes campus. Action B2 activities started at the very beginning of the LIFE E-VIA project in August 2019 and lasted up to the end of 2021. Action B2 was coordinated by UNI EIFFEL and is divided into four sub-actions:

- B2.1 "Acoustical characterisation of EVs on existing tracks", involving UNI EIFFEL;
- B2.2 "Construction of the B1-based prototype test section", involving UNI EIFFEL and UNIRC;
- B2.3 "Characterisation of the B1-based prototype test section", involving UNI EIFFEL and IPOOL;
- B2.4 "Selection of optimised EV tyres", involving UNI EIFFEL and CRD.

Sub-action B2.1 started at the beginning of the project and consisted in the acoustical characterisation of a set of EVs on six different existing road surfaces of UNI EIFFEL reference test track in Nantes. The aim was to provide reference acoustical data for EVs in order to help in the mix design of the optimised road surface developed within Action B1 and to complement action B6 dealing with the improvement of CNOSSOS-EU model for EVs. Tests included source characterisation by means of a microphone array located on the roadside and standard Controlled Pass-By (CPB) noise measurements at usual urban speeds. Different real driving conditions have been considered, i.e. constant speed, acceleration and deceleration conditions. As expected for EVs, at constant speed tyre/road noise dominates sound emission. At 50 km/h, the difference between the quietest and the loudest test sections varies from 4.8 dB(A) to 7.9 dB(A) depending on EV model. While deceleration tests in energy recovery mode leads to little difference with pass-by at constant speed, pass-by in full acceleration tests with EVs have shown a large noise increase, often exceeding 5 dB(A). The noise increase is located in the driving wheel area, including both rolling noise under torque effect and motor noise contributions. However, the ranking of road surfaces remains quite unchanged under acceleration. These results emphasise the stake of the road surface selection for reducing noise emission from EVs. The combination of sound absorption properties and low texture levels leads to the highest noise reduction.

Sub-action B2.2 started in February 2020 and ended in September 2020. This action was dedicated to the construction of a 57 m long by 8 m wide prototype of low-noise road surface on UNIEIFFEL reference test track. This step was necessary for further feedback in action B1 and prior full-scale construction of the low-noise test section in the pilot are in Florence (Italy) within action B3. Based on the main outputs of action B1, two VTAC 0/6 test sections of the same grading curve have been laid. They differ by the addition of 1.9 % of crumb rubber (CR) in one of the mixes. The construction of the prototype was performed in September 2020 without major difficulty, using classical laying procedure in road construction. The test section without CR was named P, while the other with CR was named PCR. The controls after construction have shown the conformity of the grading curve and of the bitumen content for both test sections. The evaluated thickness and air-void content were also compliant. The measured mean texture depth (MTD) was rather low on both test sections, with an average value of 0.51 mm for test section P and 0.42 mm for test section PCR.

Sub-action B2.3 dealt with the characterisation of the prototype test section. It started after its construction in September 2020 and ended in June 2021. Regarding road surface properties influencing tyre/road noise, quite low mean profile depth (MPD) and surface texture levels were measured

for both prototype test sections P and PCR. The sound absorption of both test sections is also weak, while their dynamic stiffness remains close to a conventional asphalt concrete. Regarding skid resistance, the estimated texture depth (ETD) values confirm the low macro-texture of P and PCR, but the friction coefficient and its evolution with polishing of the road surface are very satisfactory. Pass-by noise measurements with EVs show that P and PCR test sections are among the quietest road surfaces, with an average noise reduction around 4 dB(A) at 50 km/h, by comparison with a reference DAC 0/10 test section. CPX measurements confirm this good noise performance for the prototype test section, with a noise reduction around 3 dB(A) at 50 km/h for a standard commercial tyre. The noise reduction with the SRTT tyre (ISO 11891-3) reduces to 1.7 dB(A) for P and 2.4 dB(A) for PCR. Both prototype test sections meet the Core criterion of the European green public procurement (GPP) for a low-noise pavement, fixing the CPX noise level at 50 km/h below 90 dB(A). This result complies with the objectives of the project. All in all, apart from the SRTT tyre, test section P without CR is on average 0.6 dB(A) quieter than test section PCR. The series of tests carried out provides a comprehensive assessment of the prototype for further LIFE E-VIA project activities.

Sub-action B2.4 focused on the acoustical characterisation of six different tyre versions, namely V1 to V6, developed by CRD within action B7. The dimension of the tyres was 205/55 R16 and the tyre versions mainly differed by the tread pattern design. Pass-by noise measurements conforming regulation UNECE R51.03 were performed in autumn 2021. The tyres were fitted on two different vehicles, one EV and one ICEV. With these tyres, test section PCR turns out to be systematically around 0.5 dB(A) quieter than test section P. Taking tyre version V1 as a reference, the tyre version V2 is the quietest. The noise reduction may exceed 1.5 dB(A) with the EV under strong acceleration, but otherwise it does not exceed 1 dB(A) in the usual driving situations. Apart from tyre version V2, there was no major definite advantage observed for the other tested cases. Four tyre versions were also tested by the CPX method on the prototype test sections and further existing road surfaces. P and PCR are among the quietest road surfaces, with a noise reduction from a reference DAC 0/10 between -4.2 dB(A) and -5.8 dB(A). Test section PCR is generally quieter than P, with a difference up to 1.1 dB(A). Comparing to the reference tyre V1, a clear advantage is observed for tyre version V2 on test section PCR (-0.6 dB(A)), while on test section P the best performance is obtained with the tyre version V4 (-1 dB(A)). The results of sub-action B2.4 will serve for the final optimisation of the EV tyre by CRD within action B7, prior to the implementation in the pilot area in Florence.

1 Introduction

According to recent data of European Alternative Fuel Observatory (EAFO), the electric vehicle (EV) fleet in the European area is still growing exponentially. Indeed, the number of EVs, including battery electric vehicles and plug-in hybrid electric vehicles, reached 3.1 million in 2020. EVs represented 10.7% of market share of new registrations in 2020 (EAFO). The different projection scenarios proposed in IEA (2019) expect EVs to represent between 15% and 30% of the global vehicle fleet by 2030, reaching between 130 and 250 million vehicles worldwide.

The increasing number of EVs in the next years is going to change the soundscape in urban area. While electric motors of EVs are significantly quieter than their internal combustion engine counterparts, rolling noise will become the prominent source of noise in urban area from about 20 km/h at constant speed (Pallas et al., 2016). Therefore, one of the main objectives of the LIFE E-VIA project is the reduction of tyre/road noise by proper optimisation of the tyre/road interaction. In the preliminary Action A1 of the project, a literature review was conducted (Pallas et al., 2020). Among several properties of EVs pointed out in this preliminary action, it was shown that EV tyres were not necessarily the quietest. In the preliminary Action A3, the role of tyres in the new context of EVs and internal combustion engine vehicles (ICEV) was also studied (Hoever, 2020). It turned out that apart from some specific EV models, the future market of EV tyres will also stay within the standard tyre dimensions, while EVs have some specificities by comparison with ICEVs such as higher torque and curb weight.

Action B2 of the LIFE E-VIA project, namely "Tyre-pavement coupling study", was therefore necessary to focus on the tyre/road interaction in the specific context of growing EV fleet. The main goal was to select the optimal combination of road surface and tyre in order to reduce noise in urban area, prior to the implementation of the pilot test section in Florence (Italy) within Action B3. The action mainly consisted on gathering experimental data on the reference test track of UNI EIFFEL in Bouguenais close to Nantes (France). Action B2 activities started at the very beginning of the project in August 2019 and lasted up to the end of 2021. Action B2 was coordinated by UNI EIFFEL and was divided into four sub-actions:

- B2.1 "Acoustical characterisation of EVs on existing tracks", involving UNI EIFFEL;
- B2.2 "Construction of the B1-based prototype test section", involving UNI EIFFEL and UNIRC;
- B2.3 "Characterisation of the B1-based prototype test section", involving UNI EIFFEL and IPOOL;
- B2.4 "Selection of optimised EV tyres", involving UNI EIFFEL and CRD.

Sub-action B2.1 started at the beginning of the project and consisted in the acoustical characterisation of a set of EVs on six different existing road surfaces of UNI EIFFEL reference test track in Nantes. The aim was to provide reference acoustical data for EVs in order to help in the mix design of the optimised road surface developed within Action B1. Tests included source characterisation by means of a microphone array located on the roadside and standard Controlled Pass-By (CPB) noise measurements at usual urban speeds. Different real driving conditions have been considered, i.e. constant speed, acceleration and deceleration conditions. Besides recommendations for B1, these tests were also intended to complement B6-action dealing with the improvement of CNOSSOS-EU model for EVs.

Sub-action B2.2 was dedicated to the construction of a prototype on UNI EIFFEL reference test track in Nantes. It started in February 2020 and ended in September 2020 after the building of the prototype. Based on the main outputs of action B1, the specifications of two low-noise very thin asphalt concrete (VTAC) 0/6 mixes, one comprising Crumb Rubber (CR), were given by UNIRC to UNI EIFFEL. The two prototype test sections were built by a sub-contracting French road company.

The aims of building a prototype in Nantes were firstly to thoroughly assess the road surface properties and the acoustical efficiency of the proposed low-noise asphalt concretes for a set of EVs prior to full-scale implementation in Florence (sub-action B2.3), and secondly to allow the characterisation of different EV tyre models from CRD within the process of optimising tyre/road interaction, in complement to holistic laboratory testing of tyres by CRD within action B7 (sub-action B2.4).

Sub-action B2.3 dealt with the characterisation of the prototype test section. It started after its construction in September 2020 and ended in June 2021. Several tests were carried out on the prototype test section. The main properties of the road surface influencing tyre/road noise, namely texture, sound absorption and dynamic stiffness, were measured. Factors influencing skid resistance such as Mean Profile Depth (MPD), wet friction and friction durability were also tested. A large part of this action was also dedicated to the acoustical characterisation of the prototype test sections. Besides reiteration of CPB and microphone array measurements performed in B2.1 for a selection of EVs, CPX tests were carried out by UNI EIFFEL with a standard 195/60 R15 tyre and by IPOOL with a SRTT tyre conforming ISO 11819-3. The latter was necessary to make reliable comparisons with results of Action B4 dealing with the monitoring on the pilot test section built in Florence. As will be seen, the series of tests carried out produces a fairly comprehensive assessment of the prototype test sections.

Sub-action B2.4 concerns the acoustical characterisation of a set of six versions of carved prototype tyres developed by CRD within Action B7 and delivered to UNI EIFFEL for testing on the prototype test sections. The measurement campaign was performed in autumn 2021 at the end of Action B2. The tyres were representative for the standard European summer replacement market at the time of testing and their size, 205/55 R16, was representative for the European EV market. For the six tyre versions, UNI EIFFEL carried out constant speed and accelerated pass-by noise measurements according to UNECE R51.03. The pass-by measurements were performed using an EV and an ICEV which were chosen based on the outcome of action A3. Four of these tyre versions were also tested by the CPX method on the prototype test sections and further existing road surfaces. The outcome of sub-action B2.4 will serve as input for further investigations by CRD within action B7.

In the following, the report is organised per sub-action. Section 2 deals with sub-action B2.1, section 3 with sub-action B2.2, section 4 with sub-action B2.3 and section 5 with sub-action B2.4. Each section ends with a summary of the main experimental results. Some additional experimental results obtained with the microphone array are also available in the appendices. Finally, the last section of the report deals with the main findings and conclusions of the study.

2 Sub-action B2.1 – Acoustical characterisation of EVs on existing tracks

This sub-action started at the beginning of the project and consisted in the acoustical characterisation of a set of EVs on different existing road surfaces of UNI EIFFEL reference test track located in Bouguenais close to Nantes (France), i.e. a Porous Asphalt (PA) 0/6, a Very Thin Asphalt Concrete (VTAC) 0/6, a VTAC 0/4, a Dense Asphalt Concrete (DAC) 0/10, a Stone Mastic Asphalt (SMA) 0/10 and a DAC 0/8 conforming ISO 10844 standard. The aim was to provide data on EV noise emission in order to help in the design of the mix of the optimised road surface within B1. The EV fleet involved in the tests was composed of EVs available at UNI EIFFEL and others that were rented. An additional reference ICEV was also included in the measurement campaign.

Tests were performed by UNI EIFFEL and included source characterisation by means of a microphone array located on the roadside and standard Controlled Pass-By (CPB) noise measurements at usual urban speeds. Beside recommendations for action B1, these tests investigated EV noise sources in real driving conditions (cruise driving, acceleration and deceleration conditions), and may also complement the work performed in action B6 regarding the improvement of CNOSSOS-EU model for EVs.

The investigation of the set of EVs tested on the various road surfaces provides a comparison of both the road surfaces and the vehicles. It informs on the overall noise emission in a wide range of real urban and suburban driving conditions. A description of the vehicle noise source contribution completes and refines the acquired knowledge.

2.1 Description of the experimentation

2.1.1 Test site and road surfaces

Within sub-action B2.1, the acoustical characterisation of EVs has been carried out on Université Gustave Eiffel reference test track located in Bouguenais (France). This test site comprises 15 test sections with different road surface properties (Figure 2.1), which makes it a worldwide renown and frequently used place to study tyre/road interaction properties, as e.g. wet skid resistance, rolling resistance or rolling noise. It must be noticed that the test track is not open to traffic and is dedicated to tests with light or medium heavy vehicles only. Despite the lack of real traffic, this test site was found to be the ideal place to implement the prototype of low-noise road surface within the LIFE E-VIA project, before full-scale implementation in the pilot site in Florence in Italy (Action B3).

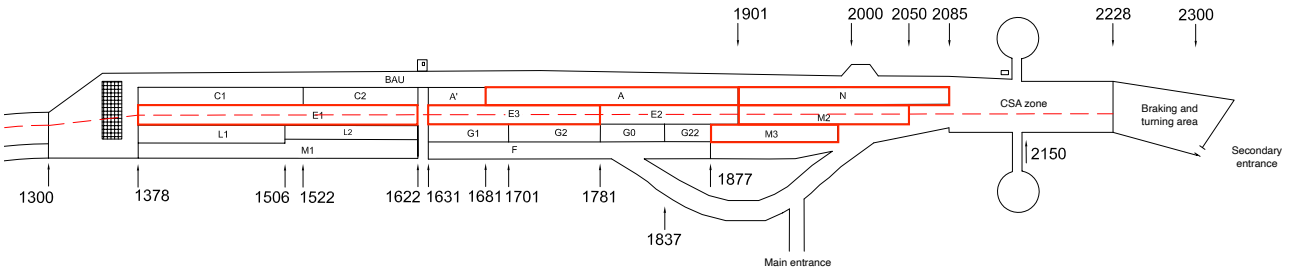

Figure 2.1: Overview of the Université Gustave Eiffel reference test track in Bouguenais (France). Test sections used within sub-action B2.1 (i.e. A, E1, E3, M2, M3 and N) are framed in red.

Six test sections have been selected for pass-by noise measurement campaigns within sub-action B2.1, namely A, E1, E3, M2, M3 and N, using the local nomenclature of the test track. These test sections are framed in red in Figure 2.1. Table 2.1 gives a description of each tested road surface:

year of construction, type, grain size, mean profile depth (MPD) as well as associated colour and marker for the presentation of results within this report. Additionally, Figure 2.2 gives a close-up

Name	Year	Type	Grain size [mm]	MPD [mm]	Color/Marker
A	2006	Porous Asphalt	0/6	1.13	+
E1	2006	Dense Asphalt Concrete	0/10	0.83	×
E3	2016	Stone Mastic Asphalt	0/10	0.91	◇
M2	2001	Very Thin Asphalt Concrete	0/6	1.29	✡
M3	2018	Very Thin Asphalt Concrete	0/4	0.60	○
N	2012	Dense Asphalt Concrete	0/8	0.31	□

Table 2.1: Description of road surfaces of the reference test track considered in sub-action B2.1. Markers and colours will be used in the following sections for road surface properties and noise results presentation.

picture of the tested road surfaces. Test sections E1, E3 and N are impervious road surfaces: E1 is a conventional Dense Asphalt Concrete (DAC) 0/10, E3 is a Stone Mastic Asphalt (SMA) 0/10 and N is a DAC 0/8 consistent with ISO 10844 (2021). The three other test sections are sound absorbing road surfaces: A is a Porous Asphalt (PA) 0/6, while test sections M2 and M3 are two Very Thin Asphalt Concretes (VTAC) of grading 0/6 and 0/4 respectively. Road surfaces A, E1, M2 and M3 are bituminous asphalt concretes that can be found on the French road network, including urban areas. Road surface E3 is rather atypical in France, but is very common in Germany and Nordic countries (most of the time in grading 0/8 or 0/11). Road surface N, with a very low MPD, is uncommon on the road network and is the type of road surface prescribed for new tyres and vehicles approval (United Nations, 1995)(United Nations, 2011).

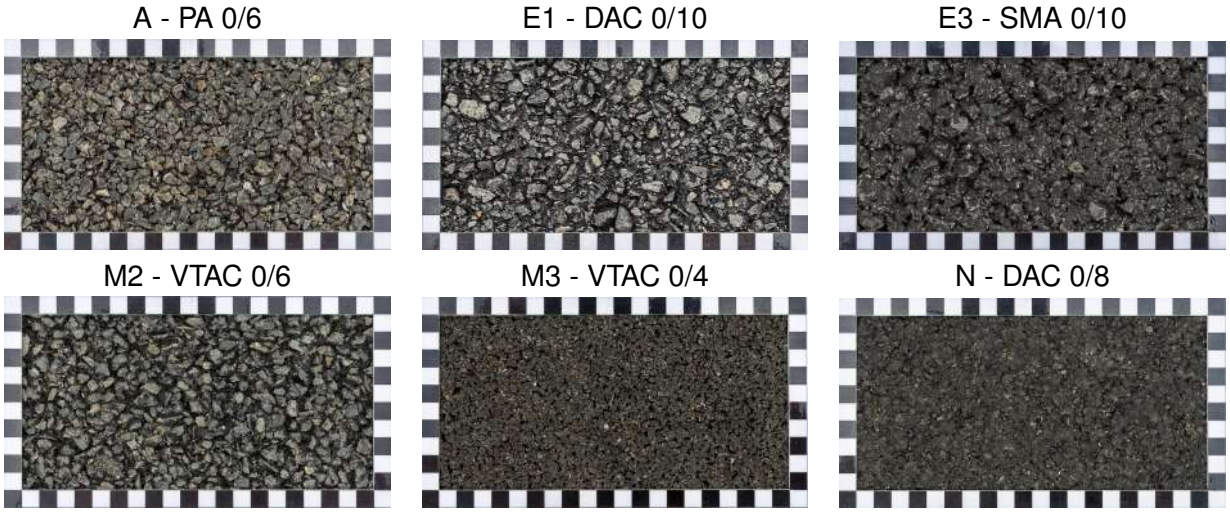

Figure 2.2: Close-up pictures of the 6 road surfaces considered for pass-by noise measurement within sub-action B2.1 (frame size: 20 cm by 10 cm).

Table 2.2 gives the mix properties of the bituminous asphalt concrete for test section A, E1, E3 and M3. The mixes basically contain several fractions of stone aggregates, fines and bitumen. The proportions are given in percent of the total weight of the mix. For test section E3, additional fibbers have been added and the fines contain a certain amount of bitumen. Hence the distinction between the percentage of filler bitumen and of total bitumen. It should be noticed that the given mix proportions are those effectively controlled after the road construction, based on the effective material laid on the test track. Regarding the apparent densities and air-void content, the data for

test section A, E3 and M3 is based on the formulation of the mix in laboratory, prior to construction of the test section, while for test section E1 it is based on *in-situ* measurement after the building of the test section. The data for test sections M2 and N is unfortunately not available with such detailed information. However, these two mixes are based on standards in which guidelines for mix formulation are given, i.e. ISO 10844 (2021) for test section N and NF EN 13108-2 (2006) for test section M2.

Mix properties	A		E1		E3		M3	
Aggregates (fraction [mm] - [%])	4/6 0/2	82.30 11.35	6/10 2/6 0/2	32.97 28.26 32.03	6.3/10 2/4 0/2	54.35 11.50 20.50	2/4 0/2	65.50 24.50
Fibbers (type - [%])					Viatop 66	0.45		
Fines [%]		0.94		0.94		7.00		4.5
Filler bitumen (type - [%])	Colflex N	5.40	35/50	5.80	35/50	6.20	50/70	5.50
Total bitumen [%]		5.40		5.80		6.35		5.50
Actual Density [g/cm^3]		2.465		2.434		2.424		2.463
Apparent Density [g/cm^3]		1.914		2.260		2.277		1.997
Air-void content [%]		22.4		7.1		6.1		18.9
Thickness [mm]		40		50		40		30

Table 2.2: Mix properties of the reference test sections A, E1, E3 and M3.

Sound absorption Sound absorption was measured according to the extended surface method of ISO 13472-1 (2002) on porous road surfaces, i.e. test sections A, M2 and M3. The other test sections have no significant absorption properties and are considered as impervious road surfaces.

The sound absorption measurement system is shown in Figure 2.3. The equipment is a stationary system composed of a sound source and a microphone respectively positioned at a distance $d_s = 1.25$ m and $d_m = 0.25$ m above the road surface. For each road surface, the absorption coefficient was first measured in the middle of the test section at five spots around the position of the pass-by microphone and averaged in the narrow bandwidth frequency domain. Then, the one-third octave band sound absorption coefficient was calculated.

Sound absorption was measured during the weeks of the pass-by noise measurement campaigns, i.e. in August 2019 and in July 2020. The results are given in Figure 2.4 for both measurement sessions. The results are quite similar for both summer 2019 and summer 2020 on test sections A and M3. It is observed that the maximum value of the absorption coefficient α is around 0.6 between 1250 Hz and 1600 Hz for surface A and around 0.7 between 800 Hz and 1000 Hz for M3, for which a second significant peak of absorption around 0.5 is observed between 2500 Hz and 3150 Hz. Regarding test section M2, a maximum absorption value of 0.2 at 800 Hz was observed in August 2019, while the maximum value was 0.3 at 630 Hz in July 2020.

Surface texture Surface texture of the six test sections was measured with a 3D profilometer. This device and the measurement procedure are described in detail in Section 4.1.1. The texture measurements for test section A, E1, E3, N and M2 had been performed within the framework of the ODSurf project (Bérengier et al., 2016). The test track being closed to traffic, it is assumed that the mega-texture and the macro-texture of the test sections did not evolve significantly during these last years. The texture measurement for test section M3, built in 2018, was performed in March 2021.

The Mean Profil Depth (MPD) and the texture spectra were calculated using longitudinal profiles extracted from the 3D texture scans, according to respectively ISO 13473-1 (2019) and ISO/TS 13473-4 (2008).

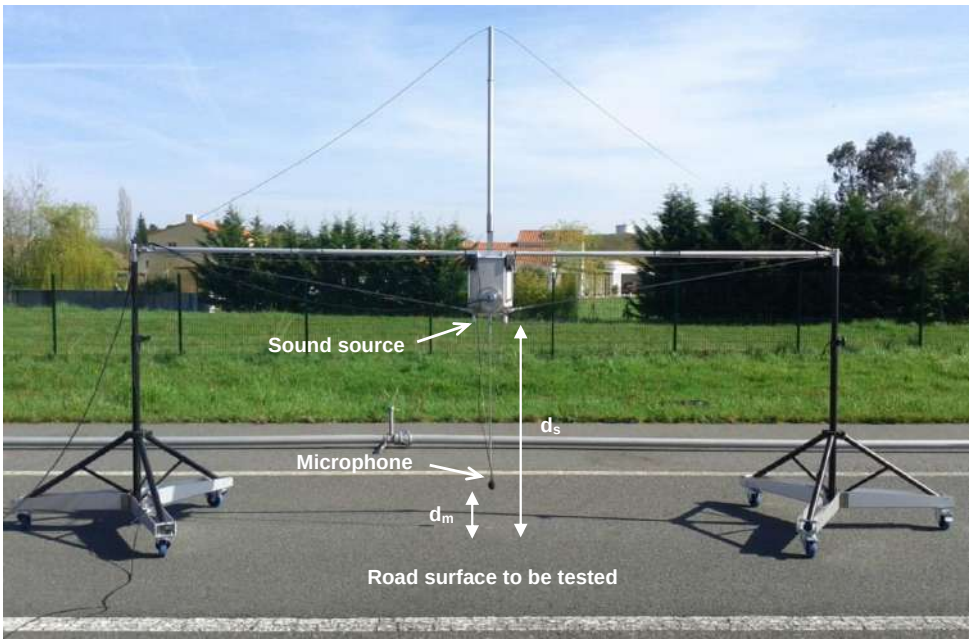

Figure 2.3: Sound absorption measurement system (here on test section A).

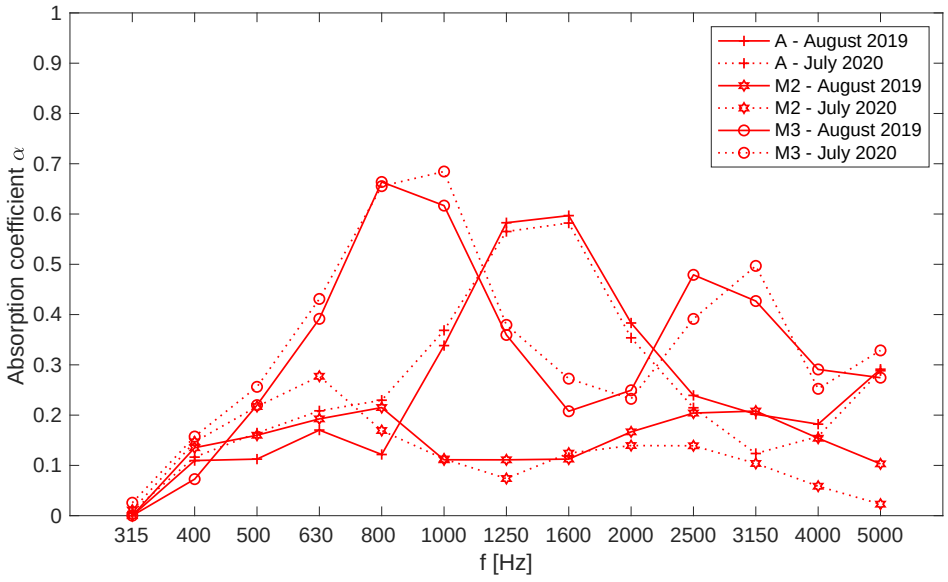

Figure 2.4: Sound absorption coefficient in one-third octave bands measured on road surfaces A, M2 and M3.

The MPD is given in Figure 2.5 for the six test sections. The lowest MPD value is obtained for the ISO surface N (0.31 mm) regarding impervious surfaces and for M3 (0.65 mm) concerning sound absorbing road surfaces. Impervious surfaces E1 and E3 have lower MPD values (respectively 0.83 mm and 0.91 mm) than sound absorbing road surfaces A and M2 (respectively 1.13 mm and 1.29 mm).

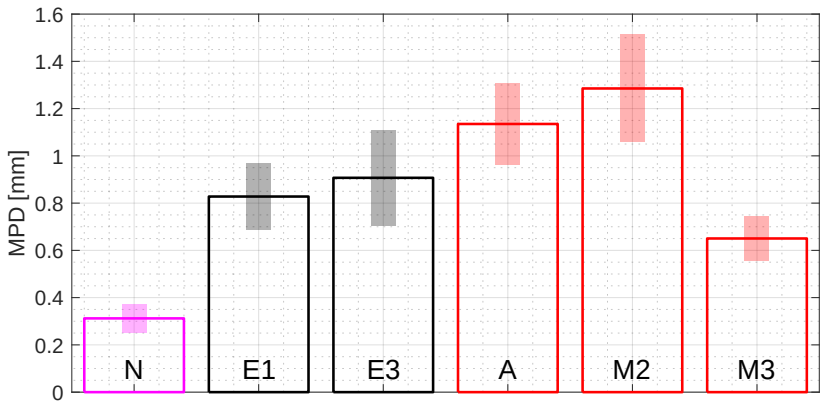

Figure 2.5: Mean Profile Depth measured on the 6 road surfaces.

The texture spectra are given in Figure 2.6 for the six test sections as a function of the texture wavelength. They represent the energy distribution of the texture signals per one-third octave bands of texture wavelength between 1 mm and 500 mm. A significant range of texture levels is observed, the lowest values being for the ISO road surface N between 1 mm and 200 mm. The wavelength range can be separated into two distinct domains. For wavelengths greater than 12.5 mm, the difference in texture levels is important and can reach up to 13 dB between N and A. The ranking of test sections remains almost unchanged between 200 mm and 12.5 mm. At wavelengths less than 8 mm, the range of texture levels is smaller and decreases from around 10 dB for 8 mm to less than 7 dB for 1 mm. In this range, the ranking of road surfaces is different from that observed at higher wavelengths. The highest levels are observed for A and M2 because of the rather narrow downward peaks and quite large amplitudes which are due to the porosity of the material.

2.1.2 Test vehicles

Vehicle models Based on EAFO data available during the period of sub-action B2.1 (i.e. 2019-2020), new registrations of EVs by volume in the European area were dominated by Battery Electric Vehicles (BEV) models. Concerning passenger cars, the Tesla Model 3 was by far dominating new registrations in 2019, followed by the Renault ZOE, the Nissan LEAF and the BMW i3. Therefore, these EV models have been involved in the pass-by noise experimental campaigns. The electric version of the new Peugeot 208 was also tested. The chosen EV models cover different segments: *supermini* segment for the Peugeot e-208 and the Renault ZOE, *small family car* segment for the BMW i3 and the Nissan LEAF and *large family car* segment for the Tesla Model 3. Additionally, in the light vehicles category, a Renault Kangoo ZE and its equivalent ICEV Renault Kangoo diesel, have been considered in the study. The six EV models tested within sub-action B2.1 are shown in Figure 2.7.

Table 2.3 gives a brief description of the tested vehicles, with ID, type (EV or ICEV), make, model, year of construction and mileage at the time of testing. It should be noticed that two Renault ZOE, namely zoe#1 and zoe#2, have been tested. In later sub-action B2.3, a different Nissan LEAF (leaf#2) was tested, hence the ID leaf#1 for the vehicle tested with sub-action B2.1. The two Renault ZOEs

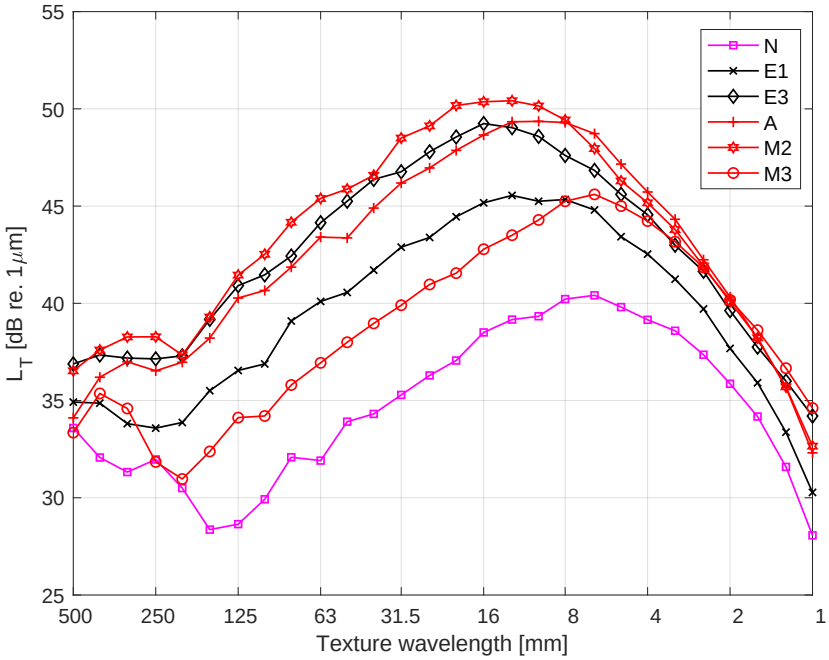

Figure 2.6: Texture spectra measured on the 6 road surfaces.

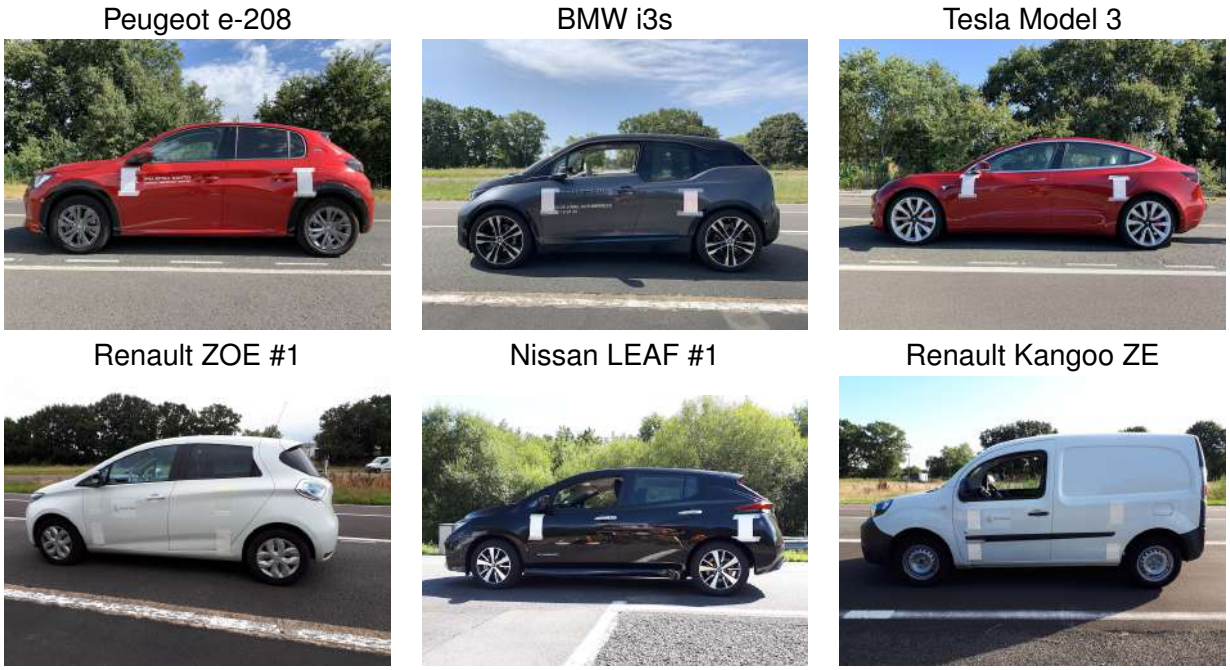

Figure 2.7: Pictures of the 6 EV models used within sub-action B2.1.

and the two Renault Kangoos were available in the vehicle fleet of Université Gustave Eiffel. The other EVs were rented or lent by car dealers for the time of testing.

ID	Type	Segment	Make	Model	Year	Mileage
e208	EV	Supermini	Peugeot	e-208	2020	3 278 km
zoe#1	EV	Supermini	Renault	ZOE	2016	18 416 km
zoe#2	EV	Supermini	Renault	ZOE	2016	5 840 km
i3	EV	Small family	BMW	i3s	2018	12 328 km
leaf#1	EV	Small family	Nissan	LEAF	2019	637 km
model3	EV	Large family	Tesla	Model 3	2019	31 498 km
kze	EV	Light commercial	Renault	Kangoo ZE	2016	12 657 km
kd	ICEV	Light commercial	Renault	Kangoo Diesel	2013	37 126 km

Table 2.3: Description of the vehicle models tested within sub-action B2.1.

Table 2.4 gives some technical specificities of the tested vehicles, i.e. power, propulsion type, battery capacity (for EVs) and curb weight. Depending on the model, the EVs can be based on traction, propulsion or even four-wheel driven.

ID	Power	Propulsion type	Battery capacity	Curb weight
e208	100 kW (136 hp)	Front wheel driven	50.0 kWh	1455 kg
zoe#1	65 kW (88 hp)	Front wheel driven	25.6 kWh	1448 kg
zoe#2	65 kW (88 hp)	Front wheel driven	25.6 kWh	1448 kg
i3	135 kW (184 hp)	Rear wheel driven	42.2 kWh	1365 kg
leaf#1	110 kW (150 hp)	Front wheel driven	40.0 kWh	1520 kg
model3	340 kW (462 hp)	All-wheel driven	77.0 kWh	1860 kg
kze	44 kW (60 hp)	Front wheel driven	33 kWh	1450 kg
kd	55 kW (75 hp)	Front wheel driven	-	1320 kg

Table 2.4: Additional properties of the vehicles tested within sub-action B2.1.

The Kangoo diesel is equipped with a 5-speed gearbox, whose ratios are given in Table 2.5.

Gear number	R1	R2	R3	R4	R5
Gear ratio	0.2683	0.4884	0.7567	1.0294	1.2187

Table 2.5: Gear ratios of the Kangoo diesel gearbox.

Tyre properties The tyres fitted on the vehicles during the tests are listed in Table 2.6. All tyres were in a reasonable state of wear. All vehicles were fitted with four identical tyre models, but the BMW i3 had different tyre dimensions at the front and at the rear of the vehicle. It should be noticed that the tyres mounted respectively on the Renault ZOE and the BMW i3 have been specifically designed for these EV models. Although not specific, the tyres on the Peugeot e-208 and the Tesla Model 3 Performance were models fitting these EVs at the time of purchase. Considering the low mileage of the Nissan LEAF tested, its tyres are also likely those delivered with the new car. Thus, this tyre panel is a representative sample of those used on the EVs investigated, though other tyres are possible for some of them. It should also be pointed out that exactly the same set of tyres was used on both Renault Kangoo vehicles.

Table 2.6 also gives additional properties of the tested tyres, i.e. the Height to Width Ratio (HWR), defined as the diameter of the unloaded tyre over the tyre width, the Shore A hardness and the inflation pressure of the tyres. The two latter were measured on cold tyres prior to the pass-by

noise testing. It should be noticed that BMW i3 tyres have a higher HWR than other tyres, which is due to their tall and narrow shape. The tyre Shore A hardness ranges between 56.1 and 67.9, respectively for the Peugeot e-208 and the Tesla Model 3. The inflation pressure was fixed following the specification of each vehicle.

ID	Tyre model	Dimensions	HWR	Hardness [Shore A]	Pressure [bars]
e208	Michelin Primacy 4	195/55 R16 87H	3.2	56.1	2.5
zoe#1	Michelin Energy E-V	185/65 R15 88Q	3.4	61.5	2.5
zoe#2	Michelin Energy E-V	185/65 R15 88Q	3.4	61.4	2.5
i3 (front)	Bridgestone Ecopia EP500	175/55 R20 89T	4.0	63.8	2.3
i3 (rear)	Bridgestone Ecopia EP500	195/50 R20 93T	3.6	64.4	2.8
leaf#1	Michelin Energy Saver	205/55 R16 91V	3.1	62.2	2.5
model3	Michelin Pilot Sport 4S	235/35 ZR20 92Y	2.9	67.9	2.9
kze(front)	Michelin Energy Saver	195/65 R15 95T	3.3	60.8	2.5
kze(rear)	Michelin Energy Saver	195/65 R15 95T	3.3	60.5	2.9
kd(front)	Michelin Energy Saver	195/65 R15 95T	3.3	60.5	2.5
kd(rear)	Michelin Energy Saver	195/65 R15 95T	3.3	60.0	2.9

Table 2.6: Description of the tyres fitted on the tested vehicles. Dimensions are followed by the load index and the speed rating. The same set of tyres has been used on both Renault Kangoos.

Figure 2.8 shows the tread pattern of the different tyre models considered during the pass-by noise test. As can be seen, the tread pattern design can be quite different from one tyre to another. For information, the European tyre labels for fuel consumption, which is important for EV range, and noise emission are given in Table 2.7[1].

Figure 2.8: Pictures of the tread pattern of the tyres fitted on the test vehicles.

[1] according to public information available on the internet in January 2022.

ID	Tyre model	Dimensions	Fuel consumption label	Noise emission label	Noise level [dB]
e208	Michelin Primacy 4	195/55 R16 87H	C	A	68
zoe#1	Michelin Energy E-V	185/65 R15 88Q	A	B	70
zoe#2	Michelin Energy E-V	185/65 R15 88Q	A	B	70
i3 (front)	Bridgestone Ecopia EP500	175/55 R20 89T	B	B	69
i3 (rear)	Bridgestone Ecopia EP500	195/50 R20 93T	B	A	69
leaf#1	Michelin Energy Saver	205/55 R16 91V	B	B	70
model3	Michelin Pilot Sport 4S	235/35 ZR20 92Y	D	B	71
kze(front)	Michelin Energy Saver	195/65 R15 95T	C	B	70
kze(rear)	Michelin Energy Saver	195/65 R15 95T	C	B	70
kd(front)	Michelin Energy Saver	195/65 R15 95T	C	B	70
kd(rear)	Michelin Energy Saver	195/65 R15 95T	C	B	70

Table 2.7: EU tyre labels of the tyres fitted on the test vehicles, concerning fuel consumption and noise emission.

2.1.3 Description of pass-by acoustical tests

The pass-by acoustical tests were performed during two distinct measurement campaigns. The first experimental campaign was performed at the beginning of the LIFE E-VIA project on August 26-30, 2019. During this first stage, only vehicles from the fleet of Université Gustave Eiffel were tested, i.e. zoe#1, kze and kd. The second measurement campaign was planned in March 2020, but finally postponed on July 20-24, 2020, due to lockdown and critical sanitary situation in link with Covid 19 pandemic in spring 2020. During this second stage, several EVs were tested, i.e. e208, zoe#2, i3, leaf#1 and model3. Additional pass-by noise measurements were also performed on the kze and the kd. The tests involved at least three operators, each in charge of an acquisition system recording pass-by noise at a given location of the reference test track. At least two drivers were also involved in the measurement campaigns. Pass-by tests were carried out in different driving conditions: at constant speed, in acceleration and in deceleration (regenerative braking).

2.1.3.1 Controlled Pass-By (CPB) noise measurement

CPB noise measurements were performed with a microphone located at the roadside, on the left of the vehicle, at the standard NF EN ISO 11819-1 (2002) position, i.e. 7.5 m from the centre of the lane and 1.20 m above the road surface. CPB tests were performed on the 6 test sections.

Figure 2.9 illustrates the experimental set-up for CPB measurement with the Nissan LEAF rolling on the test section E1. The microphone at roadside can be seen. Two infrared cells can also be observed on the road, at the left of the tested vehicle. They are respectively located at 5 meters before and after the microphone position. During pass-by, these cells detect the two reflective plates fixed on the vehicle, respectively near the front and the rear of the vehicle body (the plates are visible on vehicle pictures in Figure 2.7). The signals from the cells provide accurate information on the vehicle position and speed at pass-by.

For each run, the acoustic pressure signal $p_A(t)$ was recorded by means of a digital audio recorder and later processed according to NF EN ISO 11819-1 (2002). The A-weighted noise level L_{AF}, based on Fast time integration, was calculated as follows:

$$L_{AF}(t) = 10\log_{10}\left(\frac{1}{\tau_F}\int_{-\infty}^{t}\frac{p_A^2(\xi)e^{-(t-\xi)/\tau_F}}{p_0^2}d\xi\right) \tag{2.1}$$

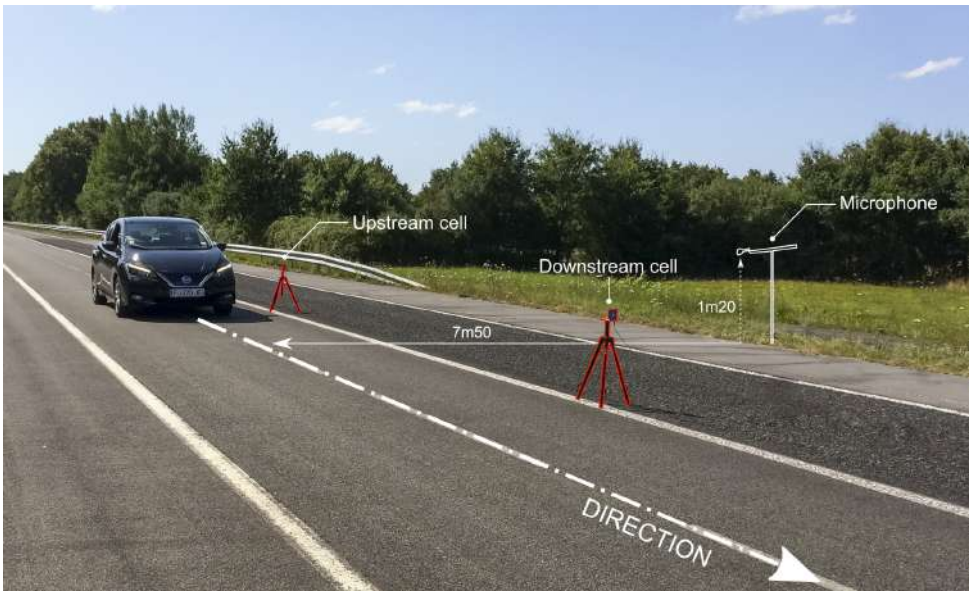

Figure 2.9: Experimental set-up for CPB noise tests (Nissan LEAF rolling on test section E1).

with constant time $\tau_F = 0.125$ s and reference acoustic pressure $p_0 = 2.10^{-5}$ Pa.

Figure 2.10 gives an example of time signature $L_{AF}(t)$ for the Nissan LEAF when passing-by at 50 km/h constant speed. The impulse signals from the infrared cells, plotted in red, are used for the calculation of the vehicle speed, as mentioned above. The time signature was analysed differently, depending on the pass-by driving conditions. The noise analysis method for each driving condition will be explained in Section 2.2.

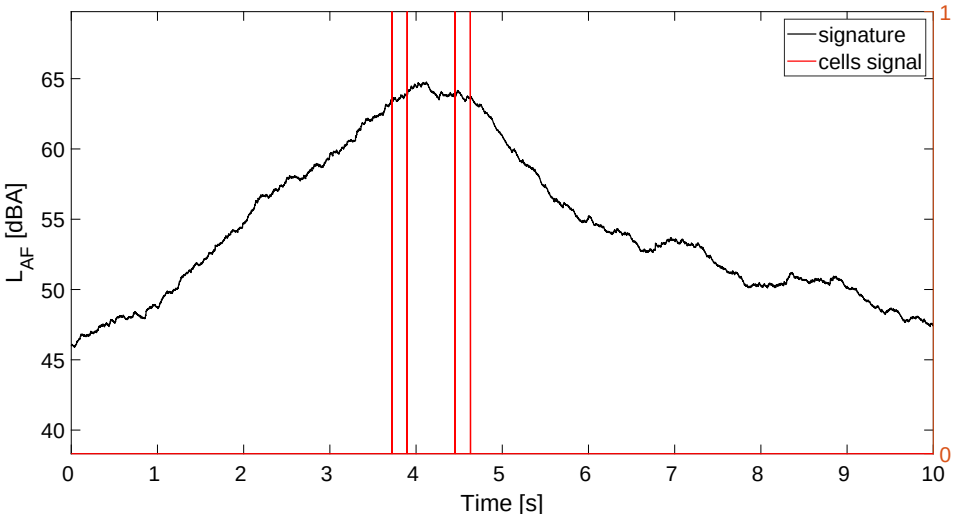

Figure 2.10: Time signature (black line) of the vehicle pass-by noise level $L_{AF}(t)$ in the case of the Nissan LEAF rolling on test section E1 at 50 km/h. Red lines are infrared cells signals.

2.1.3.2 Microphone array measurement

The microphone array, associated with a specific array processing, performs acoustic imaging of the vehicle at pass-by and offers the possibility to geometrically separate and identify noise source contributions to the vehicle noise emission. Compared to CPB measurement, which provides noise

emission from the vehicle as a whole, it allows further investigation of the origin of the noise from the vehicle driving in real conditions but is not a standard method.

The microphone array used has been designed by UMRAE (UNI EIFFEL) and is composed of 61 half-inch microphones arranged in a plane on several concentric circles (Figure 2.11). The outer circle has a diameter of 2.56 m. The array is placed at roadside, about 3.5 m from the track centre, the plane of microphone arrangement being parallel to the track (Figure 2.12). The lowest microphone is close to the ground level and precisely located.

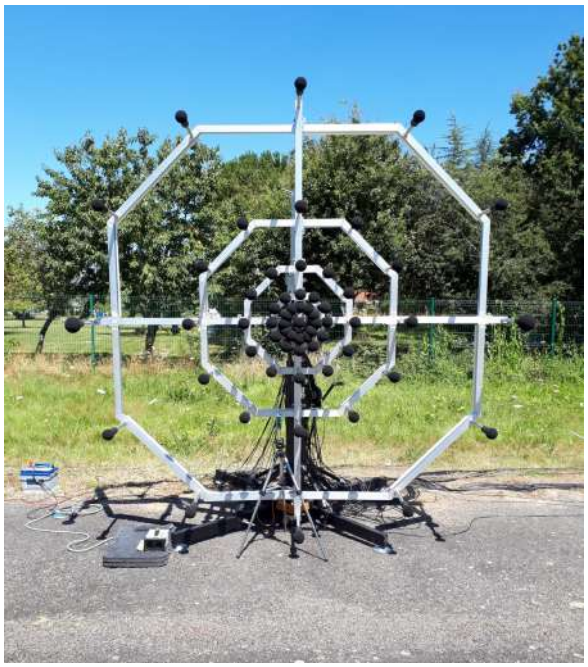

Figure 2.11: Setup of the 61-microphone plane array.

For the implementation of the array processing, kinematic information on the vehicle motion is required. This is provided by three infrared cells 10 m apart – shared with the CPB experiment – detecting two reflecting plates located on the vehicle side (Figure 2.12, right). It is completed by the use of a rangefinder, aligned with the microphone plane, which measures the distance to the front (resp. rear) tyre flange when the vehicle faces the array. This defines the position of the vertical scan plane on the vehicle side for the investigation of the noise sources. All acoustic and kinematic signals are synchronously recorded at a sampling frequency $F_s = 32768$ Hz.

It should be noticed that the microphone array tests were performed on test section N only. The different driving conditions have been considered (i.e. constant speed, acceleration or deceleration). They were carried out simultaneously with the CPB tests, the microphone array being positioned about 5 m downstream of the CPB microphone in the direction of movement.

Array signal processing

The array processing involves classical beamforming for spherical incident waves, the noise sources on the vehicles being considered as uncorrelated monopoles. Dedopplerisation is implemented on each microphone signal, on the one hand to compensate for motion-related frequency and amplitude distortions in received signals and on the other hand, to steer the focal point to any vehicle point and follow it on its trajectory in front of the array. In this way, Doppler effect and attenuation variations due to the varying propagation distance between source and microphone are resolved. The steering range is [-20°, +20°] centred on the direction normal to the array centre (i.e. perpendicularly crossing the track in front of the array centre), whatever the vehicle speed. Thus, all

Figure 2.12: Microphone array and vehicle pass-by on road surface N – Left: overview with the BMW i3 – Right: reflecting plates on the Tesla Model 3.

sources on the vehicle are examined in the same way and over the same directional range under any driving condition. The dedopplerised microphone signals are filtered in third-octave bands for next noise source investigation and imaging.

A Hanning spatial weighting of the array microphones is used for higher rejection of interference sources outside the focus direction. Beamformed arrays are well-known to behave as spatial filters and to basically offer a frequency-dependent spatial response (Johnson and Dudgeon, 1993). In order to ensure the sources to be inspected with similar spatial filters over a wide frequency range, the spatial weighting is implemented as third-octave-dependent (Pallas and Perrier, 2009), specified by an array aperture[2] $Q = 4$ from third-octave 500 Hz to 5000 Hz. At frequencies lower than 500 Hz, this aperture value cannot be satisfied and the array resolution[3] reduces with the decreasing aperture.

The beamformed signal $p_{bf,F,i}(t)$ provided at the output of the array processing is expected to be the signal emitted by the source located at the point F focused on the vehicle, in the third-octave i. The noise level delivered by the processing is the A-weighted equivalent noise level calculated on the time duration T_{scan} corresponding to the source motion within the steering range [-20°, +20°], according to:

$$L_{Aeq,F,i} = 10\log_{10}\left(\frac{1}{T_{scan}}\int_{(T_{scan})}\frac{p^2_{bf,F,i}(t)}{p_0^2}dt\right) + L_A(i) \tag{2.2}$$

where $L_A(i)$ is the standard A-weighting factor of third-octave band i. The focus point F is scanned over the vertical plane at vehicle side to provide a noise source map of the passing-by vehicle. Results in A-weighted overall levels are the energetic summation of third-octave levels from 100 Hz to 5000 Hz. For a common comparison basis between driving conditions and vehicles, the reported levels are scaled to the reference distance of 2.7 m.

2.1.3.3 Pass-by driving conditions

While CPB measurements are classically performed at constant speed, action B2 also investigated pass-bys under acceleration or deceleration, which are common situations in urban traffic. Thus, the influence of the road surface on vehicle noise emission has been assessed in various conditions encountered in real life. Tests in acceleration conditions were also motivated by the high acceleration capacity of EVs, due to the typical performance of electric motors, providing increased acceleration rates on a wide speed range in comparison with conventional vehicles (Pallas et al., 2020). By comparison with constant speed, acceleration conditions can also lead to a higher electric motor

[2]The aperture is the ratio between the array length and the wavelength at third-octave centre frequency.
[3]The array resolution characterises the ability to separate neighbour sources.

noise contribution and to an increase of rolling noise levels due to stronger torque efforts in the driving tyre/road contact areas (Hoever, 2020). Regarding deceleration conditions, most EV models have now a regenerative braking system (Pallas et al., 2020), which may lead to an additional source of noise. In the following, the procedure for each driving condition is described.

Constant speed tests On each test section, several runs were performed at constant speed in the range between 20 km/h and 110 km/h, with a 5 km/h step. At low speed, the Acoustic Vehicle Alerting System (AVAS) was switched off during the tests when this equipment was available, except for the Peugeot e-208 for which the deactivation was not possible and the speed without AVAS ranged from 30 km/h to 110 km/h. During the tests, the speed was controlled visually with an on-board accurate GPS receiver or by using the speed regulator. Table 2.8 gives a synthesis of the experiment carried out at constant speed. For each combination of test section and test vehicle, the date of measurement and the speed range are given.

	e208	zoe#1	zoe#2	i3	leaf#1	model3	kze	kd
A	07/2020	08/2019	07/2020	07/2020	07/2020	07/2020	08/2019	07/2020
V [km/h]	30 - 110	20 - 110	20 - 110	20 - 110	20 - 110	20 - 110	20 - 100	20 - 110
E1	07/2020	08/2019	07/2020	07/2020	07/2020	07/2020	08/2019	08/2019
V [km/h]	30 - 110	20 - 110	20 - 110	20 - 110	20 - 110	20 - 110	20 - 100	20 - 110
E3	07/2020	08/2019	07/2020	07/2020	07/2020	07/2020	08/2019	08/2019
V [km/h]	30 - 110	20 - 110	20 - 110	20 - 110	20 - 110	20 - 110	20 - 110	20 - 110
M2	07/2020	08/2019	07/2020	07/2020	07/2020	07/2020	08/2019	07/2020
V [km/h]	30 - 110	20 - 110	20 - 110	20 - 110	20 - 110	20 - 110	20 - 90	20 - 110
M3	07/2020	08/2019	07/2020	07/2020	07/2020	07/2020	08/2019	07/2020
V [km/h]	30 - 110	20 - 110	20 - 110	20 - 110	20 - 110	20 - 110	20 - 80	20 - 110
N	07/2020	08/2019	07/2020	07/2020	07/2020	07/2020	08/2019	08/2019
V [km/h]	30 - 110	20 - 110	20 - 110	20 - 110	20 - 110	20 - 110	20 - 80	20 - 110

Table 2.8: Synthesis of experiments performed within sub-action B2.1 at constant speed – Date and speed range for each 'vehicle / test section' configuration.

When driving with the Kangoo diesel, the gear ratio selected was the most appropriate one for the pass-by speed according to normal driving conditions (Table 2.9).

Speed range	20-25 km/h	30-40 km/h	45-55 km/h	60-110 km/h
Gear	R2	R3	R4	R5

Table 2.9: Gear ratios of the Kangoo diesel selected over the driving speed range, at constant speed.

Acceleration tests Acceleration tests were performed at full acceleration conditions, i.e. pass-by tests were carried out in full throttle. The test vehicle accelerated over a minimum length of 10 m centred on the microphone, from various initial speeds selected in 10 km/h steps. The actual range of initial speeds depended on the power of the tested vehicle. Table 2.10 gives a synthesis of the experiment carried out in accelerating conditions. For each combination of test section and test vehicle, the date of measurement and the speed range are given. EVs generally offer several driving modes, allowing the driver to select its preferred option regarding on-board energy management or torque availability. In order to test the toughest conditions, the option giving high acceleration rates was selected (Table 2.12).

	e208	zoe#1	zoe#2	i3	leaf#1	model3	kze	kd
A	07/2020	-	07/2020	07/2020	-	-	07/2020	07/2020
V [km/h]	0 - 90	-	0 - 70	0 - 80	-	-	0 - 60	0 - 70
E1	07/2020	-	07/2020	07/2020	07/2020	07/2020	08/2019	08/2019
V [km/h]	0 - 90	-	0 - 70	0 - 80	0 - 80	0 - 90	0 - 60	0 - 70
E3	07/2020	-	07/2020	07/2020	07/2020	07/2020	08/2019	08/2019
V [km/h]	0 - 90	-	0 - 70	0 - 80	0 - 80	0 - 90	0 - 60	0 - 70
M2	07/2020	-	07/2020	07/2020	07/2020	07/2020	07/2020	07/2020
V [km/h]	0 - 90	-	0 - 70	0 - 80	0 - 80	0 - 90	0 - 60	0 - 70
M3	07/2020	-	07/2020	07/2020	-	07/2020	07/2020	07/2020
V [km/h]	0 - 90	-	0 - 70	0 - 80	-	0 - 90	0 - 60	0 - 70
N	07/2020	-	07/2020	07/2020	07/2020	07/2020	08/2019	08/2019
V [km/h]	0 - 90	-	0 - 70	0 - 80	0 - 80	0 - 90	0 - 60	0 - 70

Table 2.10: Synthesis of experiments performed within sub-action B2.1 for acceleration tests – Date and range of initial speeds for each 'vehicle / test section' configuration.

Deceleration tests Pass-by noise tests in decelerating conditions were performed with the regenerative braking mode of the EV. In this mode, the vehicle decelerates when releasing the gas pedal, without pressing the brake pedal. The test vehicle decelerated from the entrance of the test section over a minimum length of 10 m centred on the microphone, with several initial speeds selected between 40 and 90 km/h. Table 2.11 gives a synthesis of the experiment carried out in decelerating conditions. For each combination of test section and test vehicle, the date of measurement and the speed range are given. EVs generally offer several driving modes, allowing the driver to select its preferred option regarding on-board energy management or torque availability. The driving mode providing the most efficient energy recovery was selected for the deceleration tests (Table 2.12).

	e208	zoe#1	zoe#2	i3	leaf#1	model3	kze	kd
A	07/2020	-	07/2020	07/2020	-	-	07/2020	-
V [km/h]	90 - 30	-	90 - 30	90 - 40	-	-	90 - 40	-
E1	07/2020	-	07/2020	07/2020	07/2020	07/2020	07/2020	-
V [km/h]	90 - 40	-	90 - 40	90 - 40	80 - 40	90 - 40	90 - 40	-
E3	07/2020	-	07/2020	07/2020	07/2020	07/2020	07/2020	-
V [km/h]	90 - 40	-	90 - 40	90 - 40	90 - 40	90 - 40	90 - 40	-
M2	07/2020	-	07/2020	07/2020	07/2020	07/2020	07/2020	-
V [km/h]	90 - 30	-	90 - 40	90 - 40	90 - 40	90 - 40	90 - 40	-
M3	07/2020	-	07/2020	07/2020	-	07/2020	07/2020	-
V [km/h]	90 - 30	-	90 - 30	90 - 40	-	90 - 40	90 - 40	-
N	07/2020	-	07/2020	07/2020	07/2020	07/2020	07/2020	-
V [km/h]	90 - 30	-	90 - 30	90 - 40	90 - 50	90 - 40	90 - 40	-

Table 2.11: Synthesis of experiments performed within sub-action B2.1 for deceleration tests – Date and range of initial speeds for each 'vehicle / test section' configuration.

ID	acceleration mode	deceleration mode
e208	sport D	ECO B
zoe#1 and #2	normal	ECO
i3	N/A	ECO Pro+
leaf#1	normal	e-pedal
model3	sport	standard
kze	standard	ECO

Table 2.12: Drive modes selected for the acceleration and deceleration tests with the EVs.

2.2 CPB results

2.2.1 Results at constant speed

2.2.1.1 Noise analysis method

Maximum pass-by noise level In the case of constant speed driving conditions, the noise analysis method is based on the maximum overall A-weighted sound pressure level $L_{Amax,m}$. For each run of the vehicle on a given test section, it was identified as the maximum value of the time signature $L_{AF}(t)$. One-third octave band instantaneous sound pressure levels $L_{Amax,m}(f)$ were also identified at the instant when the maximum noise level $L_{Amax,m}$ occurred, for one-third octave frequency bands from 100 Hz to 5 kHz.

The immunity of sound recordings to background noise of the test site was considered with care. For each combination of EV and road surface, the background noise level L_{bn} was recorded at the roadside microphone. The difference between the measured maximum noise level at vehicle pass-by and the background noise level, ΔL, is defined by:

$$\Delta L = L_{Amax,m} - L_{bn} \tag{2.3}$$

Then, if $\Delta L < 6$ dB(A), the measurement was disregarded. If $\Delta L \geq 6$ dB(A), a correction was applied to the overall and the one-third octave frequency band measured noise levels. The corrected noise level expresses as follows:

$$L_{Amax} = L_{Amax,m} - \Delta L_{Amax} \tag{2.4}$$

with:

$$\Delta L_{Amax} = -10 \log_{10} \left(1 - 10^{\frac{-\Delta L}{10}}\right) \tag{2.5}$$

It should be noticed that for the overall noise levels, in practice, the signal to background noise difference ΔL was above 10 dB(A) for most of the configurations and the correction term was minor. In the frequency domain, the correction depended on the configuration and on the background noise level at the time of the test. The influence of the background noise level was essentially critical at low vehicle speed and in the low frequency range below 315 Hz, occasionally at the highest frequencies. Figure 2.13 gives the values of ΔL as a function of frequency and vehicle speed in the case of the Nissan LEAF rolling on test section E1. It is clear that the occurrence of invalid data (i.e. $\Delta L < 6$ dB(A)) is mainly limited to very low frequency and speeds.

Noise level versus vehicle speed regression The corrected CPB overall noise level L_{Amax} increases linearly with the logarithm of speed (Fig. 2.17), which is a common behaviour when rolling noise is the dominant noise source. It was analysed trough a logarithmic regression versus vehicle speed V:

$$L_{Amax}(V) = L_{Amax}(V_{ref}) + b_{L_{Amax}} \log_{10}(V/V_{ref}) \tag{2.6}$$

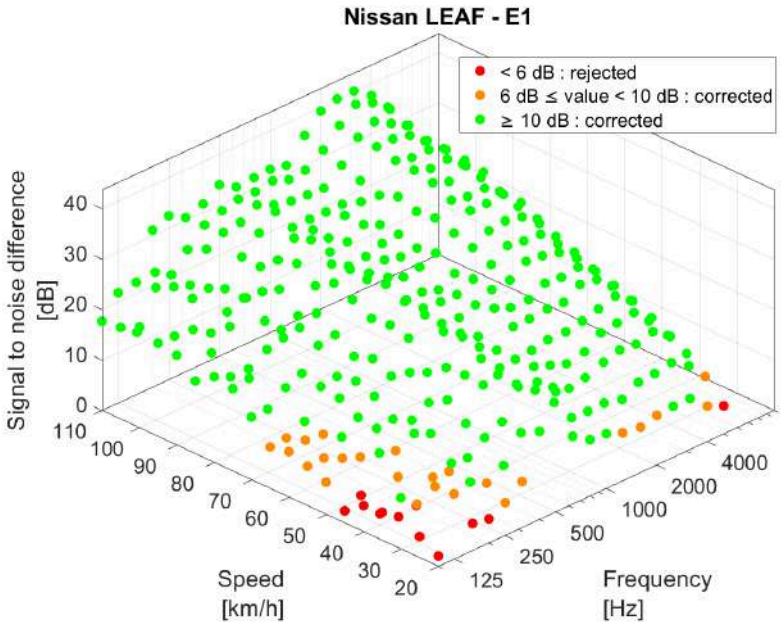

Figure 2.13: Signal to background noise difference ΔL as a function of speed and third octave frequency bands in the case of the Nissan LEAF rolling on E1 test track.

where V_{ref} is a reference speed, $L_{Amax}(V_{ref})$ is the overall regression noise level (in dB(A)) at the reference speed, and $b_{L_{Amax}}$ is the slope of the regression in dB(A) per decade of speed. The same speed dependency was assumed for one-third octave band noise levels (in dB(A)) at frequency f:

$$L_{Amax}(V, f) = L_{Amax}(V_{ref}, f) + b_{L_{Amax}}(f) \log_{10}(V/V_{ref}) \tag{2.7}$$

where $L_{Amax}(V_{ref}, f)$ is the spectral regression noise level (in dB(A)) at the reference speed, and $b_{L_{Amax}}(f)$ is the slope of the regression in dB(A) per decade of speed in the one-third octave band of central frequency f. Within the framework of the LIFE E-VIA project, dealing with noise reduction in urban areas, the reference speed is fixed to $V_{ref} = 50$ km/h.

2.2.1.2 Comparison of ICEV and EV in the case of the Renault Kangoos

The Renault Kangoo diesel and the Renault Kangoo ZE having the same set of tyres[4] and the same car body, only the propulsion technology is different between these two tested vehicles, all other things being equal. This configuration is proper for comparison of an EV with its equivalent ICEV. The main idea was to quantify noise abatement at low speed due to the quietness of the electric motor by comparison with the intern combustion engine, all else being equal.

Thus, the overall noise level of the Renault Kangoo diesel, driving at constant speed V and engine speed rpm, was assumed to be the energetic sum of a propulsion noise component $L_{Amax,p}$ and a rolling noise component $L_{Amax,r}$, which can be expressed as follows:

$$L_{Amax} = L_{Amax,p}(rpm) \oplus L_{Amax,r}(V) \tag{2.8}$$

The propulsion noise component is supposed to depend only on the engine speed rpm, whereas the rolling noise component is a function of the vehicle speed V, according to Equations (2.9) and (2.10).

$$L_{Amax,p}(rpm) = L_{Amax,p}(rpm) + b_{L_{Amax,p}} \log_{10}(rpm/rpm_{ref}) \tag{2.9}$$

$$L_{Amax,r}(V) = L_{Amax,r}(V_{ref}) + b_{L_{Amax,r}} \log_{10}(V/V_{ref}) \tag{2.10}$$

[4]Each tyre of the set was identified and was mounted in the same place on both vehicle versions.

Vehicle speed V and engine speed rpm are not uniquely linearly linked over the whole speed range but their relationship depends on the gear ratio engaged. This non-unicity defines two degrees of freedom and allows the separation of the two noise components. These were identified and separated by means of an optimisation method, minimising the mean square error between the measured pass-by noise levels and the model given by Equations (2.8) to (2.10) over the whole speed range tested (Pallas et al., 2014).

For each test section, Figure 2.14 gives the identified propulsion and rolling noise components for the Renault Kangoo diesel, and the recomposed total noise levels from the decomposition. A good agreement with the measured noise levels is observed. An atypical shape of propulsion noise versus speed relationship can be observed for test sections M3 and A, possibly due to absorption properties of the road surfaces. The cross-over speed is defined as the speed value at which the rolling noise component meets the propulsion noise component. It lies below 30 km/h for test sections E1, E3, A and M2 and is around 40 km/h for test sections N and M3. Thus, tyre/road noise exceeds the ICEV propulsion noise by 10 dB(A) from approx. 50 km/h for test sections E1, E3, A and M2 and from 70 km/h for test sections E1 and M3.

On Figure 2.14, the overall noise levels measured with the Renault Kangoo ZE are also plotted for comparison. It should be noticed that a whistling noise occurs on the Renault Kangoo ZE at speeds greater than 95 km/h (or 100 or 105 km/h depending on the test section), which is not related to tyre/road noise and makes the L_{Amax} value increase significantly[5]: since irrelevant here, the measures affected by this issue are removed from the figure. On test sections N, E1 and E3, the rolling noise component identified for the ICEV coincides with the CPB noise level of the EV above 40 km/h, while for test sections A and M2 they coincide over the whole speed range. Regarding test section M3, the relationship of noise with speed is atypical for the EV too, but the measured noise level is close to the ICEV rolling noise component, especially above 40 km/h. Below 40 km/h, for test sections N, E1, E3 and M3, the noise level can be either above or below the ICEV rolling noise level. The results support the conclusion that tyre/road noise is the dominating source of noise for the Renault Kangoo EV over the whole speed range tested. Similarly for the other tested EVs, tyre/road noise was also considered as the main source of noise over the whole speed range in constant speed driving conditions.

2.2.1.3 Comparison of Renault ZOE#1 and Renault ZOE#2

It is also interesting to compare two different test vehicles of the same model. Within sub-action B2.1, this was done with the Renault ZOEs. Test vehicles zoe#1 and zoe#2 are exactly the same EV model, as can be seen in Tables 2.3 and 2.4. The only main difference was the higher mileage for zoe#1 (18416 km) in comparison with zoe#2 (5840 km). Thus, the state of wear of the front tyres was higher for zoe#1 than for zoe#2. It should be added that both vehicles were tested at the same season (summer), but with one year interval, which may lead to different temperature conditions and slight changes in the state of the road surface during the tests (knowing that the roads are only lightly trafficked).

Figure 2.15 compares the overall maximum noise levels measured with both Renault ZOEs, the measurement points being linked for a better trend visibility. For the six test sections, the results of both vehicles are very close, in terms of shape and amplitude. Both vehicles display the same trend, but the zoe#1 is slightly less noisy on road surfaces E1, E3, M2 and M3, while the difference is not significant on N and A.

[5]When whistling occurs, a spectrum analysis points out a tone around 1270 Hz. The analysis with the microphone array locates its origin near the front of the vehicle. This noise source makes the L_{Amax} be detected as the vehicle is still approaching the microphone position, unlike the other vehicle pass-bys. It does not happen with the Kangoo diesel, which excludes any implication of tyre-road noise due to the same tyre set used on both vehicles.

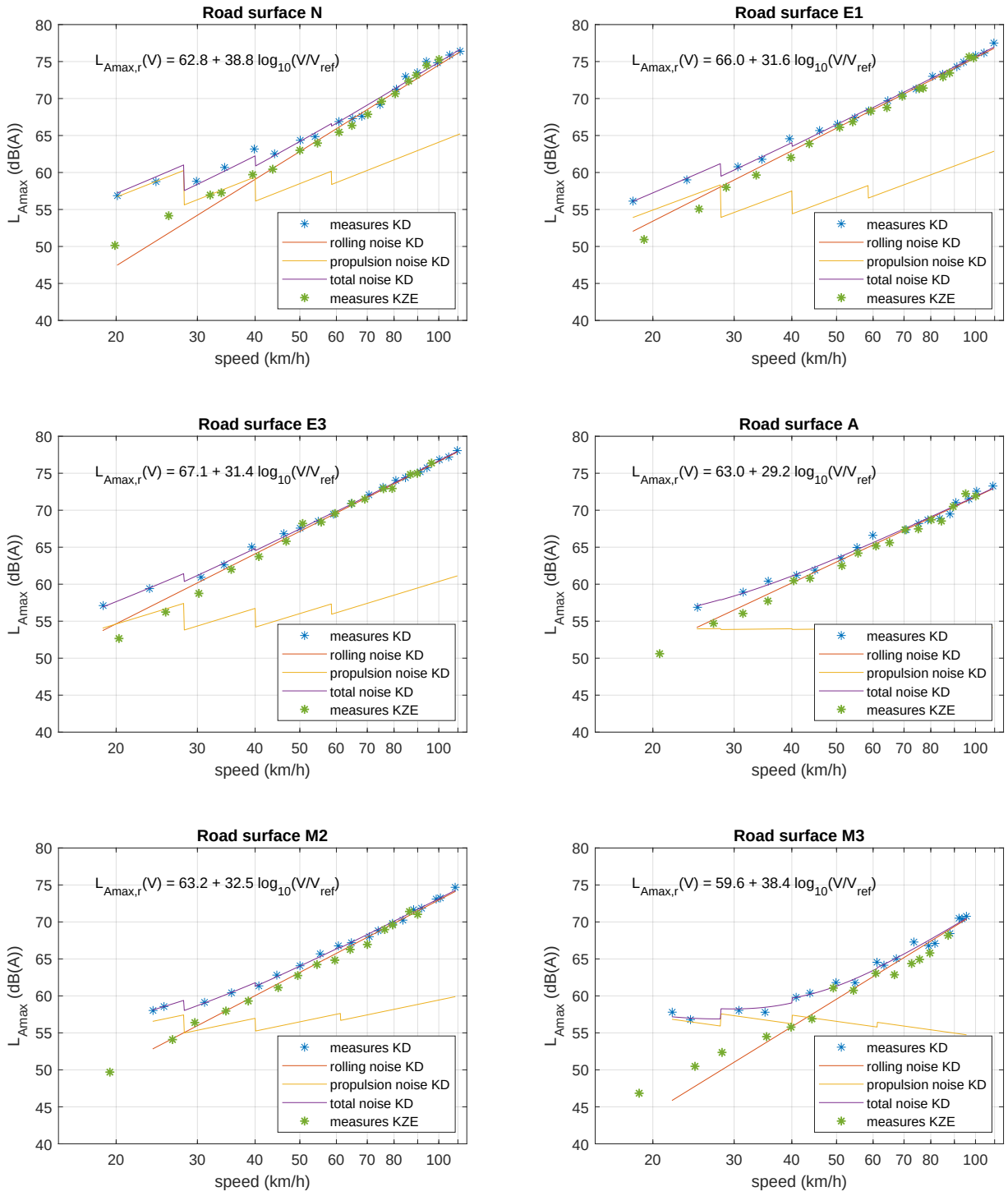

Figure 2.14: Decomposition of the measured maximum noise levels L_{Amax} into propulsion noise and rolling noise components for the Renault Kangoo Diesel (KD) at constant speed, V_{ref} = 50 km/h – Comparison with the overall maximum noise levels measured with the Kangoo ZE (KZE).

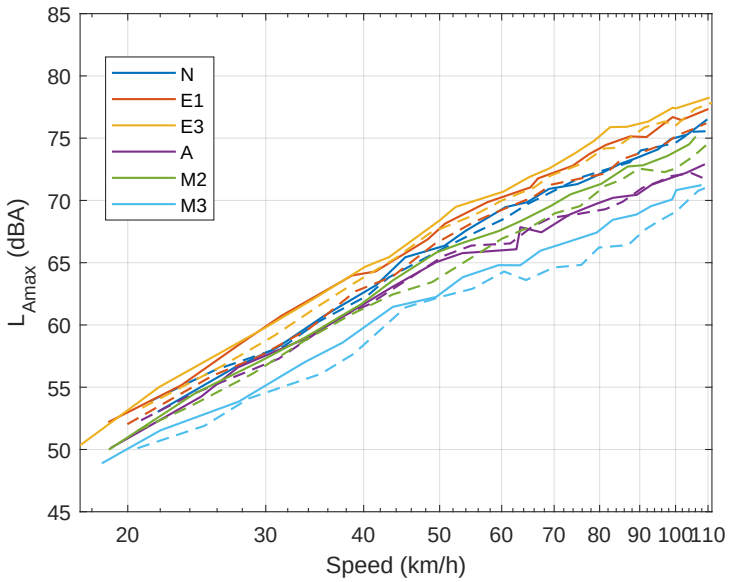

Figure 2.15: Comparison of the maximum noise level versus speed for the two examples of Renault ZOE at cpnstant speed (points connected by lines for readability: zoe#1 in dashed lines and zoe#2 in solid lines) on the six test sections. Corrected in temperature at $T_{air} = 20$ ℃.

A comparison of the spectra measured when L_{Amax} occurs is given in Figure 2.16 for pass-bys at a constant speed close to 50 km/h. No temperature correction is applied since no such procedure is definitely agreed in frequency. In a similar way for both examples of ZOE, the spectrum maximum is spread over the one-third octave bands 800 Hz and 1000 Hz for road surfaces E1, E3 and N, while it lies on 800 Hz for A, M2 and M3. All spectra also exhibit a smaller local maximum at 250 Hz.

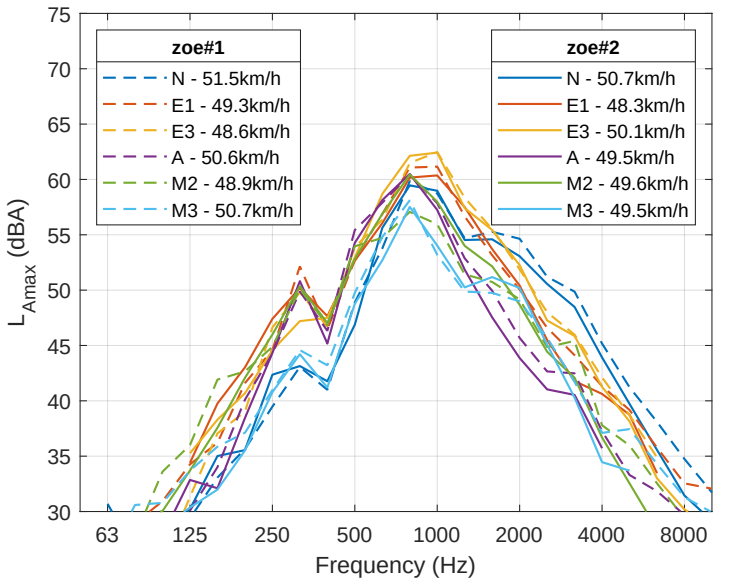

Figure 2.16: One-third octave spectra measured at the time of L_{Amax} for the two examples of Renault ZOE at a constant speed close to 50 km/h (zoe#1 in dashed lines and zoe#2 in solid lines) for the six test sections. Not temperature corrected.

Considering the results of this section, in the following only one Renault ZOE (zoe#2) will be considered in the analysis.

2.2.1.4 Regression coefficients for constant speed driving conditions

Noise data have been analysed by means of a logarithmic regression on the experimental data for each combination of EV and road surface. Figure 2.17 plots the regression line obtained from the overall noise level L_{Amax} and the vehicle speed V in the case of the Nissan LEAF rolling on the E1 test section. The values of the parameters $L_{Amax}(V_{ref})$ and $b_{L_{Amax}}$ are displayed on the graph. The standard deviation of the parameters can be estimated via the 95% confidence interval of the regression. The coefficient of determination of the regression r^2 is also indicated and is very close to 1 in most of the configurations.

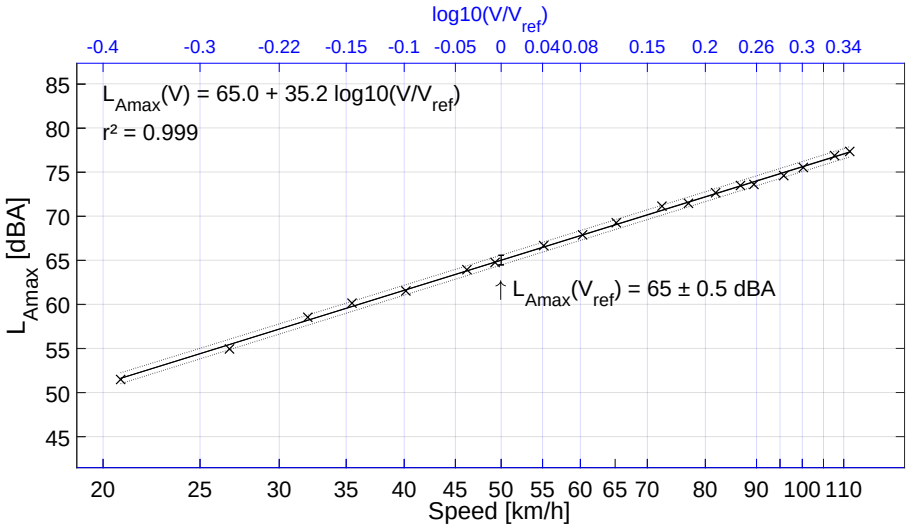

Figure 2.17: Example of logarithmic regression (solid line) of the overall maximum noise level L_{Amax} versus vehicle speed V in the case of the Nissan LEAF rolling on the E1 test section. Crosses are the experimental data. The reference speed is $V_{ref} = 50$ km/h (not corrected in temperature).

Table 2.13 gives the overall noise levels $L_{Amax}(50)$ and the regression slopes $b_{L_{Amax}}$ for the 36 combinations of EV and test section. The indicated uncertainties correspond to the standard deviation of the regression parameters. The average air temperature T_{air} during the test is also given, but the noise levels in the table are not corrected in temperature. From these data, one can estimate the CPB noise level at any vehicle speed between 20 and 110 km/h.

2.2.1.5 Ranking of EV overall noise levels at 50 km/h

In the following, the analysis focuses on the results for the overall noise levels at the reference urban speed of 50 km/h. For the sake of analysis, the overall noise levels at 50 km/h are presented in two different ways. Firstly, the classification of road surfaces is considered for each tested EV. Then, EV ranking per road surface is analysed. The noise levels are corrected in temperature according to Anfosso-Lédée and Pichaud (2007) for proper comparison of the different configurations. The reference air temperature is $T_{air} = 20$ °C.

Ranking of road surfaces per EV The classification of the six test sections is given in Figure 2.18 for each tested EV. For all EVs, the quietest road surfaces in increasing order are M3 and A and the loudest ones in increasing order are E1 and E3. In between, the ranking of road surfaces M2 and

Peugeot e-208			
Surface	T_{air} (°C)	$b_{L_{Amax}}$	$L_{Amax}(50)$
A	21.1	30.2 ± 1.1	61.6 ± 0.8
E1	27.6	34.6 ± 1.3	64.2 ± 1.0
E3	27.6	34.9 ± 1.0	65.0 ± 0.7
M2	23.3	29.6 ± 1.5	62.3 ± 1.1
M3	23.3	32.4 ± 1.6	58.7 ± 1.1
N	23.0	32.6 ± 1.5	61.6 ± 1.1

Renault ZOE#2			
Surface	T_{air} (°C)	$b_{L_{Amax}}$	$L_{Amax}(50)$
A	23.7	28.9 ± 1.8	63.6 ± 1.7
E1	28.7	33.2 ± 1.4	66.0 ± 1.3
E3	28.7	34.8 ± 1.4	66.6 ± 1.4
M2	23.6	32.1 ± 1.1	63.9 ± 1.0
M3	26.8	28.9 ± 1.2	61.5 ± 1.1
N	33.4	32.7 ± 1.6	64.2 ± 1.4

BMW i3			
Surface	T_{air} (°C)	$b_{L_{Amax}}$	$L_{Amax}(50)$
A	28.6	34.1 ± 1.6	61.4 ± 0.9
E1	26.4	34.7 ± 1.1	64.0 ± 1.1
E3	26.4	34.9 ± 1.0	65.0 ± 1.0
M2	31.4	33.9 ± 1.0	61.5 ± 1.0
M3	32.1	28.1 ± 1.8	59.3 ± 1.1
N	28.1	34.1 ± 1.4	62.0 ± 0.8

Nissan LEAF#1			
Surface	T_{air} (°C)	$b_{L_{Amax}}$	$L_{Amax}(50)$
A	28.1	31.5 ± 1.2	62.9 ± 1.0
E1	27.6	35.2 ± 0.6	65.0 ± 0.5
E3	27.6	36.4 ± 0.9	66.0 ± 0.8
M2	32.4	32.1 ± 0.9	62.7 ± 0.8
M3	32.1	28.6 ± 1.4	61.3 ± 1.3
N	28.1	37.0 ± 2.2	64.3 ± 2.0

Tesla Model 3			
Surface	T_{air} (°C)	$b_{L_{Amax}}$	$L_{Amax}(50)$
A	29.4	29.5 ± 1.6	63.1 ± 1.3
E1	26.6	32.8 ± 0.6	66.2 ± 0.6
E3	26.6	34.8 ± 0.9	67.0 ± 0.9
M2	26.6	30.3 ± 1.4	64.0 ± 1.3
M3	31.4	31.0 ± 1.7	60.1 ± 1.6
N	31.4	33.1 ± 1.0	63.0 ± 1.0

Renault Kangoo ZE			
Surface	T_{air} (°C)	$b_{L_{Amax}}$	$L_{Amax}(50)$
A	28.8	31.0 ± 1.1	62.6 ± 1.3
E1	21.4	33.9 ± 0.9	65.5 ± 0.8
E3	24.5	35.4 ± 1.1	66.8 ± 1.0
M2	24.8	32.4 ± 1.2	62.9 ± 0.9
M3	21.4	31.2 ± 2.4	59.3 ± 1.7
N	33.7	33.4 ± 1.5	63.1 ± 1.0

Table 2.13: CPB regression slopes $b_{L_{Amax}}$ (in dB(A)/dec) and overall noise levels $L_{Amax}(50)$ (in dB(A), not corrected in temperature) at 50 km/h for the 6 test sections and the 6 EV models tested.

N varies from one EV to another. It is observed that road surfaces with low texture levels (i.e. M3 and N) and/or absorption properties (A, M2 and M3) are among the quietest test sections. This is due to the reduction of tyre/road noise which is the dominant source for EVs during CPB tests at constant speed. The difference between the quietest and the loudest test sections (resp. M3 and E3) is quite influenced by the EV model and varies from 4.8 dB(A) for the Nissan LEAF to 7.9 dB(A) for the Renault Kangoo ZE. Considering the 36 road/vehicle configurations, a difference of 8.8 dB(A) was observed between the quietest and the loudest combinations (i.e. e208/M3 vs. model3/E3).

EV ranking per road surface Figure 2.19 gives the acoustical classification of the 6 tested EVs for each road surface. The Peugeot e-208 and the BMW i3 are the quietest vehicles, while in most cases the Renault ZOE is the loudest vehicle, or nearly. The ranking shows that there is no clear relationship between the EV segment and its overall noise level. The difference between the quietest and the loudest EV ranges from 2.0 dB(A) for test section E3 to 3.6 dB(A) for test section N. It is likely that tyre/road noise emission on M3 and N, with low MPD and texture levels, is more sensitive to the tyre tread pattern, which could explain the higher difference in noise levels on these test sections.

2.2.1.6 Spectral noise levels of EVs

Figure 2.20 gives the CPB regressed noise spectra at 50 km/h for each vehicle, considering the 6 test sections. Independently of the test section, a minor peak is observed at low frequency for some vehicles, i.e. at 250 Hz for the Peugeot e-208 and the Nissan LEAF, and at 315 Hz for the Renault

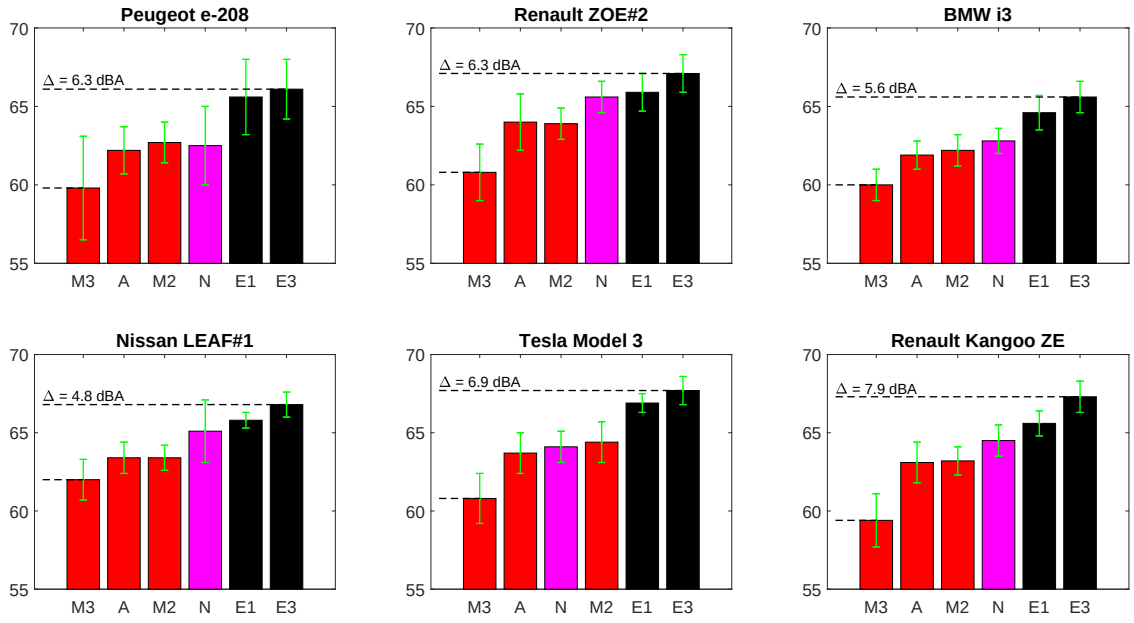

Figure 2.18: Overall noise levels ranking of the 6 road surfaces for each EV at $V_{ref} = 50$ km/h (in dB(A), corrected in temperature at $T_{air} = 20$ °C).

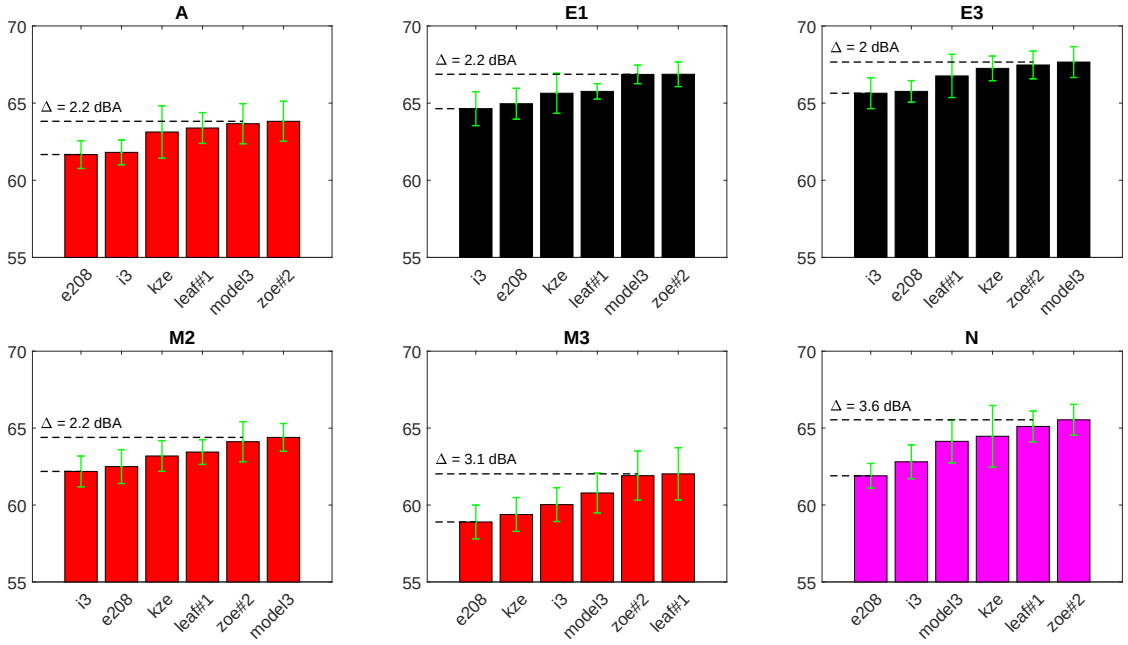

Figure 2.19: Overall noise levels ranking of the 6 EVs for each road surface at $V_{ref} = 50$ km/h (in dB(A), corrected in temperature at $T_{air} = 20$ °C).

ZOE. The dispersion among road surfaces depends on the EV model, with variations up to 15 dB(A) for the Tesla Model 3 above 630 Hz.

For the impervious road surfaces (i.e. E1, E3 and N), a maximum is observed at 1000 Hz for all EVs but the Tesla Model 3 on E3, for which the maximum is slightly shifted at 800 Hz. This peak at 1000 Hz is typical of the tyre/road noise emission on this kind of dense surfaces. It may have several origins according to Sandberg and Ejsmont (2002). For these road surfaces, it is clear that the noise levels at frequencies below 1000 Hz are smaller for the test section N due to its low texture levels over the large texture wavelength range (Fig. 2.6), reducing tyre vibration (Descornet and Sandberg, 1980). Between 1000 Hz and 2000 Hz, the difference between N and E1 or E3 depends on the configurations. At higher frequency above 2000 Hz, test section N is louder than E1 and E3. This can be explained by lower texture levels at small texture wavelengths for N (Fig. 2.6), increasing air-pumping mechanisms (Descornet and Sandberg, 1980).

In the case of the porous test sections (i.e. A, M2 and M3), the major peak is less pronounced than for dense surfaces and is shifted at a lower frequency between 630 Hz and 800 Hz, depending on the configuration. Noise level reduction at frequencies above this maximum are clearly due to the sound absorption properties of these road surfaces (Fig. 2.4). It can be noticed that for test sections A and M2, noise levels at frequencies below the peak position are in the same order of magnitude than noise levels of test sections E1 and E3. This is again due to high texture levels for A and M2 in the large texture wavelength range. On the contrary, test section M3 is quieter than A and M2 at low frequency due to lower texture levels at large texture wavelength, favourable to the reduction of tyre vibration. Combined with sound absorption properties, this makes test section M3 the quietest road surface for all tested EVs.

2.2.2 Results at variable speed

2.2.2.1 Noise analysis method

When analysing noise emission under acceleration (resp. deceleration), the noise indicator considered is the A-weighted sound pressure level L_{AF} when the vehicle centre is facing the microphone position. By definition, this quantity is less than (or equal to) the standard indicator L_{AFmax}. This focuses on wayside noise radiation, in the same relative position whatever the speed and the vehicle. It is coupled with the instantaneous speed of the vehicle at that position, calculated from the speeds at the entrance and output of the test section as provided by the cells and assuming the acceleration (resp. deceleration) to be constant within this time interval. The mean acceleration over the section is also inferred from the cell signals. The vehicle centre is defined as the middle of the wheelbase.

The immunity of sound recordings to background noise is processed as previously described in section 2.2.1.1. There is no correction related to temperature, but the air temperature values recorded during the tests are indicated for information. Overall noise levels are studied without regression with speed, since not appropriate for these conditions.

2.2.2.2 Acceleration

A description of the acceleration test procedure is given in section 2.1.3.3. The six EVs have different acceleration capacities, from rather moderate with the Renault Kangoo ZE to quite strong ones with the Tesla Model 3. In any case, the acceleration rate decreases as the vehicle speed increases. Each vehicle was tested on various road surfaces (see Table 2.10) and the results are displayed in Figure 2.21. For each vehicle, the plots of the acceleration rates on the different road surfaces highlight the high repeatability of the test conditions and attest to the possibility of comparing acoustically the road surfaces in most cases, all else being equal.

The extent of the differences between road surfaces is fairly constant with speed for the BMW i3 and the Nissan Leaf. For the other EVs there is a trend towards a smaller range of noise levels at

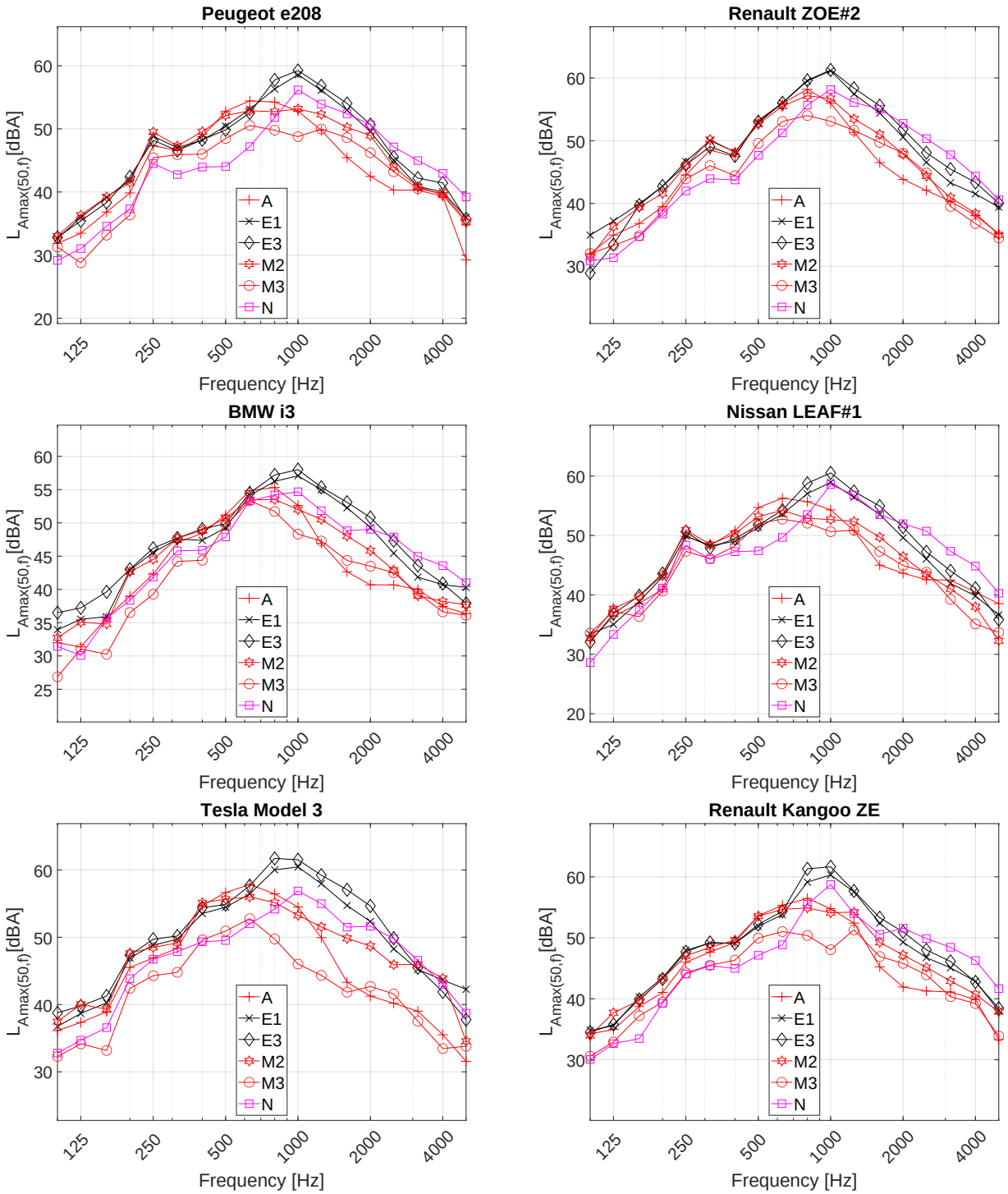

Figure 2.20: Regressed CPB noise spectra at the reference speed of 50 km/h.

lower speeds than at high speeds, reflecting a still stronger effect of wise road surface selection at high speeds. In a general way, the ranking of road surfaces remains quite unchanged with speed and is consistent with those found at constant speed (see Figure 2.18), except for road surface N which has a differentiating behaviour. While it was often ranked between the dense asphalt surfaces E1/E3 and the sound absorbing ones A/M2/M3 at constant speed, it may be closer to these dense surfaces or even become the noisiest one under acceleration of several vehicles, at least at low speeds consistent with urban conditions. A focus on this road surface will be given with the noise source analysis in section 2.3.

2.2.2.3 Deceleration

A description of the deceleration test procedure is given in section 2.1.3.3. Deceleration applies forces to tyre-road contact area for slowing down, at the same time as it loads the electric motor for energy recovery. For every EV, deceleration rates by releasing completely the accelerator pedal remain limited to about -2 m/s^2. When decelerating in this way, Renault Zoe, Renault Kangoo ZE, Nissan Leaf and Peugeot e208 do not show significant noise variation from constant speed driving. Similarly, the BMW i3 and the Tesla Model 3 on most surfaces provide a much limited increase of wayside sound radiation. But the Tesla Model 3 demonstrates a strong impact of deceleration on vehicle noise emission, yielding an increase of about 4 dB(A) over 30-40 km/h on road surface N and 3-4 dB(A) at speeds 30-45 km/h on M3 (Figure 2.22). A comparison of the noise levels from the decelerating Tesla Model 3 on several road surfaces shows the specificity of this vehicle on roads N and M3: it highlights the specific behaviour below 50 km/h, leading to a modified ranking of road surface N at the lowest speeds (Figure 2.23). This will be explored further with the noise source analysis in next section.

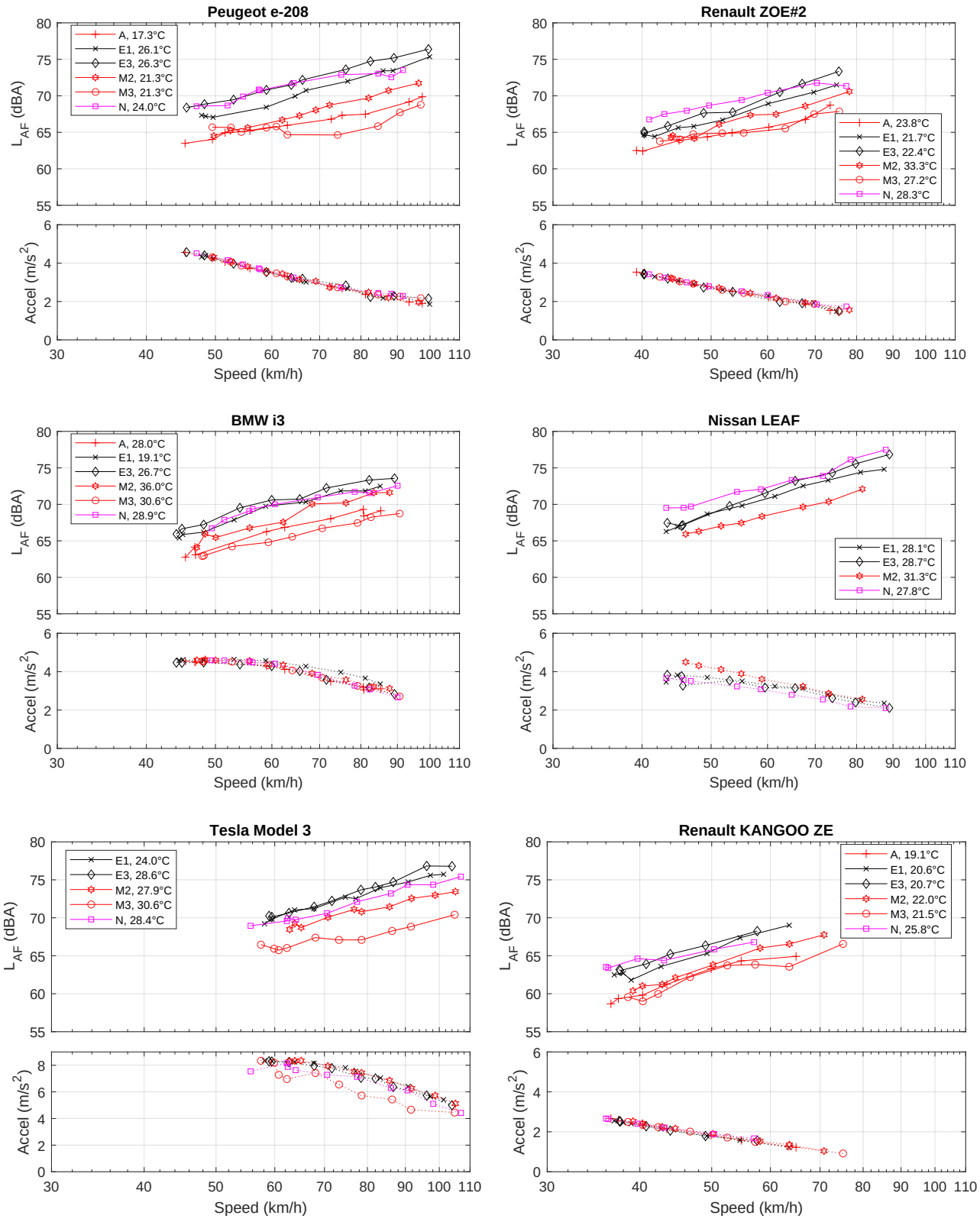

Figure 2.21: A-weighted sound pressure level under full acceleration, measured when the vehicle centre is right to the microphone at 7.5 m (not temperature corrected) – Corresponding acceleration rate of the vehicle.

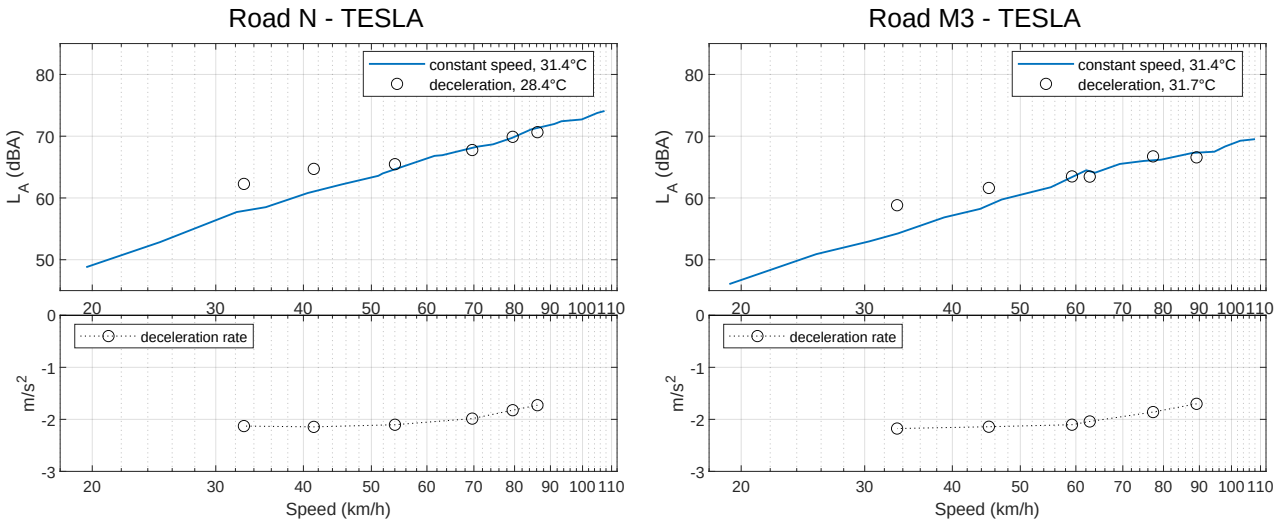

Figure 2.22: A-weighted sound pressure level of the Tesla Model 3 at constant speed (L_{Amax}) and under deceleration (L_A measured when the vehicle centre is right to the microphone at 7.5 m) as a function of speed right to microphone, on road N (left) and M3 (right) (not temperature corrected) – Corresponding deceleration rate of the vehicle (bottom).

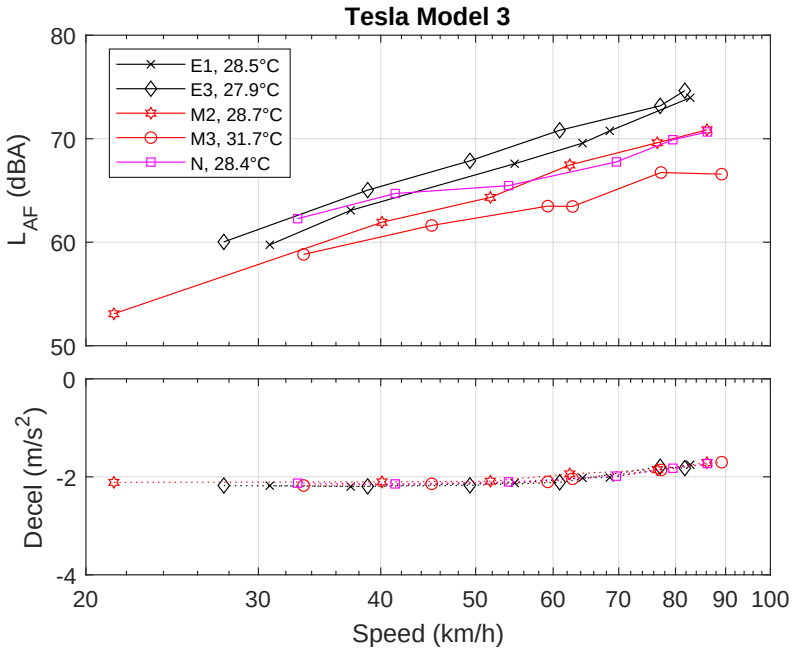

Figure 2.23: A-weighted sound pressure level of the Tesla Model 3 under deceleration (L_A measured when the vehicle centre is right to the microphone at 7.5 m) as a function of speed right to microphone, on all road surfaces tested (not temperature corrected) – Corresponding deceleration rates of the vehicle (bottom).

2.3 Investigation of the noise sources

As highlighted sooner, within sub-action B2.1 the noise source study has been carried out on road surface N only.

2.3.1 Approach with the microphone array

Since highly directional, the microphone array filters out a great part of the background noise, which therefore does not need to be considered. For each vehicle pass-by, a noise source map of the vehicle is produced in dB(A), in each one-third octave band from 100 Hz to 5000 Hz and in overall levels over the same frequency range. The noise levels received from any location on the vehicle are displayed according to a colour scale, the step of which has been fixed at 0.5 dB(A) for an easier reading of the values.

In most cases, the noise sources detected lie mainly in the neighbourhood of the wheels. They include the rolling noise but, if so, may also contain propulsion noise – when the motor is located close to the axle – with a propagation path from underneath the car body and possibly through the gap between the body and the wheel. For quantifying in a simple way the noise emission from each wheel zone, the maximum noise level received on the array from the area surrounding the wheel and the tyre/road contact has been taken. This allows the noise contribution from each wheel zone to be plotted as a function of speed and to be compared between vehicles and road surfaces.

2.3.2 Results

2.3.2.1 Main noise sources at constant speed

An illustration of the noise source maps of the six EVs is given at a constant speed of 50 km/h in Figure 2.24 in overall levels over the frequency range [100 - 5000 Hz]. The breakdown by one-third octave can be found in the appendix A. For an overview at all speeds, the contribution of each wheel zone as a function of speed is displayed in Figure 2.25, also in overall levels and over the same frequency range, and in appendix B according to frequency. In a general way, it turns out that the rear wheel zone is often the one contributing most to noise emission and that the ranking of wheel zones is not necessarily steered by the driving axle and the nearby presence of the motor:

- the Peugeot e208 (front-motor) has rather balanced contributions of both wheel zones at low speeds, but a slightly higher contribution from the rear wheel beyond 40 km/h. The larger levels on the front wheel zone below 30 km/h have no connection with rolling or motor noise but they are due to the AVAS, which is audible towards the vehicle side (see section 2.3.2.1). Frequency contribution gradually shifting from one third-octave to the next higher one over the whole speed range within the range [200-1600 Hz], similarly for both wheel zones, likely involves specificities of rolling noise (Figure B.1). A shifting high frequency component might come from the motor.
- the Renault ZOE#2 (front-motor) shows higher noise levels from the rear wheel zone by 1-2 dB(A) over most of the speed range, except above 85 km/h where wheel zone contributions are balanced. Several frequency components are frequency dependent, the most important one shifting from third-octave 315 Hz to 2000 Hz over the speed range, always more markedly on the rear wheel zone and resulting to the overall outcome (Figure B.2).
- the BMW i3 (rear-motor) offers a balanced wheel zone contribution on almost the entire speed range. Frequency component shift occurs from 315 Hz to 1600 Hz with increasing speed, generally with a slightly higher level on rear wheel zone (Figure B.3). Its coincidence with the range 800-1000 Hz explains the overall predominance of rear wheel between 70 and 90 km/h. A higher level of the rear wheel zone at low speeds and frequencies larger than 2500 Hz might be motor contribution, but with no noticeable effect on overall levels.

- the Nissan LEAF#1 (front-motor) has very unequal inputs, with a quite stronger contribution from the rear wheel zone by about 4 dB(A) at most speeds, except between 60-80 km/h with a lower difference. This is mostly due rear wheel zone dominating in the frequency range 1000-2500 Hz, the balance being quite effective at lower and higher frequencies (Figure B.4).
- the Tesla Model 3 (dual-motor) shows an increasingly higher contribution of the rear wheel zone with increasing speed. The motor management is not known, but at constant speed where the power demand remains low, one of the motors may be preferred due to own performance. The shift of a strong component is clearly visible in frequencies, more markedly on the rear wheel zone, but its presence at frequencies 200-800 Hz reduces its overall impact (Figure B.5). Both wheel zone contributions are comparable beyond third-octave 1000 Hz.
- the Renault Kangoo ZE (front-motor) has a balanced contribution from both wheel zones at all speeds. This also occurs in most frequency bands. There is only a trend for a higher contribution of the front wheel zone relative to the rear one in third-octave band 630 Hz, with no actual effect on the overall levels.

When comparing the wheel zones of all vehicles, the rear wheel of the leaf#1 and the zoe#2 differentiate by a significantly higher level at most speeds, at least over urban speed range (Figure 2.26). Then comes the zoe#2 front wheel, confirming this vehicle as the least quiet one among the vehicles tested, consistent with CPB results in Figure 2.19. Other wheel zones and vehicles are fairly clustered, with moderate spread at urban speed.

Comparison of the noise sources of Renault Kangoo ZE and Renault Kangoo D

The electric and conventional versions of the Renault Kangoo may be interestingly compared. Let us recall that both vehicles are identical in terms of their bodywork and set of tyres, the only difference being the drive technology. An illustration of their noise source maps at 50 km/h is presented in Figure 2.27. At this speed, the Kangoo D drives in 4th gear and 1625 rpm. The engine of the Kangoo D produces a leading contribution of the front wheel zone, which extends more broadly on either side of the pure wheel area. This is clearly visible on one-third octave maps, with noise radiation from underneath the vehicle body and wheel shielding in the central part (Figure A.7, for instance at 500 Hz or 1250-1600 Hz). By comparing with Kangoo ZE in Figure A.6, an increased contribution at high frequencies by a source located before the front wheel is clear. The contribution of the exhaust outlet is also noticeable, although not fully revealed due to the scan angle range to the side. Quantified contribution of each wheel zone highlights an increase by the diesel engine exceeding 5 dB(A) at 20 km/h, reducing at higher speeds because of the share of rolling noise, still noticeable up to 70 km/h in overall levels (Figure 2.28), but variably with frequency (Figure B.7).

Atypical noise sources

Some noteworthy noise sources could be noticed in specific conditions. Although not directly linked with rolling noise at the focus of this study, they deserve mentioning.

The AVAS system, which could not be switched off on the Peugeot e208, was working at low speed below 30 km/h. In these conditions it gives rise to increased contribution from the vehicle front part (Figure 2.29). Sideways, this noise comes from the area around the front wheel and the bottom of the vehicle, at specific frequencies according to the relevant regulation (Figure C.1). The scan angle range here reflects very little the forward radiation inherent in this system.

Finally, an unexpected whistling sound was produced by the Kangoo ZE at high speeds, most often prevailing beyond 95 km/h. This high-pitched acoustic outlier was detected as a narrowband tone around 1270 Hz regardless of the speed, and suspected to be radiated from the front grille towards vehicle front (Figure 2.30). When occurring at the highest speeds, it could outclass the other

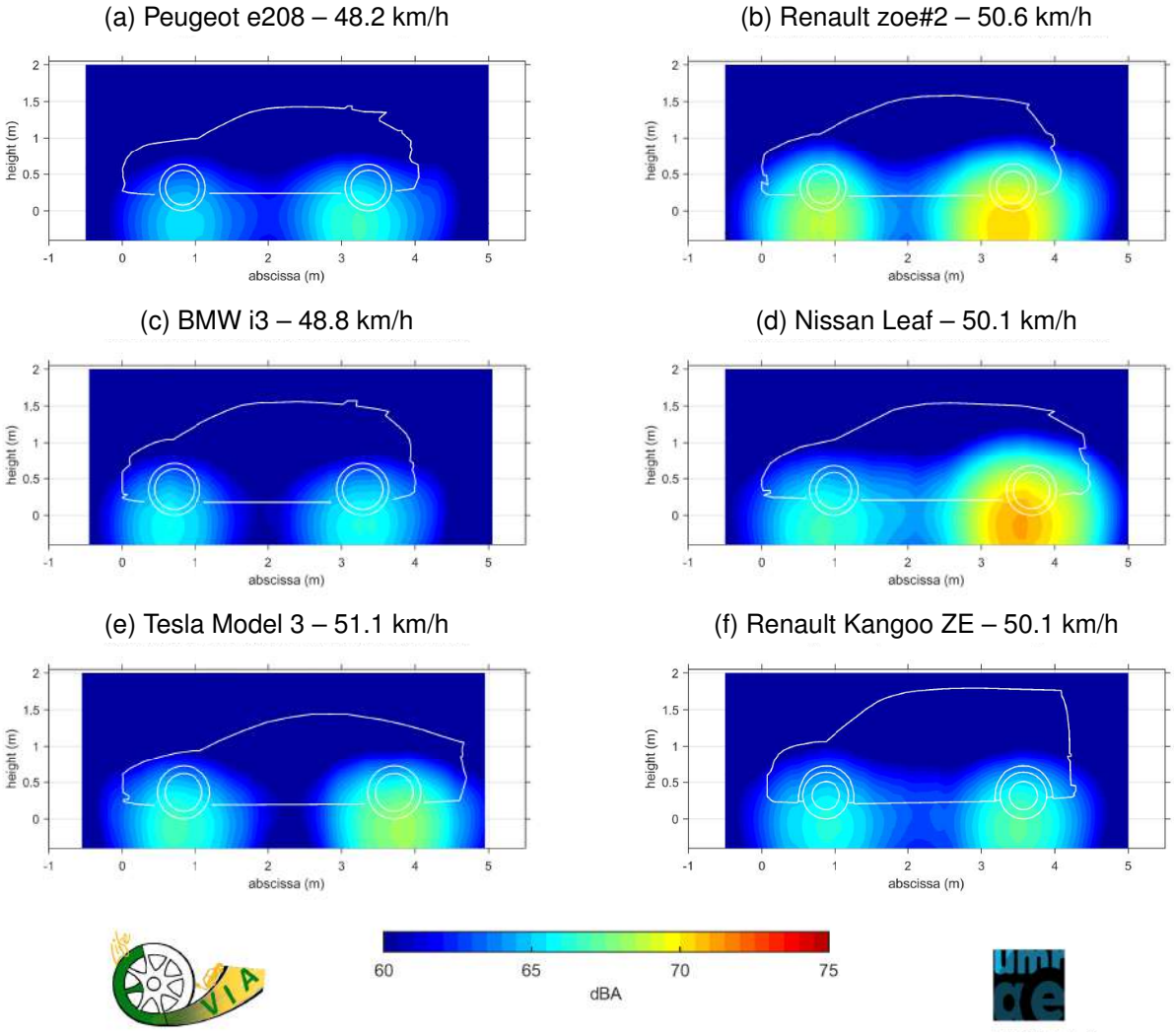

Figure 2.24: Noise source maps of the EVs at a constant speed close to 50 km/h on road surface N – A-weighted overall noise levels at the reference distance of 2.7 m – Colour scale in 0.5 dB(A) steps from 60 to 75 dB(A).

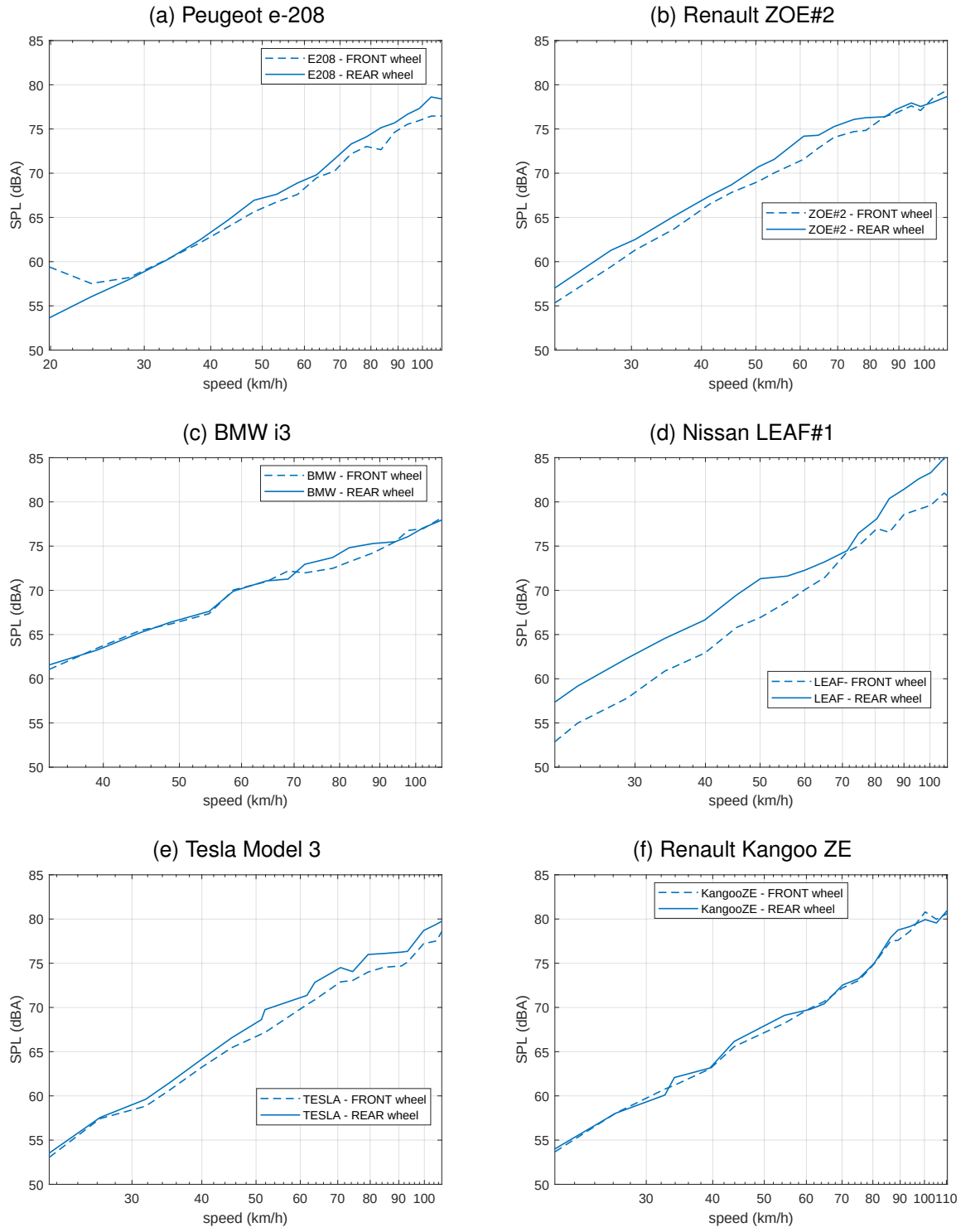

Figure 2.25: Contribution of the front wheel zone (resp. rear wheel zone) of the EVs tested as a function of speed on road surface N – A-weighted noise levels in the range [100 - 5000 Hz] at the reference distance 2.7 m.

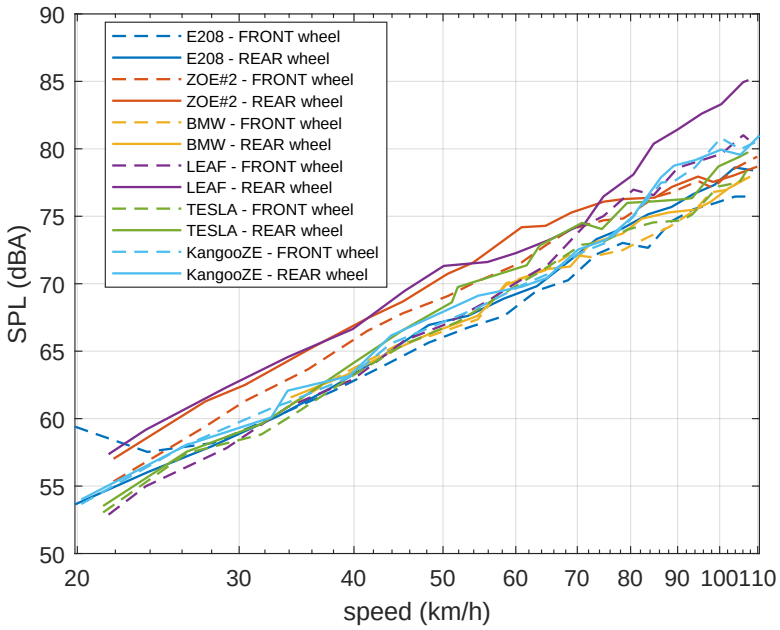

Figure 2.26: Contribution of the front wheel zone (resp. rear wheel zone) of the EVs as a function of speed on road surface N – A-weighted noise levels in the range [100 - 5000 Hz] at the reference distance of 2.7 m.

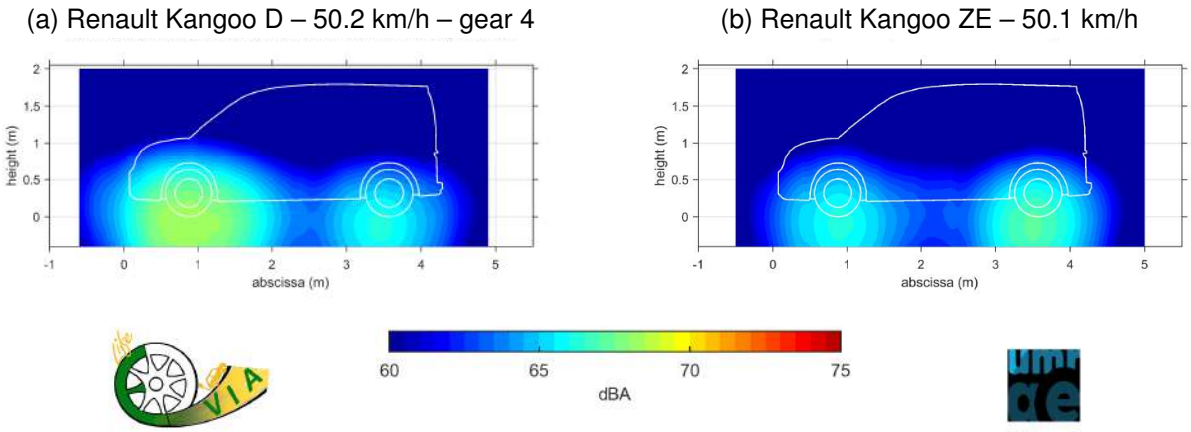

Figure 2.27: Noise source maps of the Kangoo D (left) and Kangoo ZE (right) at a constant speed close to 50 km/h – A-weighted overall noise levels at the reference distance of 2.7 m – Colour scale in 0.5 dB(A) steps from 60 to 75 dB(A).

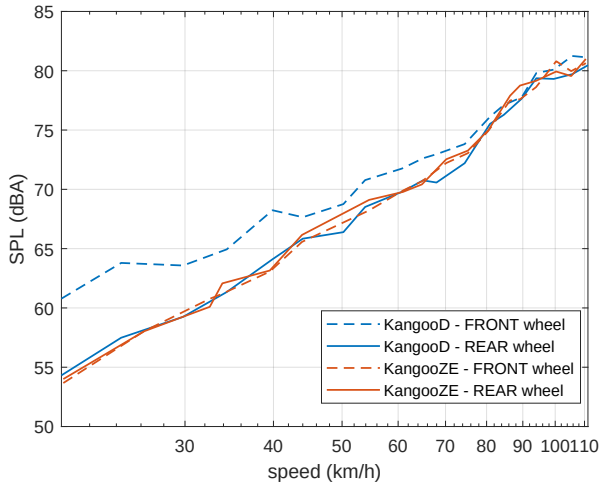

Figure 2.28: Contribution of the front wheel zone (resp. rear wheel zone) of the Kangoo ZE and Kangoo D as a function of speed on road surface N – A-weighted noise levels in the range [100 - 5000 Hz] at the reference distance of 2.7 m.

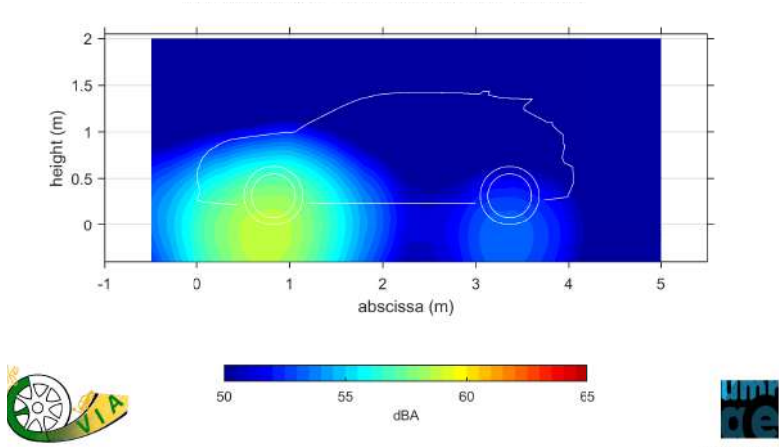

Figure 2.29: Noise source map of the Peugeot e-208 with AVAS at 19.9 km/h – A-weighted overall noise levels at the reference distance of 2.7 m – Colour scale in 0.5 dB(A) steps from 50 to 65 dB(A).

noise sources and result in the detection of L_{Amax} shifted to vehicle approach instead of a more usual sideways position, with a direct impact on spectrum content. The pass-bys concerned have been disregarded as far as possible.

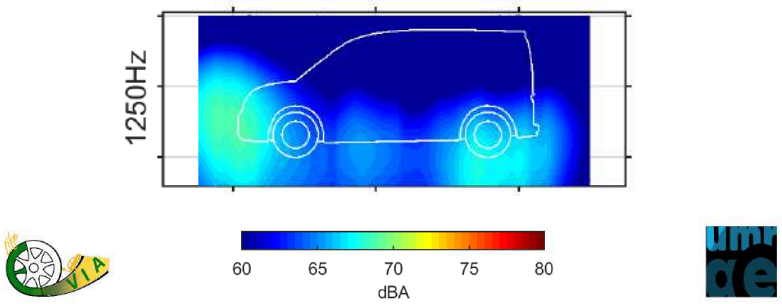

Figure 2.30: Noise source map of the Kangoo ZE whistling at 94 km/h in third-octave 1250 Hz – A-weighted noise levels at the reference distance of 2.7 m – Colour scale in 0.5 dB(A) steps from 60 to 80 dB(A).

2.3.2.2 Main noise sources at variable speed (acceleration, deceleration)

It is to be expected that noise source ranking changes at driving modes with variable speed, due to modified contributions of motor noise and of tyre/road noise, the latter resulting from increased forces in the contact area.

Noise source behaviour under full acceleration

Because of different motor performance, the acceleration rates vary from one vehicle to another, the Tesla Model 3 having the highest acceleration ability and the Kangoo ZE the lowest one among the set of vehicles tested. In addition, the higher the instantaneous speed, the lower the acceleration for any vehicle.

The main observation under vehicle acceleration relates to the significant increase of the contribution from the driving wheel areas. This is clearly highlighted on the overall noise maps illustrating accelerated pass-bys for which the vehicle was around 50 km/h when facing the microphone array[6] (Figures 2.31 and 2.32, to be compared with Figure 2.24). On top of each figure, the instantaneous speed when the front (resp. rear) wheel faces the array centre is given. The 6 vehicles have been split into two figure groups for an easier visualisation with appropriate colour scale ranges. The widening of the source area towards the front and rear of the drive wheel is most likely caused by motor noise, which cannot be factually separated here from the neighbouring rolling noise across the entire frequency range.

This is completed by Figure 2.33 for the Nissan Leaf and those in appendix D for the other EVs, superposing the contributions of each wheel zone measured at constant speed and under full acceleration as a function of instantaneous speed right to array centre. In addition, the figures show the acceleration rates recorded at each pass-by.

Relatively to constant speed conditions, the accelerating vehicles with front-motor and front-wheel-drive show a significant increase of the noise radiation from the front wheel zone, which becomes on any such EV the dominating noise source. The growth of noise from this area generally exceeds 5 dB(A) around 50 km/h and reduces with decreasing acceleration rate at higher speeds to about 4 dB(A) around 70-80 km/h (respectively around 60 km/h for the Renault Kangoo ZE having

[6]The strong acceleration ability of the Tesla Model 3 leads to speeds already exceeding 60 km/h when it gets the array, even with a standing start at the entrance of the test section.

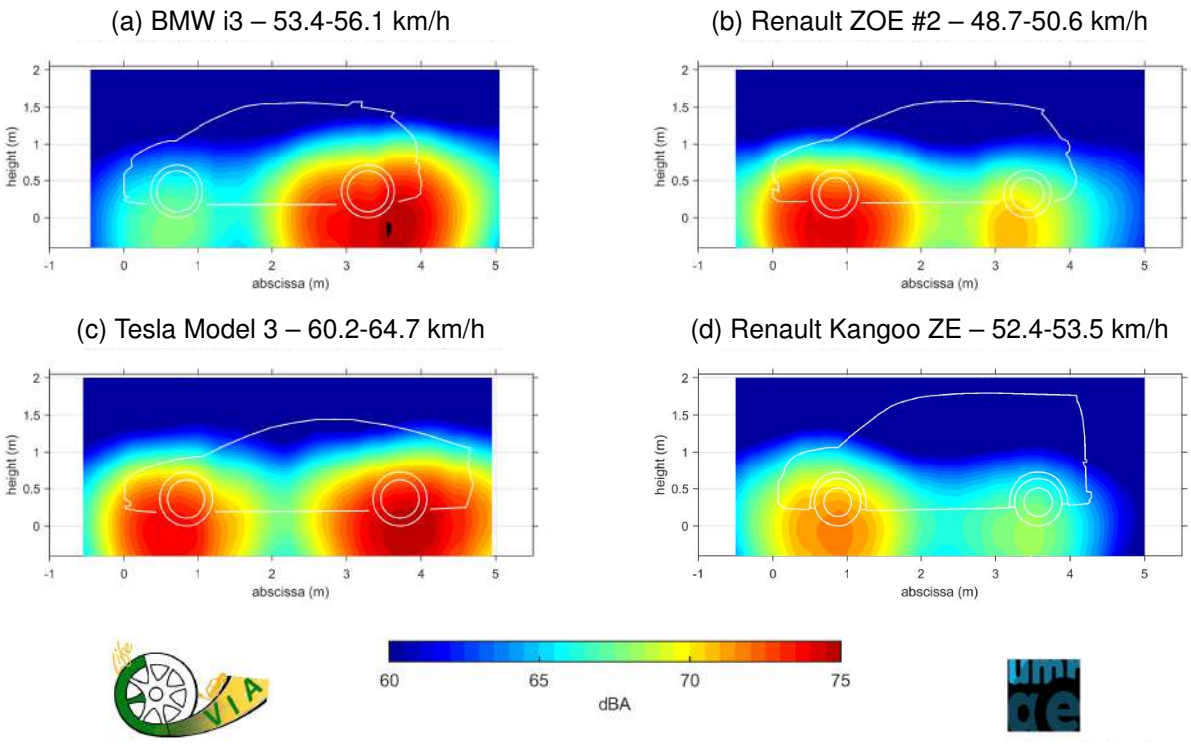

Figure 2.31: Noise source maps of 4 EVs under full acceleration around 50 km/h on road surface N – A-weighted overall noise levels at the reference distance of 2.7 m – Colour scale in 0.5 dB(A) steps from 60 to 75 dB(A).

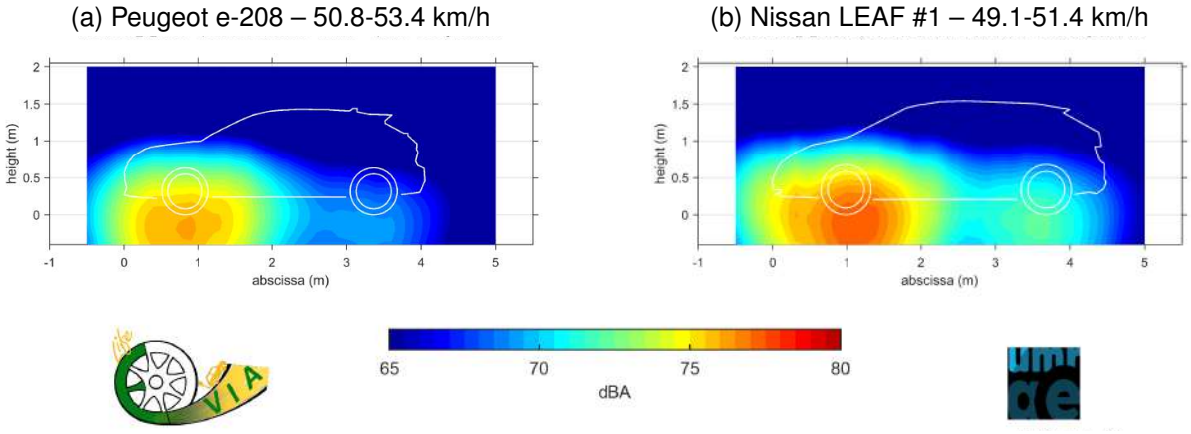

Figure 2.32: Noise source maps of 2 other EVs under full acceleration around 50 km/h on road surface N – A-weighted overall noise levels at the reference distance of 2.7 m – Colour scale in 0.5 dB(A) steps from 65 to 80 dB(A).

a lower acceleration ability). This comes from medium frequencies 500-1600 Hz with a suspected enhancement from tyre components, but also quite uniformly in the high frequency bands. By contrast, the contribution from the rear wheel zone is unchanged for the Renault Kangoo ZE, almost unchanged for the Renault ZOE#2, but with a slight increase of 1.5-2 dB(A) still to be explained for the Nissan LEAF and the Peugeot e-208. The same behaviour is observed with the rear-wheel drive BMW i3 by just reversing the roles of front and rear wheel zones. Finally, the dual-motor Tesla Model 3 with four-wheel drive spreads the effect of acceleration on noise emission between the two axles, in a reasonable degree in relation to the strong acceleration rates. It displays a moderate increase of 2-3 dB(A) for the front wheel zone, but 4-5 dB(A) for the rear wheel zone up to 90 km/h decreasing thereafter: front and rear contributions are balanced up to 90 km/h, the rear one dominating beyond.

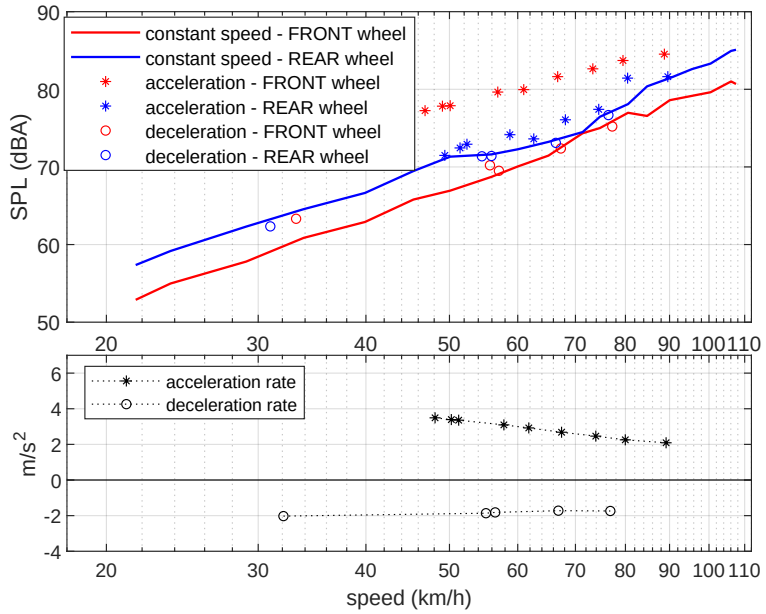

Figure 2.33: Front and rear wheel noise sources of the Nissan Leaf in all driving modes – Top: A-weighted overall noise levels at the reference distance of 2.7 m – Bottom: acceleration and deceleration rates.

Noise source behaviour under deceleration

In the deceleration tests without use of the brake, the motor is used as a generator for energy recovery from the loss of kinetic energy. Depending on vehicle, deceleration rates range from moderate (-0.6 m/s^2 for zoe#2) down to higher (-2.1 m/s^2 with model3). For every car, deceleration remains relatively constant over the speed range, with only a very slight deviation towards high speeds.

When compared to constant speed conditions, deceleration has no acoustical effect on overall sound emission from non-drive wheel zones of any vehicle (Figure 2.33 and appendix D). Its effect on drive wheel noise emission remains low, not greater than 1-2 dB(A), and only at speeds below 40-50 km/h for kze, leaf#1, zoe#2 and e208. The EVs that clearly stand out in this driving condition are:

- the BMW i3, showing an increase of noise emission from the drive-wheel zone over the whole speed range tested and estimated to about 5 dB(A) at low speed and lowering to 1.5 dB(A) over 20-80 km/h,

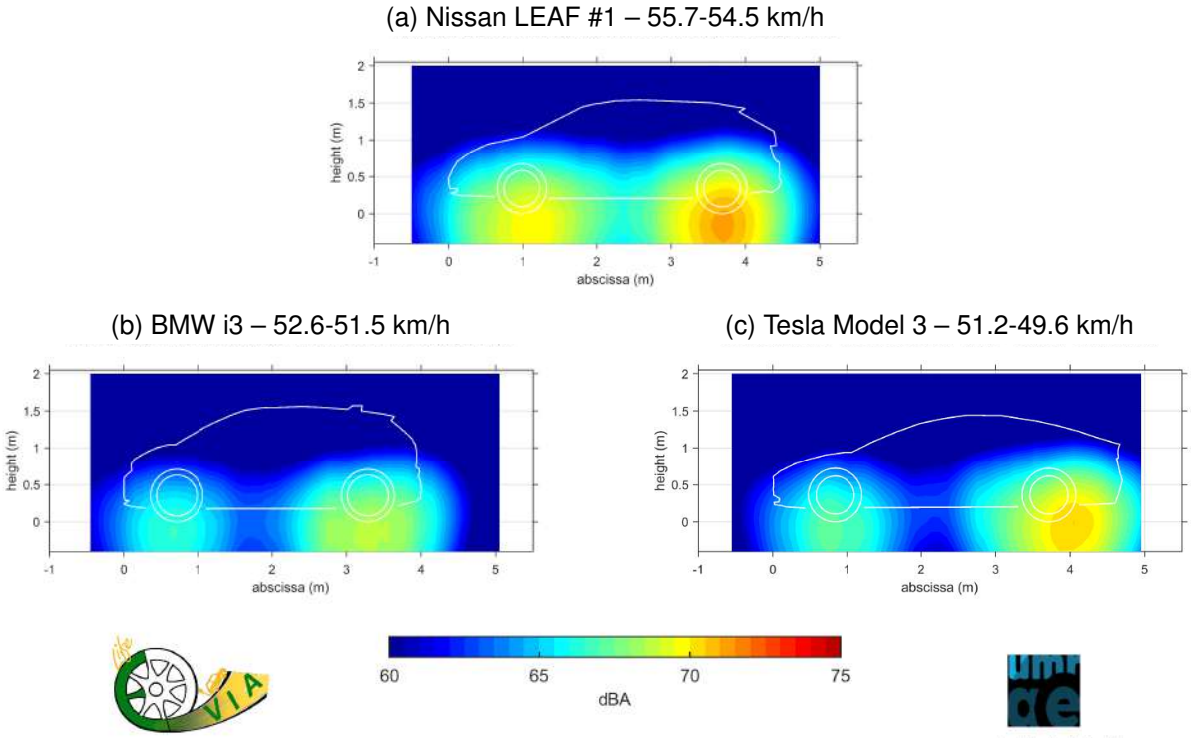

Figure 2.34: Noise source maps of the Nissan Leaf (top), the BMW i3 (bottom left) and the Tesla Model 3 bottom (right) under deceleration around 50 km/h on road surface N – A-weighted overall noise levels at the reference distance of 2.7 m – Colour scale in 0.5 dB(A) steps from 60 to 75 dB(A).

- and the Tesla Model 3 below 50 km/h – already highlighted on CPB results with the 7.5 m microphone – for which noise increase mainly comes from the rear wheel zone and is assessed to 5.5-2.5 dB(A) according to speed.

The two latter situations and also the Nissan LEAF are illustrated by noise source maps of pass-bys under deceleration with an instantaneous speed around 50 km/h when facing the array (Figure 2.34), to be compared with constant speed conditions in Figure 2.24(d) for the Nissan Leaf, Figure 2.24(c) for the BMW i3 and Figure 2.24(e) for the Tesla Model 3. The corresponding distribution in one-third octave bands is given in appendix E, highlighting distinct frequency changes on the vehicles.

2.4 Synthesis

Six EVs from different vehicle segments have been tested on six distinct road surfaces available on UNI EIFFEL reference test track, over a wide range of speeds and driving conditions, including constant speed, acceleration and deceleration. Half of these road surfaces are dense, the others are absorbing. The vehicles were fitted with their commercial tyre sets, representative of their own market.

At constant speed, investigations based on the maximum A-weighted noise level at vehicle pass-by made it possible to assess the impact of the choice of road surface on the noise emission of these vehicles. A comparison between an ICE and an electric version of the same vehicle (Renault Kangoo) confirmed the predominance of rolling noise from the EV noise emission over the whole speed range. Investigation of the noise sources showed that noise radiation from some EVs may be quite balanced between front/rear wheel zones, but the rear wheel zone is often the source area contributing most to noise received at roadside, even if not being a driving axle and without nearby electric motor. This

is particularly pronounced with Renault ZOE and mostly Nissan LEAF. For all EVs tested on the road surfaces, the overall noise emission level increases quite linearly with log(speed), but this may notably differ in frequency bands where tyre characteristics are outlined by road surface properties. A focus on the typical urban speed 50 km/h provided a road surface ranking. The difference between the quietest and the loudest test sections is influenced by the EV model and varies from 4.8 dB(A) to 7.9 dB(A) according to EV. This analysis emphasises and quantifies the challenge of the road surface selection for reducing noise emission from EVs. By contrast, the difference between the quietest and the loudest EV on any road surface ranges from 2.0 dB(A) to 3.6 dB(A). For all EVs, the quietest road surfaces in increasing order are M3 (VTAC 0/4) and A (PA 0/6), and the loudest ones in increasing order are E1 (DAC 0/10) and E3 (SMA 0/10). Road surfaces with low texture levels and/or absorption properties are among the quietest test sections. Considering the 36 road/vehicle configurations, a difference of 8.8 dB(A) was observed between the quietest and the loudest combinations. The use of absorbent vs. impervious road surfaces has also an additional effect on the frequency distribution of noise, shifted towards lower frequencies in case of porous ones. The combination of sound absorption properties and low texture levels makes test section M3 the quietest surface tested.

Since electric vehicles can offer high acceleration abilities, with a strong influence on rolling noise emission due to increased torque at the tyre/road contact area, full acceleration tests have been carried out. They have shown the large noise increase – often exceeding 5 dB(A) – from the driving wheel area, including both rolling noise and motor noise contributions, and making the front wheel zone dominate on front motor vehicles or sharing it on both axles if all-wheel driven. In a general way, the ranking of road surfaces remains quite unchanged with speed under acceleration and is consistent with those found at constant speed, except for road surface N (ISO surface, DAC 0/8) which has a differentiating behaviour at urban speeds and can even become the loudest. This underlines the importance of taking acceleration situations into account in the vehicle noise emission assessment, also in urban conditions.

Deceleration tests, without the use of braking pedal, have been performed to evaluate the possible impact of the introduction of energy recovery on noise emission and increased torque in this driving condition. Most EVs tested do not show a noise variation from constant speed driving – or with a limited effect – on wayside sound radiation when decelerating on the various road surfaces. However, the Tesla Model 3 demonstrated a strong impact of deceleration, yielding a noise increase of about 3-4 dB(A) over 30-45 km/h on road surfaces N or M3, leading to a modified ranking of road surface N at the lowest speeds.

3 Sub-action B2.2 – Construction of a B1-based test track prototype

Within sub-action B2.2, a 57m-long by 8m-large prototype has been constructed in September 2020 on UNI EIFFEL reference test track in Nantes (France). Based on the main outputs of action B1, the specifications of two very thin asphalt concrete (VTAC) 0/6 mixes were given by UNIRC to UNI EIFFEL. Both mixes are based on the same grading curve, while one differs by comprising 1.9% of crumb rubber per mix weight. Then, a call for tender was launched by UNI EIFFEL in June 2020 in order to subcontract the building of the prototype to a local road company. Finally, the two VTAC 0/6 test sections have been implemented by the Colas company. The aims of building a prototype in Nantes were the following :

1. to assess the road surface properties and the acoustical efficiency of the proposed low-noise asphalt concretes for a set of EVs prior full-scale implementation in Florence (sub-action B2.3);
2. to allow the characterisation of different EV tyre models from CRD within the process of optimising tyre/road interaction, in complement to holistic laboratory testing of tyres by CRD within action B7 (sub-action B2.4);
3. to provide feedback to action B1 and recommendations for action B3 for full-scale demonstrator construction in the pilot area in Florence.

In the following, the report first describes the preparatory actions within sub-action B2.2. Then, the different steps of the prototype construction are described. The last section deals with control of mix content and volumetrics after construction of the two VTAC 0/6 test sections.

3.1 Preparatory actions

3.1.1 Preliminary mix design within B1 action

Within B1 action, two types of mixtures were designed and partly validated through experiments in laboratory (Praticò, March 2021). Both are very thin asphalt concrete mixture of maximum aggregate size 6 mm, but one is comprising a percentage of crumb rubber in the formulation. It is expected that this addition of crumb rubber in the mix will lead to further reduction of tyre/road noise. The properties of both mixes in terms of bitumen, aggregates and bituminous mixture are reminded below. These were sent by UNIRC to UNI EIFFEL in March 2020 in order to fix the specifications in the call of tender for the prototype construction. For further details the reader is invited to refer to B1 action deliverable (Praticò, March 2021).

3.1.1.1 Bitumen and aggregates

The specifications regarding bitumen and aggregates were the same for both mixes of VTAC 0/6. Concerning bitumen, the foreseen asphalt binder from B1 action was a bitumen type 50/70. The specifications regarding the bitumen quality are given in Table 3.1. For each parameter, the reference standard for laboratory test, the unit and the value as prescribed from B1 action are given.

Regarding aggregate properties, one must distinguish coarse aggregates (retained by the 5 mm round sieve), fine aggregates (passing to the 5 mm round sieve) and filler (lower than 0.075mm). The requirements for coarse aggregates of the mix are given in Table 3.2. For each parameter, the reference standard for laboratory test, the unit and the value as prescribed from B1 action are given.

The requirements for fine aggregates of the mix are given in Table 3.3. For each parameter, the reference standard for laboratory test, the unit and the value as prescribed from B1 action are given.

Parameter	Standard	Unit	Value
Penetration at 25°C	EN1426, CNR24/71	dmm	50-70
Softening point	EN1427, CNR35/73	°C	$\geq$ 65
Breaking point (Fraass)	EN 12593, CNR43/74	°C	$\leq$ -15
Dynamic viscosity at 160°C, γ=10 s^{-1}	EN 13072	Pa.s	$\geq$ 0.4
Elastic recovery at 25°C	EN 13398	%	$\geq$ 75
Storage stability 3 days at 180°C (softening point variation)	EN 13399	°C	$\leq$ 0.5
After Rolling Thin Film Oven Test (RTFOT)	EN12607-1		
Volatility	CNR54/77	%	$\leq$ 0.8
Residual Penetration at 25°C	EN1426, CNR24/71	%	$\geq$ 60
Increase in softening	EN1427, CNR35/73	°C	$\leq$ 5

Table 3.1: Bitumen properties of VTAC 0/6 mix foreseen from action B1.

Parameter	Standard	Unit	Value
Los Angeles	CNR 34/73, UNI EN 1097-2	%	$\leq$ 20
Micro Deval	CNR 109/85, UNI EN 1097-1	%	$\leq$ 15
Crushed and broken surfaces	UNI EN 933-5	%	100
Maximum size of aggregates	CNR 23/71, UNI EN 933-1	mm	20
Freezing and thawing cycles	CNR 80/80, UNI EN 1367-1	%	$\leq$ 30
Boiling water stripping test	CNR 138/92, UNI EN 12697-11	%	0
Passing at 0.075 mm	CNR 75/80, UNI EN 933-1	%	$\leq$1
Shape coefficient	CNR 95/84, UNI EN 933-4		$\leq$ 3
Aggregate flakiness	CNR 95/84, UNI EN 933-3		$\leq$ 1.58
Flakiness index	CNR 95/84, UNI EN 933-3	%	$\leq$ 20
porosity	CNR 65/78, UNI EN 12697-8	%	$\leq$ 1.5
Polishing stone value	CNR 140/92, EN 1097-8	%	$\geq$ 45

Table 3.2: Coarse aggregate properties of VTAC 0/6 mix foreseen from action B1.

Parameter	Standard	Unit	Value
Sand equivalent	CNR 27/72, EN 933-8	%	$\geq$ 80
Passing percentage at 0.075 mm	CNR 75/80, UNI EN 933-1	%	$\leq$ 2
Percentage of crushed and broken surfaces in coarse aggregate particles	CNR 109/85 – UNI EN 933-5	%	100

Table 3.3: Fine aggregate properties of VTAC 0/6 mix foreseen from action B1.

Concerning the filler, the requirements are given in Table 3.4. For each parameter, the reference standard for laboratory test, the unit and the value as prescribed from B1 action are given.

Parameter	Standard	Unit	Value
Boiling water stripping test	CNR 138/92, UNI EN 12697-11	%	≤ 5
Passing percentage at 0.18 mm	CNR 23/71, UNI EN 933-1	%	100
Passing percentage at 0.07 5mm	CNR 75/80, UNI EN 933-1	%	≥ 80
Plasticity index	CNR-UNI 10014, ASTM D4318		N.P.
Rigden voids - voids of dry compacted filler	CNR 123/88, EN 1097-4	%	30-45
Stiffening power for 1.5 filler/bitumen ratio	CNR 122/88, EN 13179-1	ΔPA	≥ 5

Table 3.4: Filler properties of VTAC 0/6 mix foreseen from action B1.

3.1.1.2 Bituminous mixture type 1 - VTAC 0/6 without crumb rubber

The first type of bituminous mixture of VTAC 0/6 proposed from B1 action outcomes was without crumb rubber. The requirements for aggregate gradation and bitumen percentage are given in Table 3.5. Let's notice that in Table 3.5 the percentage of bitumen is given by aggregate weight. The corresponding percentage of bitumen by the total weight of the mix is 6%. The expected thickness of the compacted mixture was about 2.5 cm and the expected air void percentage was about 7%.

Sieve [mm]	Passing [%]	Range [$\pm$%]
8	100	0
5.6	100	3
4	88	5
2	58	5
1	35	5
0.5	24	5
0.25	18	3
0.063	11	2
Bitumen [%] (by aggregate weight)	6.4	0.5

Table 3.5: Aggregate gradation and bitumen percentage of VTAC 0/6 mix type 1 (without crumb rubber) foreseen from action B1.

3.1.1.3 Bituminous mixture type 2 - VTAC 0/6 with crumb rubber

The second type of bituminous mixture of VTAC 0/6 proposed from B1 action outcomes was with additional crumb rubber (dry method). The requirements for aggregate gradation and bitumen percentage are given in Table 3.6. As can be seen, the aggregate gradation is the same as for VTAC mix type 1 (Table 3.5). Let's notice that in Table 3.6 the percentage of bitumen is given by aggregate weight (including crumb rubber). The corresponding percentage of bitumen by the total weight of the mix is 6.2%. The recommendation from B1 action for the percentage of crumb rubber (with respect to aggregate weight) was in the range between 1% and 5%.

Sieve [mm]	Passing [%]	Range [±%]
8	100	0
5.6	100	3
4	88	5
2	58	5
1	35	5
0.5	24	5
0.25	18	3
0.063	11	2
Bitumen [%] (by aggregate weight)	6.6	0.7

Table 3.6: Aggregate gradation and bitumen percentage of VTAC 0/6 mix type 2 (with crumb rubber) foreseen from action B1.

3.1.2 Call for tender

A call for tender was published by UNI EIFFEL in June 2020 (Dauvergne et al., 2020a). The consultation was launched according to the "adapted" procedure in application of articles R.2123-1 and L.2123-1 of the public procurement code in force in France on April 1, 2019.

The technical specifications of the prototype were fully described by Dauvergne et al. (2020b). The prototype location on the reference test track of UNI EIFFEL in Nantes (France) is highlighted by a red circle on Figure 3.1. This prototype covers an area of 450 m^2 of bituminous asphalt concrete. It was planned to have a length of 57 meters between reference points (RP) 2085 and 2142, and a width varying from 8.0 m to 7.5 m due to the presence of a bungalow existing at the end of this area (Figure 3.2).

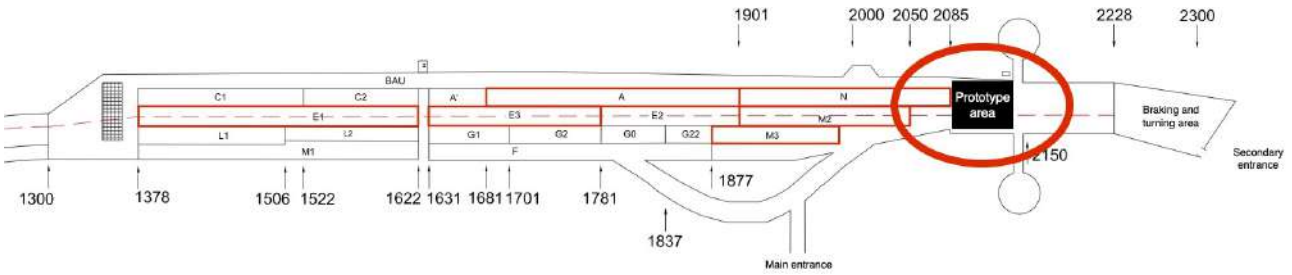

Figure 3.1: Location of the prototype area on the UNI EIFFEL reference test track in Nantes (France).

It was specified by Dauvergne et al. (2020b) that the construction works should include a planing of the existing test section in bituminous asphalt concrete up to the as-dug gravel which will have to be compacted prior laying of the new materials. It was also indicated that the under layer of the prototype VTAC 0/6 should be a bituminous dense asphalt concrete (DAC) 0/10 over the entire planed surface. Its formulation was kept free for proposition by the road company building the prototype.

Regarding the surface layer of the prototype, the call for tender indicated a basic solution and a variant solution, as illustrated in Figure 3.2. The basic solution consisted in laying a VTAC 0/6 without crumb rubber over the whole 450 m^2 area of the prototype (Figure 3.2 (a)). In the variant solution, the prototype area was divided in two test sections as shown in Figure 3.2 (b): a VTAC 0/6 with crumb rubber of particle size 2/4 mm at the top of the area and a VTAC 0/6 without crumb rubber of the same kind as the basic solution at the bottom of the area. In the call for tender, the candidates were highly encouraged to propose an offer for the basic solution and the variant solution. The specification of

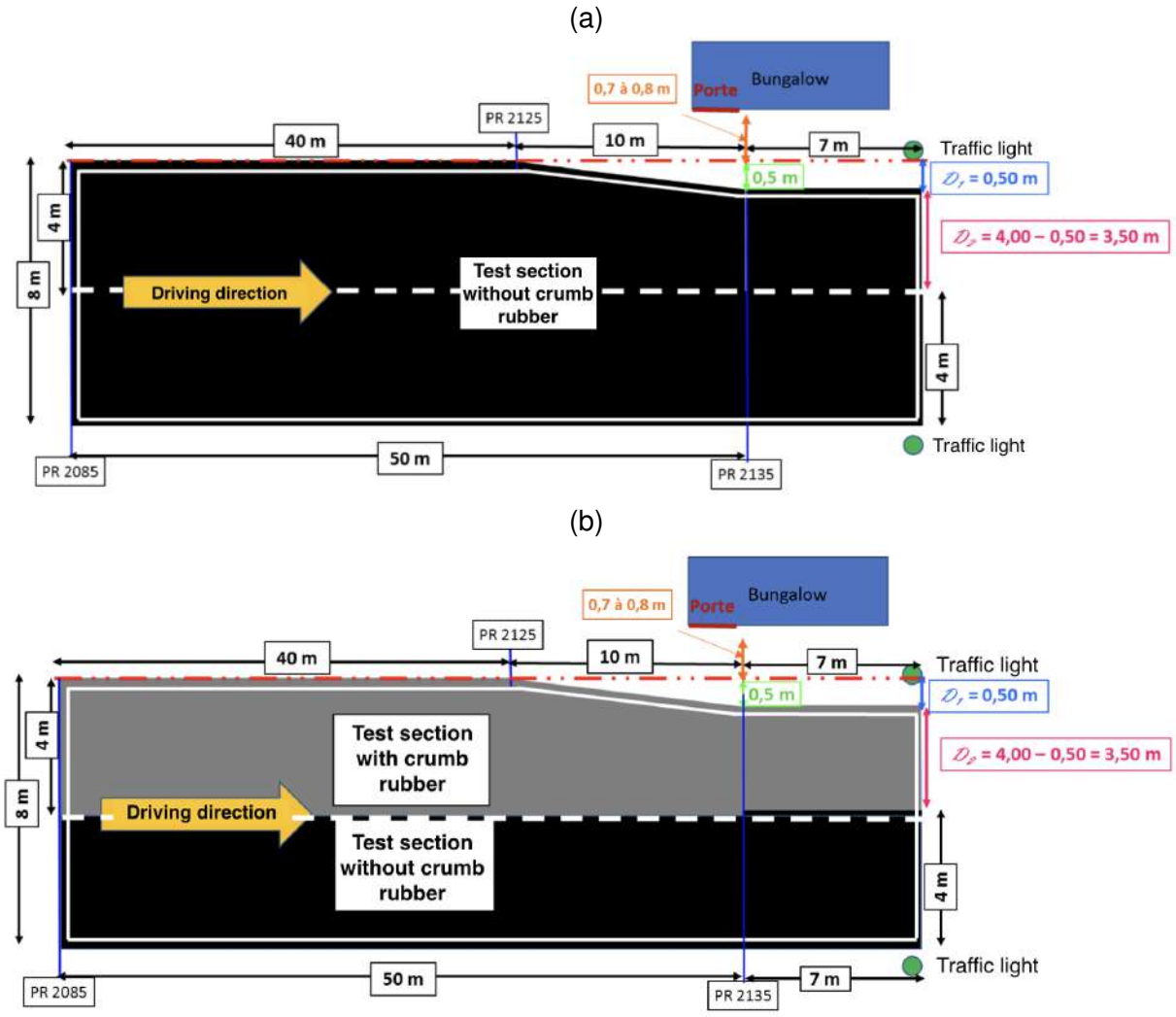

Figure 3.2: Surface layer options for the prototype construction (Dauvergne et al., 2020b): (a) the basic solution with one test section without crumb rubber, (b) the variant solution with two test sections, the first without crumb rubber and the second with crumb rubber.

VTAC 0/6 mixes from B1 action described in section 3.1.1 were fully given in the call for tender. The candidates were asked to respect as much as possible these formulations from B1 action.

Four road construction companies were consulted by UNI EIFFEL, namely Charier, Eiffage, Eurovia and Colas. Only Colas company applied for building the prototype. The offer included a proposal for both the basic solution and the variant solution. After analysis and validation of the offer, this company was selected for the construction of the prototype.

3.1.3 Formulation study prior the prototype construction

Prior to the construction of the prototype, Colas performed a detailed formulation study in laboratory in order to check the conformity of their solutions with the specifications from action B1. Both VTAC 0/6 mixes (without and with crumb rubber) are based on the same grading curve (Figure 3.3) and the amount of total bitumen was fixed to 6.4% of the total mix weight. This amount of bitumen was slightly increased by comparison with B1 specification considering Colas know-how and recommendation in the construction of very thin asphalt layers. As can be seen in Figure 3.3, the grading curve proposed by the road company is very close to the B1 reference grading curve. Thus, the black grading curve in Figure 3.3 will serve as the reference within B2 action for the prototype construction.

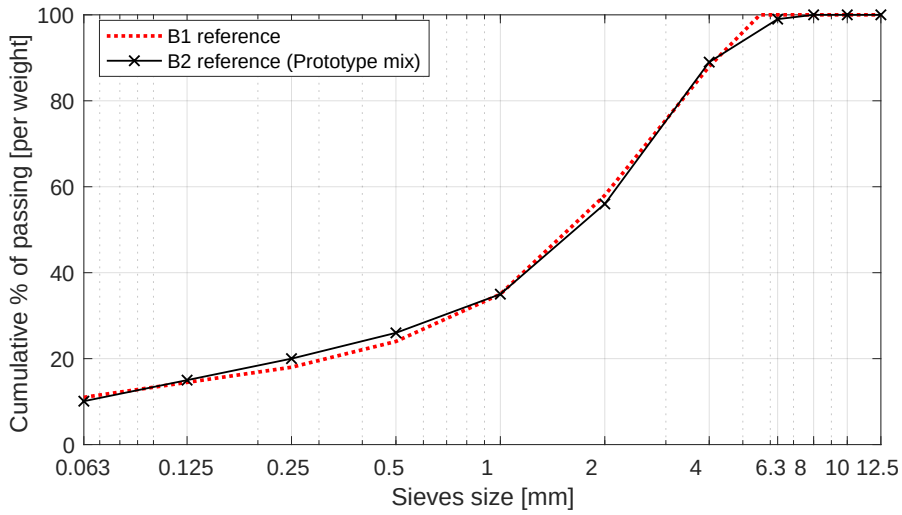

Figure 3.3: Comparison of reference grading curves from B1 and B2 actions.

The properties of the final mixes are given in Table 3.7 for the VTAC 0/6 without crumb rubber and the VTAC 0/6 with crumb rubber. The aggregates percentage for each fraction (0/2, 2/4 and 4/6.3) are given. Aggregates of fraction 0/2 come from Rouans quarry, while aggregates of fractions 2/4 and 4/6.3 are from Vairé quarry. Both quarries are close to Nantes. The fines are composed of limestone and a bitumen 50/70 is used. All these materials conform with specifications from B1 action.

In the case of the VTAC 0/6 with crumb rubber, the grading curve includes crumb rubber aggregates in the fraction 0/1 mm. In practice, the same product as the one used during the preliminary study of action B1 was used for the prototype construction, namely RARX® product (CIRTEC, 2019). RARX® is an elastomeric asphalt extender that can be added to hot mix asphalt concretes. It is composed of fine rubber granules (58%), conventional bitumen (16%) and mineral fillers (25%). As can be seen in Table 3.7 for the mix with crumb rubber, the amount of stone aggregates, fines and filler bitumen have been adjusted by Colas in order to take into account the composition of RARX®.

Mix properties	Without CR			With CR		
Aggregates (fraction [mm] - type - [%])	4/6.3	Vairé	7.0	4/6.3	Vairé	7.0
	2/4	Vairé	33.0	2/4	Vairé	33.0
	0/2	Rouans	52.0	0/2	Rouans	51.0
				0/1	RARX®	1.9
Fines (type - [%])		Limestone	1.6		Limestone	1.0
Filler bitumen (type - [%])		50/70	6.4		50/70	6.1
Total bitumen [%]			6.4			6.4
Thickness [mm]			25			25

Table 3.7: Final mix properties of the two implemented options of prototype VTAC 0/6.

3.2 Prototype construction

The 57m-long by 8m-large prototype was built from the 7th to the 10th of September 2020 on UNI EIF-FEL reference test track. It was finally decided to choose the variant option of the call for tender, i.e. to implement two different mixes of VTAC 0/6 (Figure 3.2 (b)). During the construction, the weather was sunny. The average air temperature was around 19°C and the wind did not exceed 20 km/h. The construction of the prototype was performed in four main steps:

1. Planing of the old test section on 7 September 2020;
2. Laying of the under-layer on 8 September 2020 (morning);
3. Laying of the VTAC 0/6 test sections on 8 September 2020 (afternoon);
4. Marking of the prototype area on 10 September 2020.

3.2.1 Planing of the old test section and laying of the under-layer

The old test section was removed by Colas on the 7 September 2020. Due to the small area to be removed, a small cold milling machine of make Wirtgen W 100 was used. It enables the milling over a width of 1 meter. Figure 3.4 (left) shows a picture of the equipment used during the milling of the existing road surface. The planing was finished in less than two hours and the final result after this step can be seen on Figure 3.4 (right). As can be seen, the as-dug gravel was reached on a part of the prototype area, while a non expected cement concrete under-layer was found when milling. This layer of cement concrete is about 120 mm thick and was kept in place under the prototype.

The under-layer was laid on the 8 September 2020. The under-layer was a French BBS 0/10 of type 2, i.e. a dense asphalt concrete (DAC) 0/10. The thickness of the under-layer was about 70 mm. The BBS 0/10 was laid with a finisher of type Vogele 1800-2 Sprayjet (Figure 3.5 (left)). The compactor was a vibrating tandem of make Bomag, type BW 154 AP-4 (Figure 3.5 (right)).

The under-layer was laid in two passes of approximately 3.5 cm. Prior each pass, a tack coat (bitumen emulsion) was sprayed on the surface. Figure 3.6 shows the construction site after the first pass (left) and the second pass (right) of the DAC 0/10 under-layer.

3.2.2 VTAC 0/6 test sections

The VTAC 0/6 test sections were laid on the 8 September 2020. A tack coat (bitumen emulsion) was first sprayed over the whole prototype area prior to the laying of the road surface (Figure 3.7).

Then, the VTAC 0/6 with crumb rubber was laid (Figure 3.8 (left)) and compacted (Figure 3.8 (right)). The same finisher and compactor as for the under-layer were used. Regarding the preparation of the mix with crumb rubber at the asphalt plant, the guidelines for use of RARX® have been

7 September 2020 - 9:34

7 September 2020 - 11:04

Figure 3.4: Planing of the old test section (left) and final result after milling (right).

8 September 2020 - 9:55

8 September 2020 - 10:02

Figure 3.5: Laying (left) and compacting (right) of the DAC 0/10 under-layer.

8 September 2020 - 10:31

8 September 2020 - 14:05

Figure 3.6: Construction site after laying of the under-layer. Left: first pass, Right : second pass.

8 September 2020 - 14:52

Figure 3.7: Laying of the tack coat (bitumen emulsion) prior laying of the VTAC 0/6.

followed with care (CIRTEC, 2019). No major issue was encountered during the laying and the compaction of the VTAC 0/6 test section with crumb rubber.

8 September 2020 - 15:38

8 September 2020 - 15:50

Figure 3.8: Laying (left) and compacting (right) of the VTAC 0/6 with crumb rubber.

Next, the VTAC 0/6 without crumb rubber was laid (Figure 3.9 (left)) and compacted (Figure 3.9 (right)). As can been seen on Figure 3.9 (right), a smaller tandem compactor was also used on both test sections. No major issue has been encountered during the laying and the compaction of the VTAC 0/6 test section without crumb rubber.

Figure 3.10 (left) shows the construction site the day of laying the prototype and six days later after marking of the prototype area. As can be seen on Figure 3.10 (right), the test section without crumb rubber (on the left) has been opened to the traffic of the test track, while the test section with crumb rubber (on the right) has been protected with cones. Thus, this area with crumb rubber, *a priori* more fragile, has only been travelled by vehicles within the framework of the LIFE E-VIA project (sub-actions B2.3 and B2.4).

3.2.3 Final prototype and denomination of test sections

A top view of the final prototype area is given in Figure 3.11. Both VTAC 0/6 test sections of size 4 m width and 57 m long can be seen. The VTAC 0/6 without crumb rubber was named test section P

8 September 2020 - 16:08

8 September 2020 - 16:09

Figure 3.9: Laying (left) and compacting (right) of the VTAC 0/6 without crumb rubber.

8 September 2020 - 16:47

14 September 2020 - 15:12

Figure 3.10: Final view of the construction site the day of laying and six days later after marking.

and the VTAC 0/6 with crumb rubber was named test section PCR. This nomenclature will be used in the following.

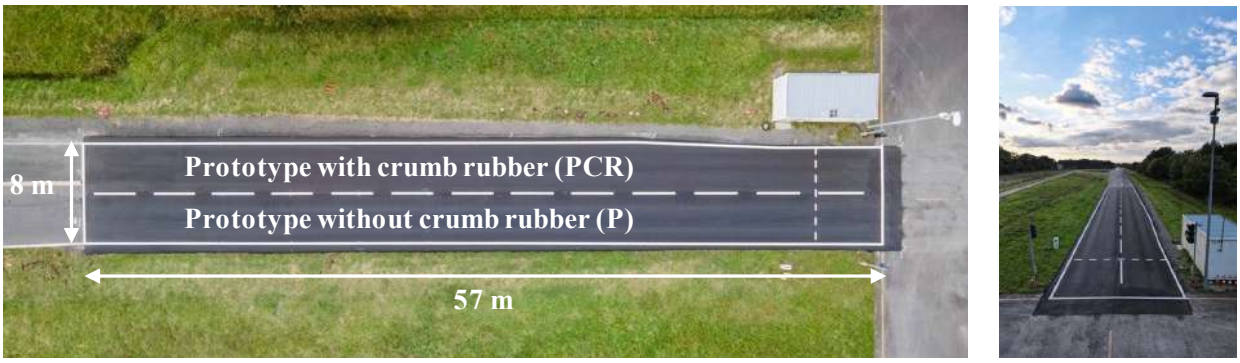

Figure 3.11: Top view of the prototype area showing test sections P (without crumb rubber) and PCR (with crumb rubber).

A close-up view of the road surfaces is given in Figure 3.12 for the prototype test sections P and PCR. They can be compared to the surface of the existing test section E1 (DAC 0/10), which serves as a reference road surface within this report. The finer grading and flattening of aggregates for test section P and PCR can be pointed out by comparison with test section E1. Surface texture of the prototype test sections will be further investigated in section 4.1.1.

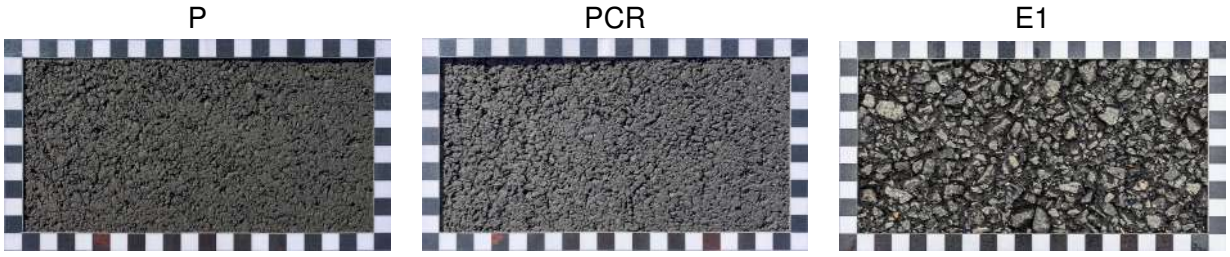

Figure 3.12: Close-up pictures of test sections P (without crumb rubber), PCR (with crumb rubber) and E1 (reference DAC 0/10). Frame size: 20 cm by 10 cm.

3.3 Controls after construction

3.3.1 Mix content

The mix content of both solutions laid on the prototype was controlled by Colas in laboratory from materials taken *in situ* during the construction. The Asphaltanalysator device was used. The binder content was controlled following NF EN 12697-1 and the grading of the mix was controlled following NF EN 12697-2. For both mixes, the binder content and the grading were found to be in conformity with the reference mix of action B2. Figure 3.13 compares the grading curve of the B2 reference mix proposed by Colas prior to the prototype construction with the grading curves of test sections P and PCR. For both P and PCR, the grading curves are in good agreement with the reference and within the tolerance margin. The binder content was 6.31% for mix P and 6.62% for mix PCR to be compared with the reference of 6.4% of total bitumen in the mix. The higher difference for PCR was attributed to the dissolution of some crumb rubber during the mix control process. The binder content was considered as conform for both test sections.

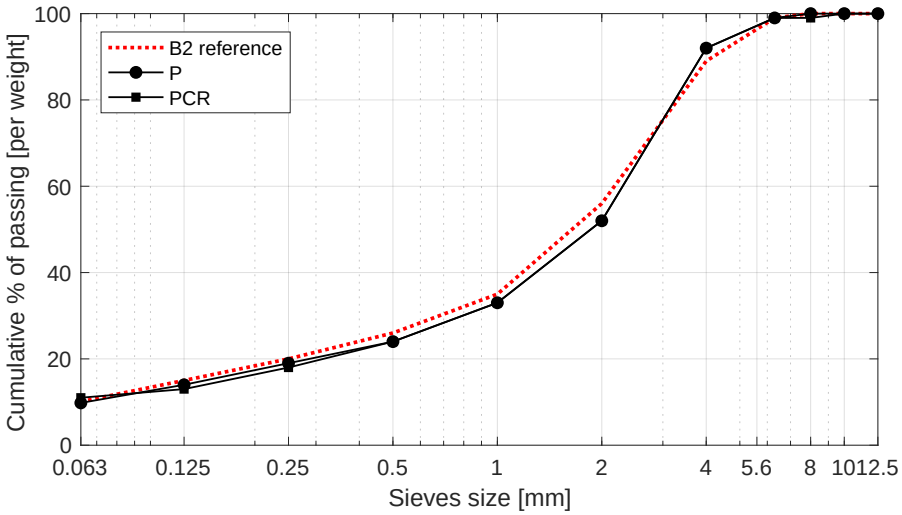

Figure 3.13: Grading curves of the controlled mixes P and PCR compared with B2 reference.

3.3.2 Mean texture depth measurement

The mean texture depth (MTD) of the road surface was measured by Colas just after the laying of the prototype test sections on the 8 September 2020. The sand patch volumetric technique was used conforming EN 13036-1. It consists in pouring a given volume V (25 cm^3) of calibrated glass beads on the pavement, spreading them using a special disc in a circular area until they are flush, and measuring the average diameter of the circle to obtain its surface S. The MTD (in mm) corresponds to the ratio between the volume V and the surface S. Figure 3.14 shows the MTD measurement by Colas on test section PCR.

Figure 3.14: Sand patch MTD measurement by Colas on 8 September 2020.

The MTD is a global indicator of the macro-texture level of the road surface. It was measured every 10 meters starting from the reference point (RP) 2090 m, RP 2085 m being the beginning of the prototype area. For each RP, a measurement was performed in the middle of the test section and in the right wheel path. These two locations are respectively denominated by "Axis" and "Right" in Table 3.8, which gives the MTD values obtained for both test sections P and PCR. The average MTD value over the 12 measurement spots was 0.51 $\pm$ 0.04 mm for test section P and 0.42 $\pm$ 0.02 mm for test section PCR. These values are much smaller than MTD values on classical VTAC 0/6 (e.g.

test section M2) or VTAC 0/4 (e.g. test section M3), but were expected due to the high percentage of aggregates in the fractions 0/2 mm (52%) and 2/4 mm (33%) in the prototype mixes.

RP [m]	MTD [mm] - P		MTD [mm] - PCR	
	Axis	Right	Axis	Right
2090	0.54	0.54	0.45	0.44
2100	0.57	0.52	0.43	0.44
2110	0.49	0.54	0.39	0.41
2120	0.51	0.50	0.41	0.42
2130	0.51	0.52	0.40	0.41
2140	0.48	0.42	0.40	0.38
Average Value	0.51		0.42	
Standard deviation	0.04		0.02	

Table 3.8: Mean Texture Depth measurement results on the prototype test sections P and PCR.

3.3.3 Air-void content

In order to measure the actual density and the air-void content of the prototype test sections, core samples have been drilled in June 2021. For each test section, three core samples have been extracted by UNI EIFFEL over the last 6 meters of the prototype area (Figure 3.15 (left)). From the core samples, it was also possible to assess the thickness of the different layers. The thickness of the VTAC 0/6 top layers ranked between 20 and 30 mm and the thickness of the DAC 0/10 under-layer was between 70 and 80 mm. For PCR, the additionnal layer of cement concrete was about 120 mm thick, as can be observed on Figure 3.15 (right).

Figure 3.15: Drilling of core samples in the prototype (left) and picture of the six core samples (right).

After complete drying, the actual density and air-void content of each sample were analysed in laboratory by means of a gamma densimeter available at the UNI EIFFEL material department premises. This equipment can be seen in Figure 3.16 and complies with EN 12697-7. After these non-destructive tests, the samples were sent to UNIRC for further analysis of the prototype mixes properties within action B1, prior to the implementation of the low-noise asphalt concrete in the pilot area in Florence in July 2021 (action B3).

The actual density of the asphalt concrete given by Colas was 2.402 g/cm^3 for both P and PCR test sections. Table 3.9 gives the apparent density and the air-void content measured on the three core samples for test sections P and PCR. The average air-void content value was 9.9% on test

Figure 3.16: Gamma densimeter used to measure actual density and air-void content from the core samples drilled on the prototype test sections.

section P, while it was 14.6% on test section PCR. Thus, the air-void content is higher by 4.7% in the VTAC with crumb rubber.

	P		PCR	
	Apparent Density [g/cm^3]	Air-void content [%]	Apparent Density [g/cm^3]	Air-void content [%]
Sample 1	2.169 $\pm$ 0.029	9.7 $\pm$ 1.2	2.064 $\pm$ 0.052	14.1 $\pm$ 2.2
Sample 2	2.179 $\pm$ 0.030	9.3 $\pm$ 1.3	2.090 $\pm$ 0.058	13.0 $\pm$ 2.4
Sample 3	2.145 $\pm$ 0.054	10.7 $\pm$ 2.3	1.997 $\pm$ 0.090	16.9$\pm$ 3.7

Table 3.9: Apparent density and air-void content of test sections P and PCR.

3.4 Synthesis of sub-action B2.2

The prototype foreseen within action B2 was successfully built in September 2020. Following a call for tender, the Colas road construction company was selected by UNI EIFFEL for the construction of two VTAC 0/6 test sections of the same grading curve, conforming B1 action reference and differing by the addition of 1.9% of crumb rubber, namely RARX®, in one of the mixes. Based on Colas know-how, the total amount of bitumen was fixed to 6.4% for both asphalt concrete mixes, which was slightly higher than the specification from B1 action. There was no major issue to point out during the construction of the prototype. The test section without crumb rubber was named P, while the other with crumb rubber was named PCR. The controls after the construction have shown the conformity of the grading curve and of the bitumen content for both test sections. The measured MTD was rather low on both test sections, with an average value of 0.51 $\pm$ 0.04 mm for test section P and 0.42 $\pm$ 0.02 mm for test section PCR. The thickness of the surface layer was also assessed from core samples drilled on P and PCR test sections. It was found to be conform to the specification of 25 mm. The air-void content of the surface layer was also assessed in laboratory with a gamma densimeter. The average air-void content value was 9.9% on test section P, while it was 14.6% on test section PCR.

4 Sub-action B2.3 – Characterisation of the prototype test sections

Following its construction, several tests have been performed from autumn 2020 until spring 2021 on the prototype test sections. Therefore, this sub-action also provided prediction and recommendation for the next implementation in the pilot area in Florence, Italy (action B3), in interaction with the track design (action B1).

Road surface properties that are likely to influence tyre/road noise emission were measured by UNI EIFFEL, i.e. road surface texture by means of a 3D-laser sensor, sound absorption by using the extended surface method (ISO13472-1) and dynamic stiffness.

Regarding skid resistance, several tests were also performed by UNI EIFFEL: SRT pendula friction tests, MPD measurements, dynamical wet friction by means of T2GO device and assessment of friction durability from road surface samples (taken during the prototype construction) by Wehner and Schulze tests in laboratory.

CPB and microphone array measurements performed in B2.1 were repeated on the prototype test sections for a selection of EVs. Noise performance of the prototype road surface was assessed at rolling speeds between 30 km/h and 70 km/h by simultaneous Close-ProXimity (CPX) and Coast-By (CB) measurements with the reference ICEV of UNI EIFFEL, a Renault Megane Scénic, fitted with 195/60 R15 tyres. The acoustical performance of the prototype test sections was also assessed by means of classical CPX measurements at 50 km/h, enabling comparison with several types of road surfaces available on UNI EIFFEL reference test track. Acoustical CPX tests have also been performed by IPOOL with the SRTT tyre conforming ISO 11819-3 in order to perform reliable comparisons in Action B4 during monitoring on the test track built in Florence.

The series of tests carried out, both physical and acoustic, produces a fairly comprehensive assessment of the properties of the prototype road surface.

4.1 Characterisation of road surface properties

4.1.1 Surface texture measurement

4.1.1.1 Texture measurement system

The texture measurements on prototype test sections were performed with a system that allows three-dimensional measurements of length comparable to the perimeter of a standard tyre and width up to 35 cm. The system consists of (Figure 4.1):

- a motorised linear axis with a stroke of 1.55 m supported by a three-legged frame,
- a 2D-profile laser sensor (model Micro-Epsilon SCAN-CONTROL 2700-50) clamped to a manual lateral positioning table with a 300 mm stroke,
- a control panel to start the measurement.

The system automatically moves the sensor longitudinally to measure strips about 55 mm wide. Eight longitudinal strips are scanned at eight lateral positions spaced 43 mm apart, ensuring an inter-strip overlap of approximately 10 mm. Profile acquisition is triggered by the movement of the sensor along the longitudinal axis every 0.1 mm. The sensor delivers a cloud of 640 points at each longitudinal position as shown in Figure 4.2.

The longitudinal strips are then merged and re-sampled in post-processing using several algorithms to obtain a single reconstructed surface with a maximum width of 35 cm and a length of about 1.5 m and lateral and longitudinal sampling intervals of 0.1 mm. The vertical resolution of the system is approximately 50 μm.

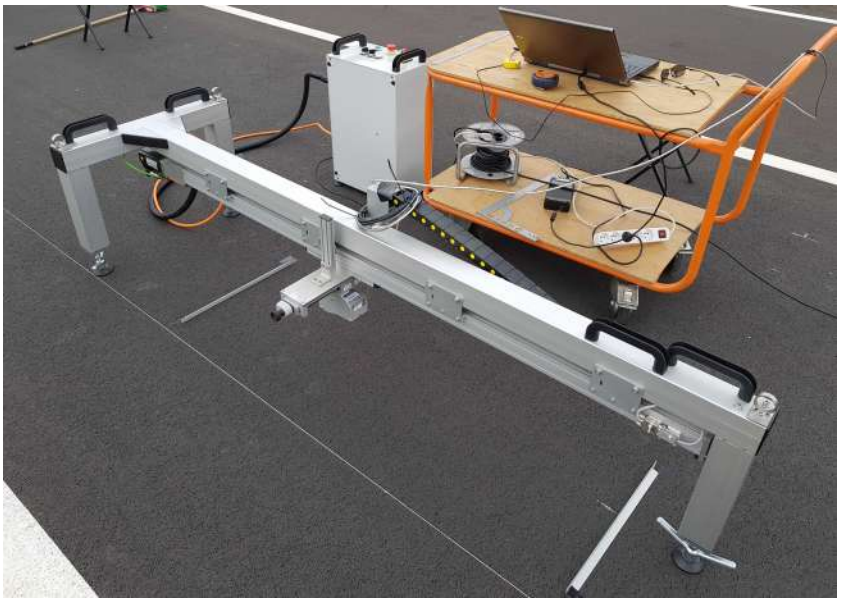

Figure 4.1: 3D texture measurement system

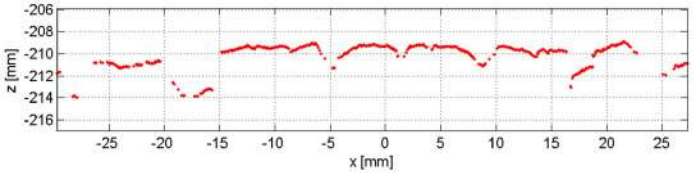

Figure 4.2: Example of a measured profile from the 2D laser sensor.

4.1.1.2 Texture measurement protocol

The protocol used for the texture measurement consists of taking several scans of each surface in the wheel paths of the acoustical test vehicle on either side of the longitudinal position of the microphone used for the pass-by noise measurements. Four scans were carried out in the wheel path on the side of the CPB microphone position chosen within sub-action B2.1 (left side of the test vehicle) and two scans in the other wheel path (see measurement configuration in Figure 4.3). Successive scans were carried out in each wheel path with 10 cm overlapping parts so as to merge them together in a single surface of several metres in length.

4.1.1.3 Texture measurement results

Measured surfaces The width and length of the surfaces reconstructed from the texture measurements carried out on the prototype test sections are given in Table 4.1. In this table and in the following results, these scans are referred to by the name shown in Figure 4.3.

Mean profile depth The mean profile depth (MPD) is defined in ISO 13473-1. It is evaluated from texture profiles extracted from reconstructed 3D texture scans at 2 cm lateral interval after resampling at 0.5 mm lateral and longitudinal spacing. The extracted profiles are first pre-filtered using digital filters that retain components of wavelengths ranging between 3 mm and 140 mm. Individual MPD values are evaluated on a segment of length 100 mm on the filtered profile. The MPD is then calculated as the difference between the arithmetic mean of the highest peaks on each half of the segment and the average height calculated over the entire segment.

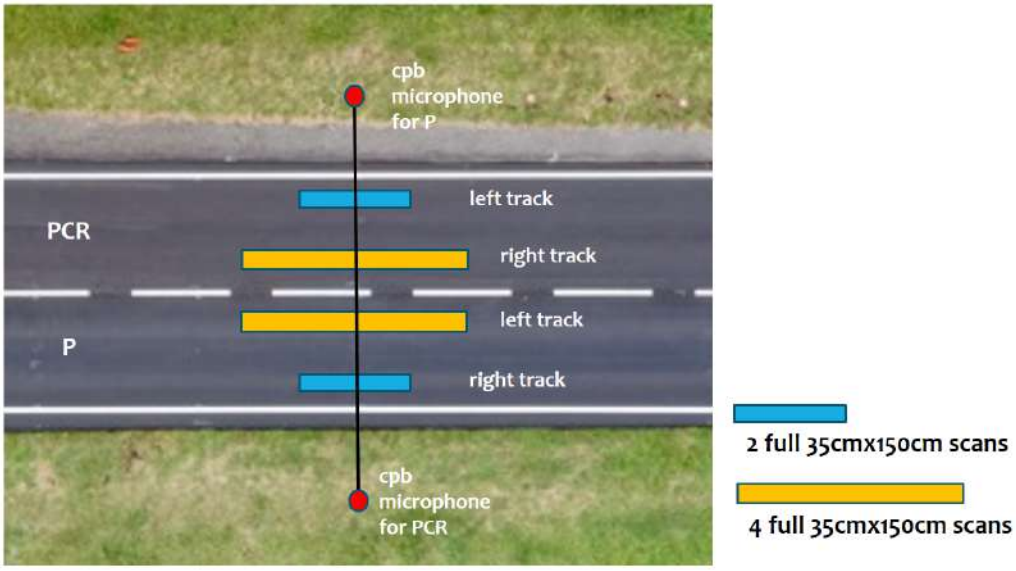

Figure 4.3: Sketch of texture measurement on prototype test sections P and PCR.

Test section	Wheel track	Nb. of scans	Width [m]	Length [m]
PCR	left	2	0.35	2.94
PCR	right	4	0.35	5.80
P	left	4	0.34	5.79
P	right	2	0.35	2.94

Table 4.1: Width and length of the texture surfaces measured on prototype test sections P and PCR.

The MPD values and associated standard deviations σ_{MPD} evaluated are given in Table 4.2. The values obtained are low. The MPD values of test sections PCR and P amount respectively to 0.30 mm and 0.39 mm. They are comparable to the MPD value obtained for the ISO 10844-like test track N. These values are compared with those obtained for the other test tracks in Figure 4.4. According to ISO 13473-1, Estimated Texture Depth (ETD) values can be obtained from MPD values by applying a multiplication factor of 1.1. These ETD values amount respectively to 0.33 mm and 0.43 mm.

Test section	Wheel track	MPD [mm]	σ_{MPD} [mm]
PCR	left	0.30	0.05
PCR	right	0.30	0.05
PCR	average	0.30	0.05
P	left	0.40	0.07
P	right	0.37	0.06
P	average	0.39	0.07

Table 4.2: MPD values and associated standard deviation of prototype test sections P and PCR (in the left and in the right wheel tracks and average value).

Texture spectrum One-third octave band texture spectra of both test sections have been evaluated from longitudinal profiles extracted every 2 cm, following the method described in ISO 13473-4. The average spectra evaluated for the left and right wheel tracks of both test sections are drawn

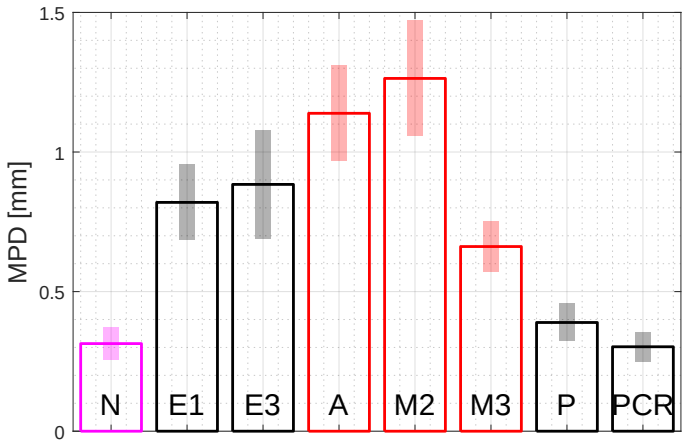

Figure 4.4: MPD values obtained on prototype test sections compared with other test sections.

in Figure 4.5. The associated spread envelopes at +/- the value of the standard deviation are also represented. There is almost no difference between the left and right wheel track spectra for the test section P except for wavelengths greater than 200 mm. The same is true for test section PCR, except for the 160 mm wavelength, at which a pronounced peak is observed for the right wheel track only.

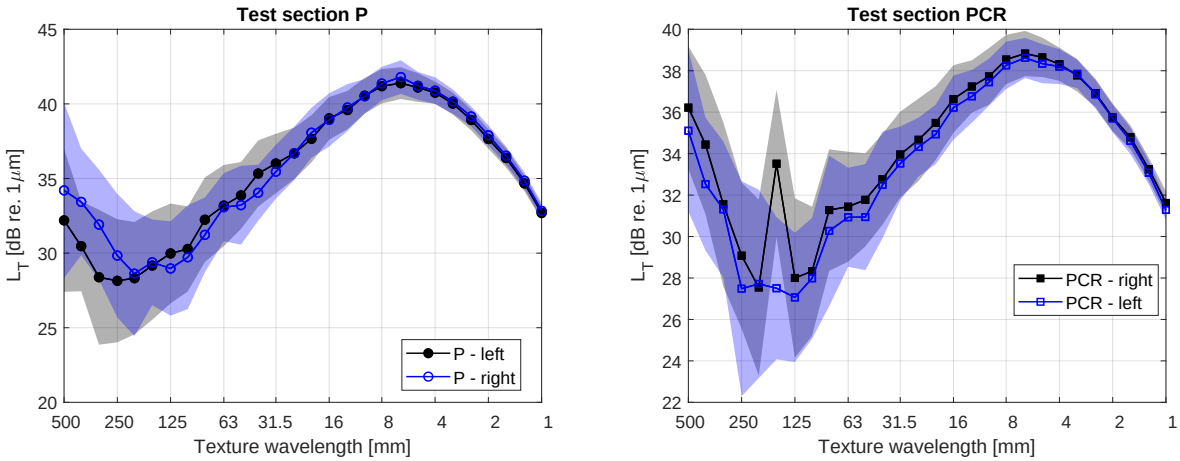

Figure 4.5: Texture spectrum of prototype test sections - Left: test section P - Right: test section PCR.

The one-third octave band texture spectra averaged over the left and right wheel tracks of both prototype test sections P and PCR are drawn in Figure 4.6 (left). The texture levels of test section P are up to 3 dB higher than those of section PCR for wavelengths lower than 125 mm, with an opposite situation for wavelengths greater than 250 mm. The peak at wavelength 160 mm observed for section PCR is partly attenuated due to averaging. These spectra are compared in Figure 4.6 (right) with those of existing test sections used in sub-action B2.1. Generally speaking, the texture levels of both test sections are in the lower range. The texture levels of test section P are quite similar to that of test track N for wavelengths ranging between 8 mm and 160 mm and become higher at shorter wavelengths. The spectrum of track N significantly drops at small wavelengths and intersects the spectrum of test section PCR around 2 mm.

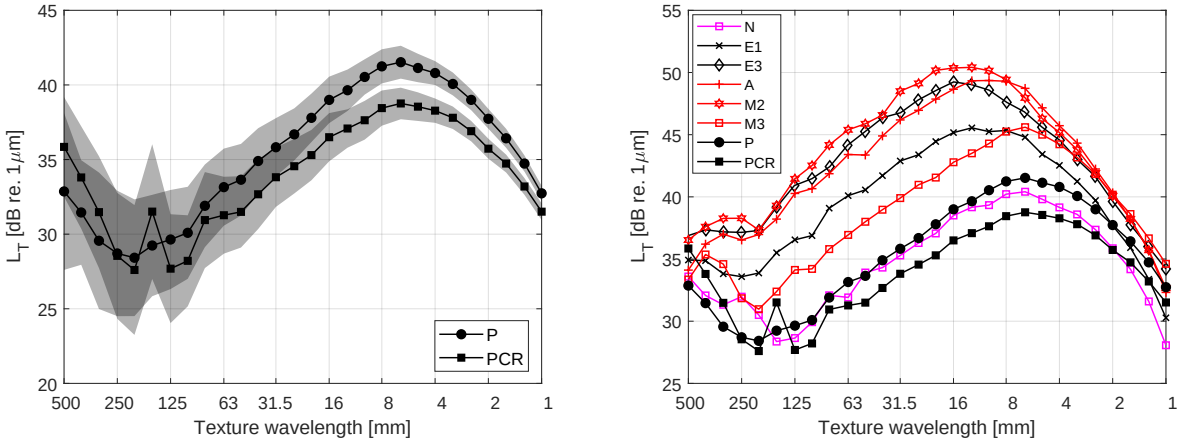

Figure 4.6: Left: Average texture spectrum of prototype test sections P and PCR. Right: comparison with exisitng test sections A, E1, E3, M2, M3 and N.

4.1.2 Sound absorption

Sound absorption was measured on test sections P and PCR following ISO 13472-1 on 28 September 2020, i.e. three weeks after the construction of the prototype. Figure 4.7 shows the measurement session on test section PCR. The same equipment as described in section 2.1.1 was used. The absorption coefficient was measured in the middle of the test section at five spots in front of the CPB microphone position (Figure 4.3) and averaged in the narrow bandwidth frequency domain. The spots were equally spaced every 2 meters.

Figure 4.7: Sound absorption measurement on the prototype test section PCR in September 2020.

Then, the sound absorption coefficient of P and PCR was calculated in one-third octave bands. The results are given in Figure 4.8 and compared to the sound absorption coefficient measured on the existing test sections A, M2 and M3 in July 2020. It can be observed that the sound absorption coefficient was rather low for both prototype test sections, with a maximum value of 0.17 and 0.26 at 2500 Hz for PCR and P respectively. Another peak around 0.1 is also observed at 500 Hz for both prototype test sections. By comparison with test sections A and M3, the sound absorption properties of P and PCR are weak. However, it can be considered of the same order of magnitude as the sound

absorption coefficient of test section M2 (VTAC 0/6), but shifted at higher frequencies (2500 Hz for P and PCR against 630 Hz for M2). This could be explained by the finer grading of test sections P and PCR compared with test section M2.

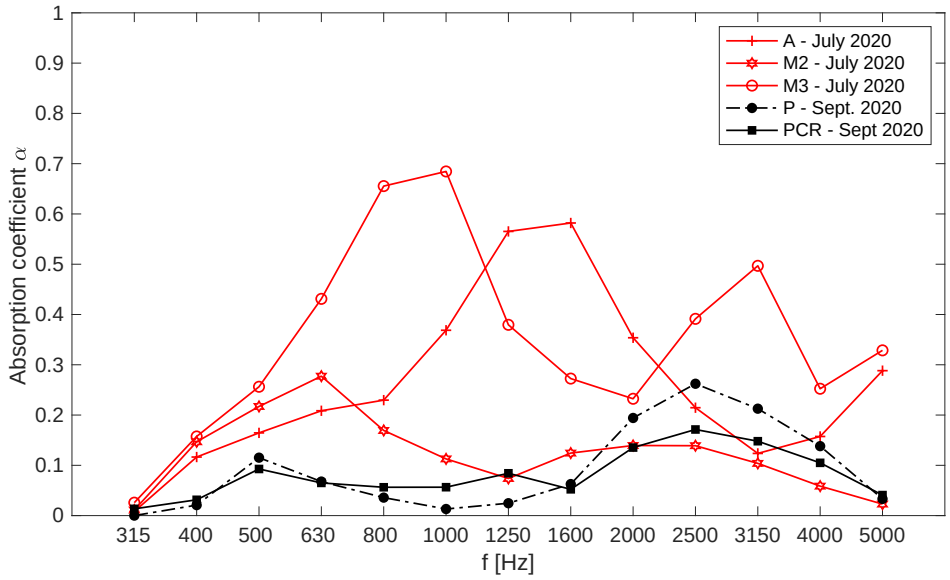

Figure 4.8: Sound absorption coefficient in one-third octave bands measured on the prototype test sections P and PCR and comparison to the existing absorbing road surfaces A, M2 and M3.

4.1.3 Dynamic stiffness

The dynamic stiffness of the prototype test sections was measured in March 2021. The measurement principle of the dynamic stiffness is given in Figure 4.9. The experimental setup is composed of an impact hammer delivering an input force $f(t)$, an impedance head measuring the direct force $f_d(t)$ and the direct acceleration $a_d(t)$ at the impact location and an accelerometer measuring the transfer acceleration $a_t(t)$ at a certain distance from the impact point. In this study, only the direct signals from the impedance head have been used.

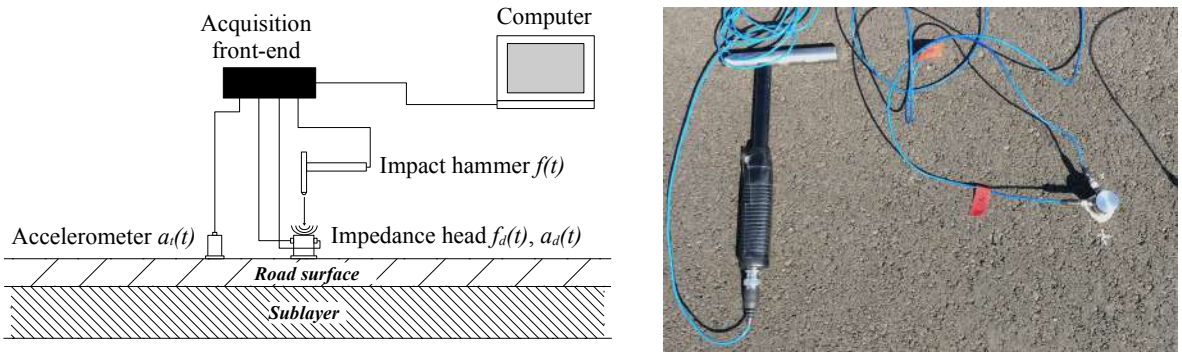

Figure 4.9: Measurement principle of dynamic stiffness (left) and impact hammer and impedance head used during the tests (right).

Defining the Fourier transform of a signal $x(t)$ by $X(\omega)$ with ω the angular frequency, the direct dynamic stiffness D_d is obtained by FFT analysis on the measured signals:

$$D_d(\omega) = F(\omega)/U_d(\omega) = -\omega^2 F(\omega)/A_d(\omega) = |D_d(\omega)|e^{j\varphi_{D_d}(\omega)} \quad (4.1)$$

where $U_d(\omega)$ is the direct displacement, $|D_d(\omega)|$ is the magnitude of D_d and $\varphi_{D_d}(\omega)$ its phase.

Five different spots were tested, located in the middle of the test section, at the same position as for sound absorption measurements. The air temperature during the test was 14℃, while the road surface temperature was 29.5℃ on test section P and 27.5℃ on test section PCR. Figure 4.10 shows the average magnitude of the dynamic stiffness $|D_d(\omega)|$ of test sections P and PCR in the frequency range between 100 Hz and 2000 Hz.

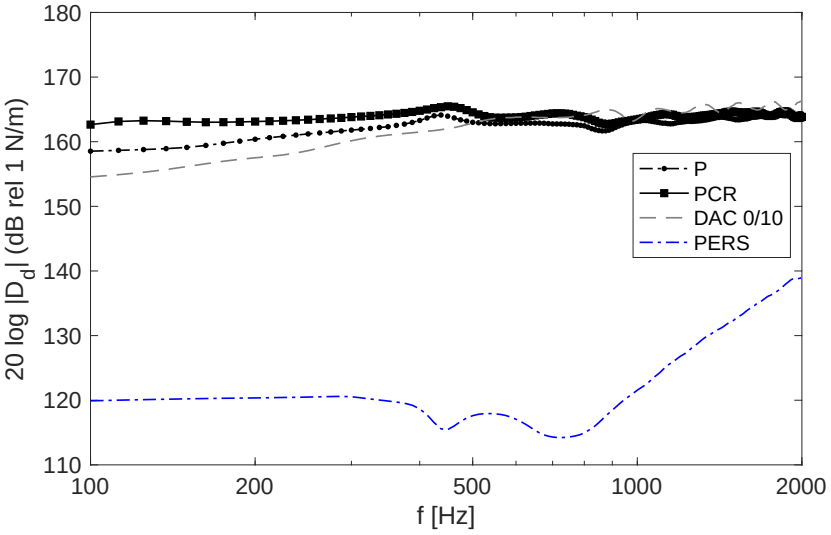

Figure 4.10: Dynamic stiffness as a function of frequency for P and PCR test sections.

The dynamic stiffness is almost constant over this frequency range, thus corresponding to an ideal spring behaviour. Although comprising crumb rubber, it is observed that PCR test section is stiffer than P test section, with a difference up to 5 dB below 400 Hz and about 2 dB above 400 Hz. As can be seen on Figure 4.10, the dynamic stiffness of test sections P and PCR is of the same order of magnitude as a DAC 0/10, and is very much higher than the dynamic stiffness of a poroelastic road surface (PERS) composed of a large amount of rubber aggregates (Bendtsen et al., 2014).

4.1.4 Skid resistance

The skid resistance properties of the prototype test sections P and PCR have been characterised through standard tests of macro-texture (MPD measurements) and friction (British pendulum and T2GO device). In parallel, two samples have been tested with the Wehner and Schulze (W&S) machine, to reproduce in laboratory the evolution of surface friction with road traffic (i.e. polishing) and to assess long term performance in terms of skid resistance.

MPD measurements

Macro-texture has been measured with the ELAtextur device. It is composed of a laser sensor mounted on a rotating arm which provides a circular 2D profile of length 400 mm. The 2D profile is analysed according ISO EN 13473-1 to calculate the MPD value. This static measurement provides a local assessment of the macro-texture of the pavement surface. Thus, the test was repeated every ten meters on the prototype to obtain a representative value of the macro-texture level along the longitudinal direction (i.e. rolling direction) of the test sections. The MPD values are used to calculate the estimated texture depth (ETD), which is the indicator currently used for road acceptance. The following relationship is applied:

$$ETD = 0.8MPD + 0.2 \tag{4.2}$$

As can be seen in Table 4.3, the average value of ETD is higher on test section P than on test section PCR. Moreover, it can be noticed that ETD values are weak on test section PCR and close to the threshold value of 0.40 mm which is the lower regulatory limit on French roads.

RP (m)	P	PCR
2090	0.49 mm	0.40 mm
2100	0.47 mm	0.39 mm
2110	0.48 mm	0.40 mm
2120	0.47 mm	0.37 mm
2130	0.51 mm	0.38 mm
2140	0.52 mm	0.38 mm
Average Value	0.49 mm	0.39 mm
Standard deviation	0.02 mm	0.01 mm

Table 4.3: ETD obtained from macro-texture measurements on P and PCR.

Friction measurements

Friction measurements were carried out by means of two different devices. On the one hand, the British pendulum provides a punctual static friction coefficient ranging between 0 (low friction) and 100 (high friction) according to standard EN 13036-4. On the other hand, the T2GO device provides a continuous friction coefficient ranging between 0 and 1 all along the longitudinal direction of the test section. Both friction coefficients are obtained at low sliding speed and on wet surface.

The British pendulum friction values measured every 10 meters on the test sections P and PCR are given in Table 4.4. On average, the static friction coefficient is higher than 70. The average friction value on test section P is approximately 10 points lower than on test section PCR, but the level of performance remains very satisfactory for both prototype pavements. Moreover, continuous friction measurements performed with the T2GO device on both test sections confirmed these good results with an average friction coefficient around 0.80.

RP (m)	P	PCR
2090	71.4	83.4
2100	68.4	78.6
2110	68.0	81.8
2120	70.8	85.2
2130	68.8	84.0
2140	74.8	81.8
Average Value	70.4	82.5
Standard deviation	2.6	2.3

Table 4.4: Static friction coefficient measured with the British Pendulum on P and PCR.

Polishing tests

The polishing tests have been carried out at UNI EIFFEL according to EN 12697-49 standard, which relies on the Wehner and Schulze (W&S) machine (Figure 4.11). The W&S machine is composed of two different rotary-heads. The first rotary-head simulates the polishing of the road surface under the action of traffic. Polishing is done by rolling three rubber cones on the surface of the pavement sample, where a mixture of water and silica flour (abrasives) is continuously spread. The second rotary-head measures the wet friction-time curve between 100 km/h and 0 km/h of a given specimen

at successive polishing states of the surface. The friction value at 60 km/h is taken into consideration for analyses. The measurements lead to a curve giving the evolution of friction coefficient with polishing stages, expressed in number of passes of the rollers.

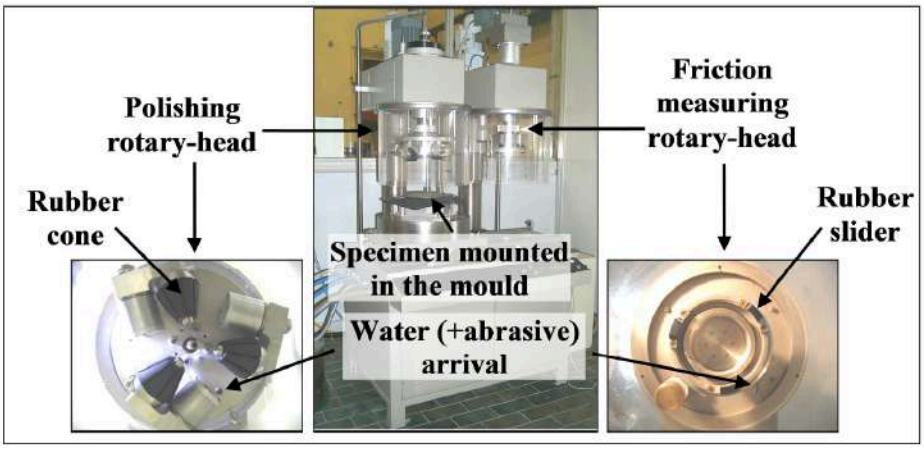

Figure 4.11: Wehner and Schulze polishing machine (Do et al., 2007).

The W&S tests have been performed on samples of diameter 225 mm which were made in laboratory from the mixes of test sections P and PCR. The friction coefficient as a function of polishing cycles is given on Figure 4.12 for both test sections P and PCR. The friction curves exhibit a classical shape with an increase of the friction coefficient in a first phase (due to bitumen removal) and a decrease of the friction coefficient in a second phase (due to polishing of aggregates). Moreover, test section P presents a lower friction coefficient value than test section PCR, but the friction coefficient always stays above 0.40, whatever the number of passes, which indicates a satisfying level of performance.

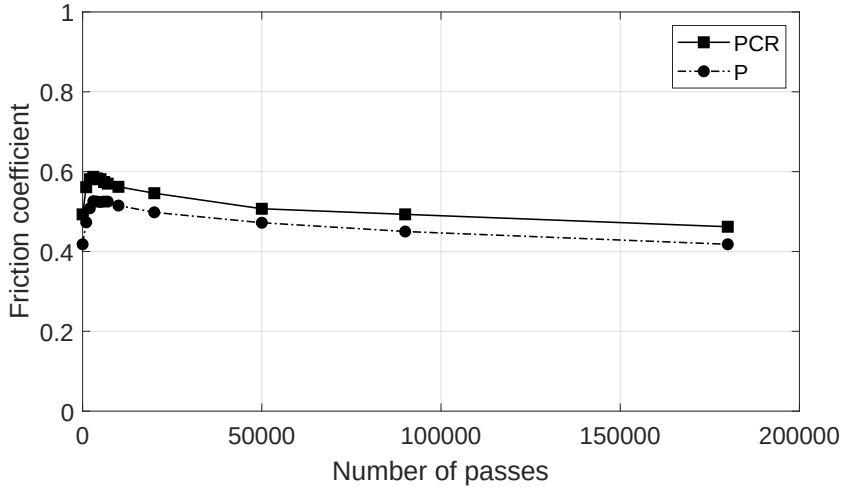

Figure 4.12: Wehner and Schulze test results on the two prototype test sections P and PCR.

4.2 Pass-By acoustical measurements

Pass-by acoustical tests were carried out similarly to those presented in sub-action B2.1 (section 2) and involved a selection of EVs driving on the prototype road surfaces. This concerned both the

standard CPB tests and the noise source analysis with the microphone array, for a comparison of the prototypes with all or some of the previous road surfaces.

4.2.1 Description of the experiment

The experimental procedure was identical to that already implemented in sub-action B2.1 and detailed in section 2.1. The common elements are not duplicated here and only those specific to B2.3 or needing clarification are outlined below.

4.2.1.1 Test site and road surfaces

The test site remains the reference test track of Université Gustave Eiffel in Nantes, France. The different road surfaces considered in this section are reminded in Table 4.5, including the existing test sections A, E1, E3, M2, M3 and N and the prototype test sections P and PCR. Figure 4.13 also gives

Name	Year	Type	Grain size [mm]	MPD [mm]	Color/Marker
A	2006	Porous Asphalt	0/6	1.13	+
E1	2006	Dense Asphalt Concrete	0/10	0.83	×
E3	2016	Stone Mastic Asphalt	0/10	0.91	◇
M2	2001	Very Thin Asphalt Concrete	0/6	1.29	✡
M3	2018	Very Thin Asphalt Concrete	0/4	0.60	○
N	2012	Dense Asphalt Concrete	0/8	0.31	□
P	2020	Very Thin Asphalt Concrete	0/6	0.39	●
PCR	2020	Very Thin Asphalt Concrete	0/6	0.30	■

Table 4.5: Description of road surfaces considered in sub-action B2.3.

a close-up picture of each road surface. The aim of the pass-by noise tests was firstly to study the noise emission of EVs on the prototype tests sections P et PCR and then to compare the results to those of sub-action B2.1 (section 2) performed on the existing test sections. For CPB measurements the results on P and PCR will be compared to all existing test sections and E1 (DAC 0/10) will be considered as the reference road surface. Regarding microphone array measurements, the results on P and PCR will be only compared to available results on test section N (taken as a reference).

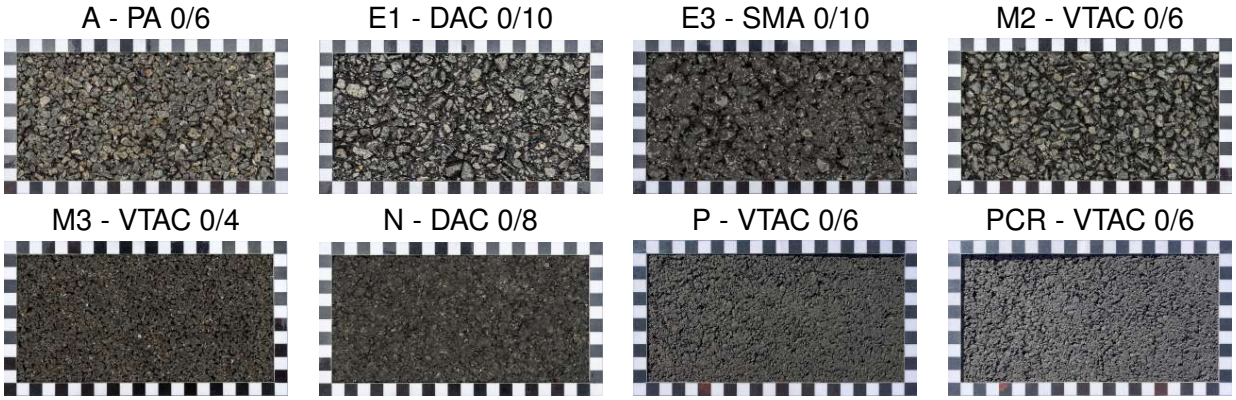

Figure 4.13: Close-up pictures of the 8 road surfaces considered for noise measurement within sub-action B2.3 (frame size: 20 cm by 10 cm).

4.2.1.2 Test vehicles

Three EVs have been tested within sub-action B2.3 for pass-by noise characterisation on the prototype test sections P and PCR (Figure 4.14). The same Renault ZOE (zoe#2) and Renault Kangoo ZE (kze) as in sub-action B2.1 were used, while a different Nissan LEAF (leaf#2) was rented.

Figure 4.14: Pictures of the 3 different types of EV models used within sub-action B2.3.

Each EV is presented in Table 4.6 giving the type, make, model, year and mileage at the time of the test in October 2020. The Nissan LEAF used within this sub-action, namely leaf#2, was older than the one used in sub-action B2.1 (leaf#1). For practical reasons, it was unfortunately not possible to rent the same vehicle at the period of the B2.3 noise measurement campaign.

ID	Type	Segment	Make	Model	Year	Mileage
zoe#2	EV	Supermini	Renault	ZOE	2016	9 131 km
leaf#2	EV	Small family	Nissan	LEAF	2013	91 035 km
kze	EV	Light commercial	Renault	Kangoo ZE	2016	13 263 km

Table 4.6: Description of the EV models tested within sub-action B2.3.

Table 4.7 summarises the main properties of the three EVs in terms of power, propulsion type, battery capacity and curb weight. The properties of the zoe#2 and kze are reminded from Table 2.4. Regarding the leaf#2, the power and battery capacity are smaller than the leaf#1 (Table 2.4), with respectively 80 kW - 24 kWh for the leaf#2 against 110 kW - 40 kWh for the leaf#1. This makes the noise emission with both Nissan LEAF hardly comparable, especially in acceleration driving conditions.

ID	Power	Propulsion type	Battery capacity	Curb weight
zoe#2	65 kW (88 hp)	Front wheel driven	25.6 kWh	1448 kg
leaf#2	80 kW (109 hp)	Front wheel driven	24 kWh	1474 kg
kze	44 kW (60 hp)	Front wheel driven	33 kWh	1450 kg

Table 4.7: Additional properties of the EVs tested within sub-action B2.3.

The properties of the tyres fitted on the EVs are described in Table 4.8. A picture of the tread pattern of each tyre model can be seen in Figure 4.15.

For the zoe#2 and the kze, the same tyres as in sub-action B2.1 have been used. For the Renault ZOE, the difference in mileage comparing to sub-action B2.1 (Table 2.3) was about 3000 km, and thus the wear of the tyres was considered as weak between both measurement campaigns. The tyres on the kze were exclusively used for the project and were not used between both experiments (apart for CRD laboratory tests within action B7), leading to a negligible wear as well. However, the tyres fitted on the leaf#2 were not of the same type as the leaf#1(Table 2.6). The wear of the tyres

ID	Tyre model	Dimensions	HWR	Hardness [Shore A]	Pressure [bars]
zoe#2	Michelin Energy E-V	185/65 R15 88Q	3.4	59.7	2.5
leaf#2	Goodyear Efficient Grip Performance	205/55 R16 91V	3.1	41.7	2.5
kze(front)	Michelin Energy Saver	195/65 R15 95T	3.3	60.0	2.5
kze(rear)	Michelin Energy Saver	195/65 R15 95T	3.3	59.6	2.9

Table 4.8: Description of the tyres fitted on the EVs tested within sub-action B2.3.

on the leaf#2 was also higher than on the leaf#1. Thus, these differences between leaf#1 and leaf#2 in terms of vehicle and tyre models make the pass-by noise comparison on road surfaces involving both EVs definitely not possible.

Figure 4.15: Tread pattern of the tyres fitted on the EVs tested within sub-action B2.3.

4.2.1.3 Description of the pass-by acoustical tests

The pass-by noise measurement campaign on the new sections P and PCR was carried out in October 2020, about one month after the prototype construction. During the vehicle pass-by, CPB and microphone array measurements were performed simultaneously.

Figure 4.16 shows the experimental set-up for each prototype test section. For the sake of visibility, indications for test section P are in blue, while those for test section PCR are in magenta. The CPB microphone was located at the standard position on the road side, 7.50 m from the centre of the vehicle path and 1.20 m above the surface of the test section. In order to limit acoustical impedance discontinuity in the vicinity of the tyre/road noise source, it was decided to put the CPB and the microphone array on the side of the track covering the largest width with P or PCR road surface along the sound propagation path. Therefore, as can be seen on Figure 4.16, testing the left side of the vehicle results in the rolling direction from West to East (W $\mapsto$ E) on test section P, while the opposite direction from East to West (E $\mapsto$ W) was used on test section PCR. The CPB microphone was located 20 meters after the entrance of the prototype area, i.e. at reference point (RP) 2105 m. The microphone array was located 5 meters after the CPB microphone along the driving direction, i.e. at RP 2110 m for tests on P and 2100 m for PCR.

Figure 4.17 gives a picture of pass-by measurement on test sections P (left) and PCR (right) in the case of the Renault Kangoo ZE. The experimental procedure was the same as in sub-action B2.1. Different driving conditions have been tested : pass-by at constant speed by 5 km/h steps, acceleration from a given cruising speed by 10 km/h steps and deceleration from a given cruising speed by 10 km/h steps. The AVAS was deactivated during the tests. The speed range covered during the tests for each driving condition is given in Table 4.9 for each EV/test section configuration. As can be seen, the speed range was more limited on PCR test section due to a limited launching

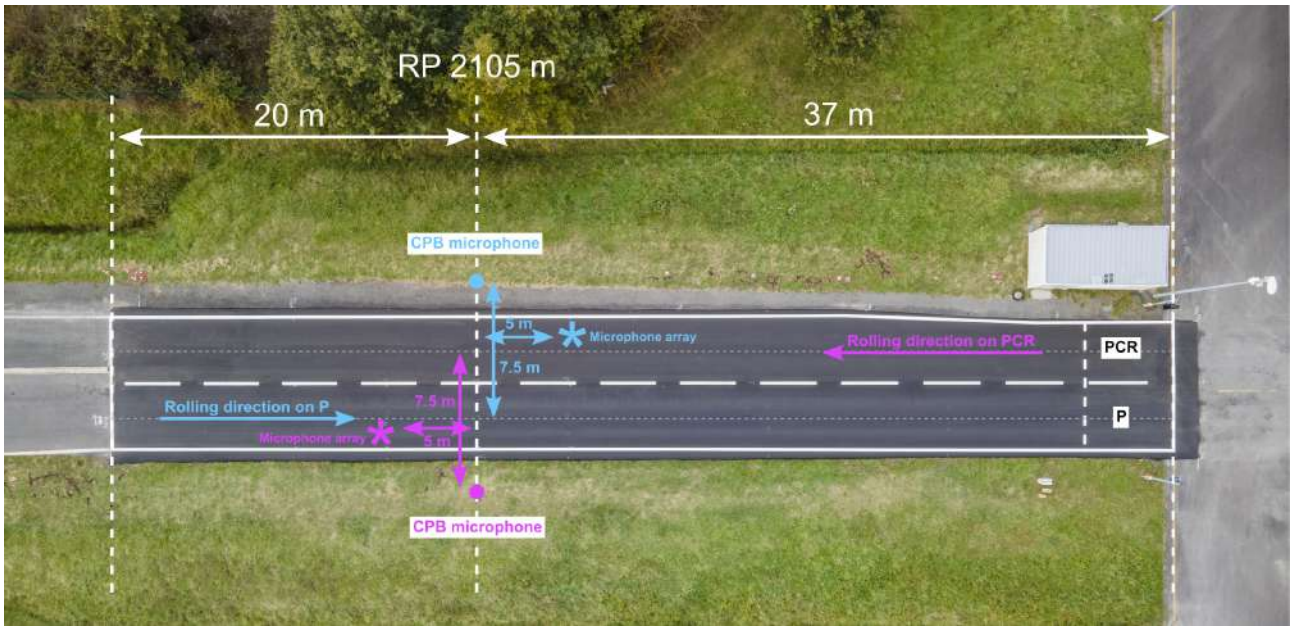

Figure 4.16: Experimental set-up for simultaneous CPB and microphone array tests on the prototype test sections P (in blue) and PCR (in magenta).

distance in the E $\mapsto$ W direction (vehicle starts from the end of the test track). The maximum speed in the E $\mapsto$ W direction is also limited by the power of the EV, e.g. kze.

(a) (b)

Figure 4.17: Pictures of the simultaneous CPB and microphone array tests on the prototype test sections P (a) and PCR (b) in the case of the Renault Kangoo ZE.

4.2.2 CPB results

4.2.2.1 Results at constant speed

The noise analysis method was the same as in sub-action B2.1, section 2.2.1.1. For each run, the maximum overall A-weighted sound pressure level L_{Amax} was identified and corrected from the background noise level. Then, a logarithmic regression versus speed was performed on CPB overall noise levels and for each one-third octave band noise levels in the frequency range between 100 Hz and 5000 Hz. The target reference speed being 50 km/h, the logarithmic regression of noise levels versus vehicle speed was performed in the speed range between 20 km/h and 70 km/h. For the sake

	Driving conditions	zoe#2	leaf#2	kze
P (W $\mapsto$ E)	Constant speed	20 - 110	20 - 110	20 - 110
	Acceleration	0 - 70	0 - 80	0 - 60
	Deceleration	90 - 40	90 - 30	90 - 40
PCR (E $\mapsto$ W)	Constant speed	20 - 90	20 - 90	20 - 75
	Acceleration	0 - 70	0 - 80	0 - 60
	Deceleration	90 - 30	90 - 30	70 - 30

Table 4.9: Speed range V in km/h covered during the experiments for each driving conditions (constant speed, acceleration, deceleration) on test sections P and PCR and for the three tested EVs.

of comparison with P and PCR, from sub-action B2.1 data the regression analysis was recalculated over the same speed range for the existing test sections A, E1, E3, M2, M3 and N. Figure 4.18 illustrates the regression analysis in the case of the leaf#2 rolling on test section PCR.

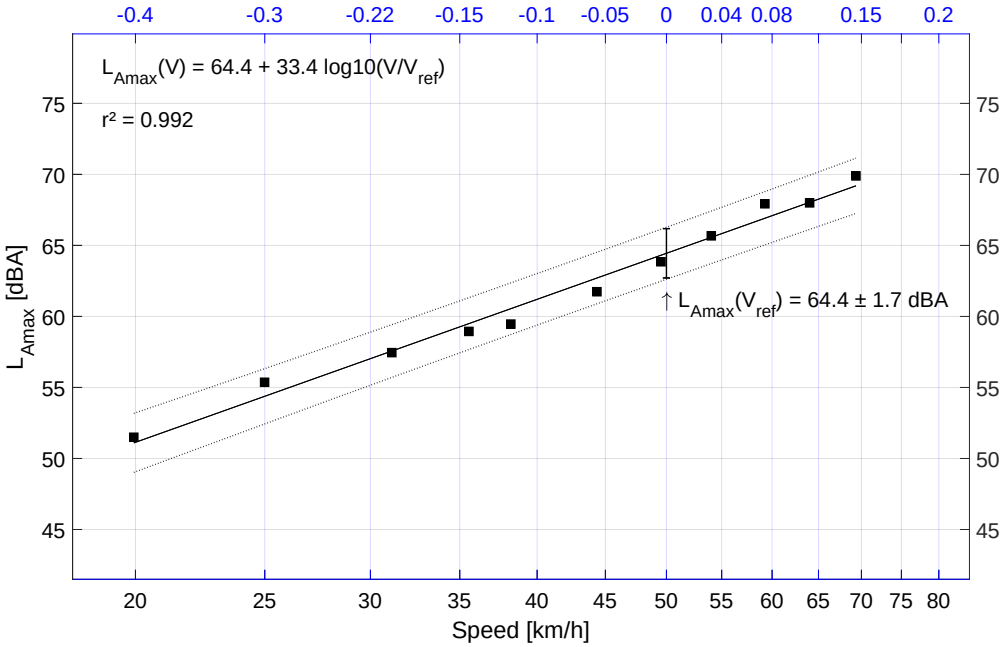

Figure 4.18: Example of logarithmic regression of the overall maximum noise level L_{Amax} versus vehicle speed V in the case of the Nissan LEAF (leaf#2) rolling on the PCR test section in the speed range [20 - 70 km/h].

Table 4.10 gives the results of the regression analysis for the Renault ZOE and the Renault Kangoo ZE. The value of the regression slope $b_{L_{Amax}}$ depends on the configuration and ranges between 30 and 37 dB(A)/dec. The overall CPB noise levels $L_{Amax}(50)$ (not corrected in temperature) at the reference speed of 50 km/h are also given for the 8 test sections.

For the sake of comparison of the different configurations, it is better to consider the overall CPB noise levels corrected in temperature at 20℃ according to Anfosso-Lédée and Pichaud (2007). This is done in Table 4.11. It can be noticed that the zoe#2 is generally louder than the kze. The difference depends on the test section. The kze is about 1.5 dB(A) quieter than the zoe#2 on the prototype test sections P and PCR. The same noise classification is obtained for both EVs, i.e. M3, P, PCR, M2, A, N, E1 and E3 from quietest to loudest road surfaces. The noise reduction at 50 km/h by comparison with the reference surface E1 is 4.2 dB(A) for PCR and 4.7 dB(A) for P in the case of the Renault ZOE#2. It is 3.9 dB(A) for PCR and 4.5 dB(A) for P in the case of the Renault KANGOO ZE.

Renault ZOE#2			
Surface	T_{air} (°C)	$b_{L_{Amax}}$	$L_{Amax}(50)$
A	23.7	34.2 ± 1.8	64.6 ± 0.9
E1	28.7	35.7 ± 1.6	66.5 ± 0.9
E3	28.7	37.1 ± 1.7	67.0 ± 1.0
M2	23.6	33.4 ± 2.2	64.1 ± 1.3
M3	26.8	30.9 ± 1.9	61.9 ± 1.2
N	33.4	36.6 ± 1.7	64.7 ± 0.9
P	12.8	32.9 ± 1.3	63.3 ± 0.7
PCR	13.3	31.7 ± 2.0	63.8 ± 1.1

Renault Kangoo ZE			
Surface	T_{air} (°C)	$b_{L_{Amax}}$	$L_{Amax}(50)$
A	28.8	31.1 ± 1.7	62.6 ± 0.9
E1	21.4	34.6 ± 1.5	65.6 ± 0.9
E3	24.5	36.5 ± 1.8	67.0 ± 1.0
M2	24.8	31.4 ± 1.5	62.7 ± 0.8
M3	21.4	31.4 ± 3.1	59.4 ± 1.9
N	33.7	32.2 ± 1.1	62.9 ± 0.6
P	13.4	33.3 ± 2.6	61.9 ± 1.5
PCR	13.7	34.2 ± 2.1	62.4 ± 1.1

Table 4.10: CPB regression slopes $b_{L_{Amax}}$ (in dB(A)/dec) and overall noise levels $L_{Amax}(50)$ (in dB(A), not corrected in temperature) at 50 km/h for the 8 test sections, available in the speed range [20 - 70 km/h].

Renault ZOE#2		
Surface	$L_{Amax}(50)$	$\Delta\ L_{Amax}(50)$
A	64.8 ± 0.9	-2.5
E1 (Ref)	67.3 ± 0.9	N/A
E3	67.8 ± 1.0	+0.5
M2	64.3 ± 1.3	-3.0
M3	62.3 ± 1.2	-5.0
N	66.0 ± 0.9	-1.3
P	62.6 ± 0.7	-4.7
PCR	63.1 ± 1.1	-4.2

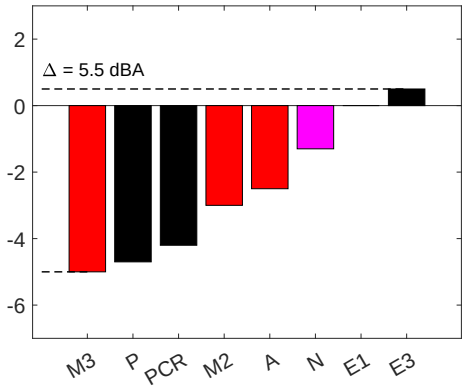

Renault Kangoo ZE		
Surface	$L_{Amax}(50)$	$\Delta\ L_{Amax}(50)$
A	63.1 ± 0.9	-2.6
E1 (Ref)	65.7 ± 0.9	N/A
E3	67.4 ± 1.0	+1.7
M2	63.0 ± 0.8	-2.7
M3	59.4 ± 1.9	-6.3
N	64.3 ± 0.6	-1.4
P	61.2 ± 1.5	-4.5
PCR	61.8 ± 1.1	-3.9

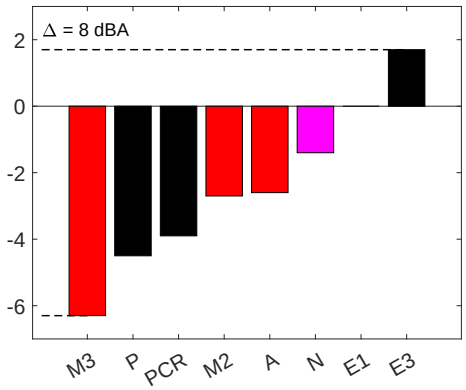

Table 4.11: CPB regression overall noise levels $L_{Amax}(50)$ (in dB(A), corrected at 20°C) at 50 km/h and differences from the reference test section E1 $\Delta\ L_{Amax}(50)$ for the 8 test sections and the 2 EV models tested in the range of speed [20 - 70 km/h].

Table 4.12 gives the CPB overall noise levels for the Nissan LEAF#2 on both prototype test sections P and PCR. For this vehicle, the regression slope is between 30 and 34 dB(A)/dec. Considering the noise levels corrected in temperature, it is observed that the leaf#2 is louder than the zoe#2 by about 0.5 dB(A) on P and PCR test sections. Test section P is 0.6 dB(A) quieter than test section PCR, which remains in the same order as the zoe#2 and the kze.

Surface	T_{air} (°C)	$b_{L_{Amax}}$	$L_{Amax}(50)$	$L_{Amax}(50)$ (20°C)
P	11.6	30.8 ± 2.4	64.0 ± 1.4	63.1 ± 1.4
PCR	12.4	33.4 ± 3.2	64.4 ± 1.7	63.7 ± 1.7

Table 4.12: CPB overall noise levels for the Nissan LEAF (leaf#2) on test sections P and PCR.

CPB noise spectra at the constant speed of 50 km/h are given in Figure 4.19 for the test sections E1, N, P and PCR regarding the Renault ZOE#2 and the Kangoo ZE and only for P and PCR regarding the Nissan LEAF#2. No temperature correction has been applied to the spectral noise levels. For the zoe#2 and the kze, noise spectra have a similar shape on the reference test section E1 and on test section N, with a clear peak at 1000 Hz. On prototype test sections, this peak is attenuated by 5 dB(A) for the zoe#2 and the maximum is shifted at 800 Hz for both P and PCR test sections. For the kze, the peak at 1000 Hz is reduced by 10 dB(A) and the maximum is shifted at 630 Hz for both P and PCR test sections. For this vehicle, a peak at 1250 Hz can be observed, but originating from another source than tyre/road noise (whistling from the motor area). For the zoe#2, a clear peak is also observed at 315 Hz and is reduced by about 5 to 6 dB(A) on the prototype test sections. While having similar spectral shapes, it is clearly observed for the three EVs that noise levels on PCR are slightly higher than noise levels on P in the frequency range between 500 Hz and 1000 Hz, while the opposite is found in the frequency range above 1250 Hz. The same tendency is observed for the Nissan LEAF#2. For this EV, a maximum peak is observed at 630 Hz and a second peak is observed at 1250 Hz on both prototype test sections P and PCR. A third peak is observed at low frequency at 250 Hz.

4.2.2.2 Results at variable speed

The noise analysis method used for pass-bys at variable speed (acceleration and deceleration) is identical to the one previously implemented in sub-action B2.1. Details are given in section 2.2.2.1.

The vehicles Renault ZOE and Renault Kangoo ZE are the same as those previously tested on the various road surfaces in sub-action B2.1. However, the Nissan LEAF #2 being different in generation and tyre, the prototype road surfaces cannot be compared with the other roads all else equal. Both Nissan LEAF models have a similar full acceleration ability, but quite different ones in deceleration without braking, around -2 m/s^2 in sub-action B2.1 but around -0.7 m/s^2 with the leaf#2 tested on P and PCR.

In the figures presented, a focus is made on a comparison of prototype test sections P and PCR with the reference dense surfaces E1 (very common) and N (consistent with ISO 10844).

Acceleration

A description of the acceleration test procedure is given in section 2.1.3.3. The vehicles Renault ZOE#2 and Nissan LEAF#2 have equivalent full acceleration rates. The Renault Kangoo ZE has a lower acceleration ability. In any case, the acceleration rate decreases as the vehicle speed increases. The results are displayed in Figure 4.20. For each vehicle, acceleration rates are identical regardless of the road surfaces, which makes road surface comparison possible. Behaviour may vary with vehicle:

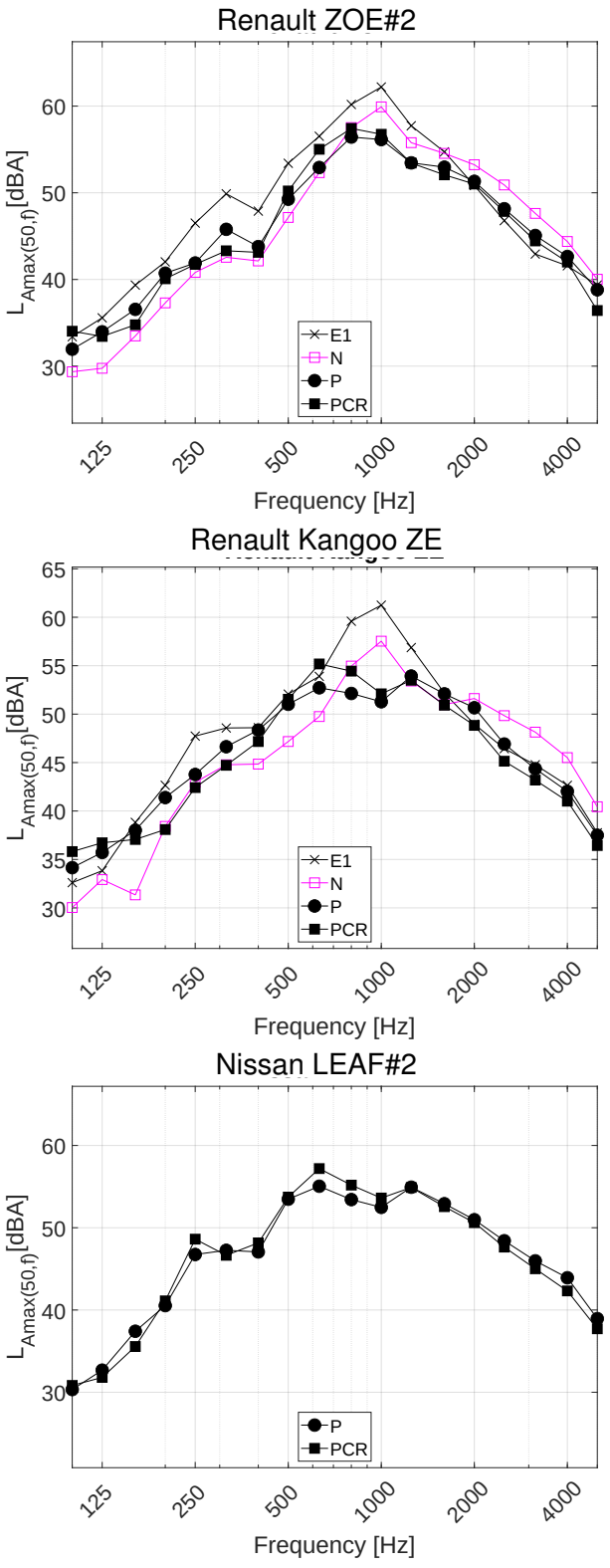

Figure 4.19: CPB noise spectra in dB(A) at 50 km/h obtained from regression in the range of speed [20 - 70 km/h] for the three tested EVs within sub-action B2.3.

- zoe#2: the tests cover an instantaneous speed range from 40 to 80 km/h. Road surface N is the noisiest across the speed range and prototype P is the quietest. The prototype PCR gives noise levels similar to those found on N at speeds 40-50 km/h, while P is close to E1 in this range. The two prototypes behave similarly as the quietest roads above 60 km/h. The unexpected loud behaviour of zoe#2 on PCR mainly comes from the 630 Hz and especially the 800 Hz third octaves, with a very strong emphasis on the vehicle front which might involve significant propulsion noise (see further in section 4.2.3.2). The distinct behaviour on prototype P in the same conditions is still unexplained.
- leaf#2: acceleration tests on both prototype test sections over speed range 40-85 km/h do not report a meaningful noise level difference between the two road surfaces up to 70 km/h. PCR gives an additional 1 dB(A) above 75 km/h.
- kze: over the 35-65 km/h speed range tested, road surfaces N and E1 are the loudest group. Prototype P provides the quietest situation at any speed, in common with PCR within 40-50 km/h. Within 35-40 km/h and 55-65 km/h, PCR happens to give a 0.5-1.5 dB(A) noisier situation than with P.

In most acceleration situations, prototype test section P provides the lowest wayside noise levels at the vehicle pass-by, with a reduction between 0 and 3.5 dB(A) compared with the reference road surface E1. Prototype test section PCR often gives similar performance to P, but is not as effective in several cases. Like at constant speed, the frequency range 630-800 Hz is often highlighted in these situations experienced with the vehicles and distinguishing the prototype test sections.

Deceleration

A description of the deceleration test procedure is given in section 2.1.3.3. Compared with constant speed pass-by, this driving condition involving deceleration with energy recovering without braking does not indicate a wayside overall noise level increase on the 7.5 m microphone with the vehicles tested. Thus, no detailed result is presented in this case.

4.2.3 Investigation of the noise sources

The approach followed for exploring the noise sources of the vehicles driving on the prototype road surfaces is fully identical to that described in section 2.3.1 and results are given according to the same pattern.

4.2.3.1 Main noise sources at constant speed

An illustration of the noise source maps of the 3 EVs tested at a constant speed of 50 km/h on prototype test sections P and PCR is given in Figure 4.21 in overall levels over the frequency range [100 - 5000 Hz]. The breakdown by third-octave can be found in the appendices F and G respectively. For comparison with the same situation on road surface N, please refer to Figure 2.24 (b) and (f) on page 32, and to Figures A.2 and A.6 in appendix A. The Nissan LEAF#2 cannot be directly compared with that of sub-action B2.1 due to differences in vehicle generations and tyres. A material problem introduced uncertainty into the zoe#2 results on PCR, and they have been discarded as a precaution.

For an overview at all speeds on road surfaces N, P and PCR, the noise level at each wheel zone is displayed as a function of speed in Figure 4.22, also in overall levels over the same frequency range, and in appendix H in each one-third octave band.

As a general overview, when comparison is possible it turns out that both prototype road surfaces compared with road N bring an overall noise reduction from both wheel zones at all speeds. The ranking of one prototype over the other is not clear and may vary according to frequency. In more details:

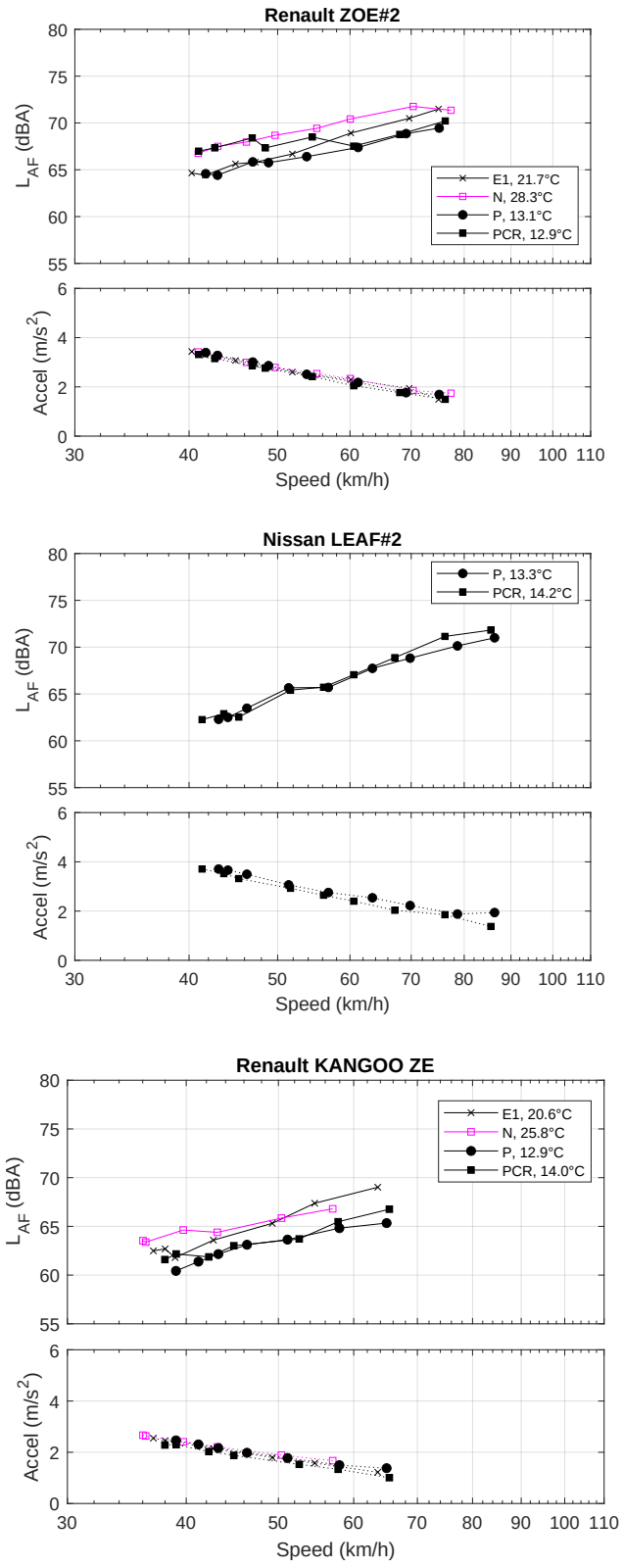

Figure 4.20: A-weighted sound pressure level under full acceleration, measured when the vehicle centre is right to the microphone at 7.5 m (not temperature corrected) – Corresponding acceleration rate of the vehicle.

- zoe#2: at 50 km/h, as well as at all speeds, the prototype road surface P brings noise reduction from wheel zones compared to road N, estimated between 1 and 3 dB(A) depending on speed. The rear one (non driving wheel) remains the louder. The general behaviour is similar in frequency, with a relatively uniform noise reduction across all frequency bands.
- leaf#2: although leaf#1 and leaf#2 cannot be readily compared, the strong predominance of the rear wheel zone (non driving wheel) is a common feature on both vehicles at any speed. At 50 km/h, this is mainly due to contributions in the 500 Hz and 1 kHz third-octave bands, but shifting in frequency with speed and strongly prominent on the rear wheel. There is no significant overall noise level difference between prototypes P and PCR.
- kze: both wheel zones have a different balance on road N or on P/PCR at 50 km/h, the front wheel being the noisier in the latter case and prevailing in the 630 Hz third-octave. The prototype test sections provide a clear noise reduction from the rear position at all speeds, the decrease is lower but effective from the front one. The frequency noise maps at 50 km/h point out the occurrence of the whistling sound previously mentioned in third-octave 1250 Hz (section 2.3.2.1), without interference on the analysis of wheel zone contributions. More generally, test sections P and PCR introduce a reduction over test section N above 800 Hz, but the opposite is true below 630 Hz.

4.2.3.2 Main noise sources at variable speed (acceleration, deceleration)

The three vehicle tested are front-wheel driven, with the electric motor located close to this area.

Noise source behaviour under full acceleration

Compared to constant speed pass-bys, the acceleration condition strongly increases the contribution from the front wheel zone of the Renault ZOE#2 and the Renault Kangoo ZE (Figure 4.23 and 4.24). This increase from the front wheel remains more moderate with the Nissan LEAF#2, despite its acceleration capacities, and the rear wheel zone is continuously dominating at all speeds. Considering the Kangoo ZE, the contribution of its rear wheel zone is unchanged with acceleration, and the front one increases by about 3 dB(A) in the range 40-60 km/h.

When comparing the three road surfaces N, P and PCR for each vehicle under full acceleration:

- zoe#2 gives lower noise levels on prototype test section P than on test section N at all speeds up to 90 km/h, for both wheel zones. The reduction is significant at frequencies beyond 800 Hz (Figure I.1).
- leaf#2 shows no significant noise level difference between both prototype road surfaces P and PCR, both overall and in frequency (Figure I.2).
- The two prototype test sections bring a noise level decrease from both wheel zones of the kze compared with test section N. This can be estimated from -1 to -2.5 dB(A) between N and P on the rear wheel zone (resp. 0 to -3 dB(A) on the front one). In frequency the noise levels with P grow relative to N up to 630 Hz, while they decrease above 800 Hz (Figure I.3).

Noise source behaviour under deceleration

Considering the observations made on the CPB results with the decelerating vehicles in section 4.2.2.2, which indicate no significant effect of deceleration at pass-by, the noise sources are not investigated further in this driving condition on P and PCR.

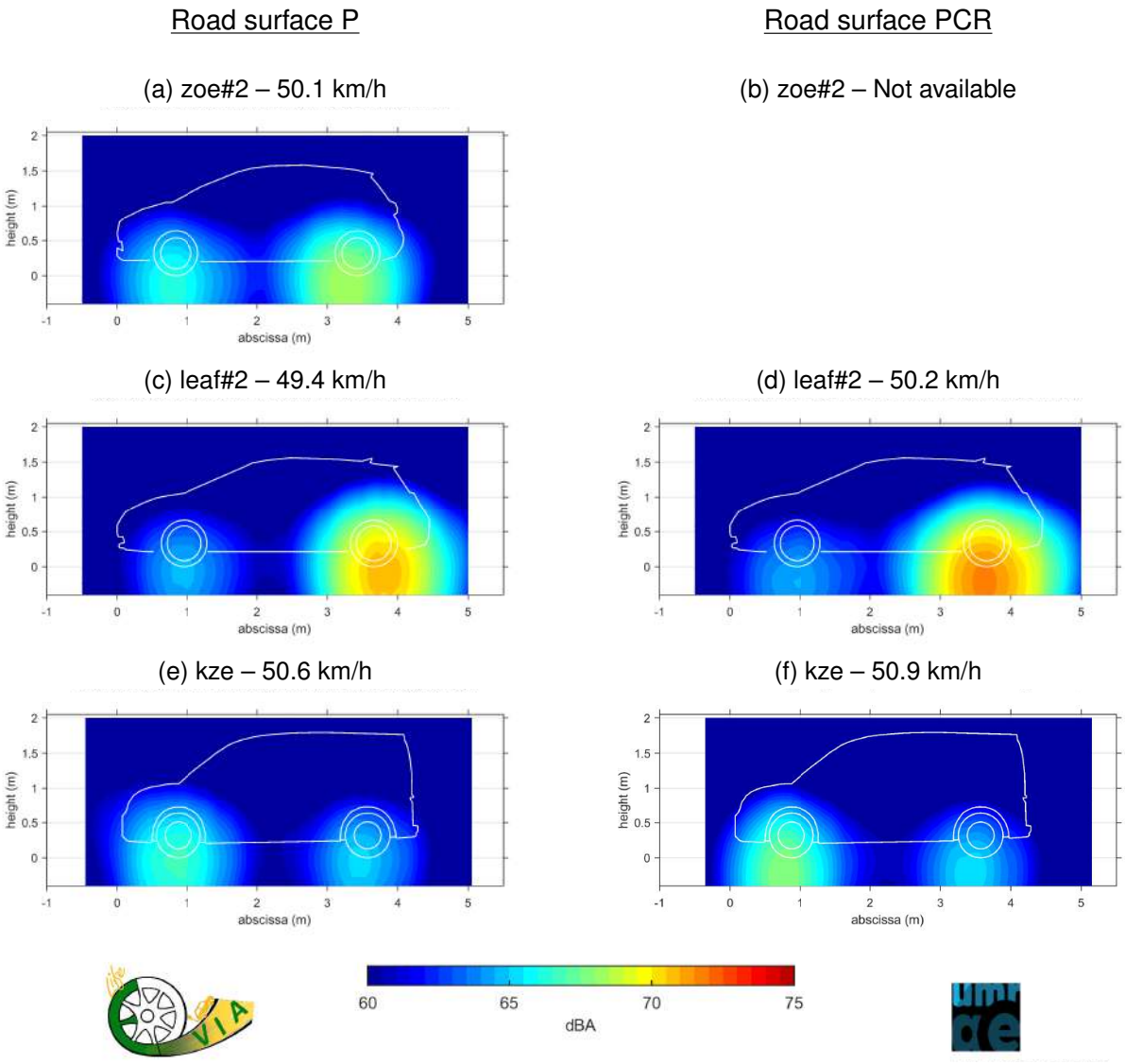

Figure 4.21: Noise source maps of the Renault ZOE#2 (top), the Nissan LEAF#2 (middle) and the Renault Kangoo ZE (bottom) at a constant speed close to 50 km/h on prototype road surfaces P (left) and PCR (right) – A-weighted overall noise levels at the reference distance of 2.7 m – Colour scale in 0.5 dB(A) steps from 60 to 75 dB(A).

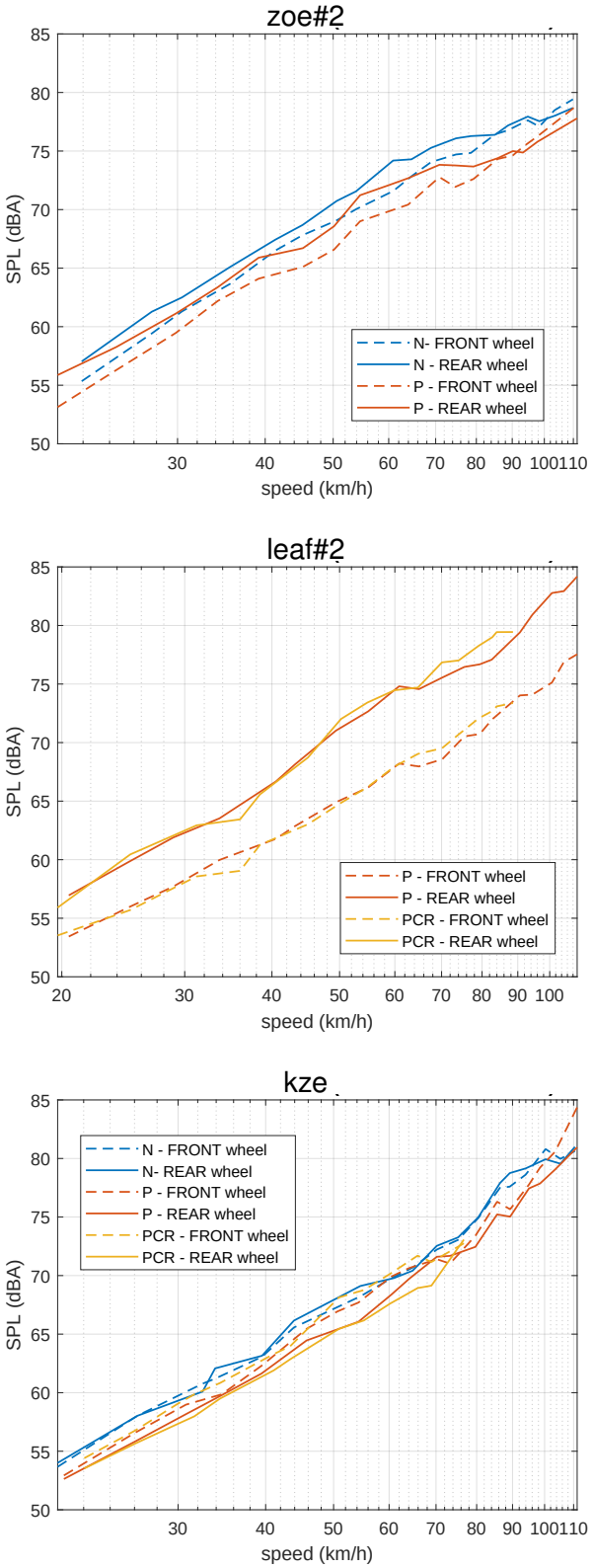

Figure 4.22: Contribution of the front wheel zone (resp. rear wheel zone) of the EVs at constant speed on road surfaces N, P and PCR – A-weighted noise levels in the range [100 - 5000 Hz] at the reference distance of 2.7 m.

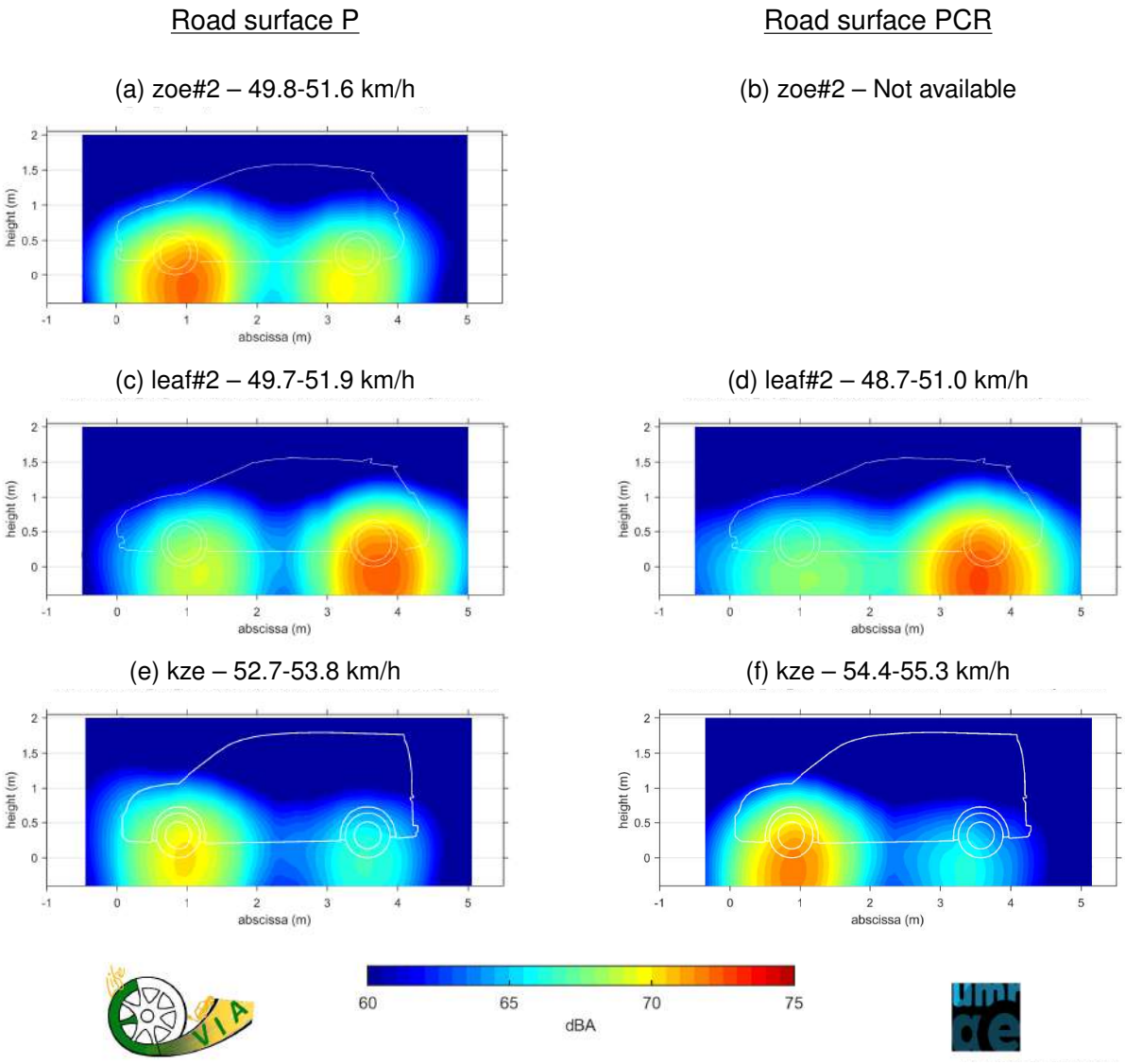

Figure 4.23: Noise source maps of the Renault ZOE#2 (top), Nissan LEAF#2 (middle) and Renault Kangoo ZE (bottom) under full acceleration around 50 km/h on prototype road surface P (left) and PCR (right) – A-weighted overall noise levels at the reference distance of 2.7 m – Colour scale in 0.5 dB(A) steps from 60 to 75 dB(A).

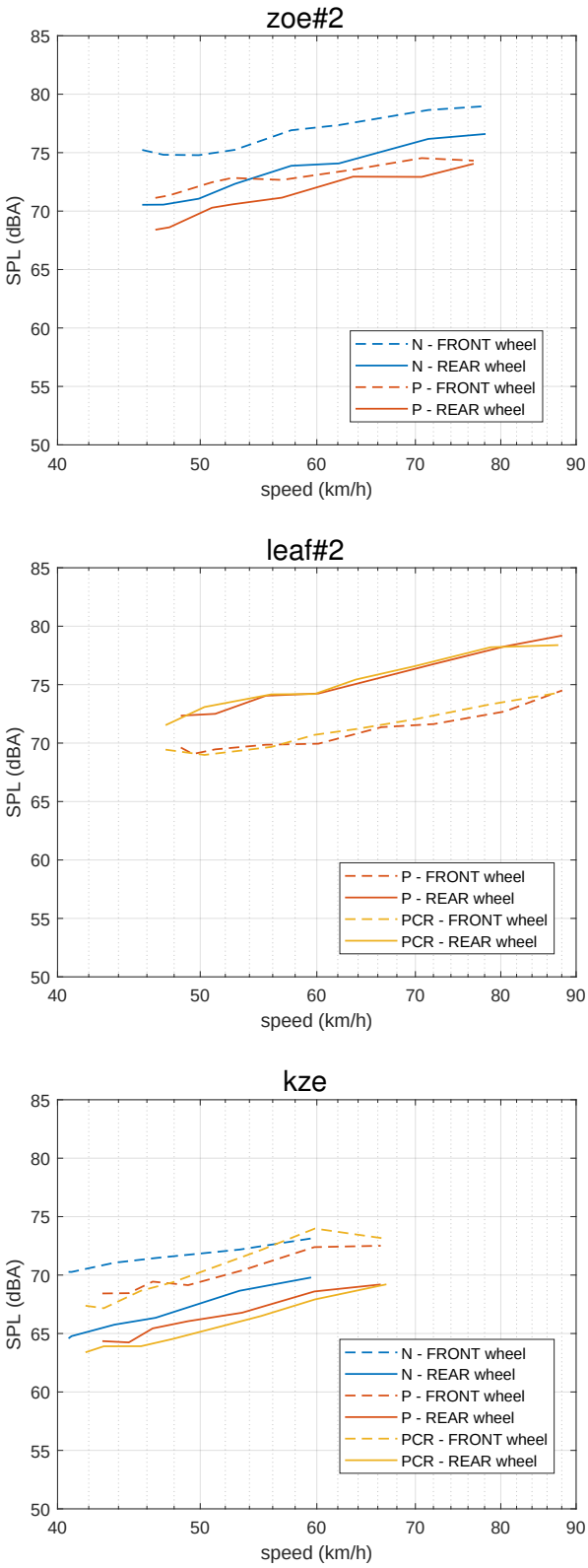

Figure 4.24: Contribution of the front wheel zone (resp. rear wheel zone) of the zoe#2 (top), the leaf#2 (middle) and the kze (bottom) under full acceleration, on road surfaces N, P and PCR – A-weighted noise levels in the range [100 - 5000 Hz] at the reference distance of 2.7 m.

4.3 Coast-By and Close-ProXimity simultaneous measurements

Coast-By (CB) and Close-ProXimity (CPX) simultaneous measurements were performed in June 2021 by UNI EIFFEL on the prototype test sections P and PCR. The procedure is detailed in Cesbron et al. (2020) and is only briefly reminded in this report.

4.3.1 Equipment and procedure

The test vehicle was a passenger car Renault Mégane Scénic 2.0 litres fitted with standard commercial tyres Michelin Energy Saver 195/60 R15 (Figure 4.25). The inflation pressure of the tyres during the tests was 2.2 bars.

Figure 4.25: Test vehicle (left) and standard commercial tyre (right) used for simultaneous CB and CPX tyre/road noise measurements.

The aim was to characterise tyre/road noise over 20 m of the prototype test sections by means of CPX and CB measurements performed simultaneously. The procedure is illustrated on Figure 4.26. Thus, the noise performance of the prototype in the vicinity of the tyre/road interface and at the road side can be compared from data acquired during the same experiment. This procedure also facilitates the study of CPX to CB propagation filter (Cesbron and Klein, 2017).

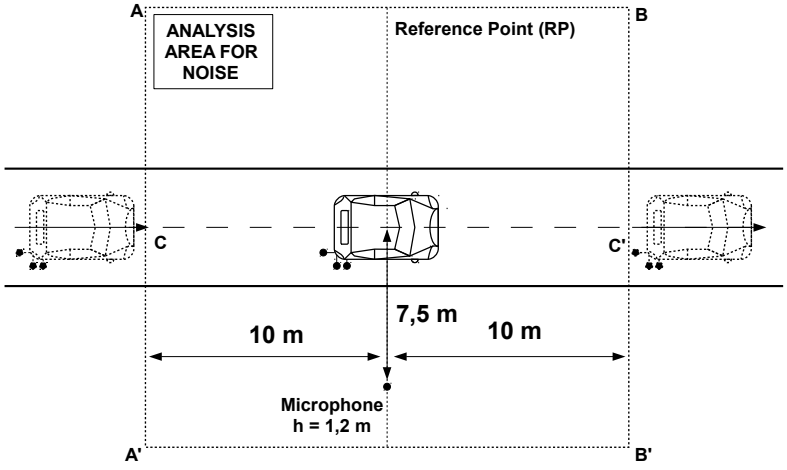

Figure 4.26: Procedure for CPX and CB simultaneous measurements.

During the tests, the vehicle was coasting at a constant speed through the test area between lines AA' and BB' (Figure 4.26). At low speeds (up to 60 km/h), the engine was switched off immediately before the vehicle reaches line AA', while from 65 km/h, the gear was set to neutral in order to minimise engine noise. On each test section, several runs were performed every 5 km/h at steady speed V from 30 km/h to a maximum speed, whose value depends on the rolling direction. In fact, for each prototype test section the tests were performed in the East to West (E $\mapsto$ W) direction up to 70 km/h and in the West to East (W $\mapsto$ E) direction up to 110 km/h. Figure 4.27 gives an example of simultaneous CPX and CB noise measurements on test section P, in the East to West direction. CPX noise measurements were performed according to ISO 11819-2 (2017), while CB measurements were performed according to the method presented in section 2.1.3.1.

Figure 4.27: Simultaneous CPX and CB noise tests on prototype test section P (E $\mapsto$ W direction).

The CPX acquisition system is illustrated in Figure 4.28. It is composed of three microphones close to the right rear wheel of the test vehicle and an infra-red switch for automatic triggering of the signals. The test section was sampled in segments of length Δx = 1.88 m corresponding to one wheel

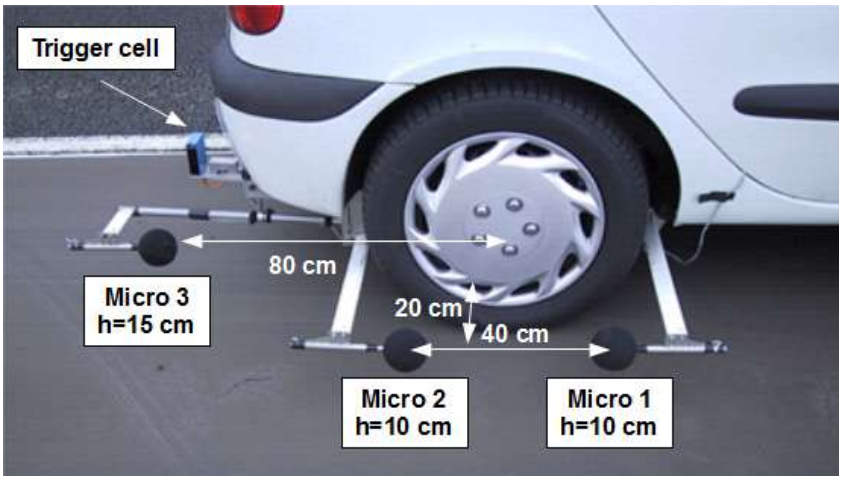

Figure 4.28: CPX measurement system.

revolution. For each interval Δx, the vehicle speed $V(\Delta x)$ was recorded, together with the equivalent sound pressure level per one-third octave band $L_{Aeq,i}(\Delta x, f)$ measured for each microphone position i. Index $i = 1$ stands for the front lateral microphone, while index $i = 2$ stands for the back lateral microphone.

4.3.2 Tyre/road noise analysis method

CB overall and spectral noise levels were analysed trough a logarithmic regression versus speed as explained in Section 2.2.1.1, in Equations (2.6) and (2.7) respectively. However, for each run the speed value used for the regression was the average vehicle speed $V = < V(\Delta x) >$, where $< . >$ denotes the arithmetic average over the CPX samples Δx between lines AA' and BB'.

Regarding CPX, the average one-third octave band noise levels $L_{Aeq,i}(V, f) = < L_{Aeq,i}(\Delta x, f) >$ were calculated for each run. Then, the energetic average of one-third octave band noise levels on lateral microphones 1 and 2 was considered:

$$\forall f, L_{Aeq}(V, f) = 10 \log_{10} \left(\frac{1}{2} \left[10^{\frac{L_{Aeq,1}(V,f)}{10}} + 10^{\frac{L_{Aeq,2}(V,f)}{10}} \right] \right) \tag{4.3}$$

Data of uncovered CPX systems may be affected by airflow noise. In this report, the Signal-to-Noise Ratio threshold (SNR) between the background airflow noise and the CPX noise levels in one-third octave bands was fixed to 6 dB(A). The one-third octave band noise levels below this SNR were not considered for the analysis, following the procedure described in Cesbron et al. (2020).

Then, the recomposed CPX overall noise levels L_{rAeq} were calculated as follows:

$$L_{rAeq}(V) = 10 \log_{10} \left(\sum_{f_1(V)}^{f_2(V)} 10^{\frac{L_{Aeq}(V,f)}{10}} \right) \tag{4.4}$$

where $f_1(V)$ and $f_2(V)$ are respectively the lower and upper valid frequencies at speed V.

Finally, a logarithmic regression versus speed was performed on recomposed CPX overall noise levels L_{rAeq} to identify $a_{L_{rAeq}}$ and $b_{L_{rAeq}}$ similarly to Equation (2.6):

$$L_{rAeq}(V) = a_{L_{rAeq}} + b_{L_{rAeq}} \log_{10}(V) \tag{4.5}$$

A logarithmic regression was also performed on the valid CPX one-third octave band noise levels at frequency f, similarly to Equation (2.7):

$$L_{Aeq}(V, f) = a_{L_{Aeq}}(f) + b_{L_{Aeq}}(f) \log_{10}(V) \tag{4.6}$$

4.3.3 Results

For the sake of comparison of E $\mapsto$ W versus W $\mapsto$ E, the regression analysis of the CB/CPX simultaneous measurements has been restricted to the speed range between 30 and 70 km/h. Considering this speed interval, the valid range of frequencies for the CPX spectral data was between $f_1(V) =$ 315 Hz and $f_2(V) =$ 5000 Hz for all speeds.

Table 4.13 gives the CPX regression slopes and overall recomposed noise levels at the reference speed of 50 km/h. The results are not corrected in temperature in this table. As can be observed, the vehicle direction has very little influence on the CPX results. The regression slopes $b_{L_{rAeq}}$ is on average close to 33 dB(A)/dec on both test sections.

Similarly, Table 4.14 gives the CB regression slopes and overall noise levels at the reference speed of 50 km/h. The results are not corrected in temperature in this table. Due to an unexpected technical issue when analysing data, the W $\mapsto$ E tests on PCR were unreliable and disregarded in

Surface	Direction	T_{air} (°C)	$b_{L_{rAeq}}$	$L_{rAeq}(50)$
P	E $\mapsto$ W	21.4	33.6 $\pm$ 1.7	83.6 $\pm$ 0.6
P	W $\mapsto$ E	21.0	33.0 $\pm$ 1.5	83.7 $\pm$ 0.5
PCR	E $\mapsto$ W	21.4	32.0 $\pm$ 2.3	84.7 $\pm$ 1.1
PCR	W $\mapsto$ E	19.8	34.0 $\pm$ 1.4	84.0 $\pm$ 0.7

Table 4.13: CPX regression slopes $b_{L_{rAeq}}$ (in dB(A)/dec) and overall noise levels $L_{rAeq}(50)$ (in dB(A), not corrected in temperature) at 50 km/h for the two test sections P and PCR in each direction.

Surface	Direction	T_{air} (°C)	$b_{L_{Amax}}$	$L_{Amax}(50)$
P	E $\mapsto$ W	21.4	31.1 $\pm$ 1.5	62.7 $\pm$ 1.0
P	W $\mapsto$ E	21.0	31.2 $\pm$ 1.5	62.5 $\pm$ 0.8
PCR	E $\mapsto$ W	21.4	33.4 $\pm$ 2.3	62.8 $\pm$ 0.8

Table 4.14: CB regression slopes $b_{L_{rAeq}}$ (in dB(A)/dec) and overall noise levels $L_{rAeq}(50)$ (in dB(A), not corrected in temperature) at 50 km/h for the two test sections in each direction.

this study. As can be observed, for test section P the vehicle direction has very little influence on the CB results and the regression slope $b_{L_{Amax}}$ is on average 31.1 dB(A)/dec. The regression slope for PCR in the E $\mapsto$ W direction is slightly higher.

The regression curves are given in Figure 4.29 for both test sections P and PCR in the E $\mapsto$ W vehicle direction for the CPX and the CB tests. The results on the prototype test sections are very similar, with a quite low dispersion of experimental points.

Table 4.15 gives the comparison between recomposed overall CPX noise levels and CB overall noise levels after temperature correction at 20°C, for both test sections P and PCR. Both vehicle directions are considered for test section P, while for test section PCR, the W $\mapsto$ E direction has been disregarded for CB measurements. Regarding test section P, the overall noise levels are almost identical in both vehicle directions, for CPX and CB measurements. However, for test section PCR a difference of 0.7 dB(A) is observed for the CPX noise levels between the W $\mapsto$ E and the E $\mapsto$ W directions. The average CPX noise level at 50 km/h $L_{rAeq}(50)$ is 83.8 dB(A) on test section P and 84.4 dB(A) on test section PCR. Thus, test section P without crumb rubber is 0.6 dB(A) quieter than test section PCR with crumb rubber. However, considering only the W $\mapsto$ E direction, the difference between both prototype test sections is reduced to 0.2 dB(A) which is negligible considering the confidence interval of the regression around 0.5 dB(A) at 50 km/h. Comparing P and PCR test sections in the E $\mapsto$ W direction, the difference between both road surface is also negligible.

Surface	Direction	$L_{rAeq}(50)$	$L_{Amax}(50)$	ΔL
P	E $\mapsto$ W	83.8 $\pm$ 0.6	62.8 $\pm$ 1.0	21.0
P	W $\mapsto$ E	83.8 $\pm$ 0.5	62.6 $\pm$ 0.8	21.2
PCR	E $\mapsto$ W	84.7 $\pm$ 0.7	62.9 $\pm$ 0.8	21.8
PCR	W $\mapsto$ E	84.0 $\pm$ 0.5	-	-

Table 4.15: Comparison between CPX recomposed regressed level L_{rAeq} and CB overall noise levels $L_{Amax}(50)$ (in dB(A), corrected in temperature at 20°C) at 50 km/h for the two prototype test sections.

Finally, the propagation filter ΔL between CB and CPX noise levels is also given in Table 4.15 and is defined as :

$$\Delta L = L_{rAeq} - L_{Amax} \tag{4.7}$$

The value of ΔL ranges between 21 dB(A) and 22 dB(A), which is in agreement with the results of Cesbron and Klein (2017).

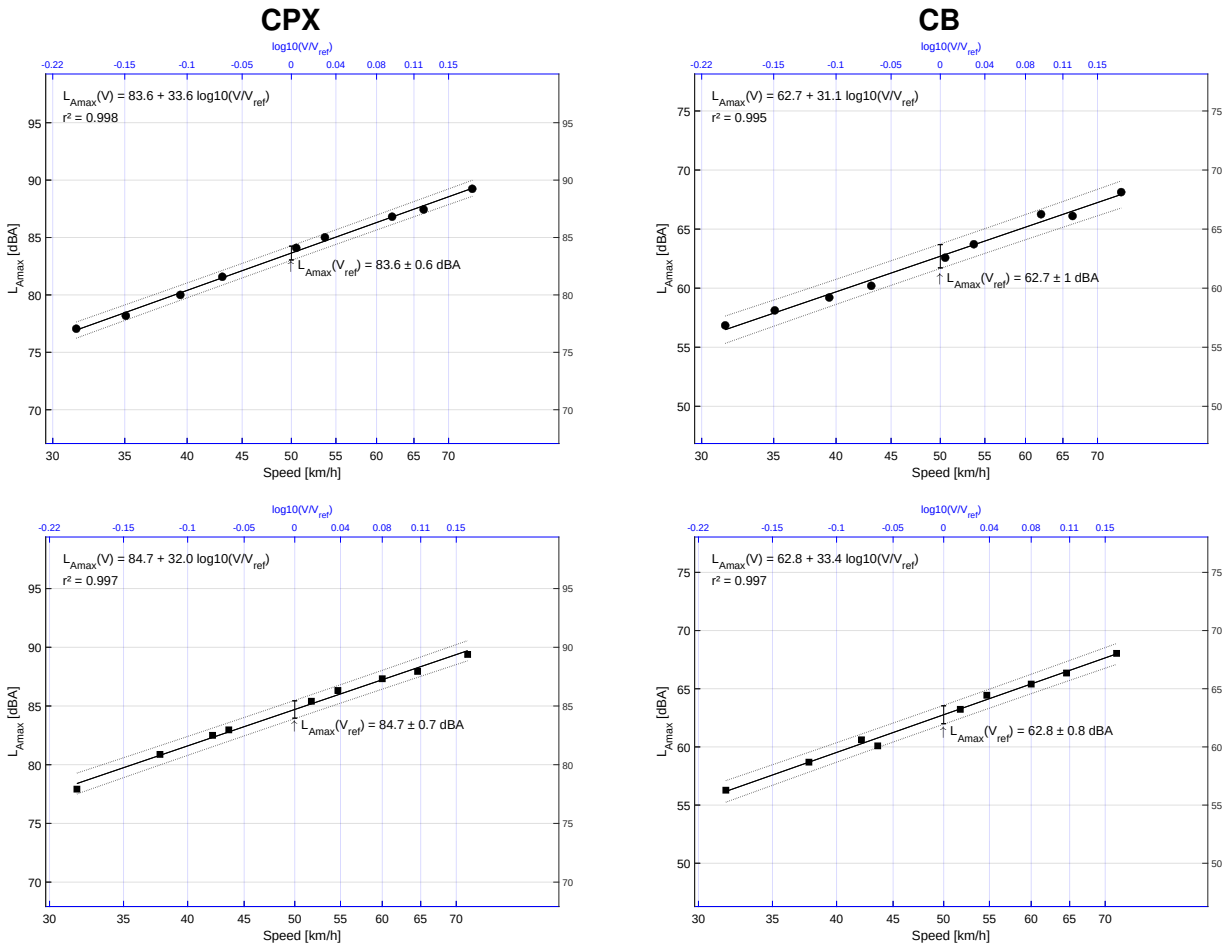

Figure 4.29: CPX (left) and CB (right) overall noise level regression of the prototype test sections P (top) and PCR (bottom) in the E $\mapsto$ W vehicle pass-by direction.

4.4 CPX measurements

Within sub-action B2.3, CPX measurements were performed according to ISO 11819-2 (2017) by UNI EIFFEL in April 2021 and by IPOOL in June 2021 on the reference test track in Nantes. Unlike CPX measurements presented in 4.3, they cover the whole test section length.

4.4.1 UNI EIFFEL CPX measurements

UNI EIFFEL CPX measurements were performed with the same equipment as described in section 4.3, i.e. the passenger car Renault Scénic 2.0 litres fitted with standard commercial tyres Michelin Energy Saver 195/60 R15 (Figure 4.25). The CPX measurement session included the existing test sections A, E1, E3, M2, M3, N for comparison with the prototype test sections P and PCR. The whole length of the test section was included in the analysis and the engine of the vehicle was kept switched on during the tests.

The noise data have been analysed with the same regression analysis procedure as for the simultaneous CB/CPX measurements (section 4.3). On each test section, several runs were performed every 5 km/h at steady speed V from 30 km/h to 70 km/h. For each run, the energetic average of one-third octave band noise levels on lateral microphones was calculated and averaged over the test section. Then, the overall CPX noise level was recomposed from the frequency range between 315 Hz and 5000 Hz. Finally, a logarithmic regression versus speed was performed on recomposed CPX overall noise levels and for each one-third octave band noise levels to get overall noise levels and spectra at 50 km/h.

Figure 4.30 shows the regression curves on the eight tested road surfaces. The dispersion of the measured data is weak. The parameters of the regression curve are given in Table 4.16 for each test section. The value of the slope $b_{L_{rAeq}}$ ranges between 34 and 39 dB(A)/dec. The noise levels $L_{rAeq}(50)$ at the reference speed of 50 km/h are not corrected in temperature in this table.

CPX regressed overall noise			
Surface	T_{air} (°C)	$b_{L_{rAeq}}$	$L_{rAeq}(50)$
A	17.9	34.7 ± 1.4	84.2 ± 0.7
E1	18.6	36.7 ± 0.8	86.8 ± 0.4
E3	18.6	38.9 ± 0.6	87.5 ± 0.3
M2	18.6	35.3 ± 0.7	85.6 ± 0.4
M3	18.0	34.7 ± 1.7	81.9 ± 0.9
N	17.9	35.1 ± 0.4	84.7 ± 0.2
P	18.6	34.6 ± 0.5	83.7 ± 0.2
PCR	17.9	36.0 ± 0.8	84.2 ± 0.4

Table 4.16: CPX regression slopes $b_{L_{rAeq}}$ (in dB(A)/dec) and overall noise levels $L_{rAeq}(50)$ (in dB(A), not corrected in temperature) at 50 km/h for the 8 test sections in the range of speed [30 - 70 km/h].

For proper comparison of CPX noise levels, Table 4.17 gives the regressed CPX overall noise levels at the reference speed of 50 km/h corrected in temperature at 20°C. For the tested tyre, the noise reduction at 50 km/h by comparison with the reference surface E1 is 3.1 dB(A) for P and 2.7 dB(A) for PCR. With a difference of 0.4 dB(A), test section P is slightly quieter than test section PCR. It can be noticed that test sections P and PCR are among the quietest, the noise classification in ascending order being M3, P, PCR, A, N, M2, E1 and E3 respectively. The difference between M3 and E3 is 5.6 dB(A), M3 being about 2 dB(A) quieter than P and PCR.

CPX noise spectra are given in Figure 4.31 for the eight test sections. No temperature correction has been applied to spectral noise levels. Both prototype test sections P and PCR have very similar

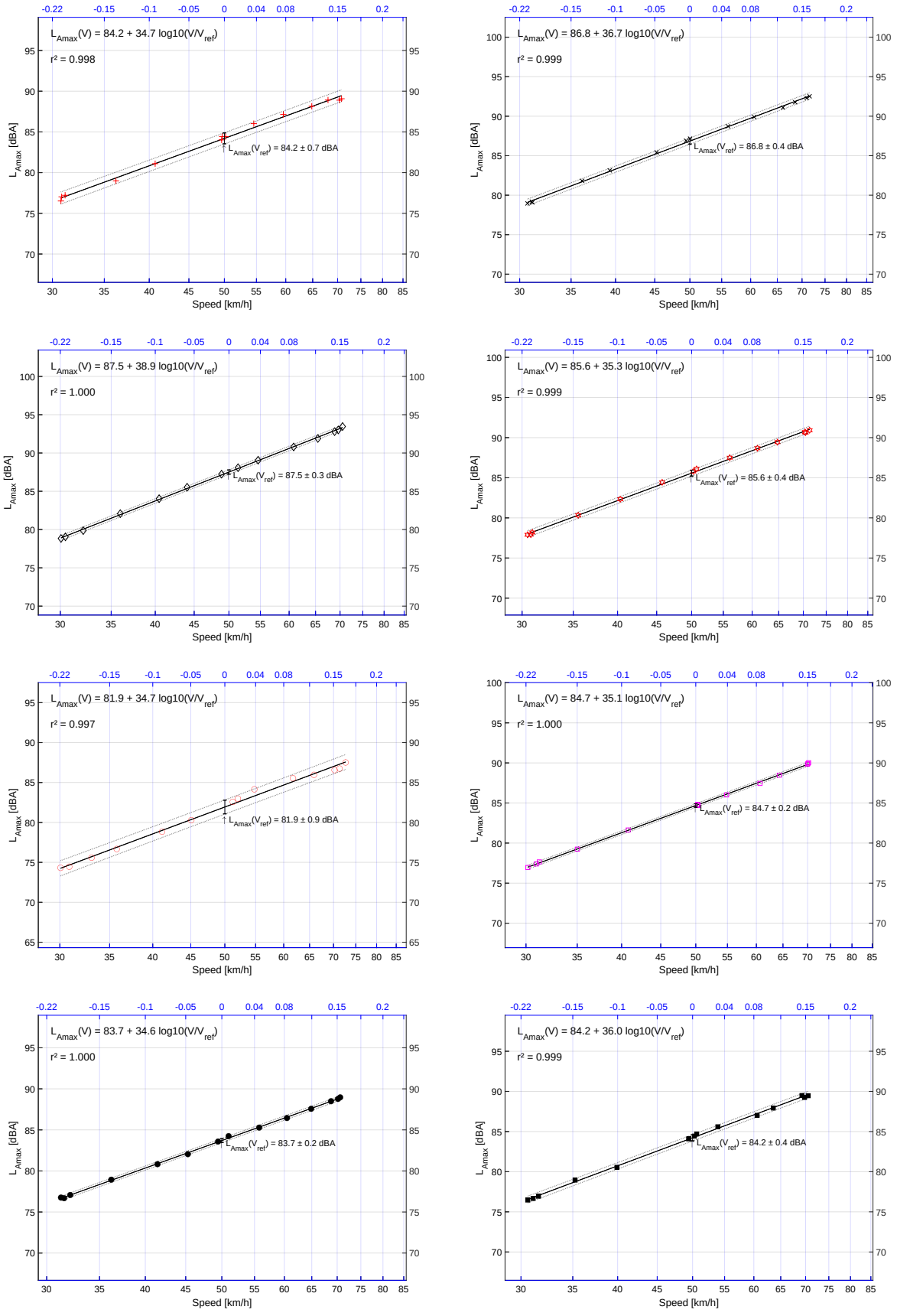

Figure 4.30: Regression analysis on UNI EIFFEL CPX overall noise levels for the existing test sections A, E1, E3, M2, M3, N and the prototype test sections P and PCR.

Surface	$L_{rAeq}(50)$	$\Delta\ L_{rAeq}(50)$
A	84.1 ± 0.7	-2.6
E1 (Ref)	86.7 ± 0.4	N/A
E3	87.4 ± 0.3	+0.7
M2	85.5 ± 0.4	-1.2
M3	81.8 ± 0.9	-4.9
N	84.5 ± 0.2	-2.2
P	83.6 ± 0.2	-3.1
PCR	84.0 ± 0.4	-2.7

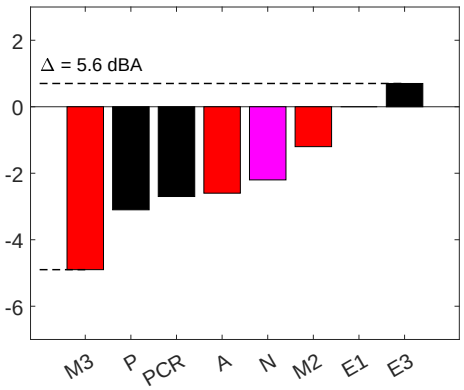

Table 4.17: CPX overall noise levels $L_{rAeq}(50)$ (in dB(A), corrected at 20°C) at 50 km/h and CPX noise difference from the reference test section E1.

spectral shapes. The maximum spectral value for P and PCR is observed at 800 Hz with the Michelin tyre. By comparison with E1, the highest noise reduction is obtained in the frequency range between 630 Hz and 2500 Hz, with a maximum of about 5 dB(A) at 1000 Hz.

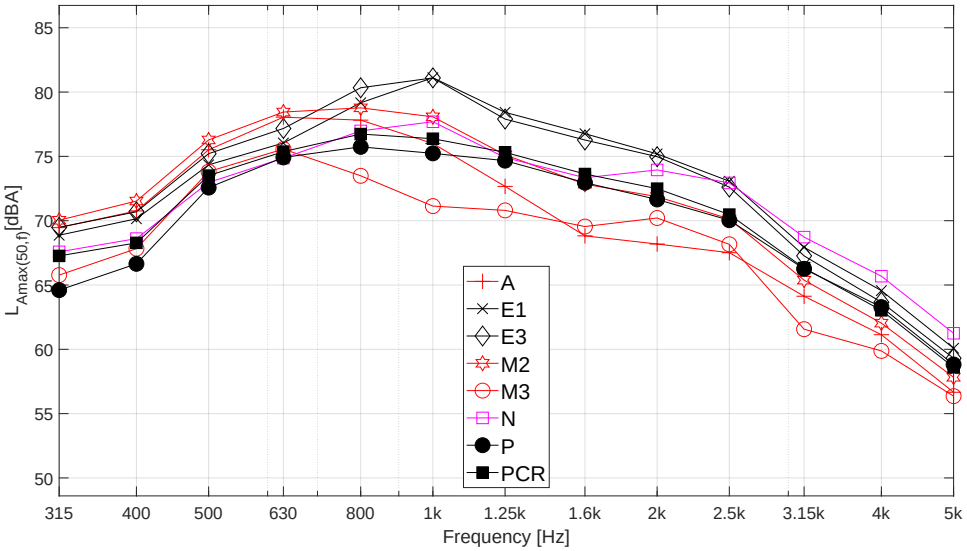

Figure 4.31: CPX noise spectra in dB(A) at 50 km/h regressed from the speed range [30 - 70 km/h].

4.4.2 IPOOL CPX measurements

The test vehicle used by IPOOL for CPX measurements was a Mercedes Vito fitted with SRTT P225/60 R16 according to ISO 11819-3 (2017) (Figure 4.32). For this set of data, the regression analysis has been performed in the speed range between 30 km/h and 110 km/h. The prototype test sections P and PCR have been tested and are compared to the reference test section E1 at the reference speed of 50 km/h. The overall noise levels have been corrected in temperature at 20°C and in tyre hardness.

In Figure 4.33, the test section has been subdivided into sections of 20.20 m over its whole length and the CPX noise levels have been averaged over each section of 20.20 m. The overall median value over the test section is also plotted for the three test sections E1, P and PCR. The Green

Figure 4.32: Test vehicle (left) and SRTT tyres (right) used by IPOOL for CPX measurements.

Public Procurement (GPP, Commission (2016)) noise limit value plus 1 dB(A) and plus 2 dB(A) are also plotted. The 57 m long test sections P and PCR comprise 3 samples, while the 200 m long test section E1 comprises 10 samples. It can be seen that the CPX noise values are far below the GPP limits for the three test sections.

Table 4.18 gives the regressed CPX overall noise levels at the reference speed of 50 km/h. For the SRTT tyre, the noise reduction by comparison with the reference road surface E1 is 1.7 dB(A) for P and 2.4 dB(A) for PCR. Opposite to the Michelin Energy tyre tested by UNI EIFFEL, for the SRTT tyre the PCR test section turns out to be 0.7 dB(A) quieter than the P test section. Both prototype test sections meet the Core criterion of the GPP for a low-noise pavement fixing the CPX noise level at 50 km/h for the SRTT tyre below 90 dB(A). The PCR test section is even close to the Comprehensive criterion of the GPP for a low-noise pavement fixing the CPX noise level at 50 km/h for the SRTT tyre below 87 dB(A).

Surface	$L_{rAeq}(50)$	$\Delta\ L_{rAeq}(50)$
E1 (Ref)	90.2 $\pm$ 0.8	N/A
P	88.5 $\pm$ 1.5	-1.7
PCR	87.8 $\pm$ 1.3	-2.4

Table 4.18: CPX overall noise levels $L_{rAeq}(50)$ (in dB(A), corrected at 20°C and in SRTT tyre hardness) at 50 km/h and CPX noise difference from the reference test section E1.

Figure 4.34 gives the regressed CPX noise level spectrum between 315 Hz and 5000 Hz at 50 km/h in the case of the SRTT tyre for the three test sections E1, P and PCR. No temperature correction is included in these data. For the SRTT tyre, the maximum observed at 800 Hz for the reference test section E1 is clearly shifted to 630 Hz for both prototype test sections P and PCR. As for the Michelin tyre, the noise spectra have very similar shapes for P and PCR. It turns out that P is slightly louder than PCR at frequencies between 1600 Hz and 5000 Hz. By comparison with E1, the highest noise reduction with P and PCR is obtained in the frequency range between 800 Hz and 1600 Hz, with a maximum of about 4 dB(A) at 1000 Hz, which is in the same order of magnitude as the Michelin Energy tyre.

4.5 Synthesis of sub-action B2.3

Within sub-action B2.3, the prototype test sections P and PCR have been fully characterised in terms of road surface properties and in terms of noise emission by pass-by and close-proximity tests. The

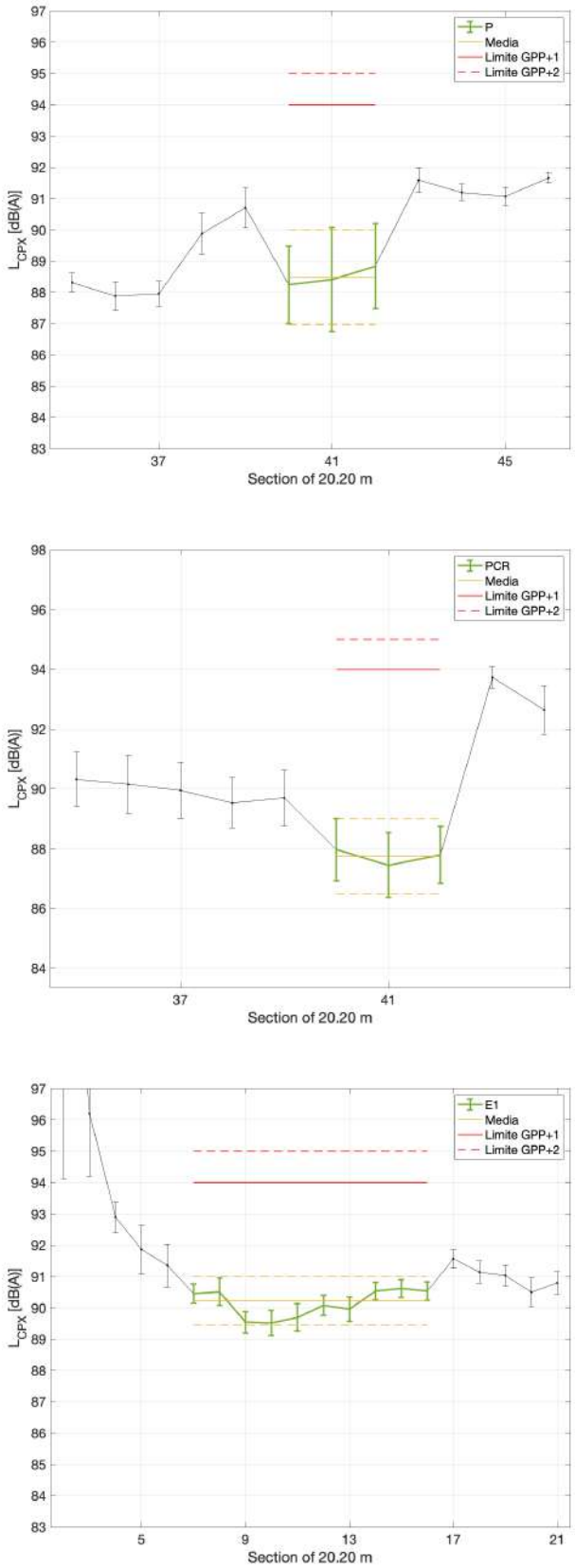

Figure 4.33: CPX overall noise levels averaged every 20.20 m for the SRTT tyre tested by IPOOL on test sections P, PCR and E1 (from top to bottom).

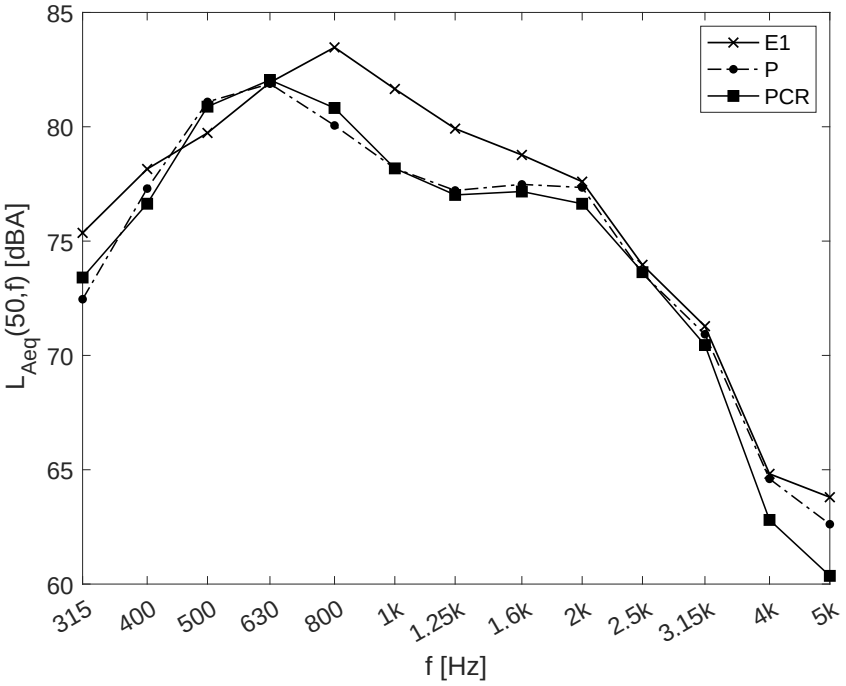

Figure 4.34: CPX noise spectra IPOOL.

measurements were performed in autumn 2020 and in spring 2021. Let's remind that P and PCR are VTAC 0/6 based on the same formulation, but PCR mix contains 1.9% of crumb rubber by weight.

Regarding 3D texture measurements, quite low MPD and surface texture levels have been measured for both prototype test sections. By comparison with other test sections, very low MPD values have been measured for P (0.39 mm) and PCR (0.30 mm), which is in the same order of magnitude as the ISO 10844 test section N. Similarly, texture levels of test sections P and PCR are quite similar to that of test section N for wavelengths ranging between 8 mm and 160 mm and become higher at shorter wavelength.

The measured acoustical absorption was relatively low on both P and PCR test sections, with a maximum absorption coefficient below 0.3 at 2500 Hz, which is weak by comparison with existing test sections A (PA 0/6) and M3 (VTAC 0/6). However, it is of the same order of magnitude as the existing test section M2 of the same kind (VTAC 0/6, sound absorption peak at 630 Hz), but shifted at higher frequencies.

Regarding the dynamic stiffness, it was unexpectedly lower on test section P without crumb rubber than on test section PCR containing crumb rubber. The dynamic stiffness for both prototype test sections is of the same order of magnitude as a conventional asphalt concrete DAC 0/10 and very much higher than the dynamic stiffness of a low-noise PERS composed of a large amount of rubber aggregates.

The skid resistance of test section P and PCR was assessed by different manners. The values of ETD confirmed the low-macro-texture of the test sections P and PCR, close to the threshold value of 0.4 mm, which is the regulatory limit on French roads. The friction coefficient values measured with the British Pendulum and T2GO devices on P and PCR were however between 70 and 82.5, which is very satisfactory on both prototype pavements. Moreover, the evolution of the friction coefficient as a function of polishing cycles was studied with the W&S machine and the friction coefficient stays above 0.40, whatever the number of passes, which indicates a satisfying level of performance.

Pass-by acoustical tests have been performed on P and PCR test sections by means of simultaneous CPB and microphone array measurements. Three EVs have been tested, namely a Renault ZOE, a Renault Kangoo ZE and a Nissan LEAF. Different driving conditions (constant speed, acceleration and deceleration) have been considered during the pass-by tests.

Concerning CPB tests at constant speed, by comparison with existing test sections, P and PCR were among the quietest road surfaces for the Renault ZOE and Kangooo ZE. At 50 km/h, the overall CPB noise level reduction for the prototype test sections, by comparison with the reference test section E1, was on average 4.4 dB(A) for the Renault ZOE and 4.2 dB(A) for the Renault Kangoo ZE. The noise spectra show a significant noise reduction in the range between 630 Hz and 1600 Hz, thus removing the peak observed at 1000 Hz for reference test section E1. For the three tested vehicles, test section P without crumb rubber was about 0.6 dB(A) quieter than test section PCR. This is mainly due to a higher noise emission on PCR in the frequency range between 630 Hz and 800 Hz. The same tendency was observed in accelerating conditions, with prototype test section P providing the lowest pass-by noise levels and a reduction up to 3.5 dB(A) by comparison with the reference road surface E1, depending on the speed range and the tested EV. Prototype test section PCR shows similar performance than P, but is less effective in several cases. For deceleration tests in regenerative braking mode, there was no significant difference in the behaviour of the prototype test sections P and PCR by comparison with the constant speed.

Concerning the microphone array measurements, the noise sources are located close to the vehicle wheels. It turns out that both prototype test section P and PCR, when compared to test section N, bring an overall noise level reduction for both wheel zones over the whole speed range. There is no clear tendency regarding the ranking of both prototypes, which may vary with the EV model and with the frequency. Knowing that the three EVs are front-wheel driven, in acceleration condition the front wheel noise contribution strongly increases for the Renault ZOE and the Kangoo ZE. For the Renault Kangoo ZE, the noise at the front wheel zone increases by about 3 dB(A) in the speed range between 40 km/h and 60 km/h. This increase at the front wheel is more moderate for the Nissan LEAF, whose rear wheel remains the dominant noise source at all speeds.

Simultaneous Coast-By (CB) and Close-Proximity (CPX) tyre/road noise measurements have also been performed on the prototype test sections. An ICEV Renault Mégane Scénic was used and fitted with Michelin Energy Saver 195/60 R15 tyres. The test sections have been tested in both East to West and West to East directions in the speed range between 30 km/h and 70 km/h. The results of the regression analysis have been compared. The values of the regression slope were very close in both directions and ranged between 31 and 34 dB(A)/dec for the CB and the CPX tests. This is a common value for tyre/road noise. On test section P, the overall noise levels were almost identical in both vehicle directions, for CPX and CB measurements. However, for test section PCR a difference of 0.7 dB(A) was observed for the CPX noise levels between the W $\mapsto$ E and the E $\mapsto$ W directions. Considering CPX data, it turned out that test section P was 0.6 dB(A) quieter than test section PCR at 50 km/h. Regarding the CB overall noise levels, no significant difference was observed between P and PCR test sections. The propagation filter between CB and CPX noise levels was between 21 dB(A) and 22 dB(A), which is consistent with literature.

CPX measurements have been performed according to ISO 11819-2 by UNI EIFFEL and IPOOL. For UNI EIFFEL, using the Michelin Energy Saver 195/60 R15, the prototype test sections P and PCR have been compared to the six existing test sections A, E1, E3, M2, M3 and N. P and PCR are among the quietest test sections, with a noise reduction at 50 km/h by comparison with the reference surface E1 of 3.1 dB(A) for P and 2.7 dB(A) for PCR. The noise reduction in the frequency domain is the most important around 1000 Hz (-5 dB(A) by comparison with test section E1). For IPOOL, the SRTT 225/60 R16 tyre of ISO 11819-3 was used. The noise reduction by comparison with E1 was 1.7 dB(A) for P and 2.4 dB(A) for PCR. Both prototype test sections meet the Core criterion of the GPP for a low-noise pavement fixing the CPX noise level at 50 km/h below 90 dB(A). However, the

Comprehensive criterion of the GPP fixing the CPX noise level at 50 km/h below 87 dB(A) was not reached, although close in the case of PCR.

Finally, CPX and CPB results have shown a significant overall noise reduction with both prototype test sections P and PCR by comparison with the reference test section E1. From spectral noise levels, this noise reduction can be mainly attributed to the noise reduction at 1000 Hz for P and PCR, and a frequency shift of the maximum noise level towards 630 Hz and 800 Hz. This abatement can be mainly attributed to the low texture levels of the prototype test sections by comparison with the reference road surface, leading to a reduction of tyre vibration. From Klein and Cesbron (2020), it has been found that the maximum spectral noise level for road surfaces with relatively high texture levels like E1 is located at 1000 Hz independently of the vehicle speed. On the contrary, for road surfaces with low texture levels as P and PCR, the maximum spectral noise level is speed dependent and is mainly influenced by the tread pattern pitch. Thus, tread pattern impacts play a major role in the noise emission for this kind of road surfaces with low texture levels. This aspect will be further investigated within sub-action B2.4. The sound absorption of P and PCR, although limited, may also partly explain the noise reduction with respect to track N above 1600 Hz. Considering all the measured configurations, test section P without crumb rubber was about 0.5 dB(A) quieter than test section PCR, which may be explained by the lower dynamic stiffness measured on test section P. The lower noise levels for P by comparison with PCR in the frequency range between 500 Hz and 1000 Hz may be explained by the lower dynamic stiffness measured for P, reducing the magnitude of tyre tread impacts and then noise levels in the medium frequency range (Beckenbauer, 2001). However, the inverse result was observed for the SRTT tyre, test section PCR being 0.7 dB(A) quieter than test section P.

5 Sub-action B2.4 – Selection of optimised EV tyres

For the selection of optimised EV tyres, CRD delivered carved prototype tyres to UNI EIFFEL for testing on the prototype test surface before autumn 2021. These tyres were technical demonstrators for testing various concepts which were investigated in action B7 at the time tyres needed to be built to be delivered to UNI EIFFEL in time for testing. The tyres are of a size which is representative for the European EV market (within the constraints given by admissible tyre sizes on the test vehicles). Independent of the state of action B7, the delivered tyres included a set of reference tyres which were representative for the standard European summer replacement market at the time of testing. The other tyres were intended to be for example tread pattern, construction and/or compound variations of the reference, aiming at optimising the balance of exterior noise performance and other tyre performances (e.g. rolling resistance, grip) for EV vehicles.

Using the mentioned tyres, UNI EIFFEL has performed constant speed and accelerated pass-by noise measurements according to UNECE R51.03 and CPX measurements on the prototype test section and further standard road surfaces. To assess the different influence of electric and internal combustion vehicles on exterior noise, the pass-by measurements were performed using EV and ICE test vehicles which were chosen based on the outcome of action A3, i.e. both the EV and the ICEV being representative for the respective markets. Because UNI EIFFEL did not have the appropriate test vehicles in their possession which fulfil these conditions, suitable cars were rented for testing.

The outcome of the noise measurement will be used as input for further investigations in action B7 and will be an initial recommendation for the tyres to be delivered for the EV festival in action B3. The optimised tyres will also be tested on the test section in Florence within B4 by IPOOL.

5.1 Pass-by noise measurements according to UNECE R51.03

5.1.1 Description of the experiment

5.1.1.1 Outline of the protocol R51.03

Regulation No 51.03 of the Economic Commission for Europe of the United Nations (UNECE, 2018) gives provisions for the approval of motor vehicles with regard to sound emissions. In particular, it provides sound level limits for driving vehicles in conditions combining constant speed and acceleration tests around 50 km/h, supposed to be representative of noise emission in normal urban driving situations. This includes both propulsion and rolling noise contributions.

At the basis of the test conditions is the power-to-mass ratio index (PMR) of the vehicle to be tested, given by the dimensionless quantity[1]:

$$PMR = \left(\frac{P_n}{m_{ro}}\right) 1000 \text{ kg/kW} \tag{5.1}$$

where P_n is the rated total engine net power in kW and m_{ro} the mass in running order in kg. The PMR helps to define the typical acceleration in urban traffic:

$$a_{urban} = 0.63 \log_{10}(PMR) - 0.09 \tag{5.2}$$

and the reference acceleration:

$$a_{wot,ref} = 1.59 \log_{10}(PMR) - 1.41 \quad \text{for } PMR \geq 25 \tag{5.3}$$

Both acceleration values guide the identification of the acceleration condition to be practically implemented in the drive-by tests, mainly the gear ratio to be selected when a gearbox is available on the vehicle tested. The same gear ratio shall be used for the constant speed test (cruise-by).

[1] For light vehicles, the PMR is also the determining parameter of the vehicle noise limit value allowed for type approval.

As a final result representing the noise emitted by the vehicle in urban driving situation, the noise level L_{urban} is:

$$L_{urban} = L_{wot} - k_p \left(L_{wot} - L_{crs} \right) \tag{5.4}$$

where L_{wot} is the reported noise level derived from the full acceleration tests and L_{crs} is the reported noise level derived from the constant speed tests. In brief, the weighting factor k_p gives the part power factor by linking the urban acceleration a_{urban} and the full acceleration, however with variants according to the characteristics of the vehicle under test.

For details and technicalities of implementation, reference to the text of the regulation is required. It will be described next in the specific cases of the two tested vehicles. For the purposes of the E-VIA project, some experimental recommendations of R51.03 have been adapted and will be specified when appropriate. The comparison of the prototype tyre versions in sub-action B2.4 focuses on the indicators L_{crs} and L_{wot}.

5.1.1.2 Implementation on the test road surfaces

Whereas type approval according to R51.03 involves driving on a surface that complies with ISO 10844 for qualifying a vehicle model, the E-VIA context considers the two prototype surfaces P and PCR implemented on the reference test track of UNI EIFFEL and described in section 3.

5.1.1.2.1 Setup and constraints

On each prototype road surface, a 20 m long test section is used, longitudinally centred on the microphone position (position PP') and extending from -10 m (position AA') to +10 m (position BB') in the direction of motion (Figure 5.1). In order to comply as much as possible with a uniform road surface width between the lane centre and the microphone, only one microphone located on the most suitable roadside is used and the vehicle drives alternately in either direction to allow investigation of both vehicle sides. Thus, the locations of AA' and BB' are interchanged depending on the driving direction during the test.

Figure 5.1: Setup of the experiment over the 20 m long test section of prototype road surface PCR.

The microphone is at a height of 1.2 m over the road plane and is 7.5 m away from the track axis. According to the respective track widths available, this distance corresponds to:

- prototype P: 5.8 m of road surface, 1.4 m of gravel surface and 0.3 m of grass width (Figure 5.2 left),
- prototype PCR: 5.97 m of road surface and 1.53 m of grass width (Figure 5.2 right).

Figure 5.2: Location of the microphone at 7.5 m relatively to the tested track: prototype test section P (left), prototype test section PCR (right).

There is no main obstacle to soundfield in the vicinity of the test section.

Measuring the left vehicle side at pass-by means driving from west to east on prototype test section P, but from east to west on prototype test section PCR.

5.1.1.2.2 Determination of vehicle kinematics

As outlined above in section 5.1.1.1, two driving conditions are investigated. In order pass-bys to be considered as valid, speed requirements shall be fulfilled, relatively to a predefined reference point on the vehicle. For a vehicle with a front motor/engine, the reference point is the foremost point of the vehicle, leading to the requirements:

- pass-by at constant speed: a speed of 50 ± 1 km/h from the reference point entering the test section in AA' to the vehicle rear end leaving it in BB',
- pass-by under acceleration: a specified acceleration condition from the time the reference point on the vehicle crosses AA' until the vehicle rear end crosses BB', and a speed of 50 ± 1 km/h when the reference point faces the microphone position at PP'.

The validity check requires reading the speeds $v_{AA'}$, $v_{BB'}$ and $v_{PP'}$, in relation to the vehicle's position. For a simultaneous assessment of vehicle position and speed at the significant locations on the test section, a combination of five 5 m apart infrared cells, spread from AA' to BB' along the test section, and of three reflecting plates carefully marked from front to rear on the vehicle side have been used. The detection of the reflecting plates passing successively in front of the cells provides samples of the vehicle's position over time. A polynomial of degree 3 may be reasonably fitted to the samples (Figure 5.3). It allows the further determination of the crossing time of the reference point or rear end of the vehicle at typical locations and, consequently, the speed at these times by using the polynomial of degree 2, first derivative of the previous one.

Incidentally, this processing may also highlight the vehicle position and speed at the time of the maximum pass-by noise level L_{Amax}.

The average acceleration of the valid pass-by over the test section is calculated in accordance with regulation R51.03:

$$a_{wot,test} = \frac{\left(\frac{v_{AA'}}{3.6}\right)^2 - \left(\frac{v_{BB'}}{3.6}\right)^2}{2(20 + l)} \tag{5.5}$$

where l is the vehicle length. $v_{AA'}$ and $v_{BB'}$ are in km/h in this formula.

5.1.1.3 Vehicles and pass-by test conditions

5.1.1.3.1 Vehicle characteristics

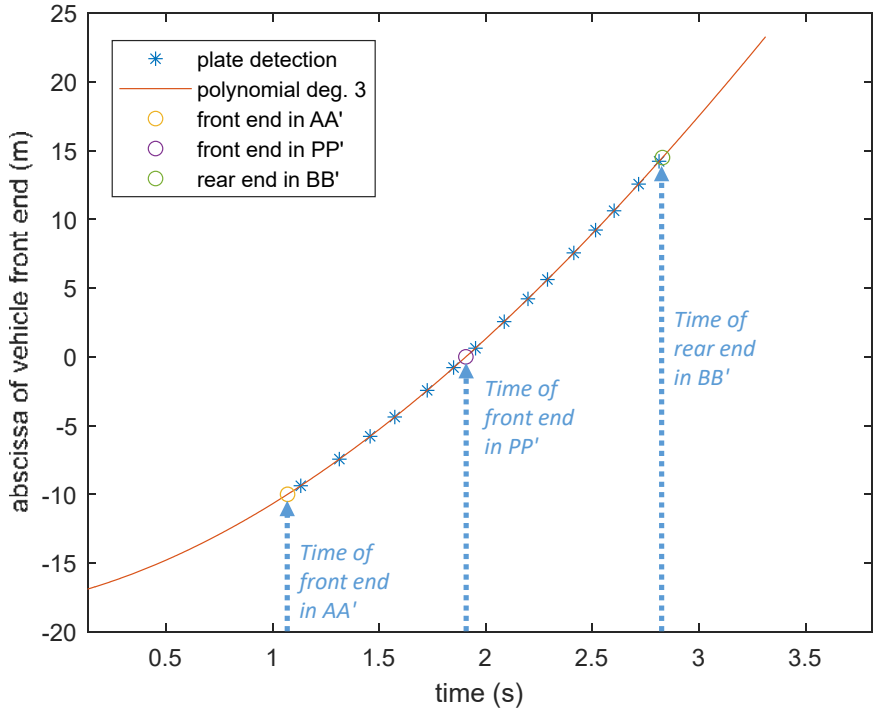

Figure 5.3: Position of the foremost point of the vehicle as a function of time during a pass-by under acceleration – Detection of the reflecting plates (∗), polynomial of degree 3 (—), specific vehicle positions (O).

The tests involve two vehicles:

- an electric Nissan LEAF (Figure 5.4 left). It is the same car as the one previously used in B2.1 tests ('leaf#1' of section 2.1.2).
- an ICE Renault KADJAR (Figure 5.4 right).

The main characteristics of these vehicles are given in Table 5.1[2].

Figure 5.4: Nissan LEAF (left) and Renault KADJAR (right) fitted with one set of test tyres and three reflecting plates.

5.1.1.3.2 Pass-by conditions with the Nissan LEAF

[2]The power value of the Nissan LEAF differs from the one previously given in Table 2.4, which is the maximum motor power, whereas the maximum net power in Table 5.1 represents the maximum 30 minute power of the vehicle.

ID	LEAF	KADJAR
Type	EV	ICEV
Energy	electricity	petrol
Make & model	Nissan LEAF	Renault KADJAR
Year	2019	2020
Mileage	7 143 km	16 985 km
Propulsion type	front wheel driven	front wheel driven
Number of gears	1	6
Mass in running order (m_{ro})	1580 kg	1408 kg
Max. net power P_n	90 kW	103 kW

Table 5.1: Characteristics of the vehicles tested within sub-action B2.4.

Using Equations (5.1) to (5.4) and data in Table 5.1, the R51.03 characteristic quantities of the Nissan LEAF are:

$$\begin{aligned} PMR &= 57.0 \\ a_{urban} &= 1.02\ m/s^2 \\ a_{wot,ref} &= 1.38\ m/s^2 \end{aligned}$$

The Nissan LEAF has a transmission with only one gear ratio. Then, the full acceleration achieved should be used instead of $a_{wot,ref}$, according to R51.03. Preliminary tests showed that full acceleration over the test section and satisfying $v_{PP'} = 50\ km/h$ corresponds to a test acceleration of about $4.1\ m/s^2$. Although an acceleration value not greater than $2.0\ m/s^2$ is recommended, it was decided to keep the full acceleration value for the acceleration tests, in order to investigate the demanding rolling conditions allowed by the vehicle. Practically, the test acceleration was in the range $[4.0, 4.2]\ m/s^2$ for all valid runs.

The runs at the constant speed 50 km/h were made with cruise control. This allowed a high repeatability of the tests.

5.1.1.3.3 Pass-by conditions with the Renault KADJAR

Using Equations 5.1 to 5.4 and data in Table 5.1, the R51.03 characteristic quantities of the Renault KADJAR are:

$$\begin{aligned} PMR &= 73.2 \\ a_{urban} &= 1.08\ m/s^2 \\ a_{wot,ref} &= 1.55\ m/s^2 \end{aligned}$$

Preliminary tests were conducted to determine the appropriate gear for the acceleration tests. No gear ratio can provide both a full acceleration close to $a_{wot,ref}$ and a speed $v_{PP'}$ of 50 km/h. This speed is possible with a full acceleration of $1.35\ m/s^2$ in gear 4, lower than $a_{wot,ref}$, and a full acceleration exceeding $2\ m/s^2$ in gear 3. In compliance with R51.03, gear 4 is selected as the sole gear ratio suitable for the acceleration tests. Practically, the test acceleration was within the range $[1.2, 1.5]\ m/s^2$ for all valid runs.

Accordingly, the cruise-by tests, achieved at the constant speed $50\ km/h$, were made with gear 4.

5.1.1.4 Optimized EV tyres

Six versions of technical demonstrator tyres of dimension 205/55 R16, named V1 to V6, have been designed for electric vehicles by Continental Reifen Deutschland (CRD) within Action B7 of LIFE E-VIA (see (Hoever, 2022) for details). Version V1 is the reference tyre version. A complete set of four

identical tyres on rims is available in each version, the wheels being alternately fitted to the electric test vehicle Nissan LEAF and the ICE test vehicle Renault KADJAR (see subsection 5.1.1.3). The four tyres in a set are strictly identified so that they are always mounted in the same position on either vehicle.

Tyres were inflated in accordance with the car manufacturer's recommendations:

- Nissan LEAF: 2.5 bars on front and rear tyres
- Renault KADJAR: 2.3 bars on front tyres and 2.1 bars on rear tyres

Before each measurement series, tyres were brought to normal operating temperature by a preliminary drive.

5.1.1.5 Environmental conditions

The measurements were taken from 23 to 26 August 2021. Weather conditions were consistent with the requirements of R51.03. A weather station was available at trackside to monitor air temperature and wind speed. In addition, the temperature of each tyre tread as well as the road surface temperature were measured at the beginning and at the end of each series of measurements involving a tyre version and a prototype road surface (i.e. constant speed and acceleration tests). Figure 5.5 gathers the temperature conditions for all tyre and road surface configurations, respectively for each vehicle:

- the tyre temperature is the average of the 8 measures (all 4 tyres of the vehicle at the beginning and end of a series),
- the road surface temperature is the average of the 2 measures (beginning and end of a series),
- the air temperature is the average of the measures recorded for all the valid pass-bys of a series.

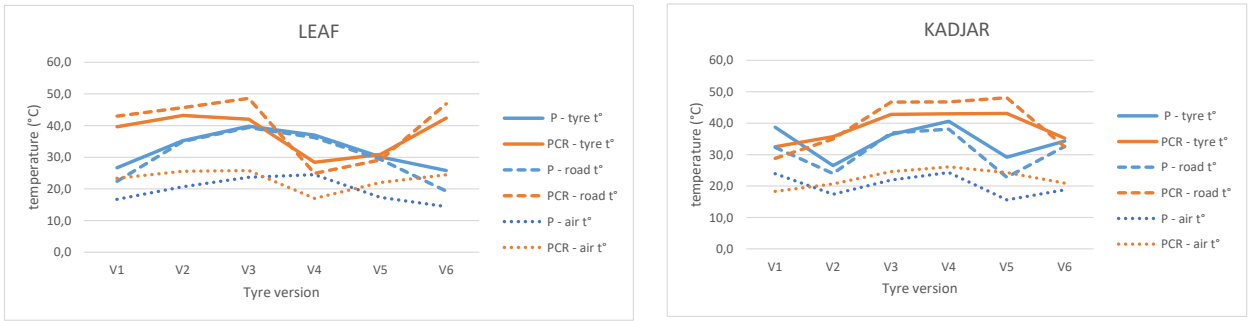

Figure 5.5: Temperature conditions during the tests with the Nissan LEAF (left) and the Renault KADJAR (right) on prototype test sections P (blue) and PCR (red) – tyre temperature (full line), road surface temperature (dashed line), air temperature (dotted line).

The background noise was recorded at the beginning of each constant speed and each acceleration series, for a duration larger than 30 seconds. In each case, the overall A-weighted average sound pressure level L_{bkgd} has been calculated and also its spectrum in one-third octave bands. The difference between the overall background noise and the measured sound of the vehicles under acceleration is always larger than 15 dB(A). This is also the case most of the time at constant speed, but it can go down to 14 or 13 dB(A) in some cases. A continuous correction has been subtracted from the readings, according to:

$$L_{corr} = L_{meas} + 10 \log_{10} \left(1 - 10^{\Delta/10}\right) \tag{5.6}$$

where L_{corr} is the corrected pass-by noise level, calculated from the measured pass-by noise level L_{meas} and the difference $\Delta = L_{meas} - L_{bkgd}$ between pass-by and background noise levels. No correction is applied to spectra in third-octave bands.

5.1.2 Overall noise results of the tyre versions

5.1.2.1 Acoustic indicators and processing

The analysis is focused on the maximum A-weighted sound pressure level indicated during each passage of the vehicle between the two lines AA' and BB', at constant speed and under full acceleration. In either case, the measured noise value is rounded to the first significant digit after the decimal place. At least four valid measurements for each constant speed test (resp. at least three valid measurements for each acceleration test) were made on each vehicle side. To be valid, the noise levels on a given side shall lie within a range of 2 dB(A). The valid results of each side are corrected with respect to background noise (see section 5.1.1.5) and then averaged separately.

Although not included in regulation R51.03, a temperature correction has been applied to the constant speed noise levels $L_{crs,corr}$ to provide corrected noise levels at the reference surface temperature $\theta_{ref} = 20$ ℃, following the indication used for tyre type approval in Regulation 117 [3]:

$$L_{crs,corr}(\theta_{ref}) = L_{crs,corr}(\theta) + K(\theta_{ref} - \theta) \tag{5.7}$$

where θ is the test surface temperature during measurement (see section 5.1.1.5), and $K = -0.03$ dB(A)/℃ when $\theta > \theta_{ref}$ and $K = -0.06$ dB(A)/℃ when $\theta < \theta_{ref}$ (United Nations, 2011). The quantity $L_{crs,corr}(\theta_{ref})$ is the noise level reported for pass-bys at 50 km/h, separately for each vehicle side. For the sake of simplicity, it is called $L_{Amax,crs}$ in the following.

No temperature correction for roadside noise levels under acceleration is widely acknowledged. The quantity $L_{crs,corr}(\theta)$ at the measurement road surface temperature θ is the noise level reported for pass-bys under acceleration, separately for each vehicle side. It is called $L_{Amax,wot}$ in the following.

5.1.2.2 Synthesis of results

The six tyres versions are compared for each vehicle separately, successively in each driving condition.

Nissan LEAF at constant speed

The reported noise levels at the constant speed of 50 km/h are given in Table 5.2 and plotted in Figure 5.6. Table 5.2 also informs on the standard deviation and the range[4] Δ of the valid noise levels included. All tyre versions provide a louder pass-by noise on prototype test section P than on prototype test section PCR, with an average difference of 0.7 dB(A) over the six tyre types and both vehicle sides. Differences between road surfaces are the smallest with tyre versions V1 and V6.

The maximum pass-by noise level at 50 km/h is always slightly larger on the left vehicle side than on the right vehicle side when driving on prototype test section P. However, the opposite is true on prototype test section PCR. One might expect a rather symmetrical noise behaviour of this vehicle. A slight track slope combined with a reverse direction for the same vehicle side from one road prototype to the other due to the reversed setup (cf. section 5.1.1.2) might be a parameter explaining this behaviour.

In any case tyre version V3 happens to be the loudest on either road surface. Versions V2 and V6 are the quietest on P, V2 and V4 on PCR. With reference to version V1, except V3 which increases

[3] Regulation 117 involves measurements at vehicle coast-by, i.e. with engine off. In the present case, rolling noise is supposed to be predominant.

[4] Difference between the maximum and the minimum values of $L_{Amax,crs}$.

	Road surface	P			PCR		
	Vehicle side	left	right	average	left	right	average
V1	$L_{Amax,crs}$	60.6	60.6	60.6	60.1	60.4	60.2
	std	*0.15*	*0.35*		*0.30*	*0.21*	
	Δ	*0.41*	*0.82*		*0.82*	*0.51*	
V2	$L_{Amax,crs}$	60.8	59.9	60.3	59.5	59.5	59.5
	std	*0.29*	*0.17*		*0.38*	*0.22*	
	Δ	*0.82*	*0.40*		*0.94*	*0.52*	
V3	$L_{Amax,crs}$	61.2	60.9	61.1	60.1	60.5	60.3
	std	*0.17*	*0.29*		*0.18*	*0.35*	
	Δ	*0.41*	*0.82*		*0.42*	*0.94*	
V4	$L_{Amax,crs}$	60.9	60.5	60.7	59.4	59.7	59.6
	std	*0.38*	*0.09*		*0.12*	*0.11*	
	Δ	*0.94*	*0.21*		*0.31*	*0.31*	
V5	$L_{Amax,crs}$	60.7	60.4	60.6	59.5	60.0	59.8
	std	*0.37*	*0.09*		*0.21*	*0.11*	
	Δ	*0.93*	*0.21*		*0.51*	*0.31*	
V6	$L_{Amax,crs}$	60.4	60.2	60.3	59.8	60.0	59.9
	std	*0.17*	*0.19*		*0.18*	*0.19*	
	Δ	*0.31*	*0.52*		*0.41*	*0.51*	

Table 5.2: Nissan LEAF at constant speed 50 km/h. Reported noise level $L_{Amax,crs}$, standard deviation std and range of values Δ of the valid pass-bys in dB(A), for each tyre version on road surfaces P and PCR. Left and right vehicle sides, average of both sides.

noise, all other tyre versions give a lower noise level, the best tyre/road configurations being V2 and V4 on prototype road surface PCR (Figure 5.7).

The maximum noise level of the LEAF at this constant speed occurs within a position range of the foremost vehicle point between 2.2 m before and 3 m after the microphone location, the latter corresponding to about 2 m after pass-by of the front wheel right to microphone. It is possibly often associated with noise emission from the front part of the vehicle.

Nissan LEAF under acceleration

Due to the strong contact forces with the high acceleration rate tested with the Nissan LEAF, the differences between tyre versions are hightened (Table 5.3 and Figure 5.8). However, on average over tyre versions and sides, the difference between road prototypes is only 0.4 dB(A), PCR being again the quieter.

As with constant speed, there is a trend for a difference between sides, reversed between one and the other prototype and in line with the slight difference in the acceleration rate with the direction.

Under strong acceleration, tyre version V2 is the quietest on both road surfaces, the loudest ones being V3 and V6. Compared with the reference tyre V1, V4 and V5 also provide a noise reduction, lower than 0.5 dB(A) and only on prototype test section PCR (Figure 5.9).

The maximum noise level of the LEAF under full acceleration occurs after the pass-by of the vehicle in front of the microphone, within a position range that roughly extends up to 5 m (exceptionally 5.7 m) after pass-by of the rearmost vehicle point right to microphone location. It is most likely associated with noise emission from the rear part of the vehicle. At these positions, the instantaneous speed of the accelerating vehicle is much higher than 50 km/h (56 to 58 km/h, exceptionally 59 km/h).

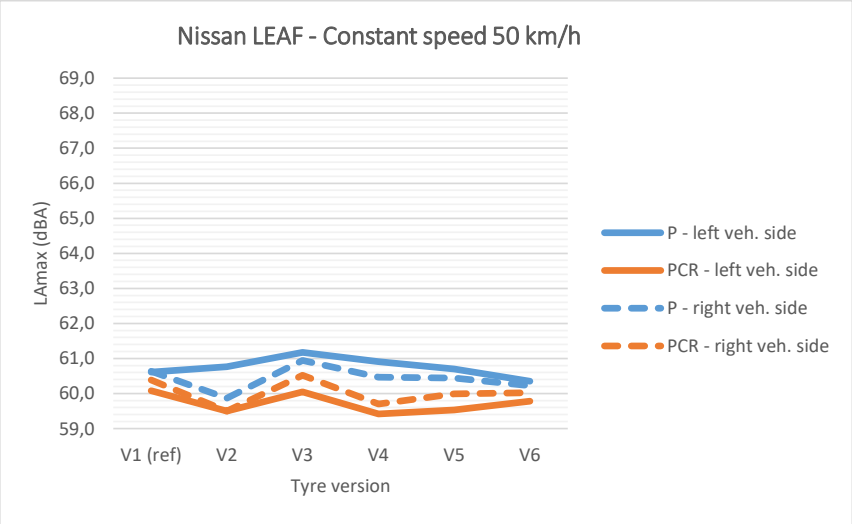

Figure 5.6: Overall $L_{Amax,crs}$ of the Nissan LEAF with tyre versions V1 to V6, at the constant speed of 50 km/h on prototype test sections P (blue) and PCR (red), left (full line) and right (dashed line) vehicle sides, temperature corrected at 20°C.

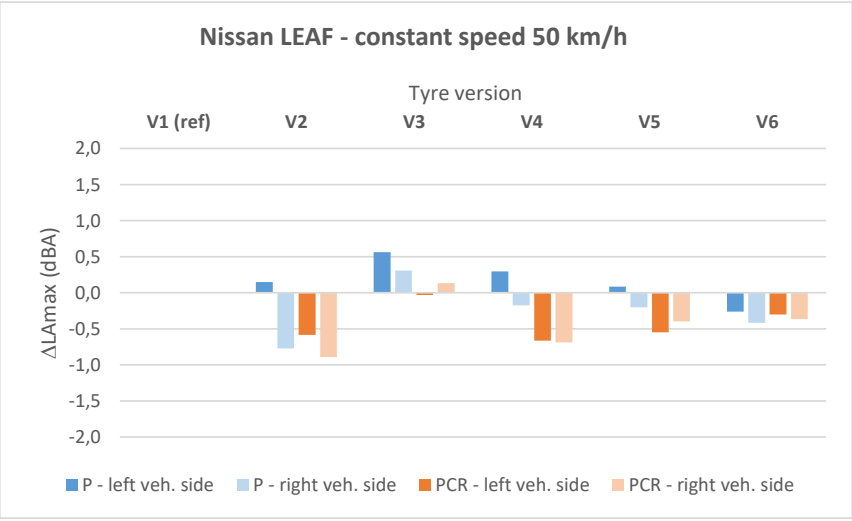

Figure 5.7: Variation of the overall $L_{Amax,crs}$ with tyre versions V2 to V6 fitted to the LEAF by reference to tyre version V1, at constant the speed of 50 km/h on prototype test sections P (blue) and PCR (red), left (bright colour) and right (light colour) vehicle sides, temperature corrected at 20°C.

	Road surface	P			PCR		
	Vehicle side	left	right	average	left	right	average
V1	$L_{Amax,wot}$	66.3	66.1	66.2	66.4	67.0	66.7
	std	*0.48*	*0.29*		*0.12*	*0.24*	
	Δ	*1.1*	*0.7*		*0.3*	*0.6*	
V2	$L_{Amax,wot}$	65.7	65.3	65.5	64.7	65.2	65.0
	std	*0.50*	*0.31*		*0.25*	*0.25*	
	Δ	*1.1*	*0.7*		*0.6*	*0.6*	
V3	$L_{Amax,wot}$	67.4	67.1	67.3	67.0	68.5	67.8
	std	*0.04*	*0.54*		*0.59*	*0.29*	
	Δ	*0.1*	*1.3*		*1.3*	*0.7*	
V4	$L_{Amax,wot}$	67.5	66.8	67.1	65.4	66.2	65.8
	std	*0.25*	*0.09*		*0.12*	*0.19*	
	Δ	*0.6*	*0.2*		*0.3*	*0.4*	
V5	$L_{Amax,wot}$	66.3	66.3	66.3	65.5	66.5	66.0
	std	*0.05*	*0.05*		*0.05*	*0.12*	
	Δ	*0.1*	*0.1*		*0.1*	*0.3*	
V6	$L_{Amax,wot}$	66.6	67.5	67.0	67.1	68.0	67.5
	std	*0.17*	*0.33*		*0.21*	*0.19*	
	Δ	*0.4*	*0.8*		*0.5*	*0.4*	

Table 5.3: Nissan LEAF under full acceleration (instantaneous speed 50 km/h). Reported noise level $L_{Amax,wot}$, standard deviation std and range of values Δ of the valid pass-bys in dB(A), for each tyre version on road surfaces P and PCR. Left and right vehicle sides, average of both sides.

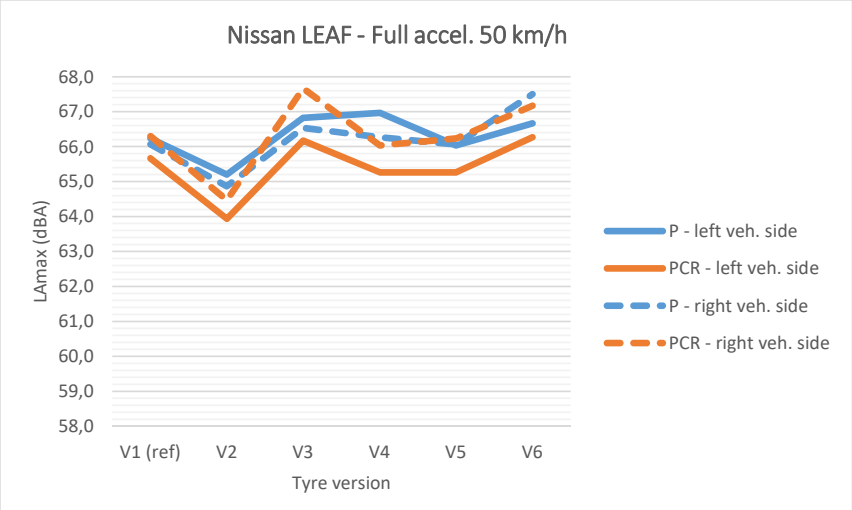

Figure 5.8: Overall $L_{Amax,wot}$ of the Nissan LEAF with tyre versions V1 to V6, at full acceleration with 50 km/h right to microphone, on prototype test sections P (blue) and PCR (red), left (full line) and right (dashed line) vehicle sides, not temperature corrected.

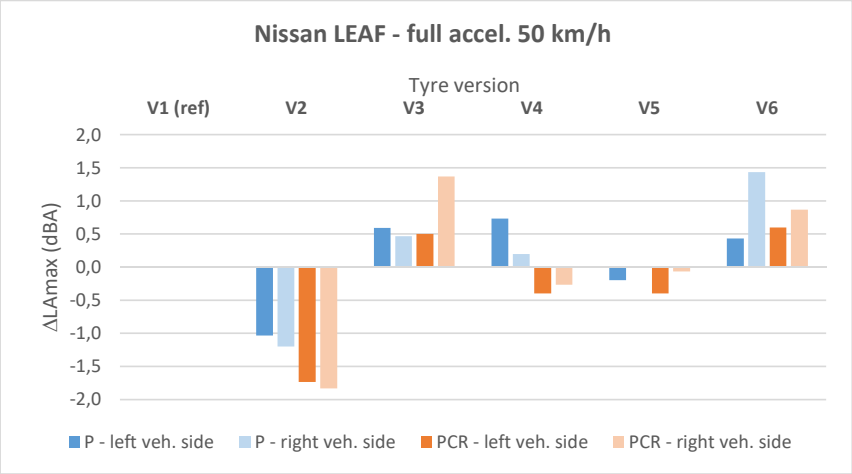

Figure 5.9: Variation of the overall $L_{Amax,wot}$ with tyre versions V2 to V6 fitted to the Nissan LEAF by reference to tyre version V1, under full acceleration with 50 km/h right to microphone on P (blue) and PCR (red), left (bright colour) and right (light colour) vehicle sides, not temperature corrected.

Renault KADJAR at constant speed

The reported noise levels at the constant of speed 50 km/h are represented in Table 5.4 and in Figure 5.10. All tyre versions except V5 provide a louder pass-by noise on prototype P than on prototype PCR, with an average difference of 0.5 dB(A) over the six tyre types and both vehicle sides. Differences between road surfaces are the smallest with tyre versions V1 and V5. The maximum pass-by noise level at 50 km/h is always slightly greater on the left vehicle side than on the right vehicle side on both surfaces, and is sometimes equal. This is consistent with a likely asymmetry in noise behaviour of this vehicle, in particular the position of the exhaust outlet.

In any case tyre version V3 happens to be louder on either road surface, otherwise V5 on road surface PCR only. Version V2 is the quietest one in any case. With reference to version V1, V2 is the only tyre version to bring a slight noise reduction on both prototype test sections, otherwise V5 on P only and V6 on PCR only with a quite limited benefit (Figure 5.11).

The maximum noise level of the Renault KADJAR at constant speed occurs within a position range of the foremost vehicle point between 2 m before and 2.1 m (exceptionally higher) after the microphone location, the latter corresponding to about 1.2 m after pass-by of the front wheel right to microphone. It is possibly associated with noise emission from the front part of the vehicle.

Renault KADJAR under acceleration

The acceleration rate tested with the Renault KADJAR is medium. On average over tyre versions and sides, the difference between prototype test sections is only 0.2 dB(A), PCR being again the quieter. (Table 5.5 and Figure 5.12)

As with constant speed, there is a trend for a difference between sides, always with a higher noise level on left vehicle side, probably originating from the powertrain noise contribution. Noise level differences with tyre versions are lower on the left vehicle side than on the right side, consistent with a possible higher role of powertrain.

In this acceleration condition, when compared with the reference version V1, all tyre versions except V5 bring a noise reduction on both vehicle sides with road surface PCR, the most effective being V2. Version V4 also improves noise levels by more than 0.5 dB(A) (Figure 5.13). On road surface P, improvements are noticeable with V4 and V6 on the right vehicle side only.

	Road surface	P			PCR		
	Vehicle side	left	right	average	left	right	average
V1	$L_{Amax,crs}$	62.1	61.9	62.0	61.7	61.5	61.6
	std	*0.46*	*0.29*		*0.26*	*0.32*	
	Δ	*1.02*	*0.71*		*0.62*	*0.82*	
V2	$L_{Amax,crs}$	61.9	61.6	61.7	61.0	61.0	61.0
	std	*0.24*	*0.51*		*0.28*	*0.28*	
	Δ	*0.61*	*1.22*		*0.72*	*0.72*	
V3	$L_{Amax,crs}$	62.6	62.3	62.5	62.0	61.8	61.9
	std	*0.26*	*0.55*		*0.67*	*0.23*	
	Δ	*0.71*	*1.43*		*1.74*	*0.61*	
V4	$L_{Amax,crs}$	62.3	62.5	62.4	61.8	61.2	61.5
	std	*0.34*	*0.22*		*0.44*	*0.23*	
	Δ	*0.92*	*0.51*		*1.02*	*0.61*	
V5	$L_{Amax,crs}$	62.0	61.4	61.7	62.4	61.7	62.1
	std	*0.49*	*0.21*		*0.15*	*0.24*	
	Δ	*1.23*	*0.51*		*0.41*	*0.61*	
V6	$L_{Amax,crs}$	62.1	62.4	62.3	61.5	61.3	61.4
	std	*0.35*	*0.19*		*0.27*	*0.37*	
	Δ	*0.92*	*0.51*		*0.71*	*1.02*	

Table 5.4: Renault Kadjar (ICEV) at the constant speed of 50 km/h (gear 4). Reported noise level $L_{Amax,crs}$, standard deviation std and range of values Δ of the valid pass-bys in dB(A), for each tyre version on road surfaces P and PCR. Left and right vehicle sides, average of both sides.

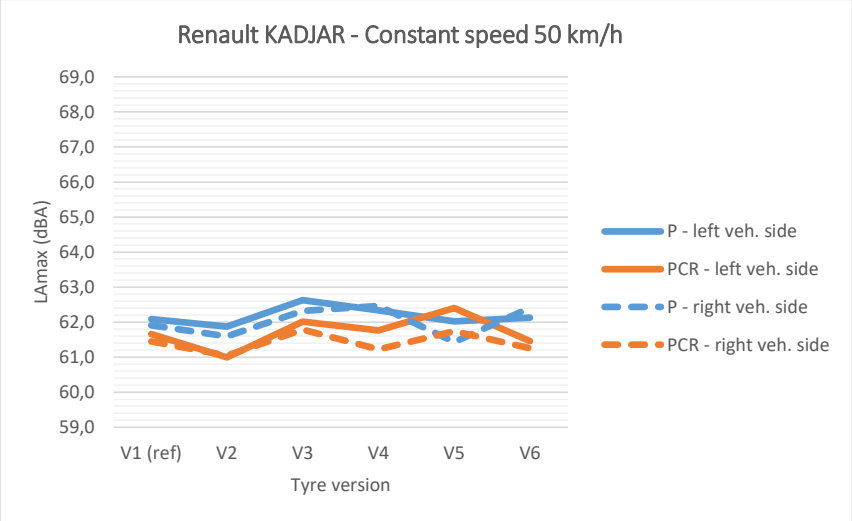

Figure 5.10: Overall $L_{Amax,crs}$ of the Renault KADJAR with tyre versions V1 to V6, at the constant speed of 50 km/h on prototype test sections P (blue) and PCR (red), left (full line) and right (dashed line) vehicle sides, temperature corrected at 20℃.

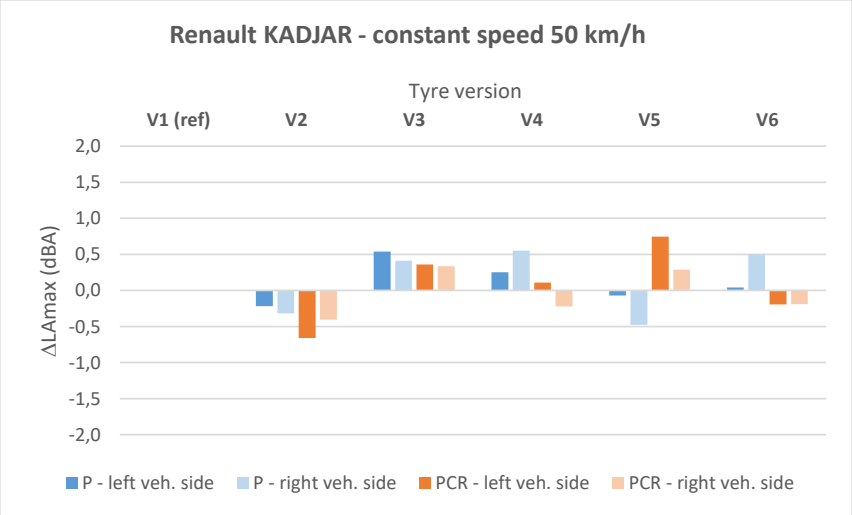

Figure 5.11: Variation of the overall $L_{Amax,crs}$ with tyre versions V2 to V6 fitted to the Renault KADJAR by reference to tyre version V1, at the constant speed of 50 km/h on prototype test sections P (blue) and PCR (red), left (bright colour) and right (light colour) vehicle sides, temperature corrected at 20℃.

	Road surface	P			PCR		
	Vehicle side	left	right	average	left	right	average
V1	$L_{Amax,wot}$	65.4	64.8	65.1	65.2	64.6	64.9
	std	*0.31*	*0.17*		*0.26*	*0.21*	
	Δ	*0.7*	*0.4*		*0.6*	*0.5*	
V2	$L_{Amax,wot}$	64.7	63.9	64.3	64.5	63.8	64.1
	std	*0.26*	*0.16*		*0.17*	*0.00*	
	Δ	*0.6*	*0.4*		*0.4*	*0.0*	
V3	$L_{Amax,wot}$	65.4	65.1	65.3	65.3	64.9	65.1
	std	*0.48*	*0.36*		*0.40*	*0.25*	
	Δ	*1.1*	*0.8*		*0.9*	*0.6*	
V4	$L_{Amax,wot}$	65.6	64.4	65.0	64.9	64.8	64.8
	std	*0.19*	*0.19*		*0.31*	*0.22*	
	Δ	*0.4*	*0.4*		*0.7*	*0.5*	
V5	$L_{Amax,wot}$	65.1	64.6	64.8	65.6	65.7	65.7
	std	*0.19*	*0.25*		*0.05*	*0.00*	
	Δ	*0.4*	*0.6*		*0.1*	*0.0*	
V6	$L_{Amax,wot}$	65.3	64.0	64.7	64.9	64.3	64.6
	std	*0.09*	*0.54*		*0.28*	*0.29*	
	Δ	*0.2*	*1.3*		*0.6*	*0.7*	

Table 5.5: Renault Kadjar (ICEV) under full acceleration (instantaneous speed of 50 km/h, gear 4). Reported noise level $L_{Amax,wot}$, standard deviation std and range of values Δ of the valid pass-bys in dB(A), for each tyre version on road surfaces P and PCR. Left and right vehicle sides, average of both sides.

The maximum noise level of the KADJAR under medium acceleration occurs within a wide position range, which roughly extends from 0.5 m to over 7 m after pass-by of the foremost vehicle point right to microphone location. This position range is much larger than what can be observed with the Nissan LEAF. Due to the moderate acceleration rate, the instantaneous speed of the accelerating vehicle differs not so much from 50 km/h over this position range.

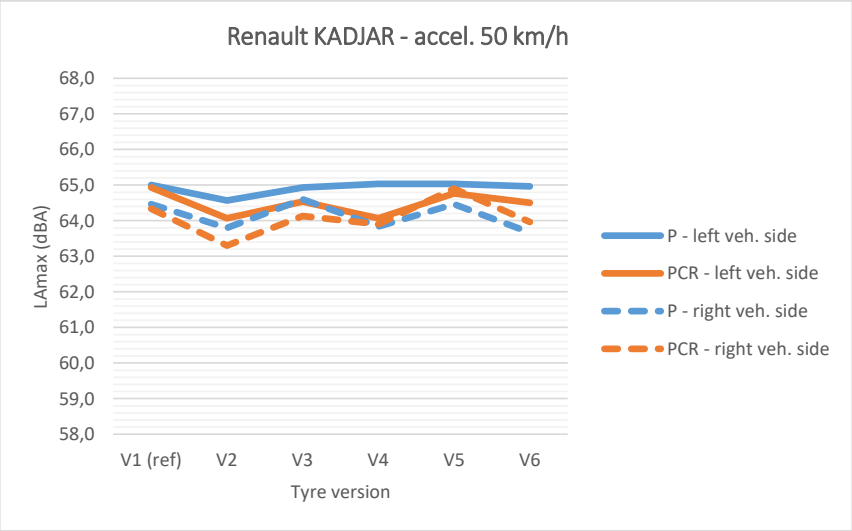

Figure 5.12: Overall $L_{Amax,wot}$ of the Renault KADJAR with tyre versions V1 to V6, under acceleration with 50 km/h right to the microphone, on prototype test sections P (blue) and PCR (red), left (full line) and right (dashed line) vehicle sides, not temperature corrected.

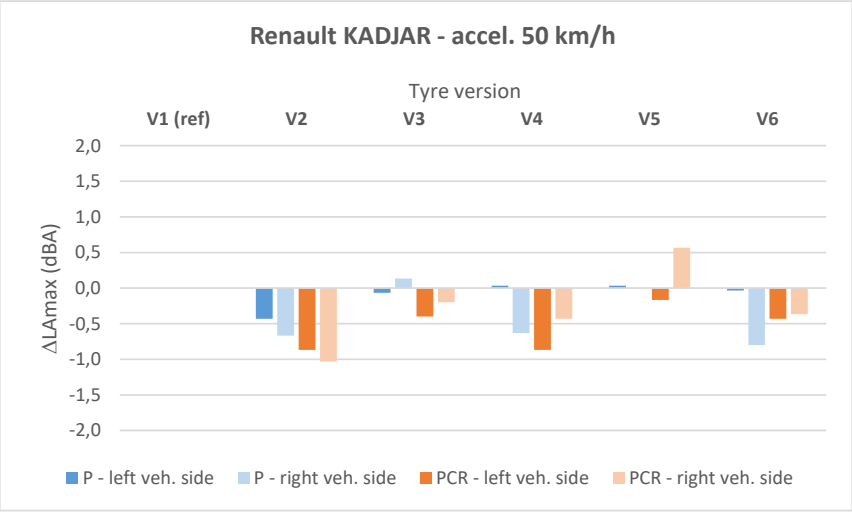

Figure 5.13: Variation of the overall $L_{Amax,wot}$ with tyre versions V2 to V6 fitted to the Renault KADJAR by reference to tyre version V1, under acceleration with 50 km/h right to the microphone on prototype test sections P (blue) and PCR (red), left (bright colour) and right (light colour) vehicle sides, not temperature corrected.

Analysis summary

Considering the six tyre versions and the two driving conditions with the electric and the ICE vehicles, there is systematically a slightly higher advantage for noise reduction with prototype test section PCR over P. The tyre version V2 is the quietest in any case, the reduction may exceed 1.5 dB(A) with the electric Nissan LEAF under strong acceleration, but otherwise remains within 1 dB(A) in the more usual driving situations.

Apart from tyre version V2, there is no strong advantage of a particular tyre version for all the cases tested. The acoustic performance of version V3 seems comparatively weak. Regarding the electric vehicle, V4 and V5 provide a small benefit over the reference V1 especially at constant speed and on road surface PCR. More generally, too low differences between noise levels from tyre versions may be within the margin of error of measurement and detailed conclusions are not relevant.

Further study of Action B7 completes acoustic properties with other important physical features to make a holistic choice of relevant tyre versions for electric vehicles.

5.1.3 Spectra characteristics of the optimised tyres

The valid and consistent spectra taken at the time of L_{Amax} of the previous pass-bys, respectively at constant speed or acceleration, have been averaged within either test condition defined by vehicle, tyre version, driving style and vehicle side. Finally, the mean spectrum of both side averages were calculated to be reported. They are presented successively for the Nissan LEAF and the Renault KADJAR. Spectra are not corrected in temperature.

Nissan LEAF on road surfaces P and PCR

At constant speed on P and PCR (Figure 5.14, top), the spectra from each tyre version are quite flat between 1000 and 2000 Hz, then drop off rapidly in a similar way for all tyre versions. On either road surface, V3 has a secondary peak at 500 Hz – particularly noticeable on PCR – while V5 has it at 630 Hz.

Drive-by under full acceleration strongly accentuates differences between tyre versions, with contributions in two more particular ranges: 1000-2000 Hz and 500-630 Hz (Figure 5.14, bottom). While V6 has its spectrum maximum at 1000 Hz on both road surfaces, V1, V2 and V5 spectra are maximum at 1250 Hz. However, V3 spectrum distributes its maximum contribution over the third-octave bands 500-630 Hz on P and PCR, as does V4 spectrum on PCR only. V5 spectrum is featured by a peak at 630 Hz.

Renault KADJAR on road surfaces P and PCR

On road surface P with the Renault KADJAR at constant speed, the spectra associated to the tyre versions differ only in the details. They are maximum in the range 1250-2000 Hz. More differences can be seen with PCR, with an enlargement down to 1000 Hz for V1 and V6. As previously noticed with the Nissan LEAF, V3 spectrum exceeds others at 400-500 Hz, like V5 spectrum at 630 Hz.

Differences in noise level between tyre versions are less outlined than with the Nissan LEAF, due to the moderate acceleration rates. Let's also recall that the instantaneous speed at time of L_{Amax} is lower than previously with the Nissan LEAF. The two road surfaces differentiate in their noise spectrum shape. The most contributing frequency range is 1000-2000 Hz in any case, with uneven involvement at 1000 Hz on test section PCR. A secondary peak still exists at 500 Hz with any tyre version. The next peak at 200 Hz, non-existent with the Nissan LEAF, might be engine noise.

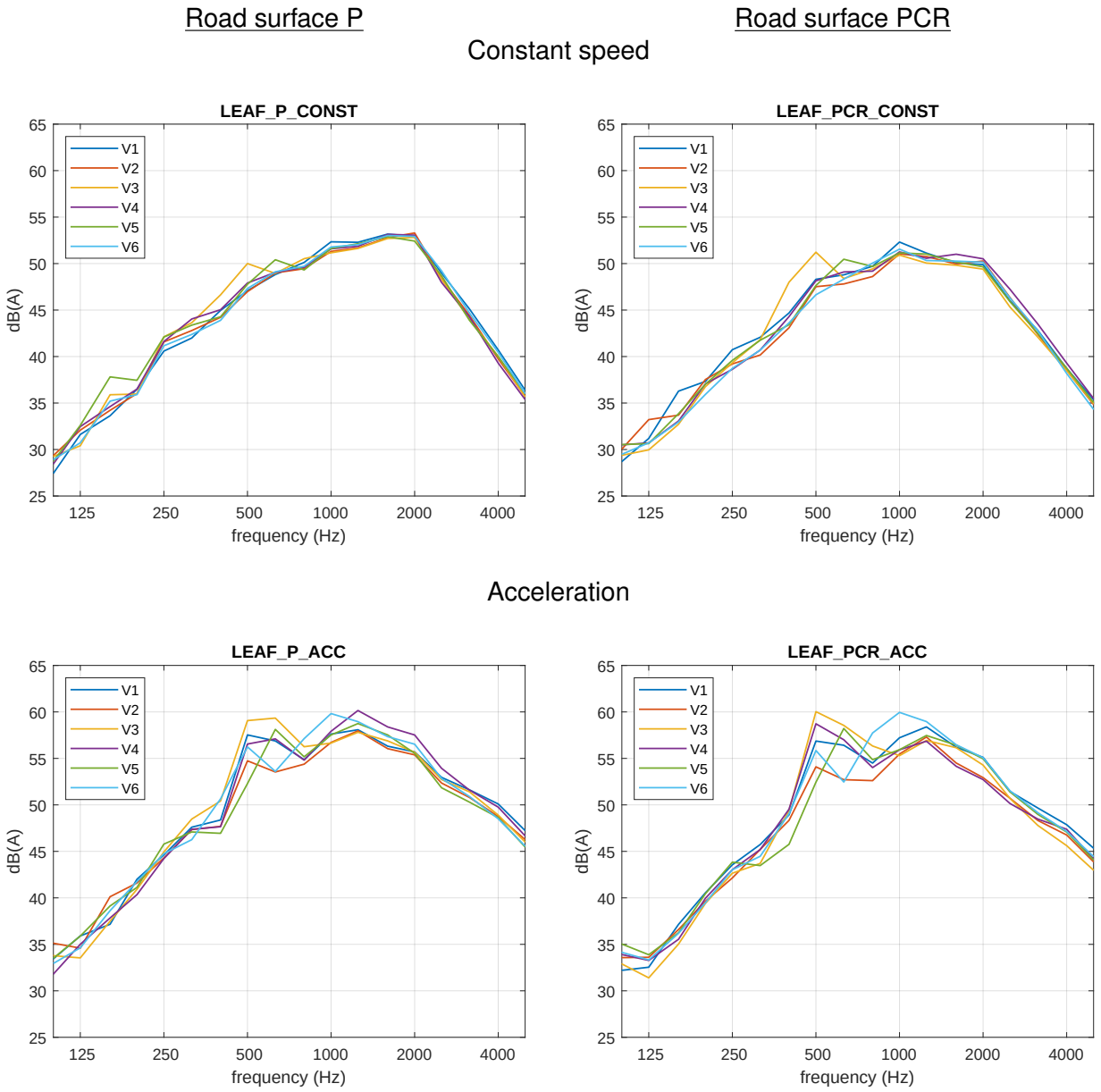

Figure 5.14: Average spectrum of $L_{Amax,crs}$ at the constant speed of 50 km/h (top) and of $L_{Amax,acc}$ under acceleration (bottom), with tyre versions V1 to V6 fitted to the Nissan LEAF on prototype test sections P (left) and PCR (right), not temperature corrected.

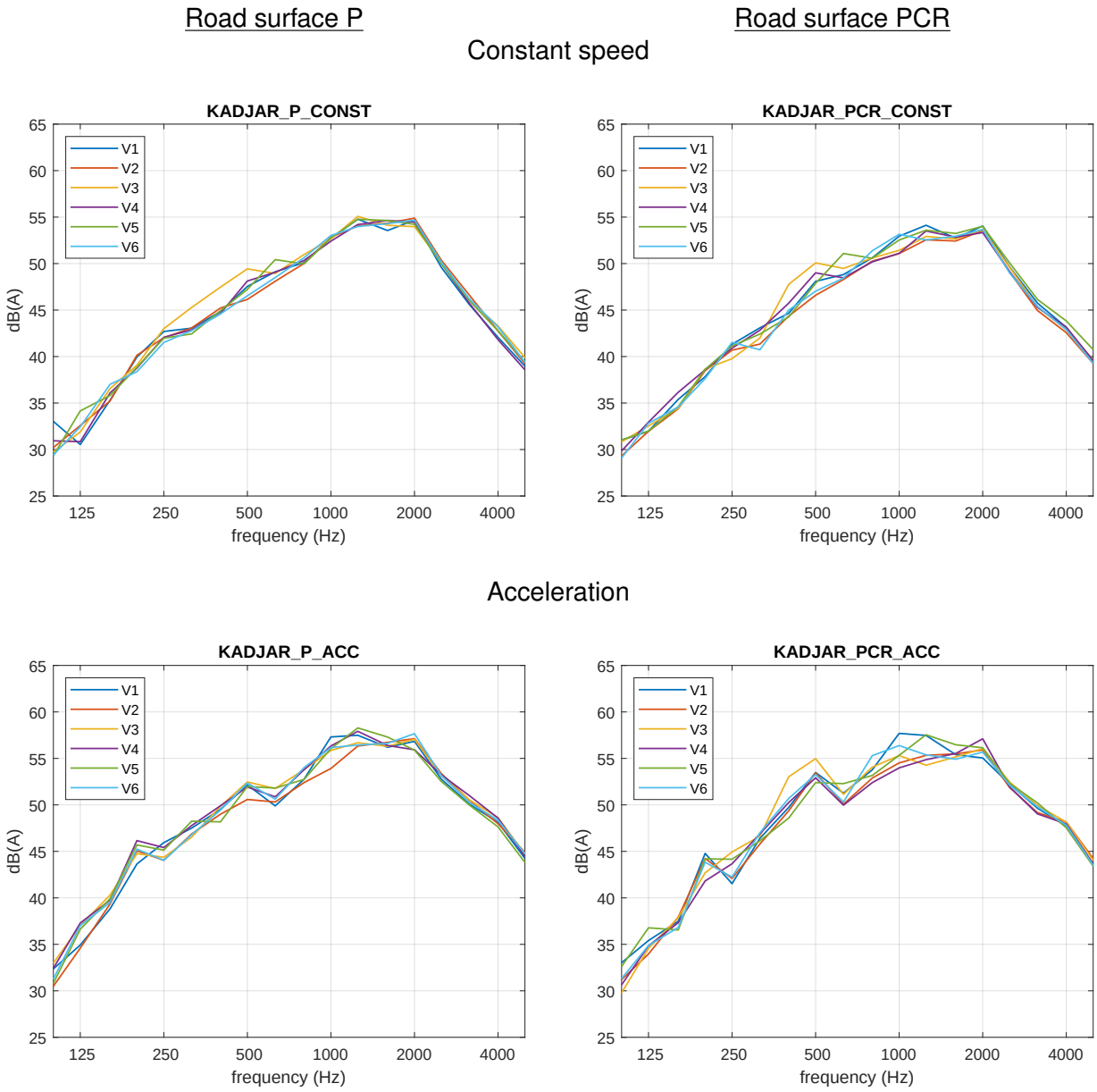

Figure 5.15: Average spectrum of $L_{Amax,crs}$ at the constant speed of 50 km/h (top) and of $L_{Amax,acc}$ under acceleration (bottom), with tyre versions V1 to V6 fitted to the Renault KADJAR on prototype test sections P (left) and PCR (right), not temperature corrected.

5.2 CPX measurements

Within sub-action B2.4, CPX measurements have been performed by UNI EIFFEL. The test vehicle was the Renault Mégane Scénic described in section 4.3, Figure 4.25 (left). Tyre versions V1, V2, V3 and V4 were tested in September 2021. The inflation pressure of the tyre during the tests was 2.2 bars. The two prototype test sections P and PCR and the six existing test sections A, E1, E3, M2, M3 and N have been involved in the study. Test sections A, E1, E3, M2, N, P and PCR were tested in West to East direction. Test section M3 was tested in the East to West direction.

The CPX data have been processed as explained in section 4.3.2 by Equations (4.3) and (4.4). However, no regression analysis was carried out. Instead, the CPX noise levels have been averaged over the full length of the test section for three runs at the constant speed of 50 km/h. Table 5.6 gives the CPX results for the 32 configurations of tyre and pavements. The average speed V and recomposed CPX noise levels L_{rAeq} are given together with the standard deviation over the length of the test section. The noise reduction ΔL_{rAeq} from the reference test section E1 is also given.

V1			
Surface	V	L_{rAeq}	ΔL_{rAeq}
M3	50.3±0.5	80.1±0.3	-7.7
PCR	50.0±0.8	82.4±0.4	-5.4
P	50.7±0.8	83.1±0.4	-4.7
A	50.5±0.5	84.5±0.9	-3.3
N	50.3±0.5	85.7±0.6	-2.1
M2	50.6±0.4	86.2±0.9	-1.6
E1	50.6±0.6	87.8±0.7	NA
E3	50.4±0.7	88.3±0.5	+0.5

V2			
Surface	V	L_{rAeq}	ΔL_{rAeq}
M3	50.4±0.5	79.8±0.5	-7.7
PCR	50.2±0.3	81.8±0.8	-5.6
P	50.7±0.3	82.8±0.5	-4.6
A	50.4±0.8	84.5±1.0	-2.9
N	50.7±0.6	85.3±0.6	-2.1
M2	50.0±0.5	85.9±0.7	-1.5
E1	50.1±0.5	87.4±0.7	NA
E3	50.1±0.4	87.9±0.4	+0.5

V3			
Surface	V	L_{rAeq}	ΔL_{rAeq}
M3	50.3±0.4	80.1±0.5	-7.4
PCR	50.3±0.3	82.2±0.5	-5.3
P	51.3±0.7	83.3±0.4	-4.2
A	50.3±0.8	84.3±1.0	-3.2
N	50.5±0.7	85.4±0.6	-2.1
M2	50.6±0.6	86.2±0.8	-1.3
E1	50.0±0.6	87.5±0.7	NA
E3	49.7±0.5	87.9±0.5	+0.4

V4			
Surface	V	L_{rAeq}	ΔL_{rAeq}
M3	50.0±0.7	79.2±0.4	-8.6
PCR	50.3±0.8	82.0±0.9	-5.8
P	50.2±1.3	82.1±0.6	-5.7
A	50.4±0.4	84.2±1.0	-3.6
N	50.1±0.5	85.1±0.6	-2.7
M2	50.8±0.7	86.0±0.9	-1.8
E1	50.7±0.6	87.8±0.7	NA
E3	50.2±0.9	88.1±0.6	+0.3

Table 5.6: Vehicle speed V (in km/h, averaged over 3 passing-by) and CPX measured overall noise levels $L_{rAeq}(50)$ (in dB(A), averaged over 3 passing-by, corrected in temperature, recomposed between 315 Hz and 5000 Hz) at 50 km/h for the 8 test sections and the 4 tyre models tested. Classification from the quietest to the loudest test section. ΔL_{rAeq} is the noise reduction from the reference test section E1.

In Table 5.6 the test sections are ordered from the quietest to the loudest road surface. The classification in ascending order is the same for the four tyre versions, i.e. M3, PCR, P, A, N, M2, E1, E3. Thus, the prototype test sections are among the quietest road surfaces, with a noise reduction from E1 test section between -4.2 dB(A) and -5.8 dB(A). Test section PCR is generally quieter than

test section P, with a difference of 0.7 dB(A) for tyre V1, 1.0 dB(A) for tyre V2, 1.1 dB(A) for tyre V3 and 0.1 dB(A) for tyre V4.

Table 5.7 gives the difference in overall CPX noise level from the reference tyre V1 for tyres V2, V3 and V4 at the speed of 50 km/h. The same results are illustrated in Figure 5.16. It turns out that the three tyre versions V2, V3 and V4 are quieter or equivalent to the reference V1 for all road surfaces, but tyre V3 on test section P (+0.2 dB(A)). For tyre V2, the reduction is between 0.3 and 0.4 dB(A), except for PCR reaching a noise reduction of 0.6 dB(A) by comparison with tyre V1. For tyre V3, there is no noise reduction for test sections M2 and M3 and the noise difference by tyre V2 is between -0.2 and -0.4 dB(A) for the other road surfaces. Comparing tyres V1 and V4, there is no noise reduction on E1, a difference between -0.2 and -0.4 dB(A) for test sections A, E3, M2 and PCR and between -0.6 and -1.0 dB(A) for test sections M3, N and P. Thus, the most important noise abatement when compared to the reference tyre V1 is obtained for tyre V4 on the prototype test section P. In this configuration there is almost no difference between test sections P and PCR.

	V1 (Ref)	**V2**	**V3**	**V4**
Surface	$\Delta\ L_{rAeq}(50)$	$\Delta\ L_{rAeq}(50)$	$\Delta\ L_{rAeq}(50)$	$\Delta\ L_{rAeq}(50)$
A	-	0.0	-0.2	-0.3
E1	-	-0.4	-0.3	0.0
E3	-	-0.4	-0.4	-0.2
M2	-	-0.3	0.0	-0.2
M3	-	-0.3	0.0	-0.9
N	-	-0.4	-0.3	-0.6
P	-	-0.3	+0.2	-1.0
PCR	-	-0.6	-0.2	-0.4

Table 5.7: Differences for each tyre from the reference tyre V1 on the CPX measured overall recomposed noise levels $L_{rAeq}(50)$.

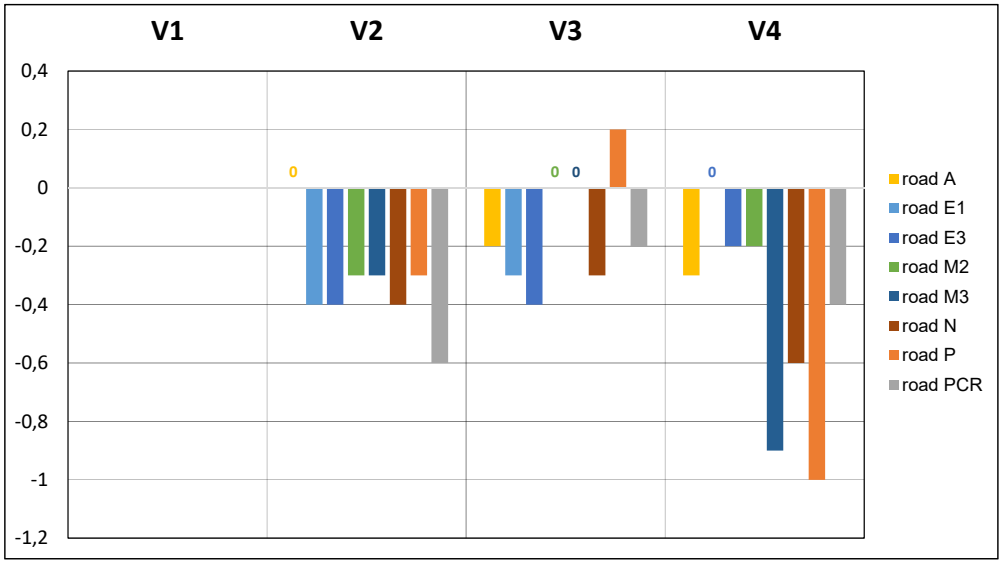

Figure 5.16: Variation of the overall CPX recomposed noise levels L_{rAeq} with tyre versions V2 to V4 fitted to the Renault Mégane Scénic by reference to tyre version V1, at constant speed of 50 km/h on the 8 test sections, temperature corrected at 20℃.

The average CPX spectra at 50 km/h for the four tyres V1, V2, V3 and V4 are given in Figure 5.17 and 5.18 respectively for test sections A, E1, E2 and M2 and for test sections M3, N, P and PCR. In Figure 5.17, for the loudest test sections E1 and E3 a clear peak is observed at 1000 Hz, while the peak is shifted at 800 Hz for road surface A and M2 due to sound absorption properties. Below the peak, the spectra are very close for the four tyre versions. The main noise differences between tyres are observed above the peak at higher frequencies, especially for road surface A.

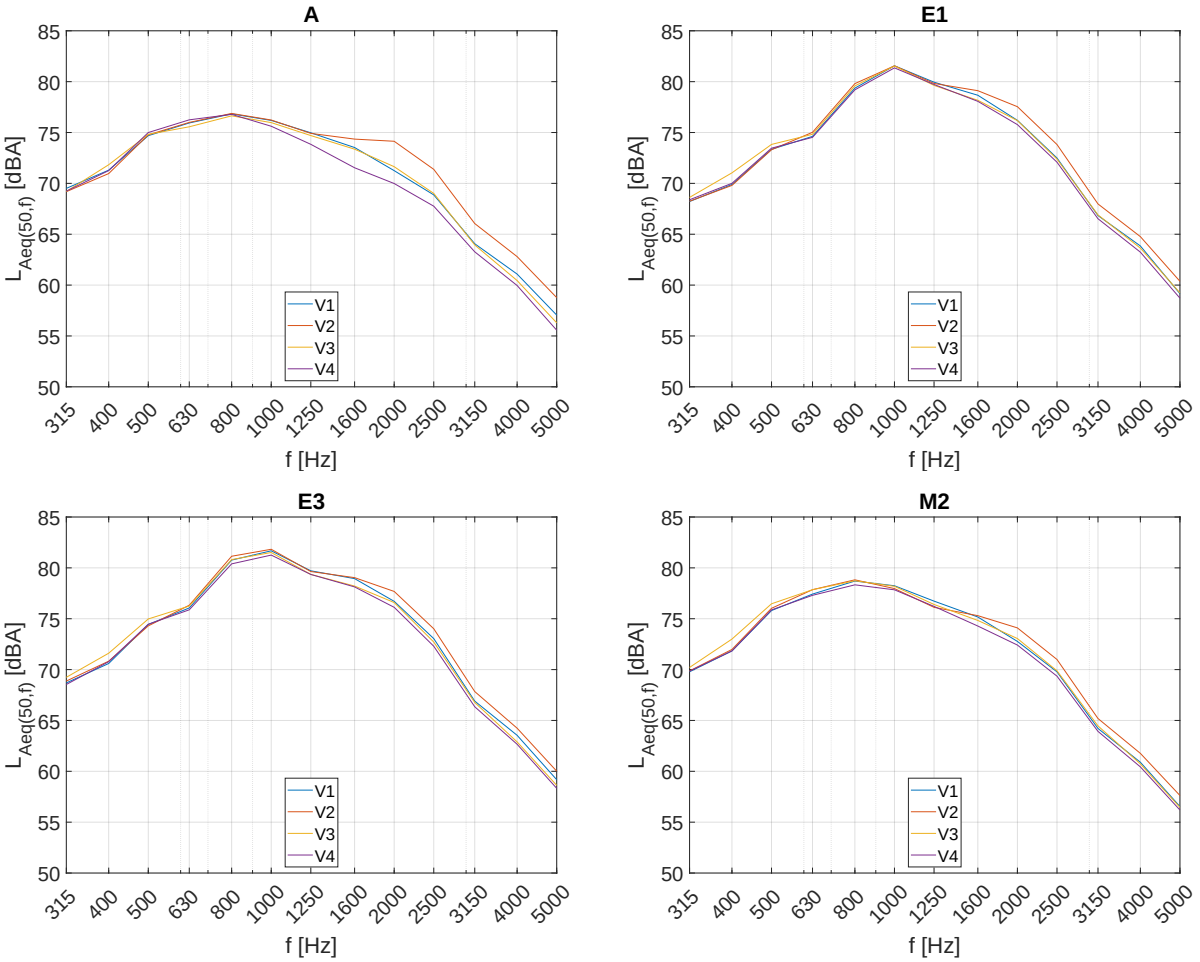

Figure 5.17: CPX mean measured spectrum at 50 km/h for test sections A, E1, E3, M2, and the 4 tyre models tested.

However, in Figure 5.18 the differences between tyre versions can be observed over the whole frequency range between 315 Hz and 5000 Hz. For test section N, clear peaks are observed at 1000 Hz and 2000 Hz, and secondarily at 500 Hz. The first peak at 500 Hz is also observed on the prototype test sections P and PCR, while the noise levels are reduced in the frequency range between 800 Hz and 2500 Hz. The flatness of M3 spectra between 500 Hz and 2000 Hz is remarkable, leading to the highest noise reduction due to low macro-texture and sound absorption properties of this road surface. On the prototype test section P, tyre V4 is clearly quieter than the other tyre versions in the frequency range between 800 Hz and 2500 Hz.

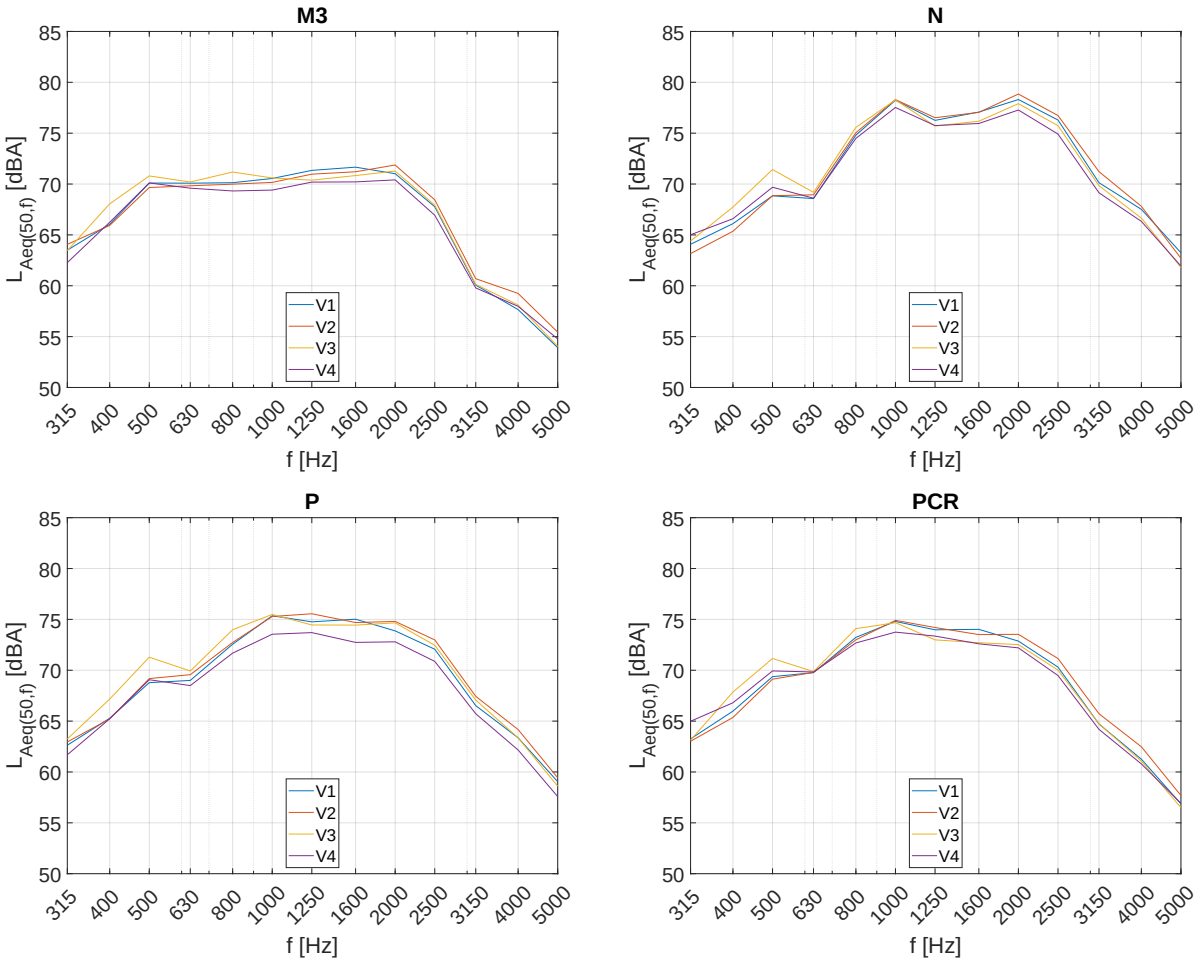

Figure 5.18: CPX mean measured spectrum at 50 km/h (averaged over 3 passing-by) for test sections M3, N, P and PCR and the 4 tyre models tested.

5.3 Synthesis of sub-action B2.4

Sub-action B2.4 has been focused on the acoustical characterisation of six different technical demonstrator tyre developed by CRD within action B7 dealing with the holistic approach for optimisation of EV tyres. The dimension of the tyres was 205/55 R16 and the tyre versions mainly differed by the tread pattern design. The six tyre version, namely V1 to V6, have been involved in pass-by noise measurements at constant speed and in acceleration conditions, conforming with the requirements of UNECE regulation R51.03. The tyres have been fitted on two different vehicles. The first tested vehicle was an EV, namely a Nissan LEAF, and was the same as the one tested in sub-action B2.1 (leaf#1). The second test vehicle was an ICEV, namely a Renault Kadjar. Tyre versions V1 to V4 have also been fitted on the UNI EIFFEL Renault Mégane Scénic and tested by the CPX method on the prototype test sections P and PCR and compared to the existing test sections A, E1, E3, M2, M3 and N.

Regarding pass-by test results, considering the six tyre versions and both driving conditions with the tested EV and ICEV, it was observed a slight systematic advantage for noise reduction with prototype test section PCR over test section P. Indeed, for the Nissan LEAF, the difference between P and PCR was on average 0.7 dB(A) at constant speed and 0.4 dB(A) in acceleration. Regarding the Renault Kadjar, the difference between P and PCR was on average 0.5 dB(A) at constant speed and reduces to 0.2 dB(A) in acceleration. Taking tyre version V1 as a reference, the tyre version V2

was the quietest in any case. The noise reduction may exceed 1.5 dB(A) with the EV under strong acceleration, but otherwise it did not exceed 1 dB(A) in the usual driving situations. Apart from tyre version V2, there was no major definite advantage observed for the other tested cases. The acoustic performance of tyre version V3 was comparatively weak. Regarding the EV, tyre versions V4 and V5 provide a small benefit over the reference V1 especially at constant speed and on road surface PCR. However, some of the differences observed remained within the level of uncertainty of tests and thus too detailed conclusions should be considered with care. Regarding the noise spectra, a flat shape was observed between 1000 Hz and 2000 Hz for all configurations. For some tyre versions, a secondary peak was observed around 500-630 Hz. This low frequency peak around 500-600 Hz was more pronounced in accelerating conditions, especially for the Nissan LEAF with high acceleration rate, as well as the second peak appearing around 1000-1250 Hz. This is due to a torque effect and a higher sensitivity of the tyre tread pattern in accelerating conditions.

Regarding CPX test results, for all tyre versions from V1 to V4 it was observed that the prototype test sections P and PCR are among the quietest road surfaces, with a noise reduction from the reference test section E1 between -4.2 dB(A) and -5.8 dB(A). Test section PCR was generally quieter than P, with a difference ranging between 0.1 dB(A) and 1.1 dB(A) (respectively tyre versions V4 and V3). Comparing to the reference tyre V1, a clear advantage was observed for tyre version V2 on test section PCR (-0.6 dB(A)), while on test section P the best performance was obtained with tyre version V4 (-1 dB(A)).

Finally, further study by CRD within the holistic action B7 by means of virtual tools and laboratory facilities will complete results on acoustical properties with other important physical features and will lead to the final optimised tyre version for EVs.

6 Conclusions

Action B2 of the LIFE E-VIA project dealt with tyre/pavement coupling study and prototype implementation. This action ran from July 2019 to November 2021 and involved many measurement campaigns on the UNI EIFFEL reference test track in Nantes (France). It was sub-divided in four sub-actions, each having a specific aim. In the following, the main results of each sub-action are summarised and the conclusions in the light of the project's objectives are pointed out.

Sub-action B2.1 The aim of sub-action B2.1 was to study noise emission of EVs on existing test sections of the reference test track in Nantes. The main objectives were to quantify pass-by noise levels, to estimate noise source localisation on EVs and to gauge the potential noise reduction for EVs when acting on the road surface. Thus, six EVs from different vehicle segments have been tested on six distinct road surfaces, over a wide range of speeds and driving conditions, including constant speed, acceleration and deceleration. Half of these road surfaces were dense, the others were absorbing. The vehicles were fitted with their commercial tyre sets, representative of their own market.

As expected, at constant speed the predominance of rolling noise from EV noise emission was confirmed over the whole speed range. Noise sources are clearly located in the wheel zones. The rear wheel is often the source area contributing most to noise received at roadside, even if not being a driving axle and without nearby electric motor. At the typical urban speed of 50 km/h, the difference between the quietest and the loudest test sections varied from 4.8 dB(A) to 7.9 dB(A) depending on EV model. This result emphasises the stake of the road surface selection for reducing noise emission from EVs. By contrast, the difference between the quietest and the loudest EVs on a given road surface ranged from 2.0 dB(A) to 3.6 dB(A). Considering the 36 road/vehicle configurations, a difference of 8.8 dB(A) was observed between the quietest and the loudest configuration. The combination of sound absorption properties and low texture levels leads to the highest noise reduction.

Full acceleration tests with EVs have shown a large noise increase, often exceeding 5 dB(A), from the driving wheel area, including both rolling noise and motor noise contributions. When compared to constant speed the ranking of road surfaces remains quite unchanged under acceleration, except for ISO 10844 road surface N which became the loudest in some cases. This underlines the importance of taking acceleration situations into account in the vehicle noise emission assessment. Regarding deceleration tests in energy recovery mode, most EVs have shown a very limited noise variation from constant speed driving on the various road surfaces. However, for one EV, the impact of deceleration was strong on test sections with low macro-texture, yielding to a noise increase of about 3 to 4 dB(A) over the urban speed range between 30 and 45 km/h.

Sub-action B2.2 The aim of sub-action B2.2 was the construction of a prototype of low-noise road surface based on the outcomes of action B1. This step was necessary for further feedback in action B1 and prior full-scale construction of the low-noise test section in the pilot area in Florence (Italy) within action B3. The 57 m long by 8 m wide prototype was successfully built on the UNI EIFFEL reference test track in Nantes in September 2020, by a sub-contracting French road company. The prototype comprises two VTAC 0/6 test sections of the same grading curve, conforming B1 action reference, and differing by the addition of 1.9 % of crumb rubber (CR) in one of the mixes. The test section without crumb rubber was named P, while the other with crumb rubber was named PCR. The controls after the construction have shown the conformity of the grading curve and of the bitumen content for both test sections. The measured MTD was rather low on both test sections, with an average value of 0.51 $\pm$ 0.04 mm for test section P and 0.42 $\pm$ 0.02 mm for test section PCR. The thickness of the surface layer was also assessed from core samples drilled on P and PCR test sections. It was found to be conform to the specification of 25 mm. The air-void content of the surface

layer was assessed in laboratory with a gamma densimeter. The average air-void content value was 9.9% on test section P and 14.6% on test section PCR.

Sub-action B2.3 The aim of sub-action B2.3 was to fully characterise the prototype test sections P and PCR in terms of road surface properties and in terms of noise emission by pass-by and Close-Proximity tests. The measurements were performed in autumn 2020 and in spring 2021.

Regarding road surface properties influencing tyre/road noise, quite low MPD and surface texture levels, in the same order of magnitude as the ISO 10844 test section N, were measured for both prototype test sections P and PCR. The sound absorption of both test sections was relatively poor, with a maximum absorption coefficient below 0.3 at 2500 Hz. The dynamic stiffness was unexpectedly lower on test section P (without crumb rubber) than on test section PCR (with crumb rubber), and remained close to that of a conventional asphalt concrete.

Regarding skid resistance, the ETD values confirmed the low macro-texture of P and PCR test sections, close to the threshold value of 0.4 mm which is the regulatory limit on French roads. The friction coefficient values measured with the British Pendulum and T2GO devices on P and PCR were however between 70 and 82.5, which is very satisfactory on both prototype pavements. Moreover, the evolution of the friction coefficient as a function of polishing cycles was studied with the W&S machine and the friction coefficient stays above 0.40, whatever the number of passes, which indicates a satisfying level of performance.

Simultaneous CPB and microphone array measurements have been performed for three EVs in different driving conditions (constant speed, acceleration and deceleration). By comparison with existing test sections, P and PCR were among the quietest road surfaces, with an average noise reduction around 4 dB(A) at 50 km/h, by comparison with the reference DAC 0/10 test section E1. For the three tested EVs, test section P without crumb rubber was about 0.6 dB(A) quieter than test section PCR. While increasing noise levels, the same tendency was observed in accelerating conditions, with a noise reduction up to 3.5 dB(A) and test section PCR being slightly less effective than P. Noise sources for P and PCR are still located close to the vehicle wheels, but bring an overall noise level reduction for both wheel zones when compared to the ISO 10844 test section N.

CPX measurements have been also performed according to ISO 11819-2 by UNI EIFFEL and IPOOL. For UNI EIFFEL, using the Michelin Energy Saver 195/60 R15, the prototype test sections P and PCR have been compared to the six existing test sections. P and PCR are among the quietest test sections, with a noise reduction relative to E1 test section around 3 dB(A) at 50 km/h. For IPOOL, the SRTT 225/60 R16 tyre of ISO 11819-3 was tested. The noise reduction by comparison with E1 was 1.7 dB(A) for P and 2.4 dB(A) for PCR. Both prototype test sections met the Core criterion of the GPP for a low-noise pavement fixing the CPX noise level at 50 km/h below 90 dB(A). However, despite very good acoustical performance of both test sections, the Comprehensive criterion of the GPP fixing the CPX noise level at 50 km/h below 87 dB(A) was not reached, although close in the case of PCR.

Sub-action B2.4 Sub-action B2.4 was focused on the acoustical characterisation of six different tyre versions, namely V1 to V6, developed by CRD within action B7. The dimension of the tyres was 205/55 R16 and the tyre versions mainly differed by the tread pattern design.

Pass-by noise measurements at constant speed and in acceleration conditions were performed conforming regulation R51.03. The tyres have been fitted on two different vehicles, one EV and one ICEV. It was observed that test section PCR was systematically around 0.5 dB(A) quieter than test section P. Taking tyre version V1 as a reference, the tyre version V2 was the quietest in any case. The noise reduction may exceed 1.5 dB(A) with the EV under strong acceleration, but otherwise it did not exceed 1 dB(A) in the usual driving situations. Apart from tyre version V2, there was no major advantage observed for the other tested cases. The acoustic performance of tyre version V3 was

comparatively weak. Regarding the EV, tyre versions V4 and V5 provide a small benefit over the reference V1 especially at constant speed and on road surface PCR.

Tyre versions V1 to V4 have also been tested by the CPX method on the prototype test sections P and PCR and compared to the existing test sections. For all tyre versions from V1 to V4 it was observed that the prototype test sections P and PCR are among the quietest road surfaces, with a noise reduction from the reference test section E1 between -4.2 dB(A) and -5.8 dB(A). Test section PCR was generally quieter than P, with a difference up to 1.1 dB(A). Comparing to the reference tyre V1, a clear advantage was observed for tyre version V2 on test section PCR (-0.6 dB(A)), while on test section P the best performance was obtained with tyre version V4 (-1 dB(A)).

The results of sub-action B2.4 will serve for the final optimisation of the EV tyre by CRD within action B7, prior to the implementation on the pilot area in Florence.

Bibliography

ISO 10844. Acoustics - Specification of test tracks for measuring sound emitted by road vehicles and their tyres, December 2021.

NF EN ISO 11819-1. Acoustics - Measurement of the influence of road surfaces on traffic noise - Part 1: Statistical Pass-By method, March 2002.

ISO 11819-2. Acoustics - Measurement of the influence of road surfaces on traffic noise - Part 2: The close-proximity method, March 2017.

ISO 11819-3. Acoustics - Measurement of the influence of road surfaces on traffic noise - Part 3: Reference tyres, March 2017.

NF EN 13108-2. Bituminous mixtures - Material specifications - Part 2 : asphalt concrete for very thin layers, December 2006.

ISO 13472-1. Acoustics - Measurement of sound absorption properties of road surfaces in situ - Part 1: extended surface method, June 2002.

ISO 13473-1. Characterization of pavement texture by use of surface profiles - Part 1: Determination of mean profile depth, 2019.

ISO/TS 13473-4. Characterization of pavement texture by use of surface profiles - Part 4: Spectral analysis of surface profiles, 2008.

Fabienne Anfosso-Lédée and Yves Pichaud. Temperature effect on tyre-road noise. *Applied Acoustics*, 68(1):1–16, 2007. ISSN 0003-682X. doi: 16/j.apacoust.2006.06.001.

Thomas Beckenbauer. Akustische Eigenschaften von Fahrbahnoberflächen. *Bearing capacity of roads, railways and airfields*, pages 553–56, 2001.

Hans Bendtsen, Rasmus Stahlfest Holck Skov, Bent Andersen, Erik Olesen, Annette Neidel, Jørn Raaberg, and Julien Cesbron. Performance of PERS at the Kalvehave test site. PERSUADE European Projet, Seventh Framework Programme - Contract No. 226313 - Deliverable D.5.1, DRD, IFSTTAR, May 2014.

Michel Bérengier, Julien Cesbron, and Peter Gusia. ODSURF project: modelling and experimental optimization of low noise pavements. In *Proceeding of Inter-Noise 2016*, pages 6973–6984, Hamburg, Germany, August 2016.

Julien Cesbron and Philippe Klein. Correlation between tyre/road noise levels measured by the Coast-By and the Close-ProXimity methods. *Applied Acoustics*, 126:36–46, November 2017. ISSN 0003-682X. doi: 10.1016/j.apacoust.2017.05.005.

Julien Cesbron, Simon Bianchetti, Philippe Klein, and Vincent Gary. Acoustical assessment of road surfaces at urban and peri-urban speeds by simultaneous Coast-By and Close-ProXimity measurements. In *Proc. 9th Forum Acusticum*, pages 2229–2235, Lyon, France, December 2020.

CIRTEC. Technical data sheet use of RARX, January 2019.

European Commission. EU Green Public Procurement criteria for road design, construction and maintenance, 2016.

Sylvie Dauvergne, Véronique Cerezo, and Julien Cesbron. Modalités de mise en concurrence : Remise des offres sur demande de devis - Marché n°2020TRAV006NTE : Travaux de construction d'un prototype de surface routière sur la piste de référence et expérimentations routières (PRER) - Université Gustave Eiffel – Campus de Nantes, June 2020a.

Sylvie Dauvergne, Véronique Cerezo, and Julien Cesbron. Travaux de construction d'un prototype de surface routière sur la piste de référence et expérimentations routières (PRER) à l'Universié Gustave Eiffel - Campus de NANTES - Cahier des Clauses Particulières (CCP) - Marché n°2020TRAV006NTE, June 2020b.

G. Descornet and U. Sandberg. Road surface influence on tire/road noise. pages 1–16, Miami, Florida, USA, 1980.

M-T. Do, Z. Tang, M. Kane, and F. de Larrard. Pavement polishing–Development of a dedicated laboratory test and its correlation with road results. *Wear*, 263(1-6):36–42, 2007. ISSN 0043-1648. doi: 16/j.wear.2006.12.086.

EAFO. European Alternative Fuel Observatory. URL `https://www.eafo.eu/vehicles-and-fleet/m1`.

Carsten Hoever. Review on noise relevant differences between ICEV and EV tyres. Deliverable Technical Report Actions A1, A2, A3, European Commission, July 2020.

Carsten Hoever. Deliverable of Action B7 of LIFE E-VIA project. Deliverable LIFE project E-VIA (LIFE18 ENV/IT/000201), 2022.

IEA. Global EV Outlook 2019 - Scaling-up the transition to electric mobility. Technical report, IEA, Paris (France), May 2019. URL `https://www.iea.org/reports/global-ev-outlook-2019`.

Don H. Johnson and Dan E. Dudgeon. *Array signal processing: concepts and techniques*. Prentice-Hall signal processing series. P T R Prentice Hall, Englewood Cliffs, NJ, 1993. ISBN 978-0-13-048513-7.

Philippe Klein and Julien Cesbron. Prediction of Coast-By tyre/road noise levels at peri-urban and urban speeds. In *Proc. 9th Forum Acusticum*, pages 2517–2524, Lyon, France, December 2020.

Marie-Agnès Pallas and Régis Perrier. Nearfield noise source localisation with constant directivity arrays : a comparison - Application to tram noise. Rotterdam, The Netherlands, March 2009.

Marie-Agnès Pallas, Roger Chatagnon, and Joël Lelong. Noise emission assessment of a hybrid electric mid-size truck. *Applied Acoustics*, 76:280–290, February 2014. ISSN 0003682X. doi: 10.1016/j.apacoust.2013.08.012.

Marie-Agnès Pallas, Michel Bérengier, Roger Chatagnon, Martin Czuka, Marco Conter, and Matthew Muirhead. Towards a model for electric vehicle noise emission in the European prediction method CNOSSOS-EU. *Applied Acoustics*, 113:89–101, December 2016. ISSN 0003-682X. doi: 10.1016/j.apacoust.2016.06.012.

Marie-Agnès Pallas, Julien Cesbron, Sergio Luzzi, Lucia Busa, Gianfrancesco Colucci, and Raffaella Bellomini. Review on electric vehicles and their noise emission. Deliverable LIFE project E-VIA (LIFE18 ENV/IT/000201) Technical Report Actions A1, A2, A3, European Commission, June 2020.

Filippo G. Praticò. Technical report on action B1. Deliverable LIFE project E-VIA (LIFE18 ENV/IT/000201) B1 report, European Commission, March 2021.

Ulf Sandberg and Jerzy A. Ejsmont. *Tyre/road noise: reference book*. INFORMEX Ejsmont & Sandberg Handelsbolag, Kisa, Sweden, First edition, 2002. ISBN 978-91-631-2610-9.

UNECE. Regulation No 51 of the Economic Commission for Europe of the United Nations - Uniform provisions concerning the approval of motor vehicles having at least four wheels with regard to their sound emissions [2018/798], 2018.

United Nations. Agreement concerning the adoption of uniform technical prescriptions for wheeled vehicles, equipment and parts which can be fitted and/or be used on wheeled vehicles and the conditions for reciprocal recognition of approvals granted on the basis of these prescriptions, 1995.

United Nations. Regulation No. 117 - Uniform provisions concerning the approval of tyres with regard to rolling sound emissions and to adhesion on wet surfaces and/or to rolling resistance, 2011.

A Sub-action B2.1 : Third-octave noise source maps of the EVs and Kangoo D on road surface N at constant speed 50 km/h

Note: figures begin on next page.

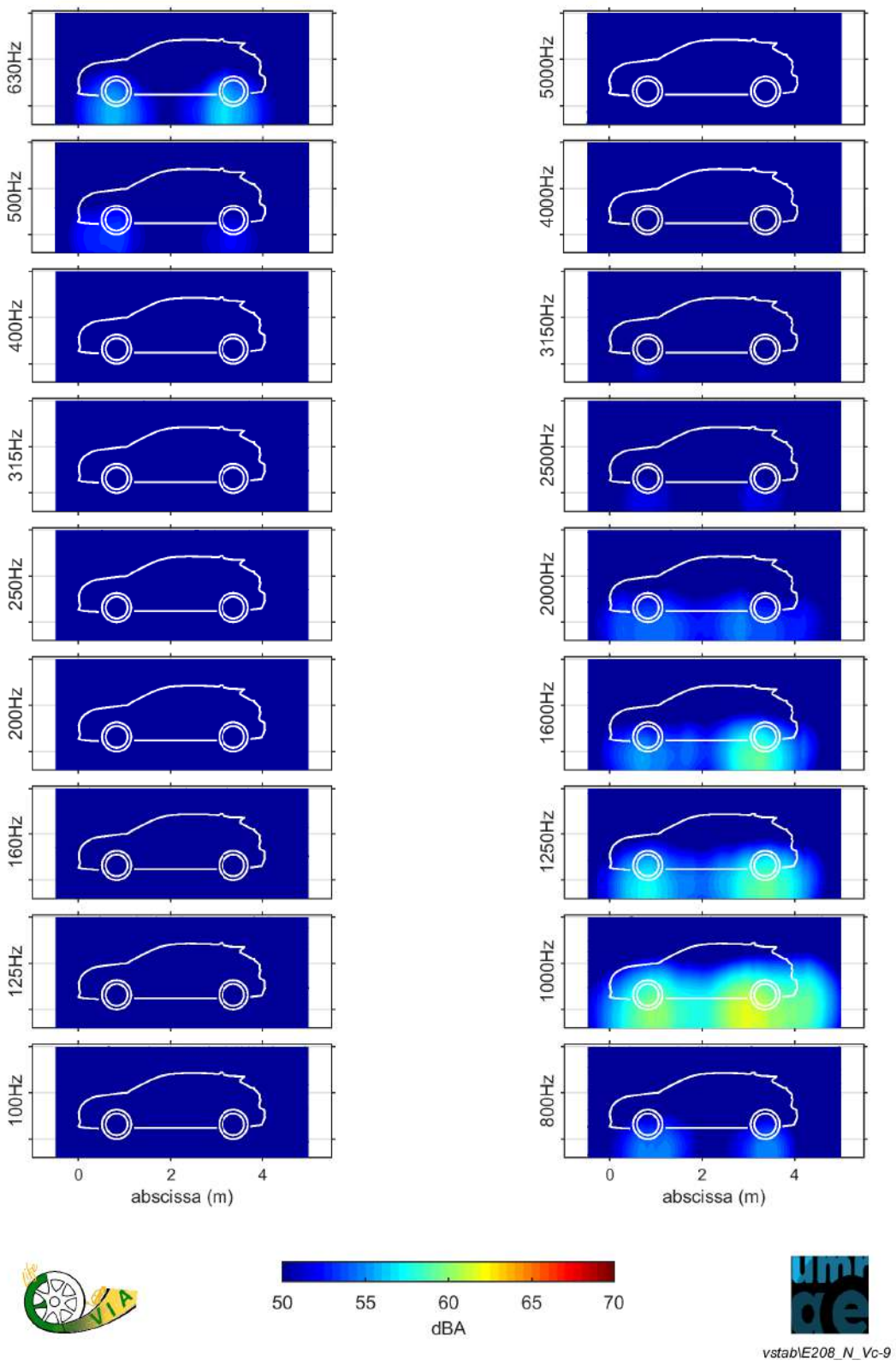

Figure A.1: Third-octave noise source maps of the Peugeot e-208 at constant speed 48.2 km/h on road N – A-weighted noise levels at the reference distance 2.7 m – Colour scale in 0.5 dB(A) steps.

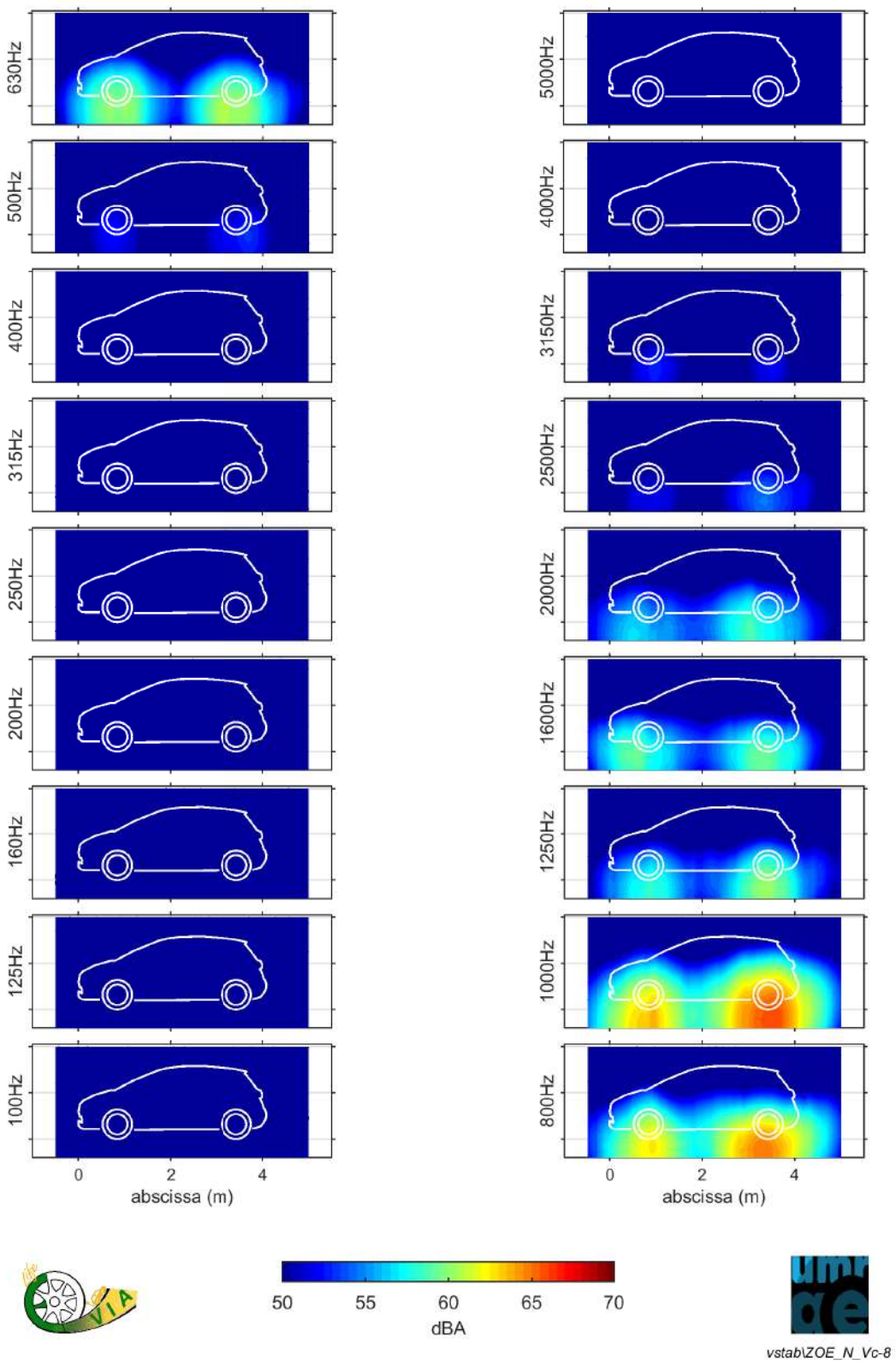

Figure A.2: Third-octave noise source maps of the Renault ZOE#2 at constant speed 50.6 km/h on road N – A-weighted noise levels at the reference distance 2.7 m – Colour scale in 0.5 dB(A) steps.

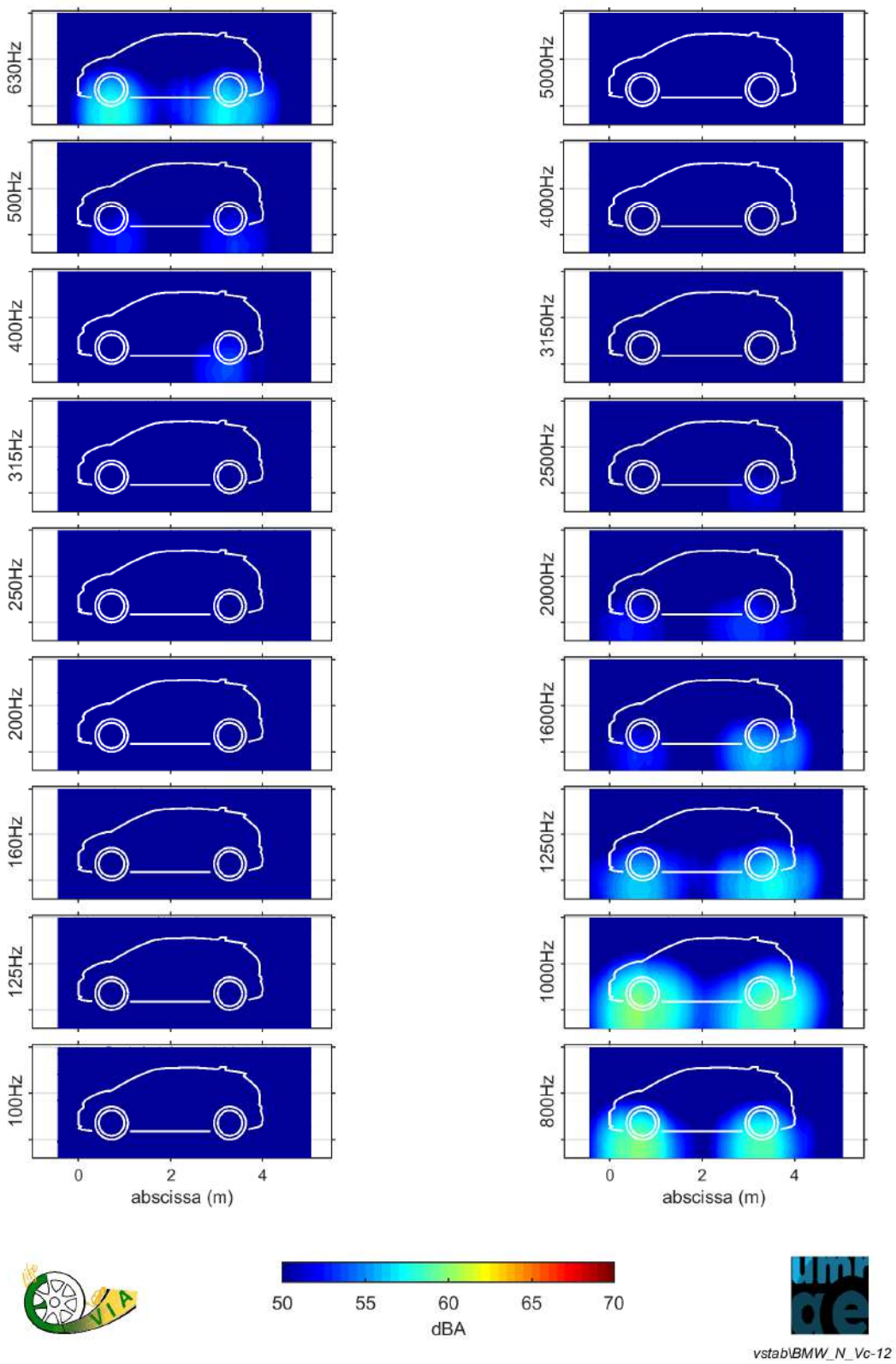

Figure A.3: Third-octave noise source maps of the BMW i3 at constant speed 48.8 km/h on road N – A-weighted noise levels at the reference distance 2.7 m – Colour scale in 0.5 dB(A) steps.

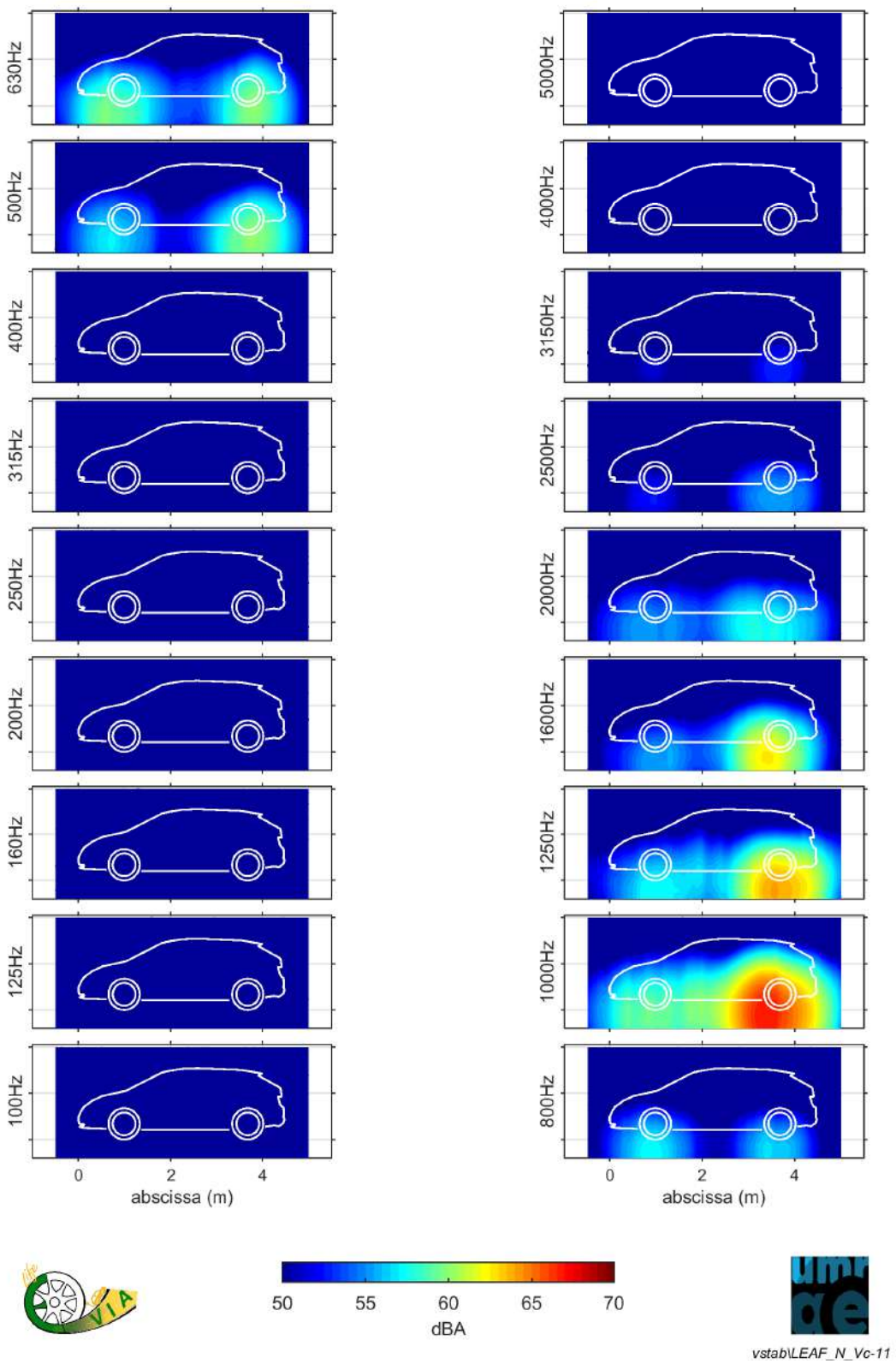

Figure A.4: Third-octave noise source maps of the Nissan LEAF#1 at constant speed 50.1 km/h on road N – A-weighted noise levels at the reference distance 2.7 m – Colour scale in 0.5 dB(A) steps.

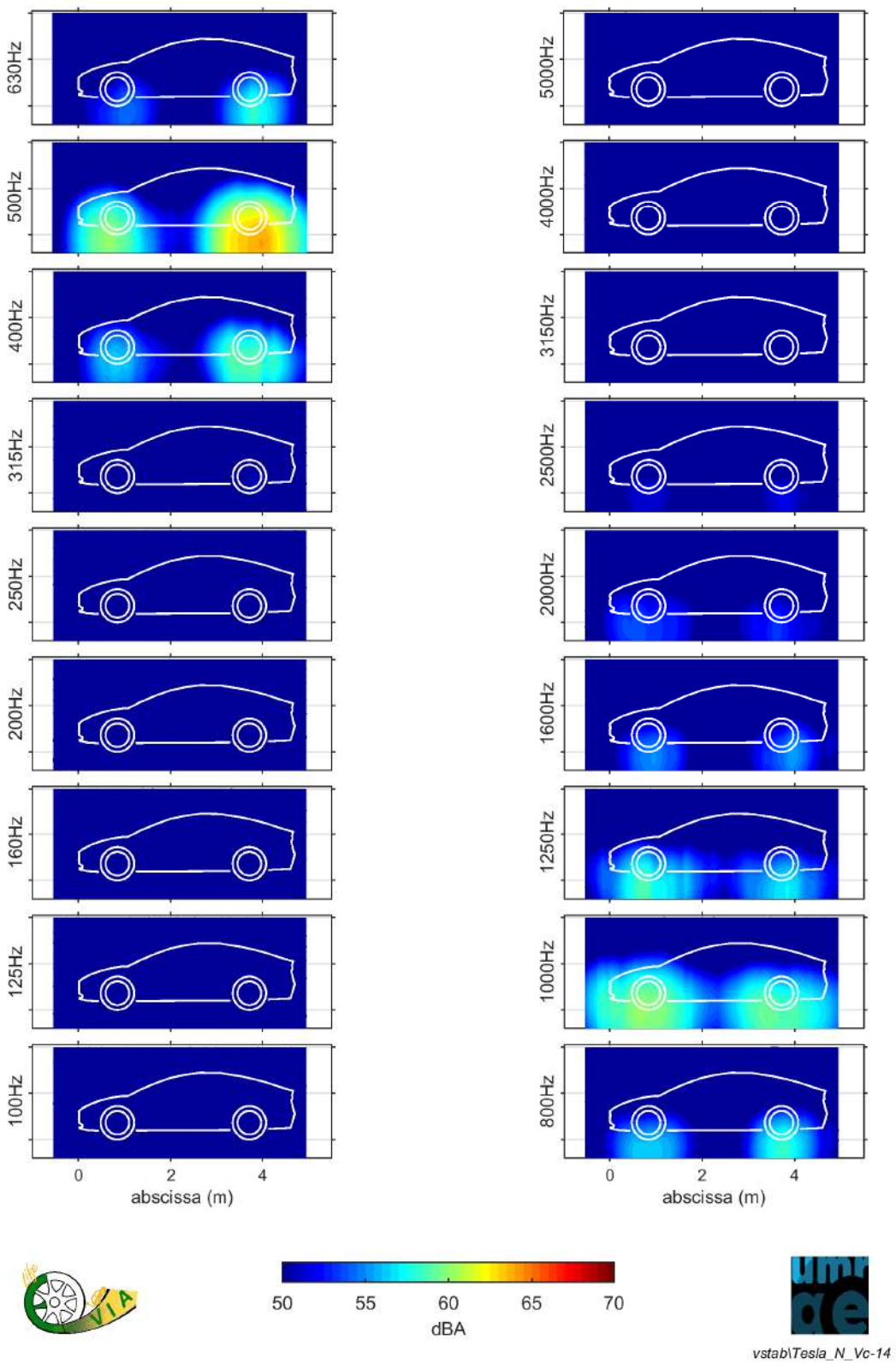

Figure A.5: Third-octave noise source maps of the Tesla Model 3 at constant speed 51.1 km/h on road N - A-weighted noise levels at the reference distance 2.7 m - Colour scale in 0.5 dB(A) steps.

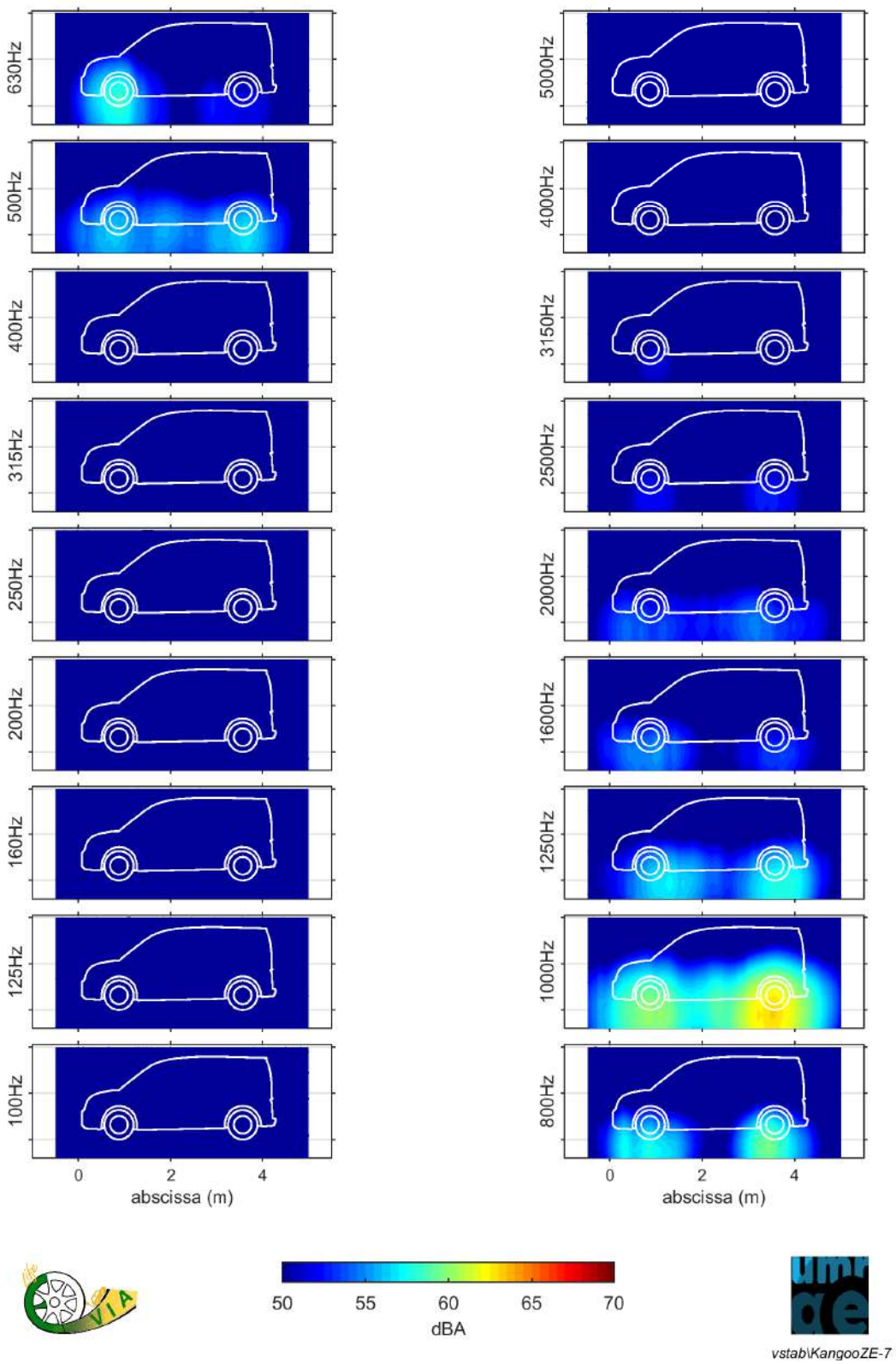

Figure A.6: Third-octave noise source maps of the Renault Kangoo ZE at constant speed 50.1 km/h on road N - A-weighted noise levels at the reference distance 2.7 m - Colour scale in 0.5 dB(A) steps.

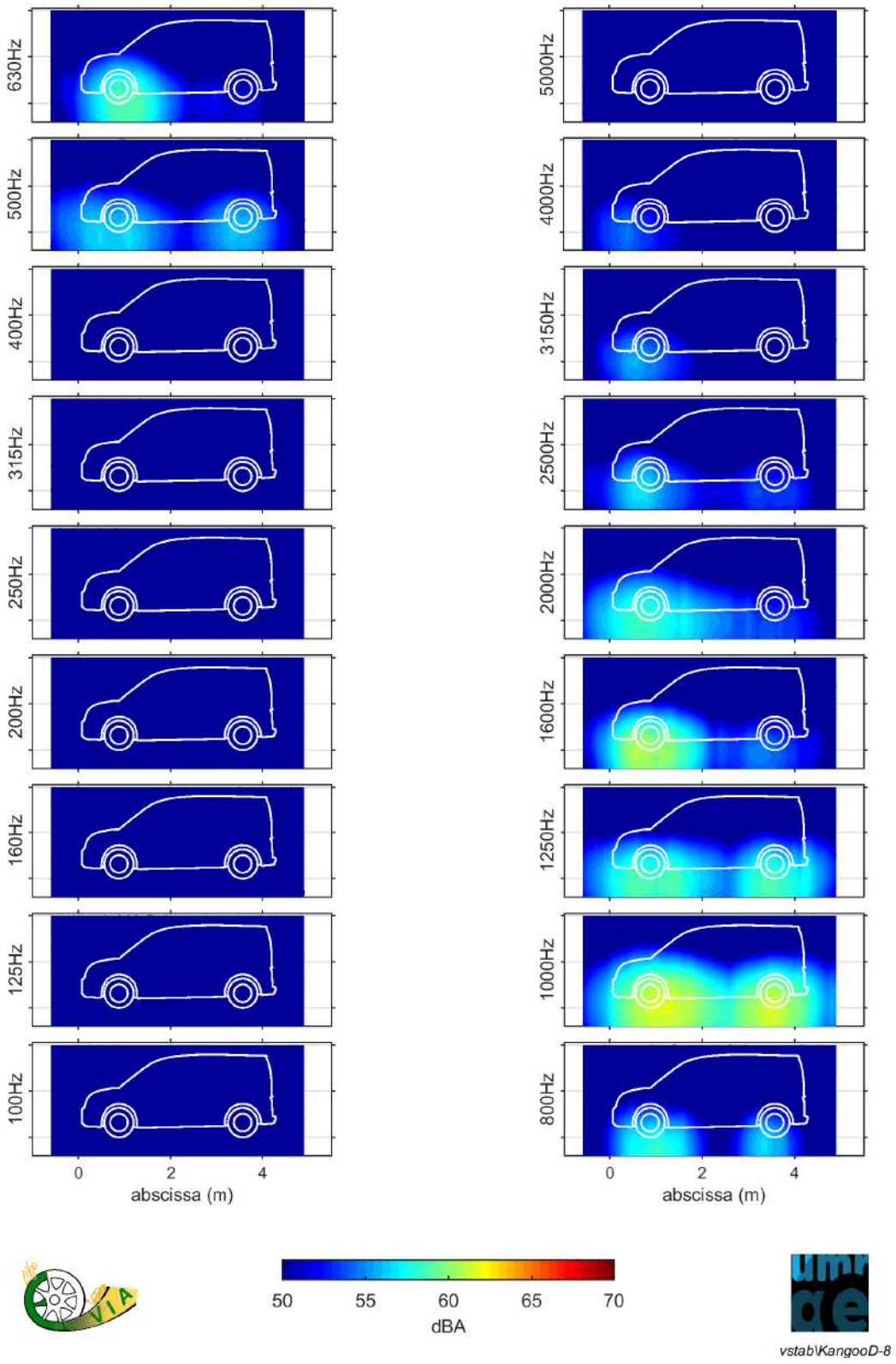

Figure A.7: Third-octave noise source maps of the Renault Kangoo Diesel at constant speed 50.2 km/h, 1625 rpm, gear 4 on road N - A-weighted noise levels at the reference distance 2.7 m - Colour scale in 0.5 dB(A) steps.

B Sub-action B2.1 : Third-octave contribution of the front and rear wheel zones at constant speed on road surface N

Note: figures begin on next page.

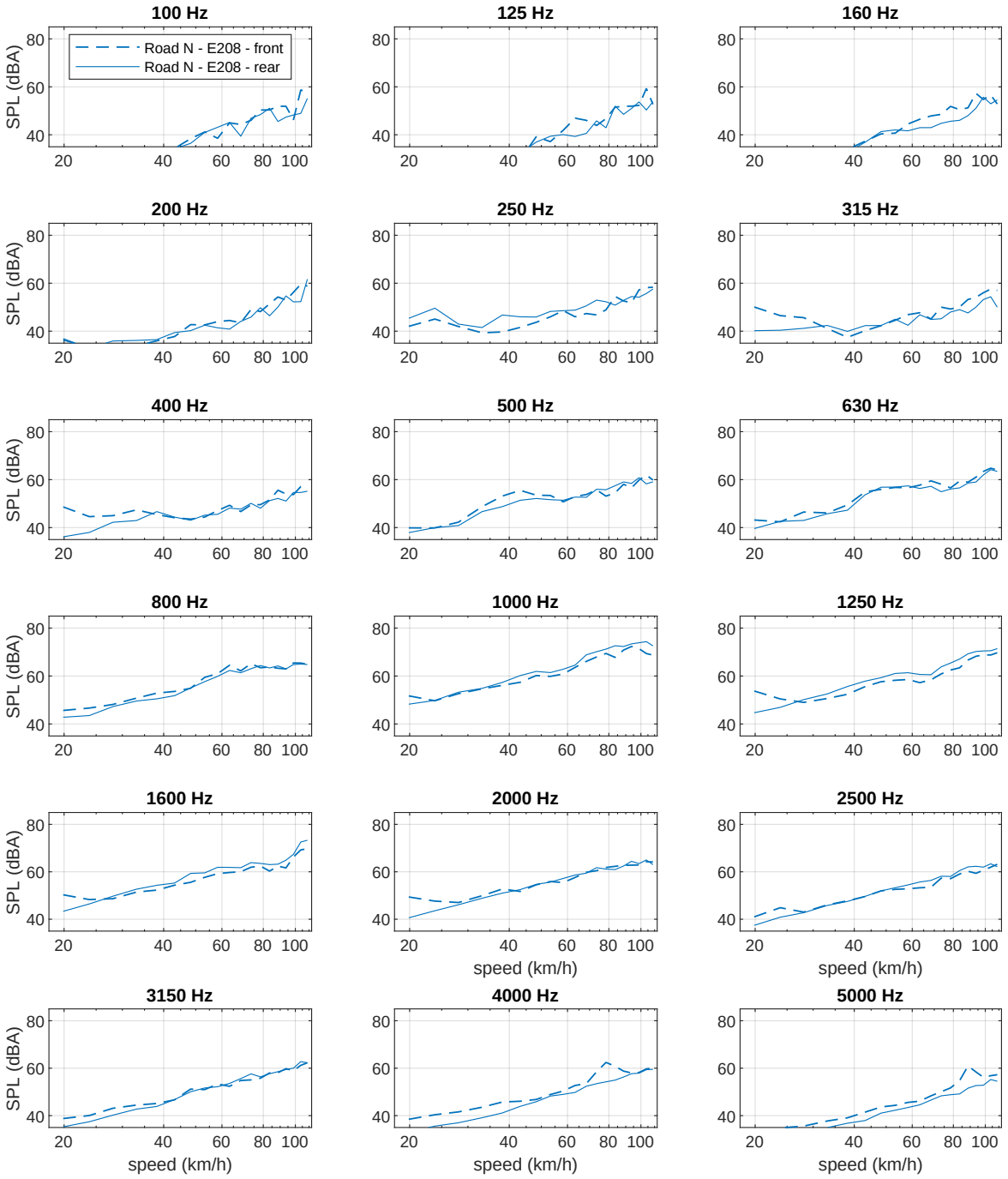

Figure B.1: Third-octave contribution of the front and rear wheel zones of the Peugeot e-208 at constant speed on road surface N – A-weighted noise levels at the reference distance 2.7 m.

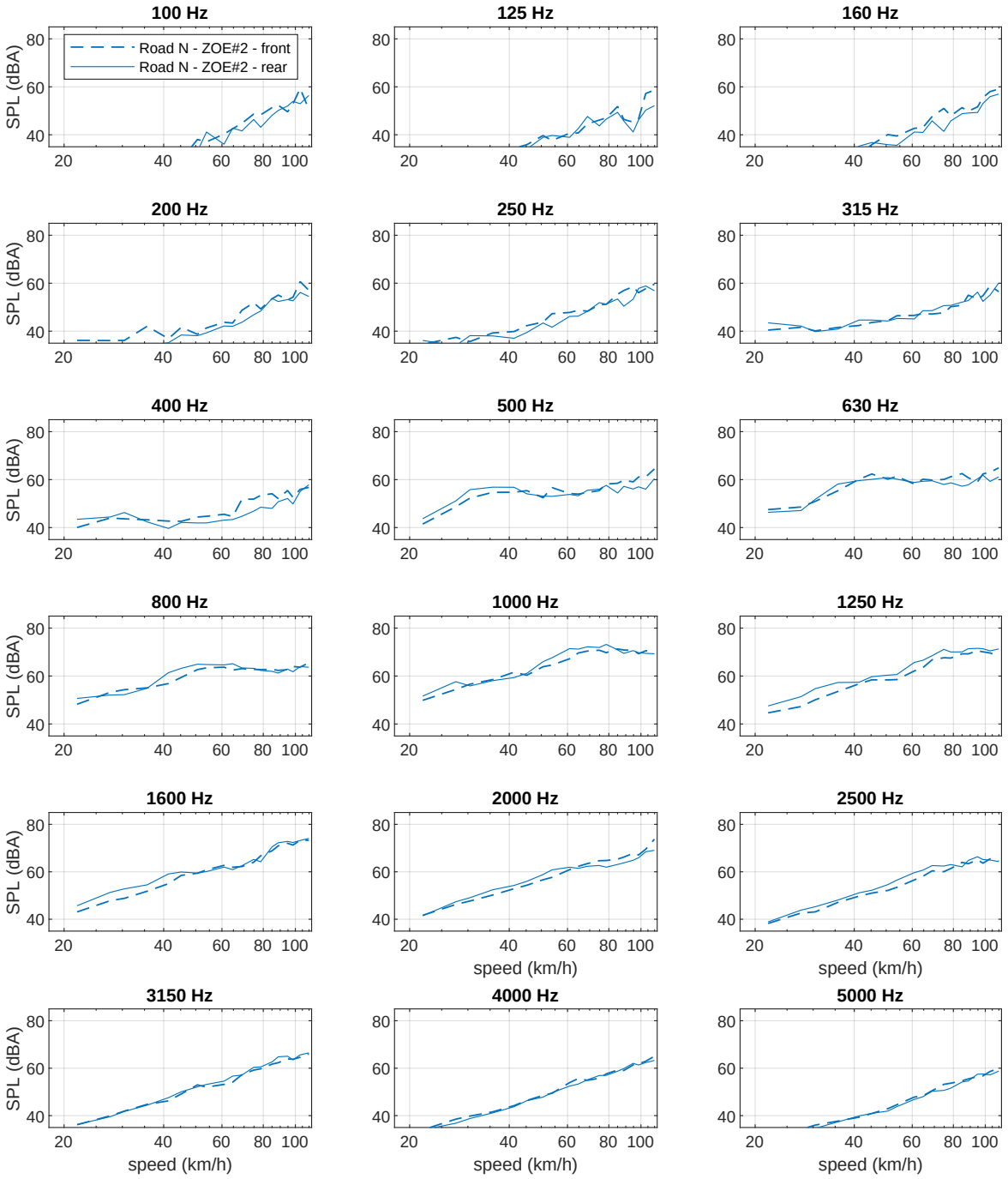

Figure B.2: Third-octave contribution of the front and rear wheel zones of the Renault ZOE#2 at constant speed on road surface N – A-weighted noise levels at the reference distance 2.7 m.

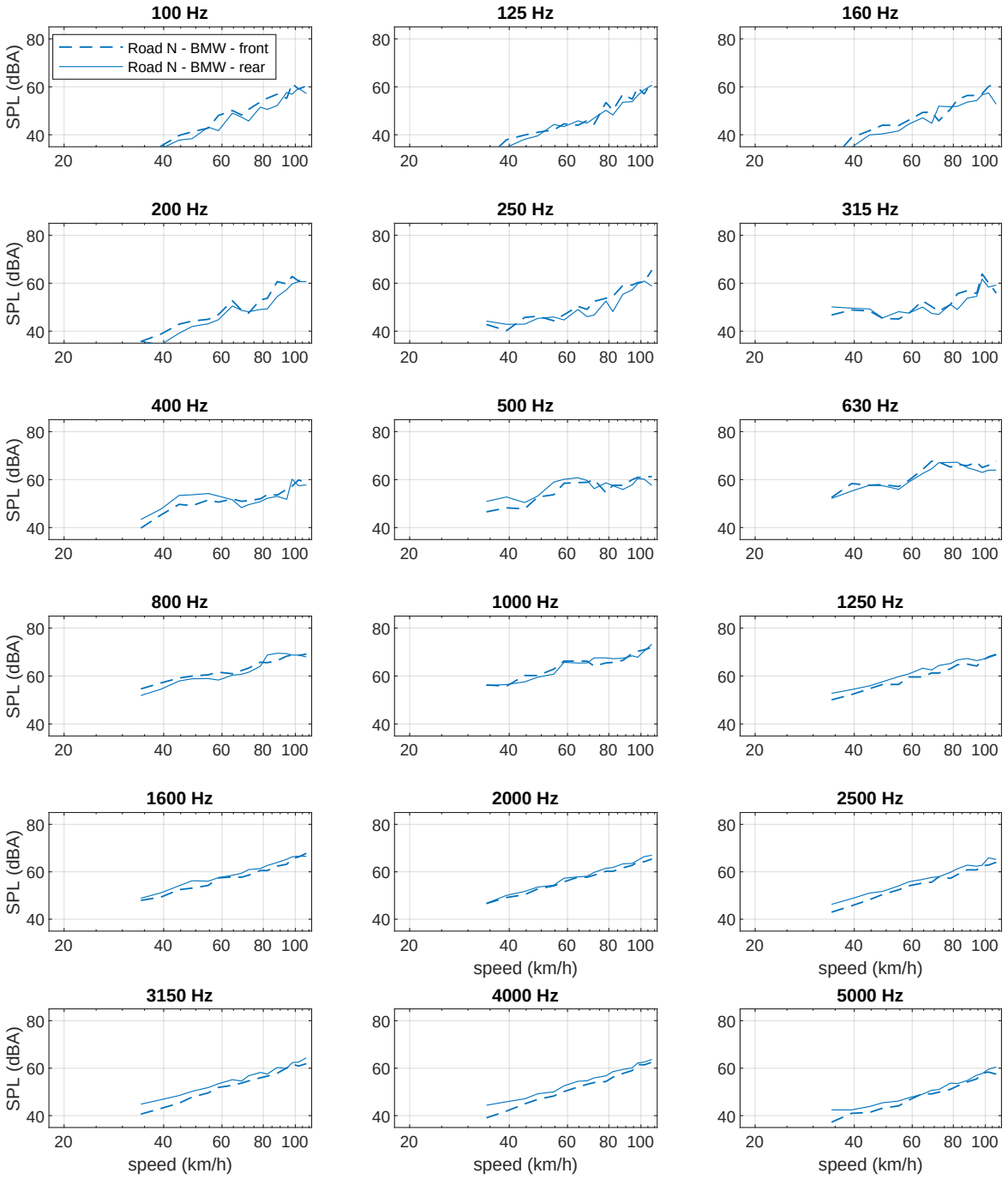

Figure B.3: Third-octave contribution of the front and rear wheel zones of the BMW i3 at constant speed on road surface N – A-weighted noise levels at the reference distance 2.7 m.

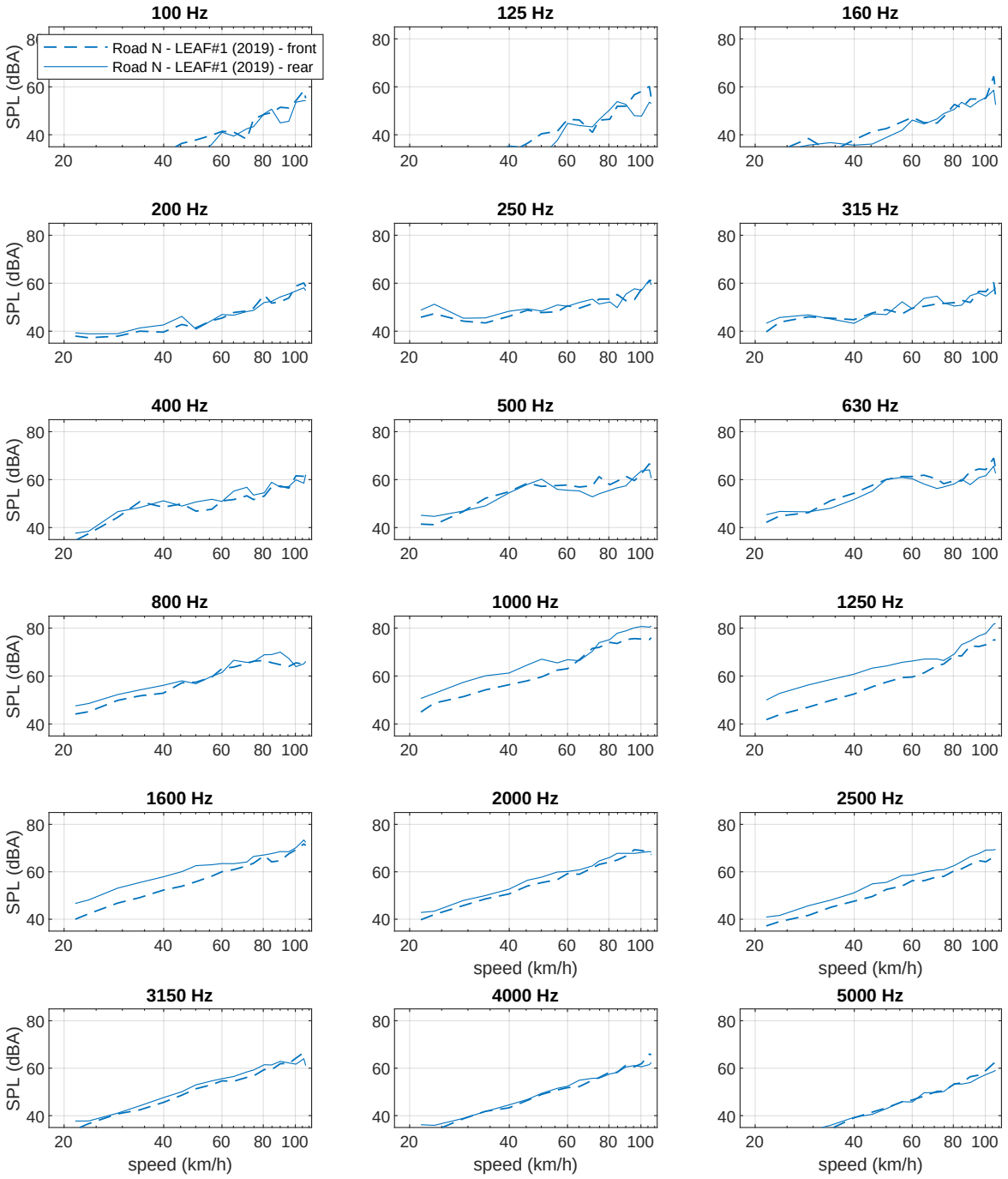

Figure B.4: Third-octave contribution of the front and rear wheel zones of the Nissan LEAF#1 at constant speed on road surface N – A-weighted noise levels at the reference distance 2.7 m.

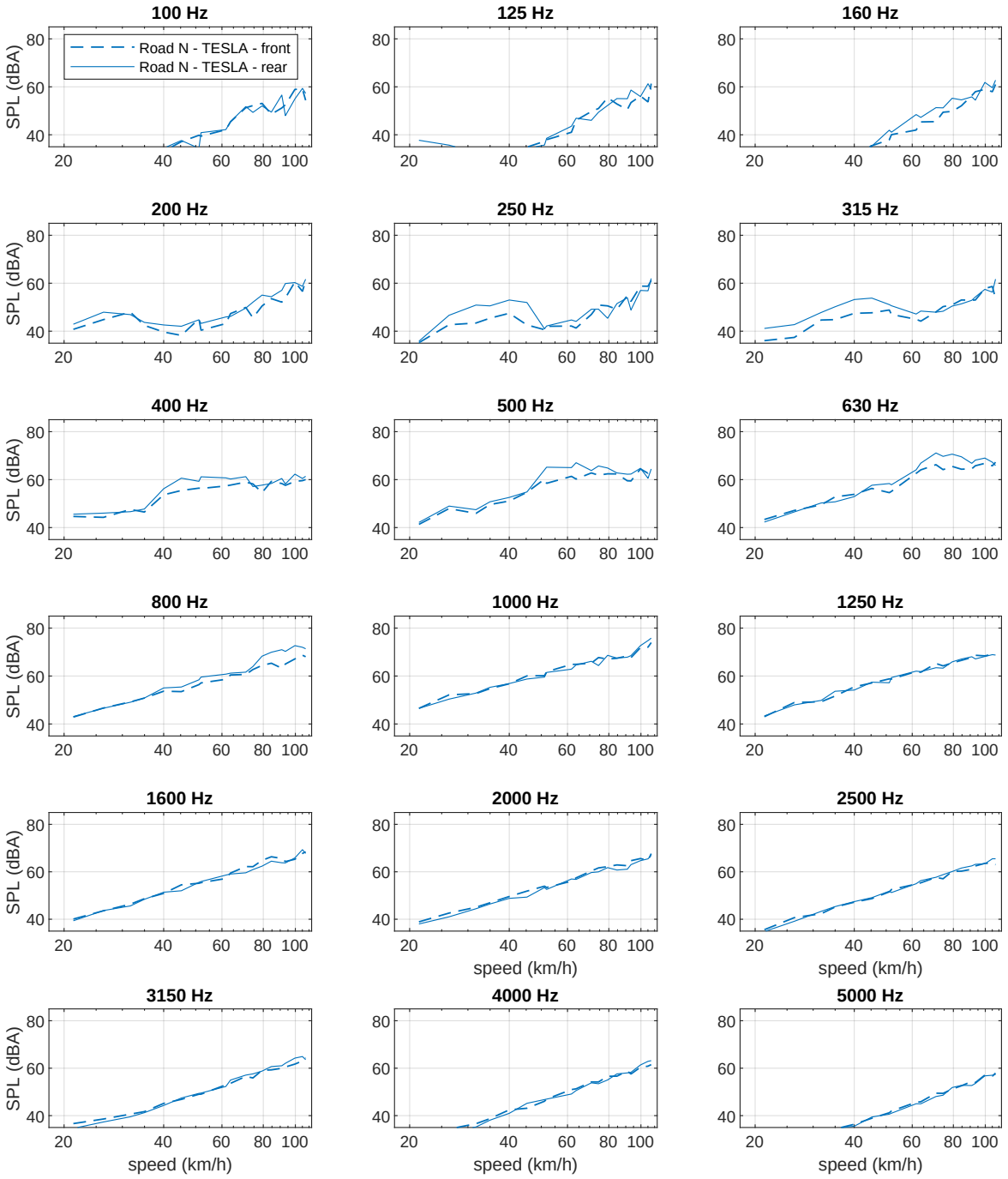

Figure B.5: Third-octave contribution of the front and rear wheel zones of the Tesla Model 3 at constant speed on road surface N – A-weighted noise levels at the reference distance 2.7 m.

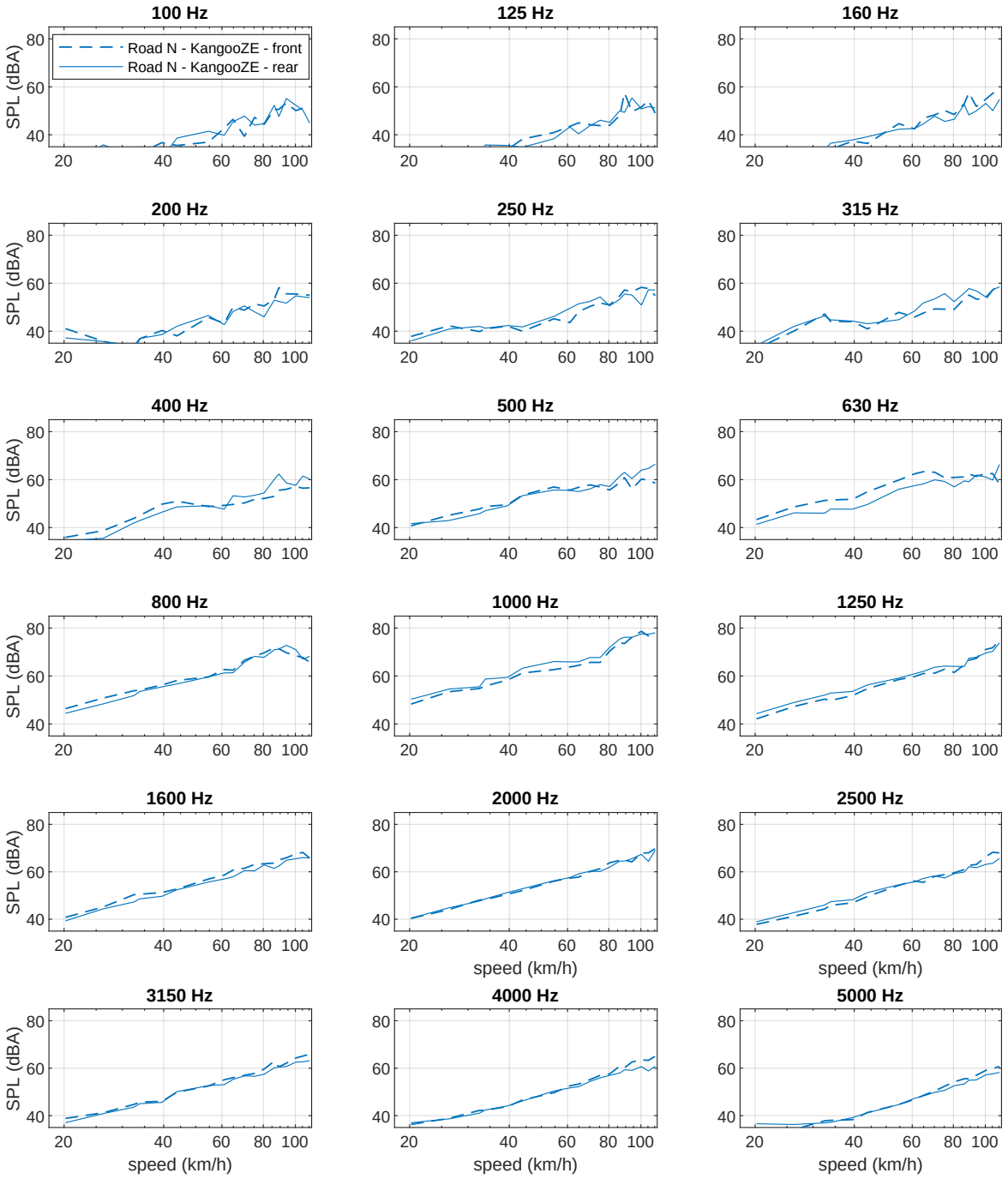

Figure B.6: Third-octave contribution of the front and rear wheel zones of the Renault Kangoo ZE at constant speed on road surface N – A-weighted noise levels at the reference distance 2.7 m.

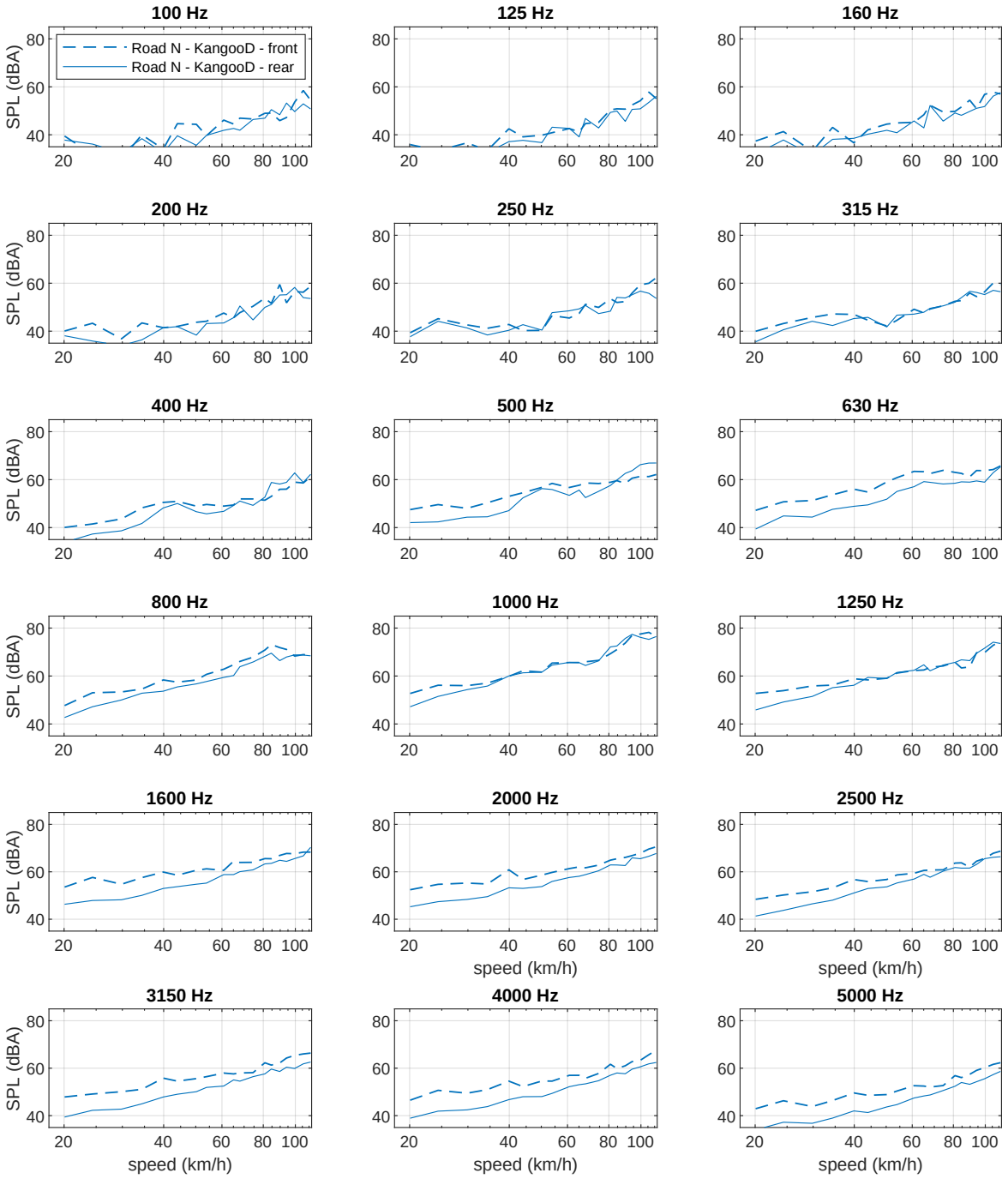

Figure B.7: Third-octave contribution of the front and rear wheel zones of the Renault Kangoo Diesel at constant speed on road surface N – A-weighted noise levels at the reference distance 2.7 m.

C Sub-action B2.1 : Third-octave noise source maps of the Peugeot e208 with AVAS on road surface N

Note: figures begin on next page.

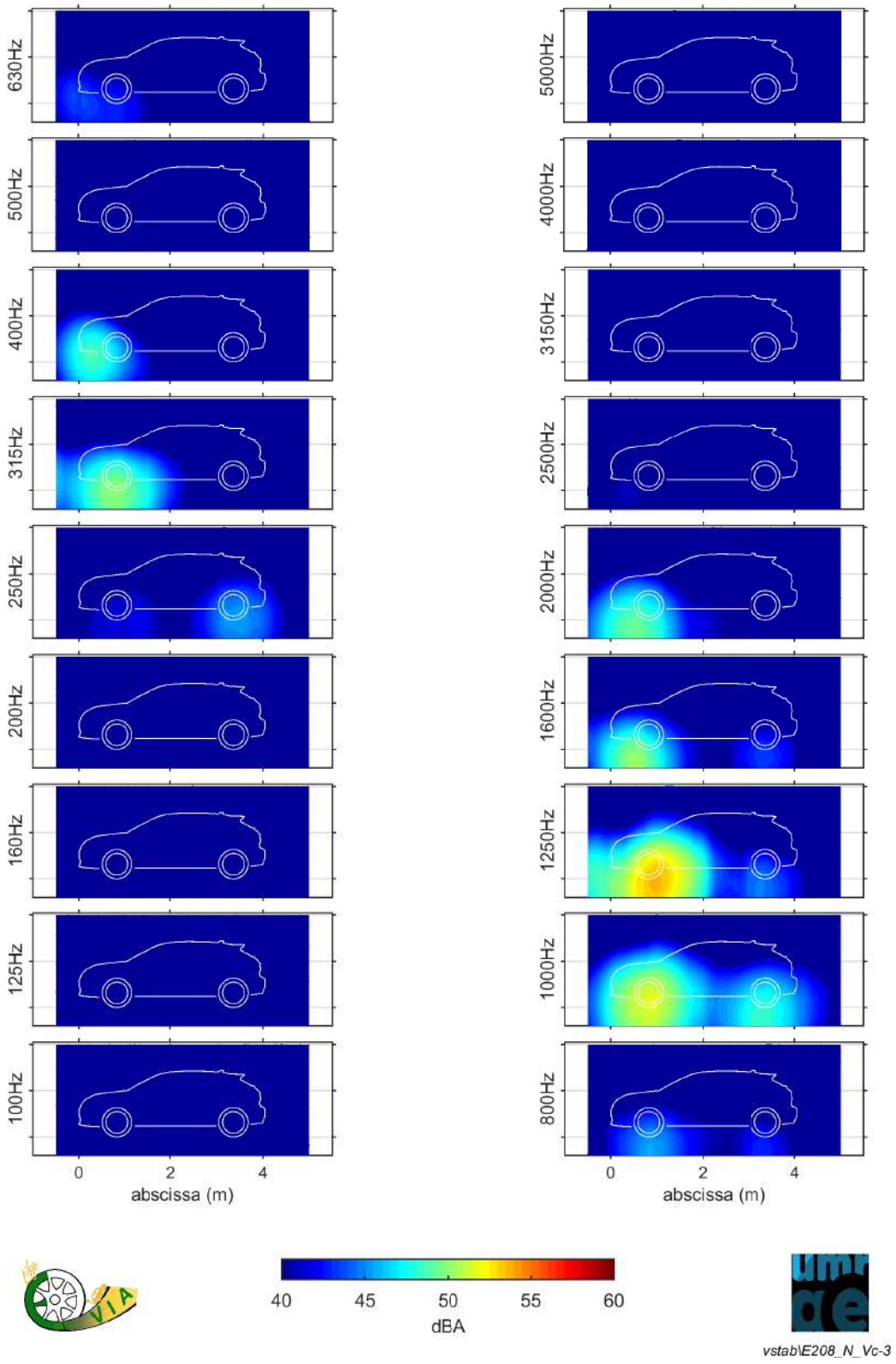

Figure C.1: Third-octave noise source maps of the Peugeot e-208 with AVAS on at constant speed 19.9 km/h on road N – A-weighted noise levels at the reference distance 2.7 m – Colour scale in 0.5 dB(A) steps.

D Sub-action B2.1 : Noise source levels at front and rear wheel in all driving modes on road surface N

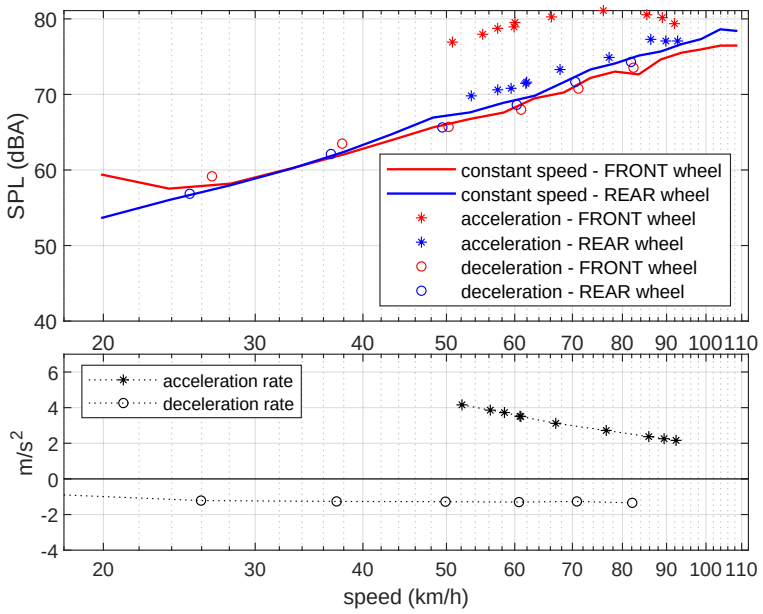

Figure D.1: Front and rear wheel noise sources of the Peugeot e-208 in all driving modes on road N – Top: A-weighted overall noise levels at the reference distance of 2.7 m – Bottom: acceleration and deceleration rates.

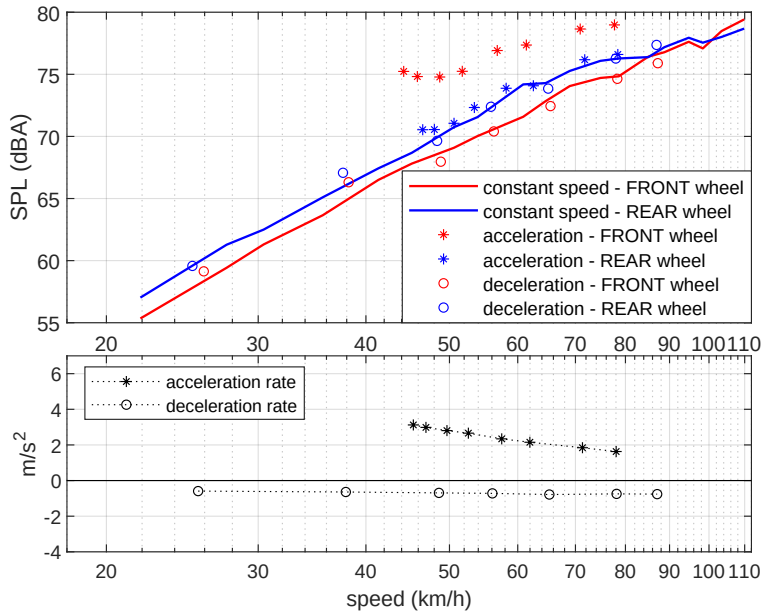

Figure D.2: Front and rear wheel noise sources of the Renault ZOE#2 in all driving modes on road N – Top: A-weighted overall noise levels at the reference distance of 2.7 m – Bottom: acceleration and deceleration rates.

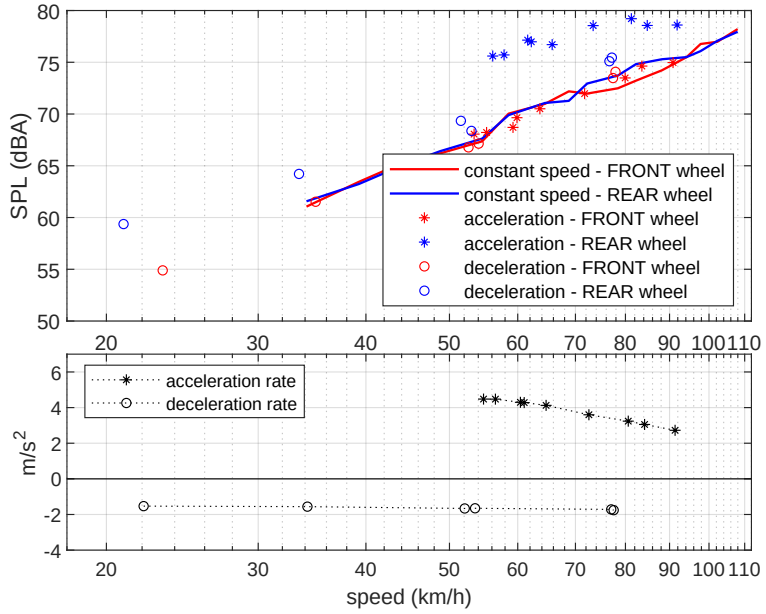

Figure D.3: Front and rear wheel noise sources of the BMW i3 in all driving modes on road N – Top: A-weighted overall noise levels at the reference distance of 2.7 m – Bottom: acceleration and deceleration rates.

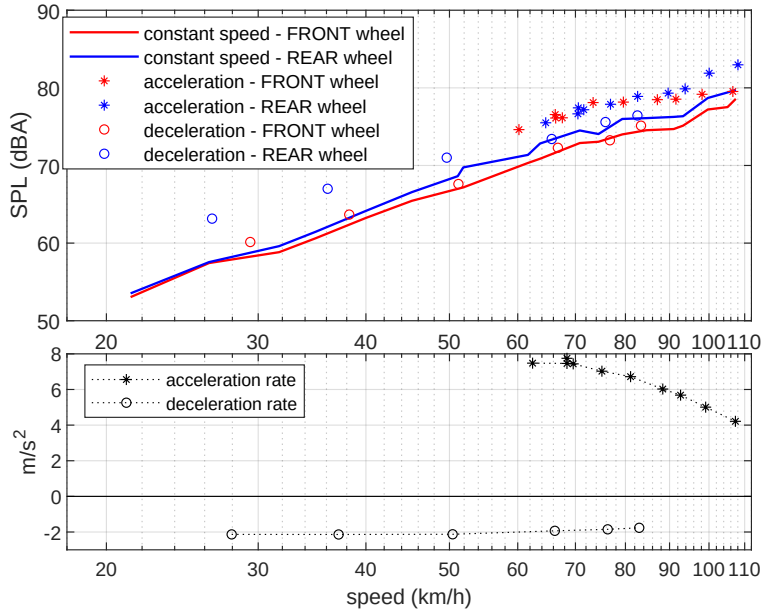

Figure D.4: Front and rear wheel noise sources of the Tesla Model3 in all driving modes on road N – Top: A-weighted overall noise levels at the reference distance of 2.7 m – Bottom: acceleration and deceleration rates.

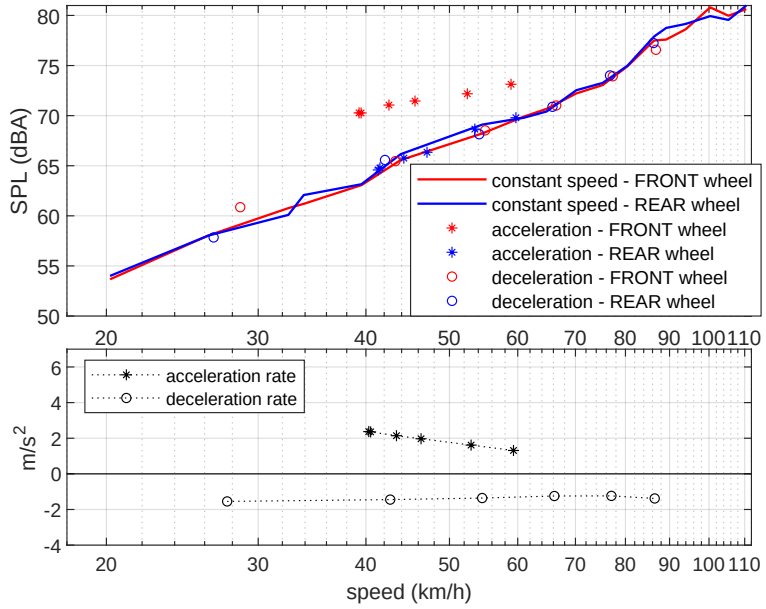

Figure D.5: Front and rear wheel noise sources of the Renault Kangoo ZE in all driving modes on road N – Top: A-weighted overall noise levels at the reference distance of 2.7 m – Bottom: acceleration and deceleration rates.

E Sub-action B2.1 : Third-octave noise source maps of the Nissan LEAF#1, the BMW i3 and the Tesla Model 3 on road surface N under deceleration

Note: figures begin on next page.

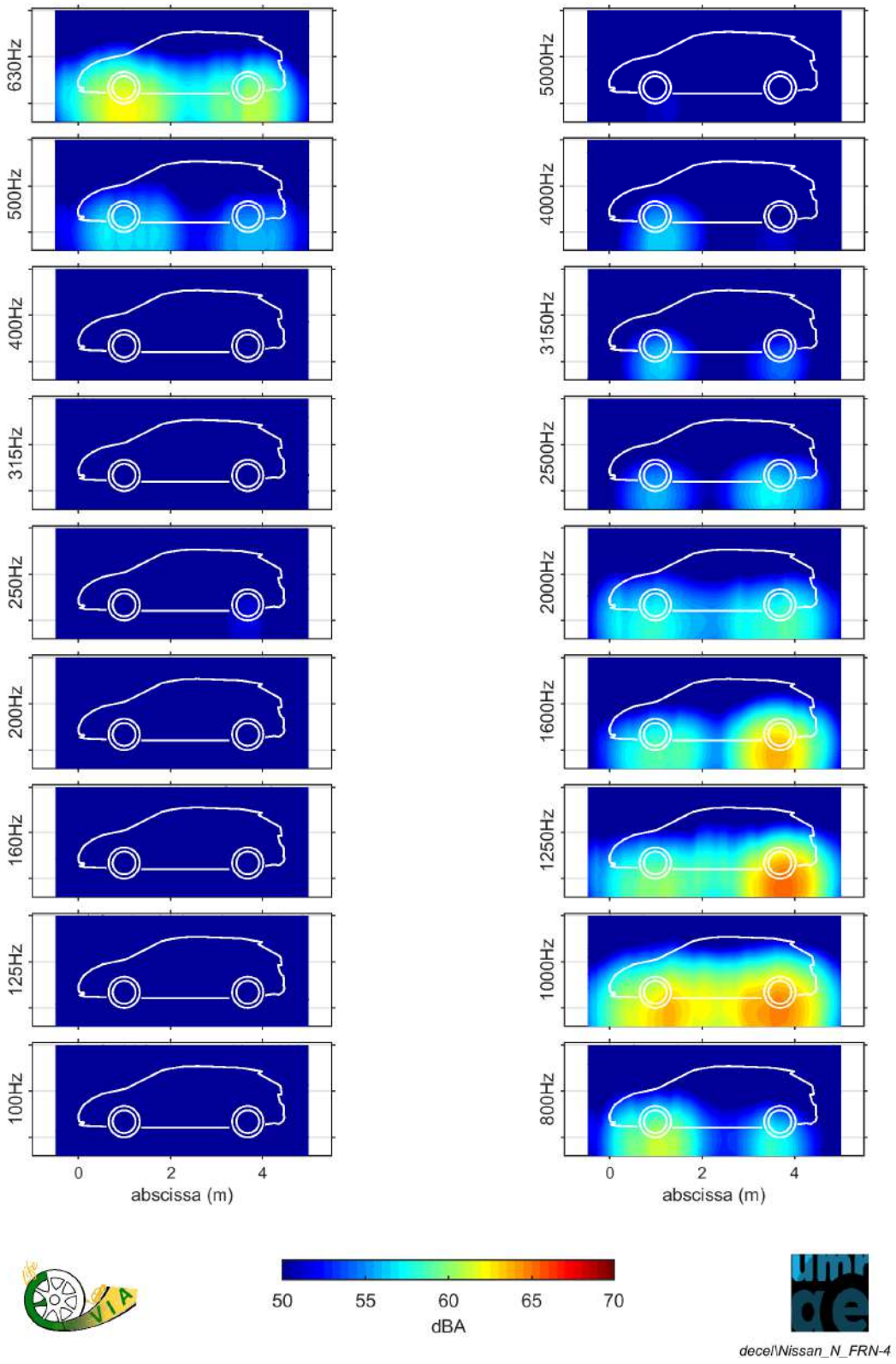

Figure E.1: Third-octave noise source maps of the Nissan LEAF#1 under deceleration on road surface N (speed in front of array: front wheel 55.7 km/h, rear wheel 54.5 km/h) – A-weighted noise levels at the reference distance 2.7 m – Colour scale in 0.5 dB(A) steps.

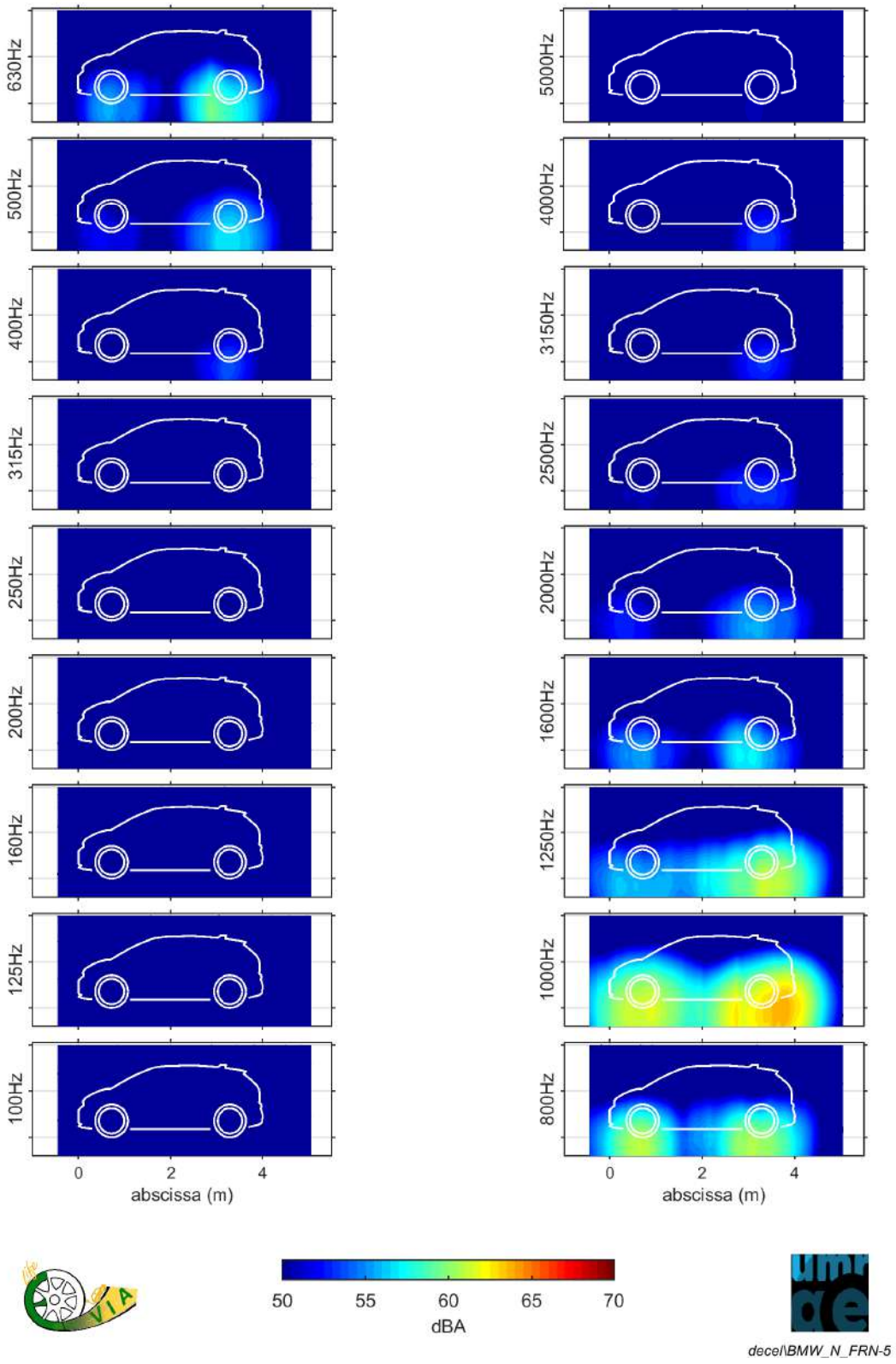

Figure E.2: Third-octave noise source maps of the BMW i3 under deceleration on road surface N (speed in front of array: front wheel 52.6 km/h, rear wheel 51.5 km/h) – A-weighted noise levels at the reference distance 2.7 m – Colour scale in 0.5 dB(A) steps.

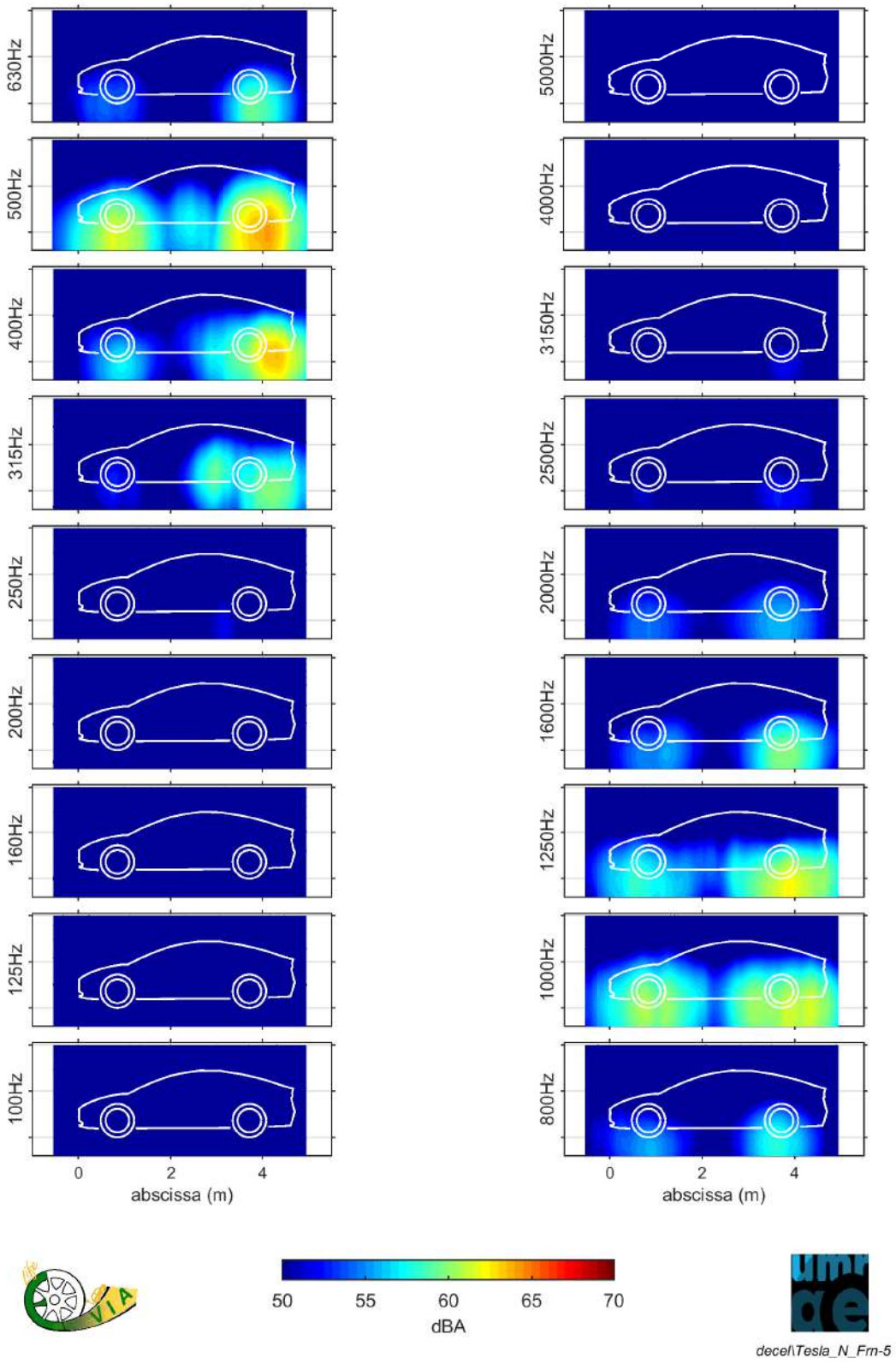

Figure E.3: Third-octave noise source maps of the Tesla Model 3 under deceleration on road surface N (speed in front of array: front wheel 51.2 km/h, rear wheel 49.6 km/h) – A-weighted noise levels at the reference distance 2.7 m – Colour scale in 0.5 dB(A) steps.

F Sub-action B2.3 : Third-octave noise source maps of the EVs on prototype road surface P at constant speed 50 km/h

Note: figures begin on next page.

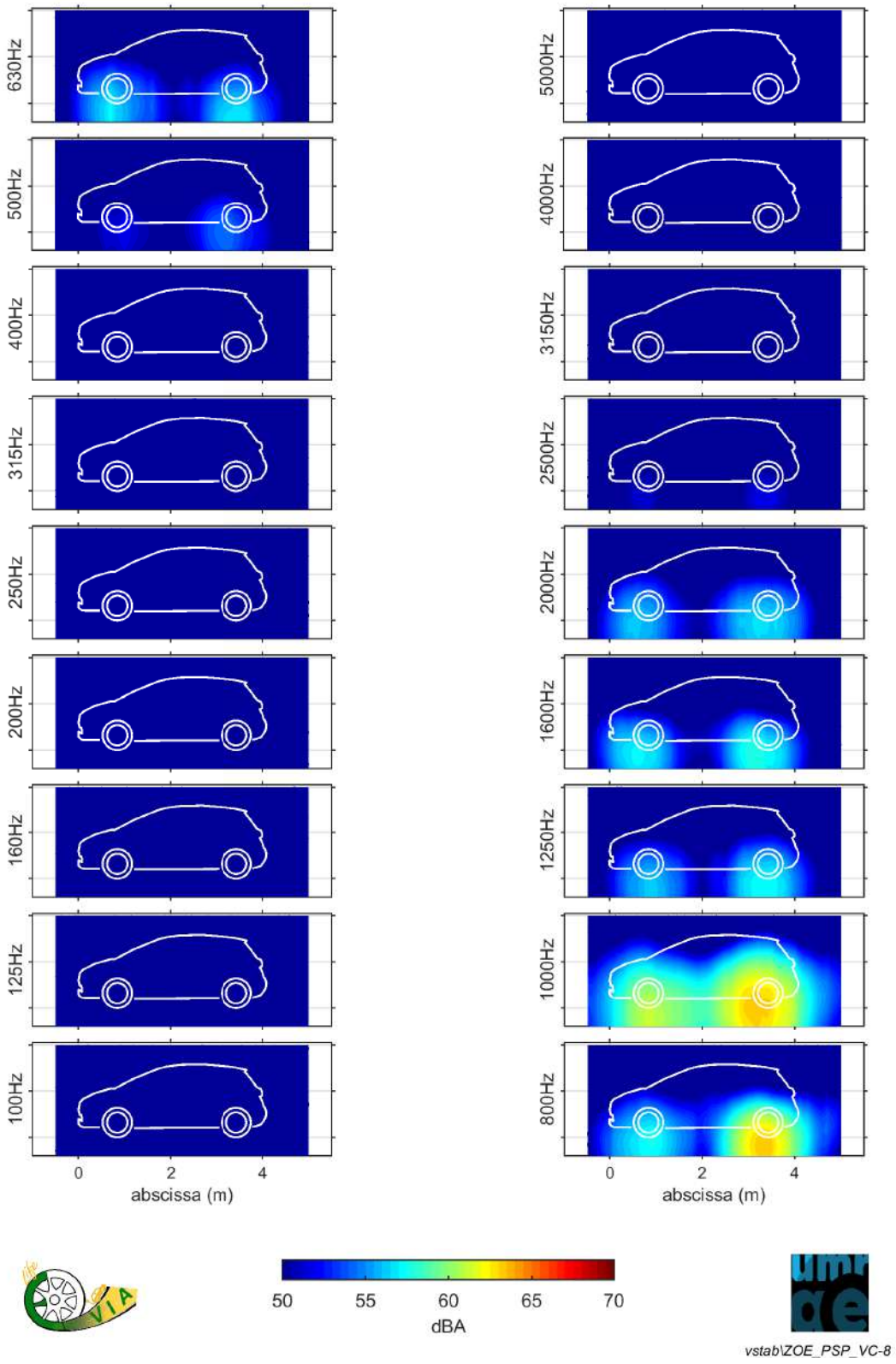

Figure F.1: Third-octave noise source maps of the Renault ZOE#2 at constant speed 50.1 km/h on test section P – A-weighted noise levels at the reference distance 2.7 m – Colour scale in 0.5 dB(A) steps.

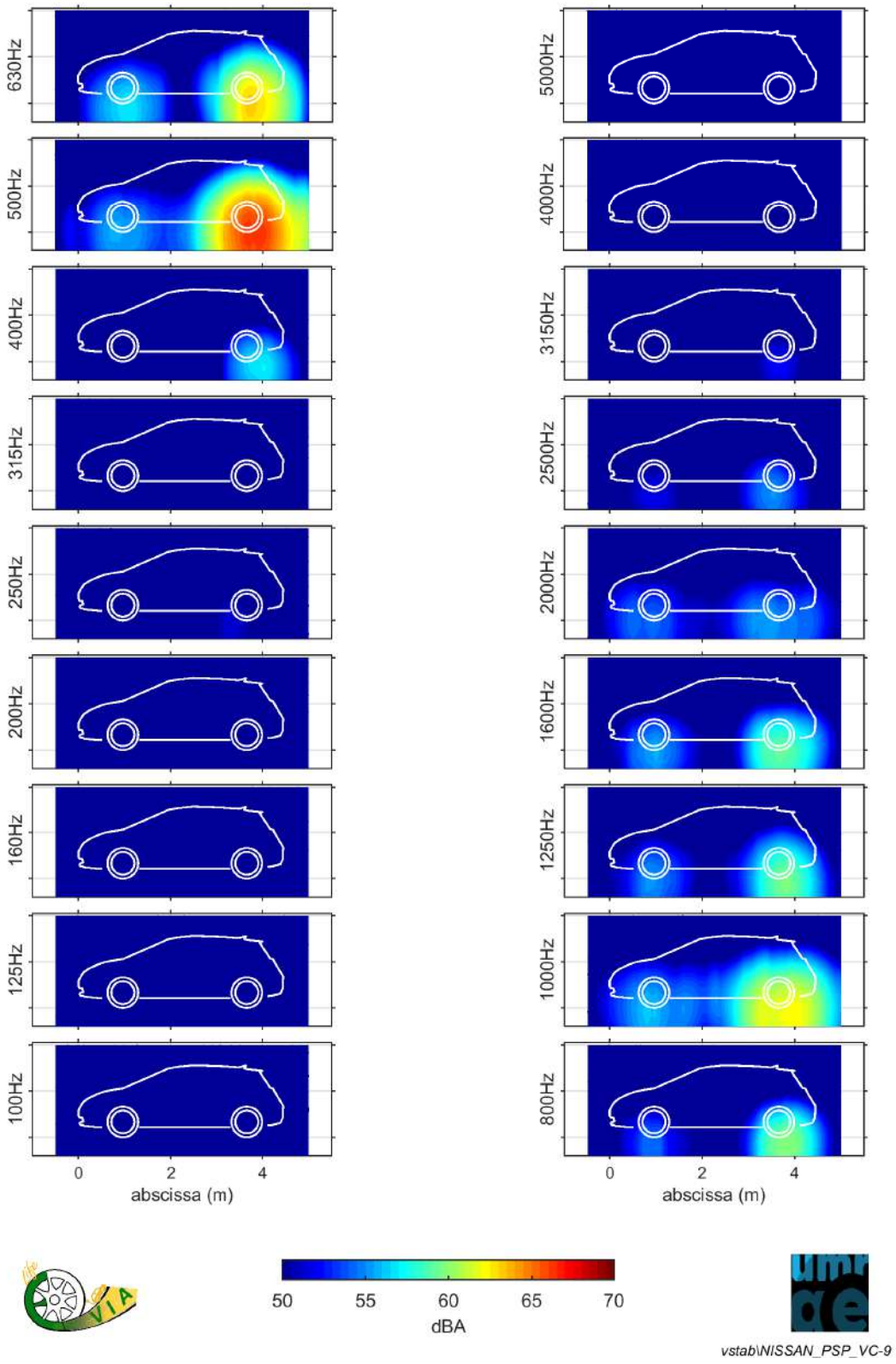

Figure F.2: Third-octave noise source maps of the Nissan LEAF#2 at constant speed 49.4 km/h on test section P – A-weighted noise levels at the reference distance 2.7 m – Colour scale in 0.5 dB(A) steps.

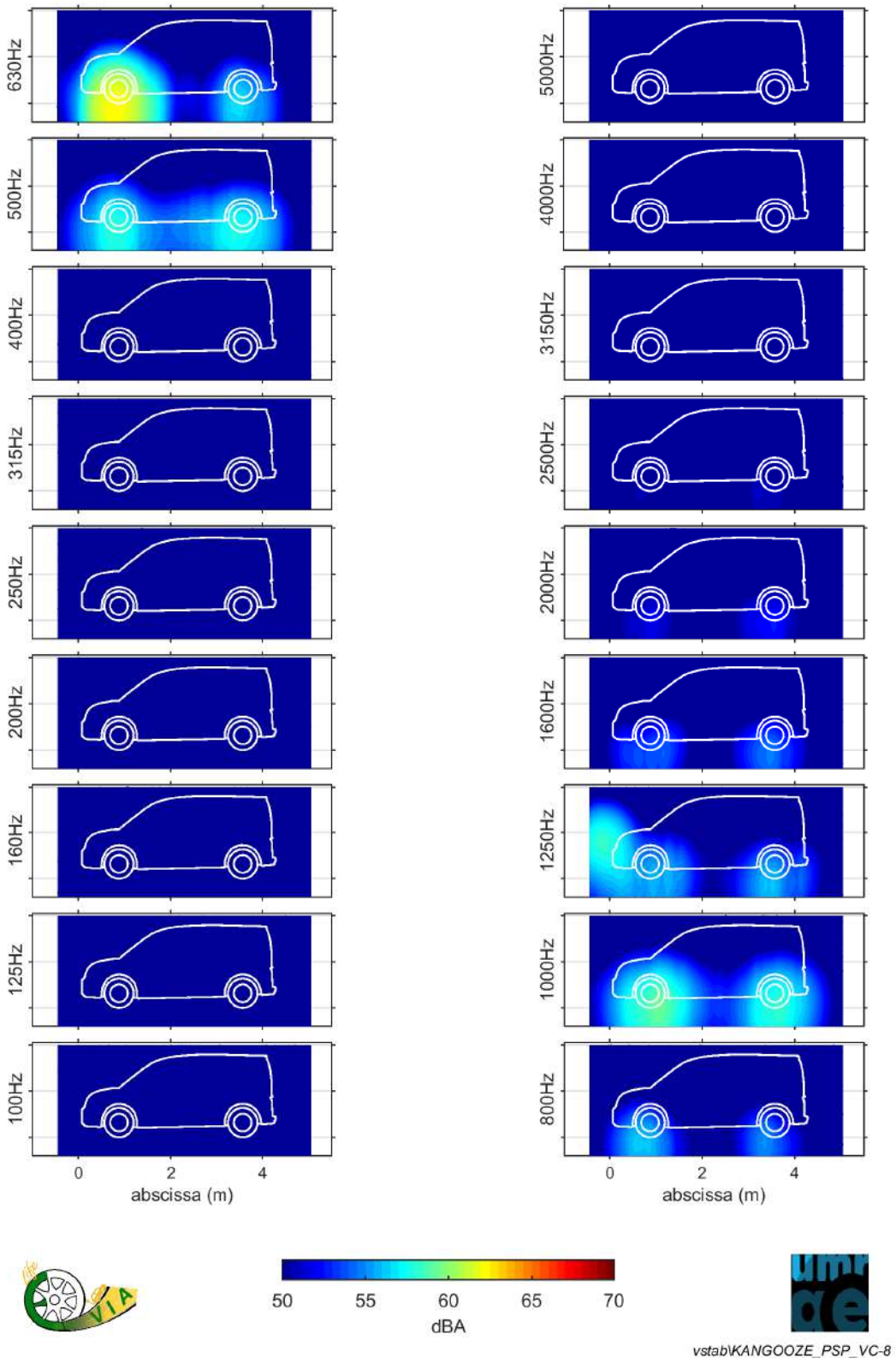

Figure F.3: Third-octave noise source maps of the Renault Kangoo ZE at constant speed 50.6 km/h on test section P – A-weighted noise levels at the reference distance 2.7 m – Colour scale in 0.5 dB(A) steps.

G Sub-action B2.3 : Third-octave noise source maps of the EVs on prototype road surface PCR at constant speed 50 km/h

Note: figures begin on next page.

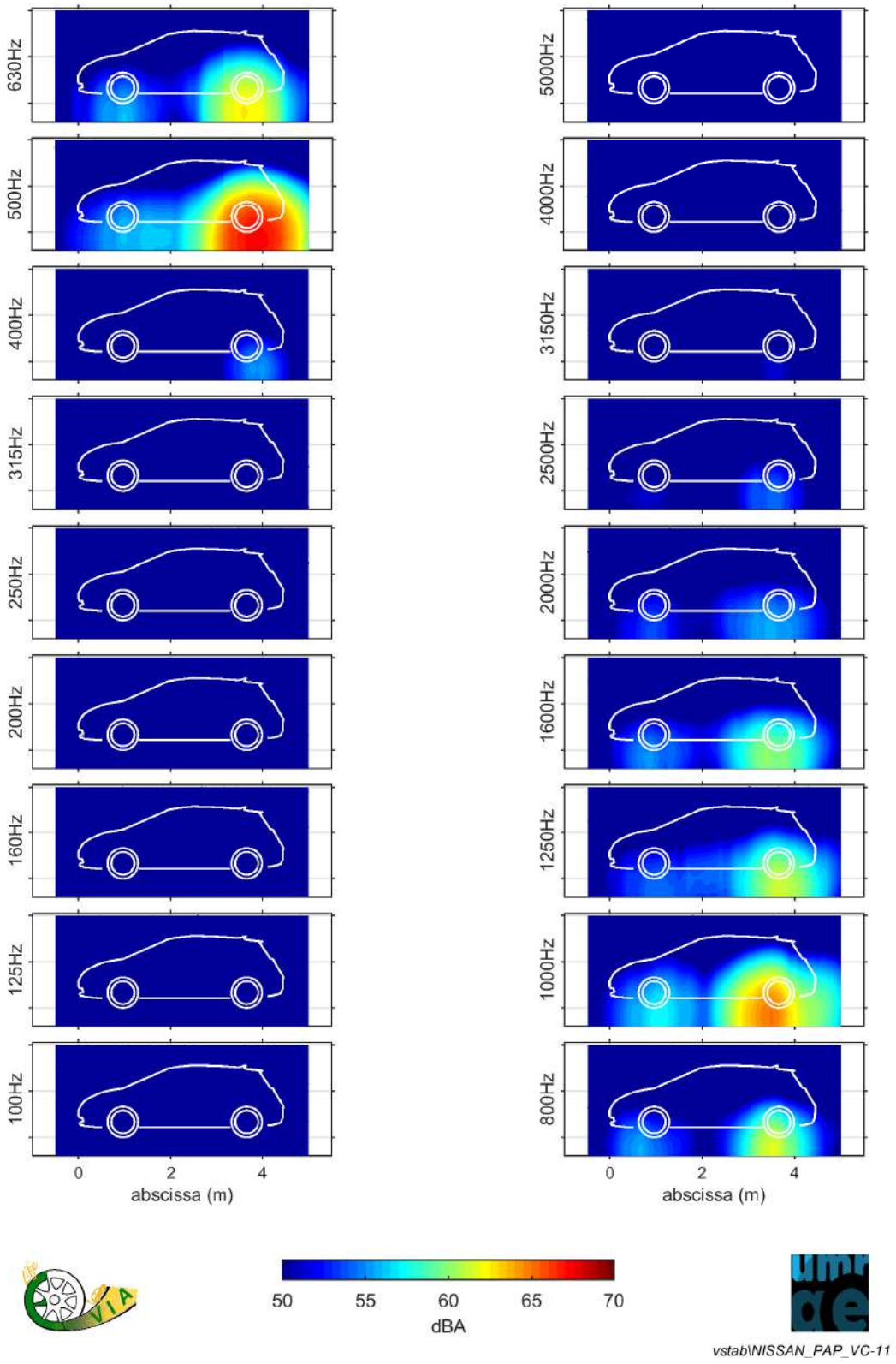

Figure G.1: Third-octave noise source maps of the Nissan LEAF#2 at constant speed 50.2 km/h on test section PCR – A-weighted noise levels at the reference distance 2.7 m – Colour scale in 0.5 dB(A) steps.

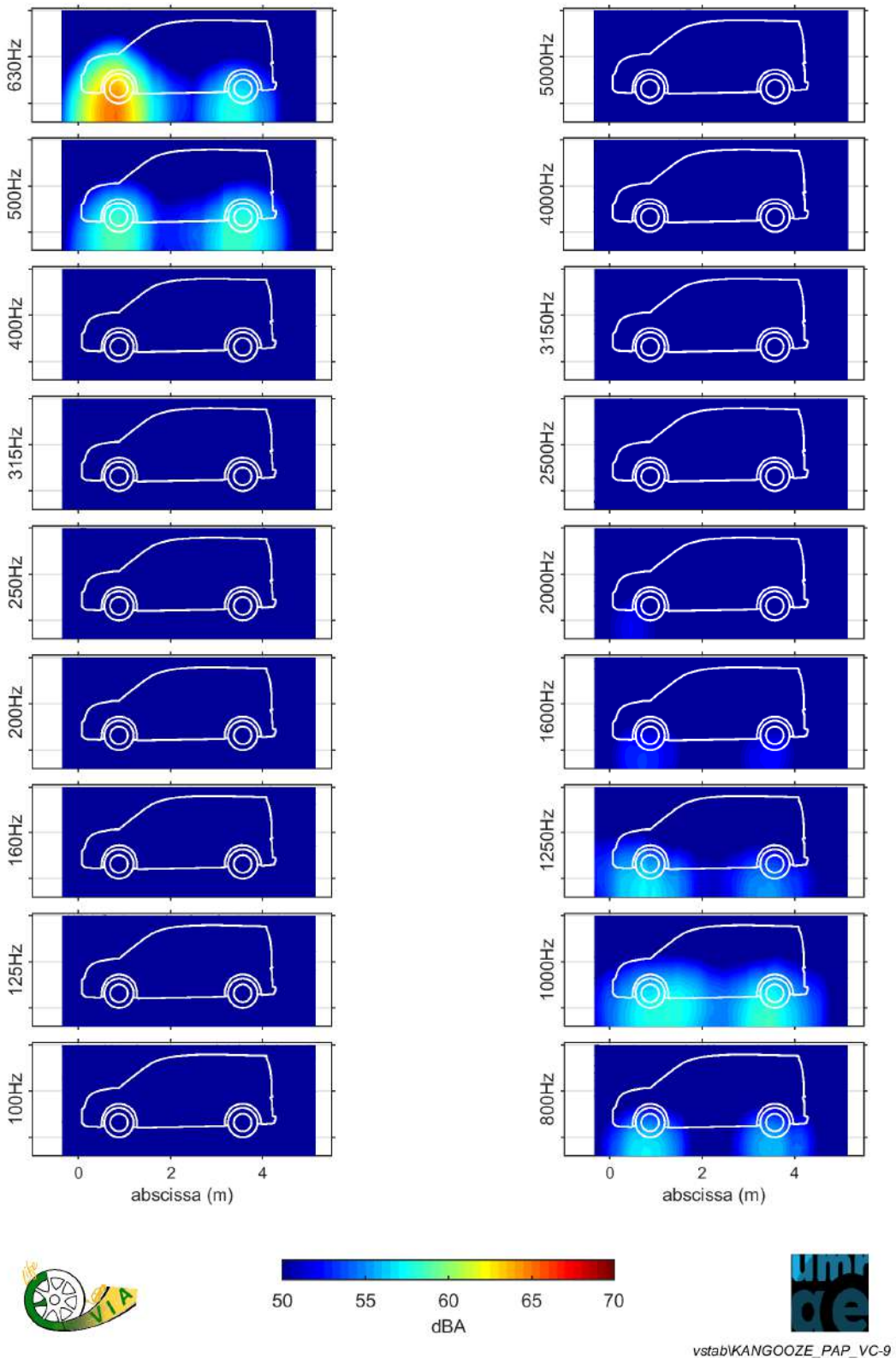

Figure G.2: Third-octave noise source maps of the Renault Kangoo ZE at constant speed 50.9 km/h on test section PCR – A-weighted noise levels at the reference distance 2.7 m – Colour scale in 0.5 dB(A) steps.

H Sub-action B2.3 : Third-octave contribution of the front and rear wheel zones at constant speed on prototype road surfaces P and PCR

Note: figures begin on next page.

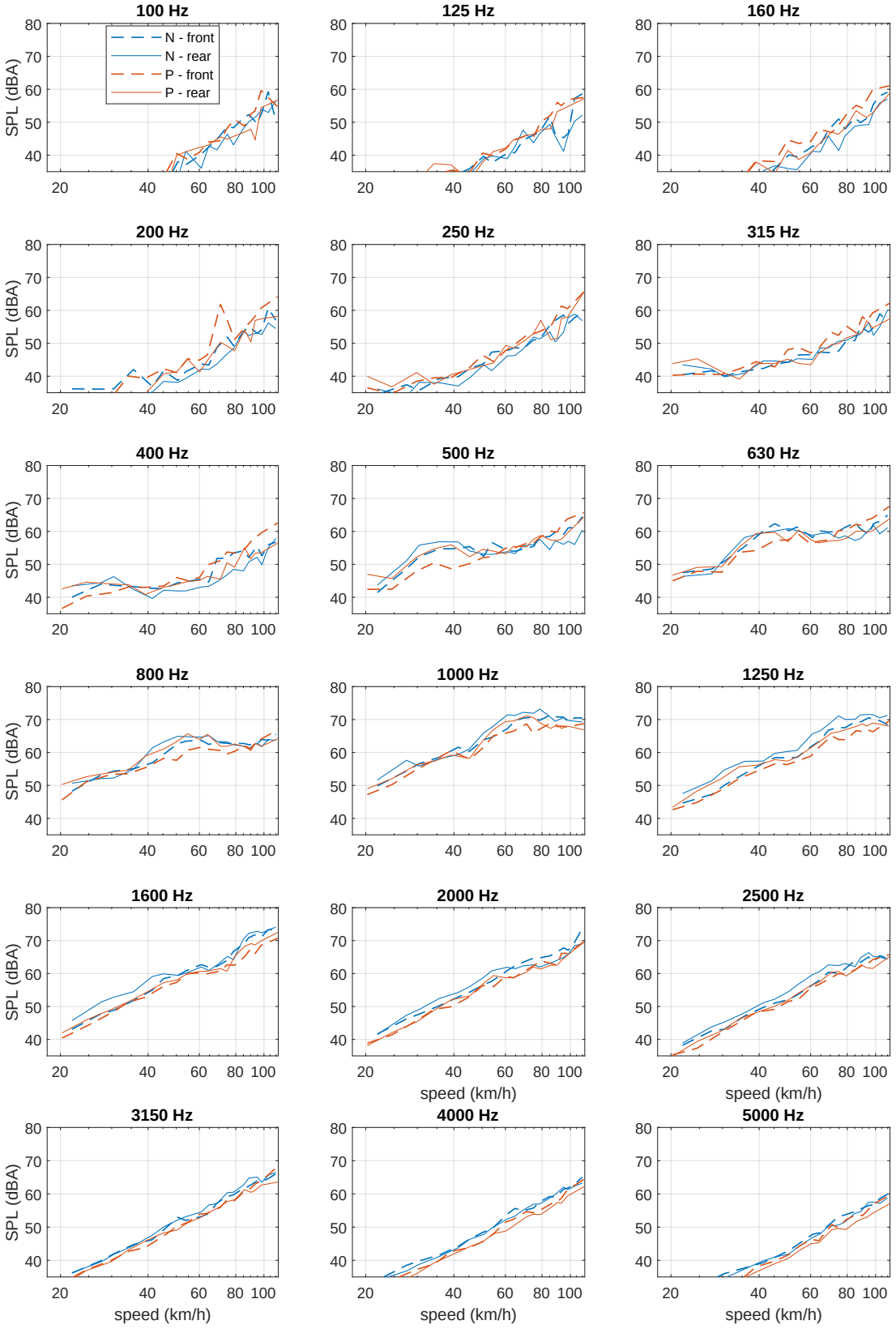

Figure H.1: Third-octave contribution of the front and rear wheel zones of the Renault ZOE#2 at constant speed on road surfaces N and P – A-weighted noise levels at the reference distance 2.7 m.

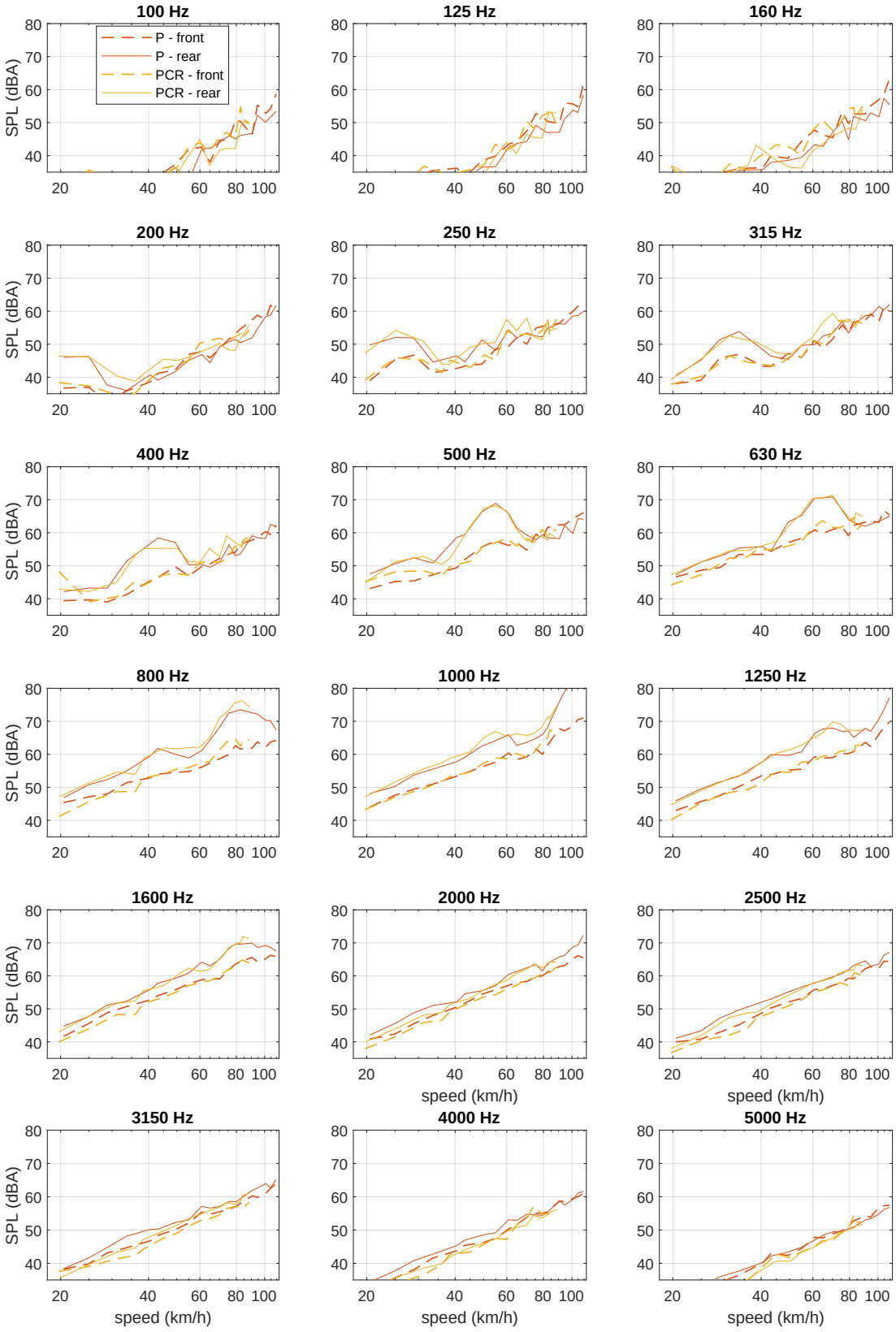

Figure H.2: Third-octave contribution of the front and rear wheel zones of the Nissan LEAF#2 at constant speed on road surfaces P and PCR – A-weighted noise levels at the reference distance 2.7 m.

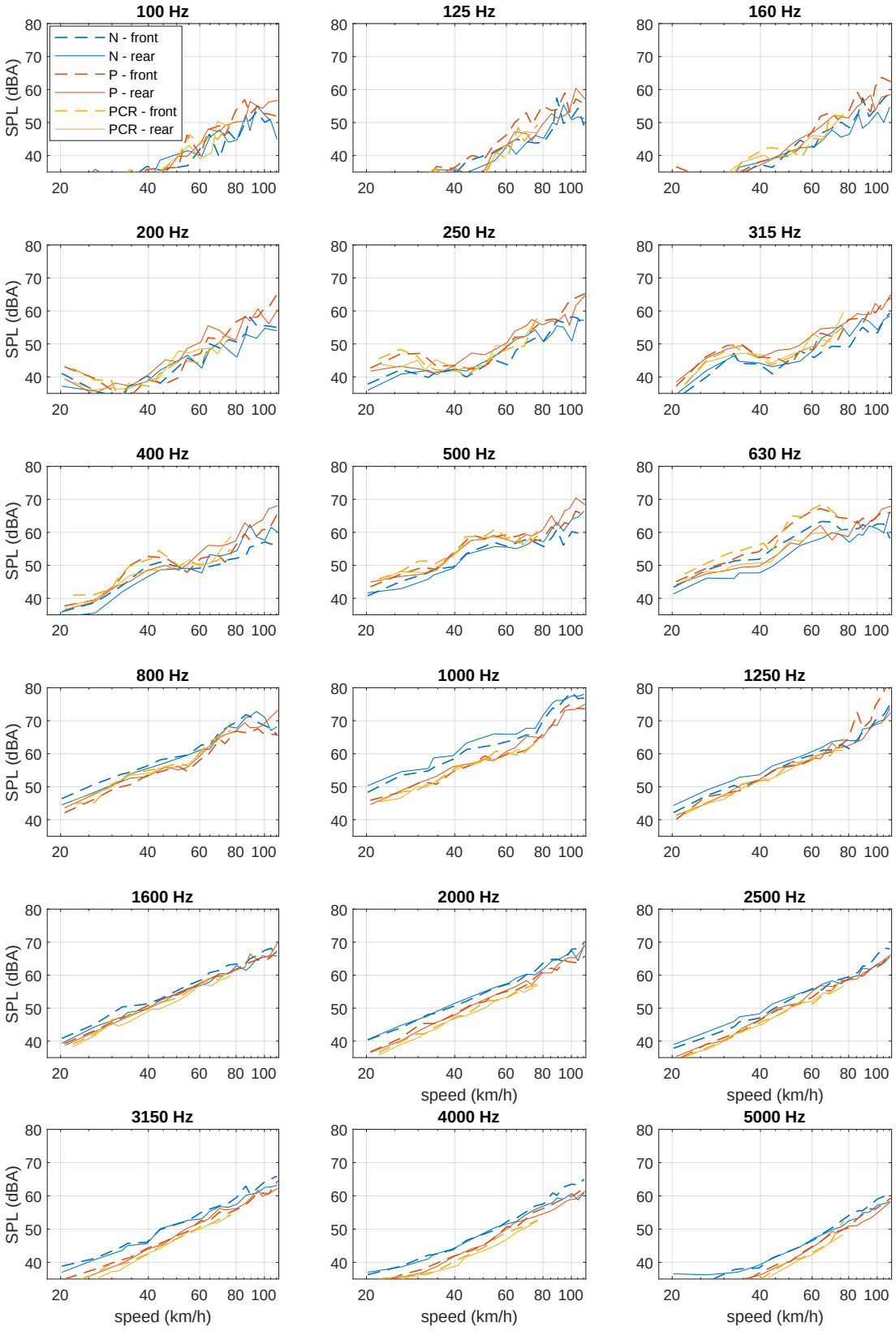

Figure H.3: Third-octave contribution of the front and rear wheel zones of the Renault Kangoo ZE at constant speed on road surfaces N, P and PCR – A-weighted noise levels at the reference distance 2.7 m.

I Sub-action B2.3 : Third-octave contribution of the front and rear wheel zones under acceleration on prototype road surfaces P and PCR

Note: figures begin on next page.

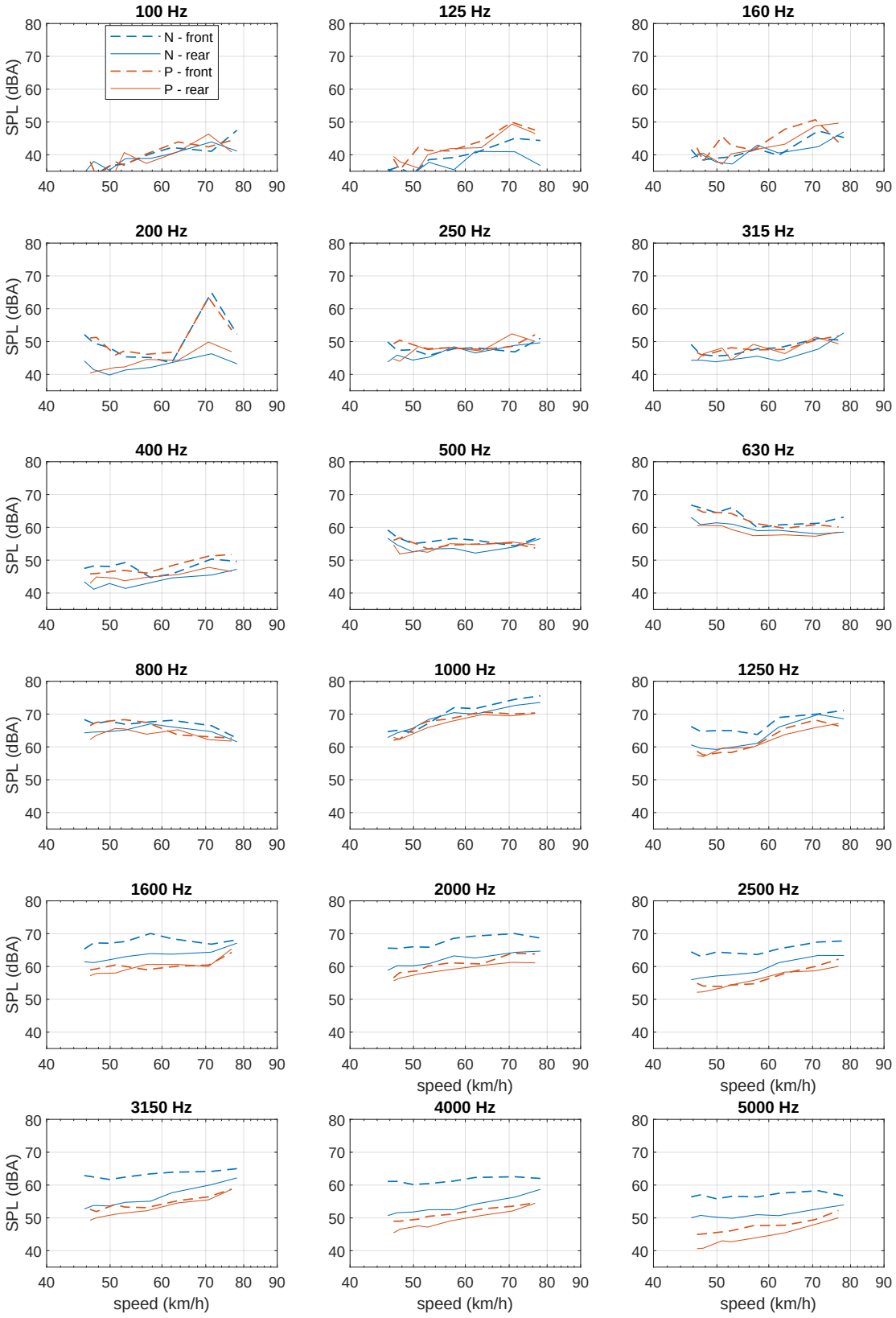

Figure I.1: Third-octave contribution of the front and rear wheel zones of the Renault ZOE#2 under acceleration on road surfaces N and P – A-weighted noise levels at the reference distance 2.7 m.

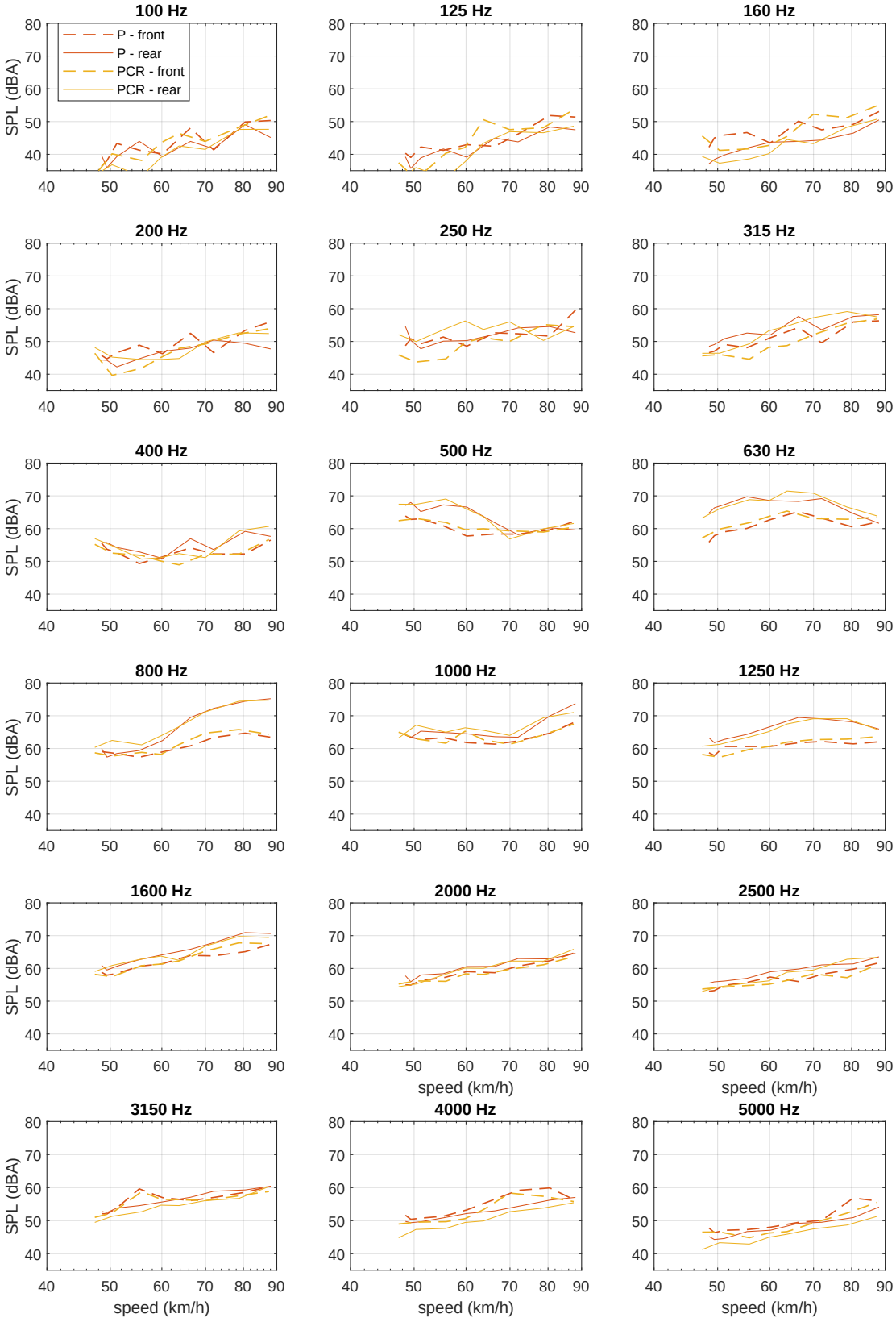

Figure I.2: Third-octave contribution of the front and rear wheel zones of the Nissan LEAF#2 under acceleration on road surfaces P and PCR – A-weighted noise levels at the reference distance 2.7 m.

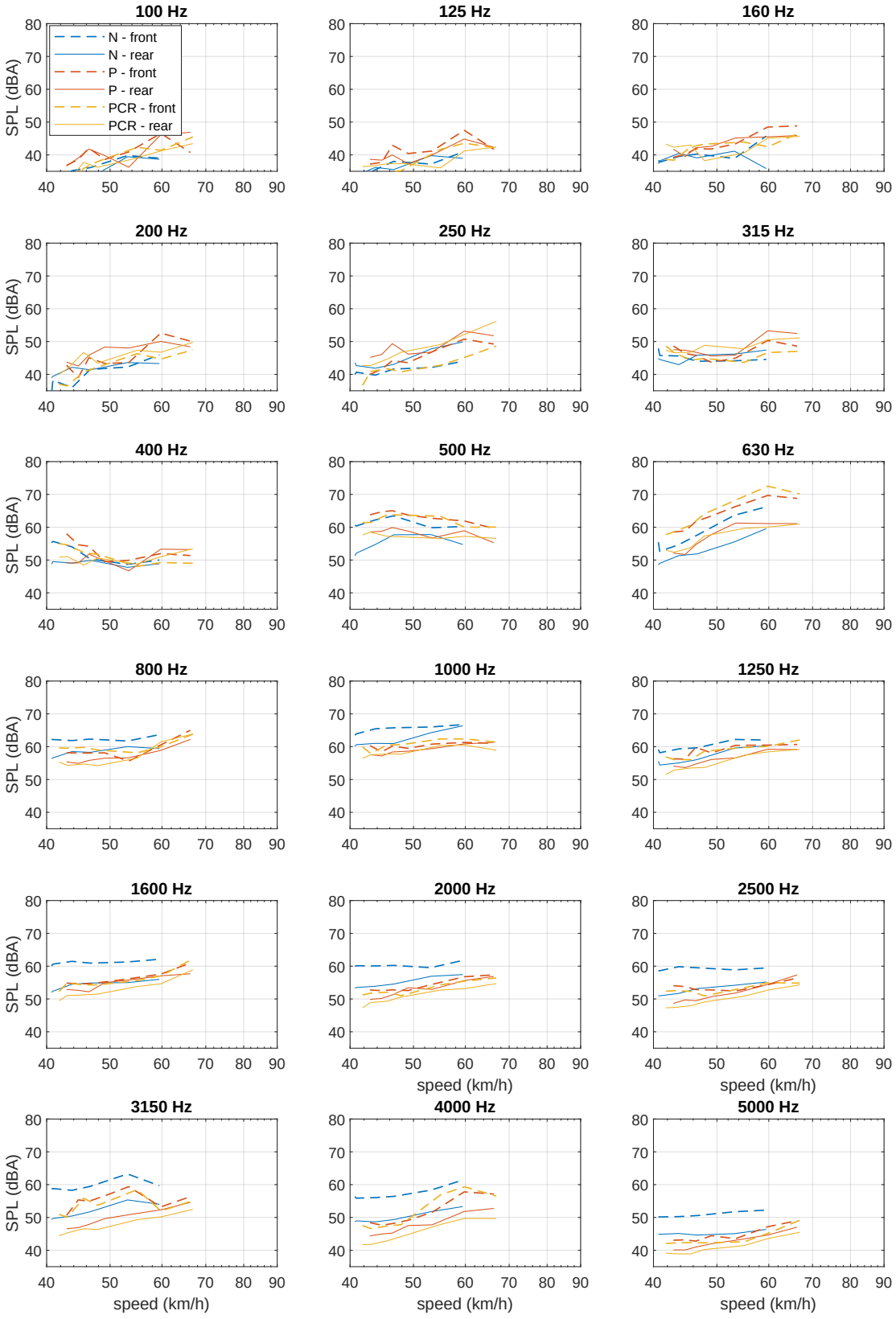

Figure I.3: Third-octave contribution of the front and rear wheel zones of the Renault Kangoo ZE under acceleration on road surfaces N, P and PCR – A-weighted noise levels at the reference distance 2.7 m.